



**DIELECTRIC PROPERTIES
OF TRANSFORMER BOARDS AND PAPERS IMPREGNATED
WITH ALTERNATIVE INSULATING FLUIDS**

Institute of High Voltage Engineering and System management,
Faculty of Electrical Engineering and Information Technique, Graz University of Technology
2014

*Dedicated to my wife, mother and brother whose support and love
has given me joy in life.*

Abstract

In the beginning of fluid-filled transformers, insulating fluids have two important functions which are providing electrical insulation and removing the heat generated from the windings. For more than one hundred years, the widely used insulating fluid in transformers is mineral oil. Along with time, key issues on the utilization of insulating fluids in transformers have been shifting toward environmental protection. Thus, ester fluids attract interest as a potential substitute for mineral oil due to its biodegradation rates, high flash point properties and high moisture tolerance. To utilize ester fluids in a transformer efficiently requires a proper understanding of the dielectric properties behavior of solid-fluid insulating system. Hence, this thesis is intended to improve knowledge regarding the dielectric properties of solids impregnated with ester fluids.

There are three goals of this work. The first goal is to measure and analyse the dielectric response of solids impregnated with ester fluids. The measurements are dependent on material properties such as density, thickness, polymer of solids (cellulose and aramid) and temperature. The second goal is to investigate the dielectric properties of solid samples after insulating fluid replacement as in the case of retrofilling. The last goal is to propose a new-semi empirical formula to estimate effective relative permittivity of solids impregnated with ester fluids.

To achieve those goals, the dielectric properties were evaluated in time domain by means of DC conductivity from long duration charging current measurement and in frequency domain by means of relative permittivity and dielectric dissipation factor $\tan \delta$ over a frequency range of 1mHz-5kHz.

The investigations were performed on homogenous solid samples which were impregnated with mineral oil Nytro 4000X (as reference), synthetic ester MI7131 and natural ester Envirotemp FR3. To study the temperature dependent behaviour, the measurements were performed at three temperature levels, 25°C, 60°C and 90°C respectively. For retrofilling investigation, the solid were first impregnated with mineral oil and then, the insulating fluids were replaced with ester fluids. After that, the change of dielectric response behaviour with time after fluid replacement was investigated.

The results of these investigation show that the dielectric properties of solid impregnated with ester fluids demonstrates different characteristic with solid impregnated with mineral oil. In time domain, it is indicated by higher DC conductivity. Meanwhile, in frequency domain, it is indicated by difference interfacial space charge polarization characteristic which is marked by additional loss peak in dielectric response $\tan \delta$ and higher relative permittivity in low frequency.

It was demonstrated that the dielectric response curve does not alter drastically with change of temperature and it shifts into a single curve which called a "master curve".

The shift in dielectric response curve with change of temperature is characterized by activation energy of DC conductivity and polarization. For solids impregnated with mineral oil, it was found that the activation energy of DC conductivity and polarization is equal and therefore, the master curve of dielectric properties is a perfect fit. However, for solids impregnated with ester fluids, the activation energy of DC conductivity is not necessarily equal to that of polarization.

From retrofilling experiment, it was demonstrated that the dielectric response of solid after fluid replacement is changing with time. The new dielectric response resembles the dielectric response of solids impregnated with ester fluids. The rapid changes of dielectric response might be caused by the interfacial polarization that occurs on the surface of pressboard rather than inside the pressboard itself.

Finally, the proposal of a new semi-empirical formula to estimate the effective relative permittivity of solid impregnated with ester fluids. The formula is an extension of Lichtenecker formula with an additional new factor to consider the influence of interfacial polarization on the surface of pressboard. The formula has been verified with measurement results with a margin of error less than the standard deviation of the measurement.

The results of these investigations will improve knowledge on the dielectric properties characteristic of solids impregnated with ester fluids.

Kurzfassung

Zu Beginn des fluidgefüllten Transformatoren, Isolierflüssigkeit haben zwei wichtige Funktionen, die Bereitstellung elektrischer Isolierung und Entfernen des von den Wicklungen erzeugten Wärme. Die weit verbreitete Isolierflüssigkeit in Transformatoren ist Mineralöl für mehr als hundert Jahren. Zusammen mit der Zeit haben die zentrale Fragen über die Verwendung des Isolierflüssigkeit in Transformatoren zum Umweltschutz verlagert worden. Deshalb Ester Flüssigkeiten verzinnt als potenzieller Ersatz für Mineralöl aufgrund seiner biologischen Abbaubarkeit hohen Brennpunkt Eigenschaften und eine hohe Feuchtigkeitstoleranz. Es erfordert ein richtiges Verständnis der dielektrischen Eigenschaften Verhalten Fest-Flüssig-Isolationssystem Ester Flüssigkeiten in einem Transformator effizient zu nutzen.

Es gibt drei Ziele dieser Arbeit. Das erste Ziel ist es, zu messen und zu analysieren, die dielektrischen Eigenschaften von Ester imprägnierten Materialien. Die Messung ist in abhängig von Materialeigenschaften wie Dichte, Dicke und Art des Polymerfeststoff (Cellulose-und Aramid) und Temperatur. Das zweite Ziel ist zu untersuchen, die dielektrischen Eigenschaften der imprägnierten Materialien nach isolierendem Flüssigkeitsersatz, wie im Fall der Retrofilling. Das letzte Ziel ist, eine neue empirische Formel, um effektive Permittivitätszahlen von Ester imprägnierten Materialien abschätzen.

Um diese Ziele zu erreichen, wurden die dielektrischen Eigenschaften im Zeitbereich durch Gleichstromleitfähigkeit bewertet und im Frequenzbereich durch Permittivitätszahlen und die dielektrischen Verlustfaktoren $\tan \delta$ über einen Frequenzbereich von 1 MHz-5kHz.

Die Untersuchungen wurden auf homogenen festen Materialien durchgeführt, die mit Mineralöl Nytro 4000X (als Referenz), synthetische Ester Flüssigkeiten MI7131 und natürliche Ester Flüssigkeiten Envirottemp FR3 imprägniert wurden. Die Messungen wurden an drei Temperaturniveaus durchgeführt wird, 25°C, 60°C und 90°C, um das temperaturabhängige Verhalten zu studiere. Für Experiment Retrofilling wurden die Materialien ersten mit Mineralöl imprägniert und dann wurden die Isolierflüssigkeit mit Ester-Flüssigkeiten ersetzt. Danach untersuchten wir die Änderung der dielektrischen Eigenschaften Verhalten mit der Zeit nach dem Flüssigkeitsersatz.

Die Ergebnisse dieser Untersuchung zeigen, dass die dielektrischen Eigenschaften von Ester imprägnierten Materialien demonstriert verschiedene Kennlinie mit mineralölimprägnierten Materialien. Im Zeitbereich wird durch eine höhere Gleichstromleitfähigkeit angegeben. Im Frequenzbereich wird durch Differenzgrenzpolarisationscharakteristik, die durch zusätzliche Verlustspitze in dielektrischen Verlustfaktoren $\tan \delta$ und eine höhere relative Permittivitätszahlen niedriger Frequenz gekennzeichnet ist, angegeben.

Es wurde gezeigt, dass die dielektrischen Kennlinien nicht drastisch ändern mit der Änderung der Temperatur und in einer einzigen Kurve, die eine "Master Curve" bezeichnet verschiebt. Die Verschiebung der dielektrischen Kennlinie mit der Änderung der Temperatur wird durch Aktivierungsenergie von DC Leitung und Polarisation gekennzeichnet. Für mineralölimprägnierten Materialien wurde gefunden, daß die Aktivierungsenergie des DC Leitung und Polarisation sind gleich, und daher wird der "Master Curve" von dielektrischen Eigenschaften perfekt sein. Für Ester imprägnierten Materialien, ist die Aktivierungsenergie DC Leitung nicht notwendigerweise gleich der Aktivierungsenergie Polarisation.

Schließlich schlagen wir eine neue semi-empirische Formel, um die effektive Permittivitätszahlen von Ester imprägnierten Materialien abschätzen. Die Formel ist eine Erweiterung von Lichtenecker Formel mit einem zusätzlichen neuen Faktor, um den Einfluss der Grenzflächenpolarisation auf der Oberfläche der Pressboard berücksichtigen. Die Formel wurde mit Messergebnisse verifiziert.

Schließlich schlagen wir eine neue semi-empirische Formel, um die effektive Permittivitätszahlen von Ester imprägnierten Materialien abschätzen. Die Formel ist eine Erweiterung von Lichtenecker Formel mit einem zusätzlichen neuen Faktor, um den Einfluss der Grenzflächenpolarisation auf der Oberfläche der Pressspan berücksichtigen. Die Formel wurde mit Messergebnisse verifiziert.

Die Ergebnisse dieser Untersuchungen würde die Kenntnis von den dielektrischen charakteristischen Eigenschaften der Ester imprägnierten Materialien verbessern.

Acknowledgement

For the last three and a half years, I have had the opportunity to study at the Institute of High Voltage Engineering and System Management (IHS) of Graz University of Technology, Graz, Austria. Finally, the work is finished and resulted in this PhD thesis.

I wish to express my deepest gratitude to my supervisor, Em.-Prof. Dipl.-Ing. Dr. techn. Dr.h.c. Michael Muhr for giving me the opportunity to do this project, for his endless support and guidance during the whole project. This project would not be possible without him.

I would like to thank Dipl.-Ing. Dr. techn. Georg J. Pukel and Dipl.-Ing. Dr. techn. Robert Schwarz for their support and fruitful discussion during the project.

I specially thank my former advisor, Prof. Dr. Suwarno for encouraging me to continue my studies in high voltage engineering.

I would also like to thank Dr. techn. Norasage Pattanadech for his friendship throughout my study time and for being a great mentor for me.

I am very grateful to Dipl.-Ing. Dr. techn. Thomas Judendorfer for his invaluable suggestion during the preparation of this thesis, to Ms. Bettina Wieser and Dipl.-Ing Julia Podesser for their help throughout the project, to Univ.-Doz. Dipl.-Ing. Dr. techn. Christoph Sumereder for his guidance on the measurement set-up, Dipl.-Ing Christian Auer and Mr. Irvin Majic for building the power supply, Mrs. Karin Wukounig for helping me with various things, Mr. Anton Schriebl and Mr. Markus Rappold for technical assistance when building the test cell.

I would like to thank the rest of the staff and colleague at the institute for these years which have helped me on so many levels, that I cannot mention them all here.

I wish to acknowledge the financial support from ÖaD Scholarship and Siemens AG Österreich Transformers Weiz, Weiz, Austria.

The last but not least, I would like to express my gratitude to my wife, Prima Elda, for her love and support. She has been my source of confidence in hardship. I also wish to thank my mother, Endang Fajarsari and brother, Riza Yukananto M.Sc for their never ending support.

Fari Pratomosiwi
Graz
March 5th, 2014

Contents

1. Introduction.....	1
1.1. Background.....	1
1.2. Thesis objectives	1
1.3. Thesis structure	2
2. Transformers insulation system.....	4
2.1 Insulating fluid.....	4
2.1.1. <i>Historical development</i>	4
2.1.2. <i>Overview of alternative insulating fluids</i>	6
2.2. Solid – fluid insulating system	17
2.2.1. <i>Basic of solid insulation in transformer</i>	17
2.2.2. <i>Intrinsic viscosity</i>	21
2.2.3. <i>Research on dielectric properties of solid-fluid insulating system</i>	21
2.3. Retrofilling	22
2.3.1. <i>Introduction</i>	22
2.3.2. <i>Reasons for retrofilling</i>	22
2.3.3. <i>What happened to transformer insulation after retrofilling</i>	23
2.3.4. <i>Research on retrofiling</i>	24
3. Theory of dielectric materials.....	26
3.1. Introduction	26
3.1.1. <i>Polarization Mechanism in Dielectrics</i>	26
3.1.2. <i>Electrical conduction mechanism of solid-fluid insulating system</i>	29
3.2. Dielectric response.....	34
3.2.1. <i>Dielectric response in time domain</i>	34
3.2.2. <i>Dielectric response in frequency domain</i>	37
3.3. Practical consideration of measurement and analysis	38
3.3.1. <i>Time domain measurement</i>	38
3.3.2. <i>Frequency domain measurement</i>	42
3.3.3. <i>Equivalent circuit of pressboard impregnated system</i>	43
3.3.4. <i>Dielectric relaxation in solid: review on analytical method</i>	47
3.4. Temperature dependent behavior of dielectric properties.....	53
3.5. Composite dielectric	55

4. Test object investigated and test set-up	60
4.1. Laboratory samples.....	60
4.1.1. <i>Pressboard and transformer papers samples</i>	60
4.1.2. <i>Insulating fluid samples</i>	61
4.2. Test vessel.....	61
4.3. Measurement performed on test objects	63
4.3.1. <i>Pressboard and transformer papers samples</i>	63
4.3.2. <i>Insulating fluid samples</i>	64
4.4. Experiment scheme.....	65
4.5. Measurement set-up.....	66
4.5.1. <i>Complex capacitance - $\tan \delta$</i>	66
4.5.2. <i>Electrical conductivity</i>	67
5. Investigation results and discussion	68
5.1. Linearity properties of samples	68
5.1.1. <i>DC conductivity</i>	68
5.1.2. <i>Capacitance - $\tan \delta$</i>	69
5.2. DC conductivity of solid impregnated with ester fluids.....	71
5.3. Dielectric response on frequency range of 1mHz - 5kHz	78
5.3.1. <i>Basic knowledge</i>	78
5.3.2. <i>Influence of insulating fluids on dielectric response</i>	80
5.3.3. <i>Influence of polymer material on the dielectric response</i>	84
5.3.4. <i>Temperature dependent behaviour of dielectric response</i>	87
5.3.5. <i>Imaginary part of susceptibility</i>	92
5.3.6. <i>Loss characteristics of solid impregnated with ester fluids</i>	96
5.3.7. <i>Master curve</i>	98
5.4. Relative permittivity - $\tan \delta$ at 50Hz.....	103
5.4.1. <i>Influence of density, thickness and polymer material of pressboard</i>	103
5.4.2. <i>Influence of density and thickness of transformer papers</i>	105
5.4.3. <i>Influence of insulating fluid and temperature</i>	107
6. Replacement of insulating fluids: laboratory test of retrofilling	113
6.1. Introduction	113
6.2. Procedure of fluid replacement.....	114
6.3. Time behavior of dielectric response after fluid replacement	114
6.3.1. <i>In frequency domain</i>	114

6.3.2. <i>In time domain</i>	124
6.4. Polarization on surface of pressboard after insulating fluid replacement.....	126
7. Estimating dielectric properties of solid impregnated with ester fluids.	131
7.1. Introduction	131
7.2. Effective relative permittivity	131
7.2.1. <i>Estimation of relative permittivity at power frequency of 50Hz</i>	131
7.2.2. <i>Estimation of relative permittivity as a function of frequency</i>	135
7.3. Dielectric dissipation factor, $\tan \delta$	136
7.4. DC conductivity	138
8. Summary and Conclusions	139
9. Future works	144
Reference.....	145
Appendix A - Direct inter-electrode capacitance for three electrodes system.....	155
Appendix B - Derivation of equivalent circuit.....	156
Appendix C - Design of electrode and test vessel	159
C.1. Electrode corner shape for measuring dielectric properties.....	159
C.2. Electrode's pressure on the measured dielectric properties.....	165
C.3. Detail of experiment vessel and electrode.....	168
Appendix D - Table of dielectric properties.....	172

List of symbols

W_{rel}	Relative moisture (water) content at a given temperature	%
W_{abs}	Absolute moisture (water) content at a given temperature	ppm
$W_L(T)$	Moisture (water) saturation limit at a given temperature	ppm
p	Dipole moment	$C \cdot m$
q	Electric charges	C
d	Displacement vector	m
α	Polarizability	$C \cdot m^2/V$
E	Static electric field stress	V/m
P	Polarization	C/m^2
χ	Electric susceptibility of the material. It accounts for all kinds of polarization processes within dielectric.	dimensionless
ϵ_0	Relative permittivity of vacuum = 8.85419×10^{-12}	F/m
e	Elementary charge	C
k	Boltzman constant = 8.6173324×10^{-5}	eV/K
T	Temperature	K
ρ	DC resistivity	$\Omega \cdot m$
E_{DC}	Activation energy of DC conductivity	1 eV = 96,5 kJ/mol
E_P	Activation energy of polarization	1 eV = 96,5 kJ/mol
R_{dc}	DC resistance	Ω
τ	Relaxation time	s
f_m	Absorption frequency	Hz
h	Sample thickness	mm
v	Mean velocity of charge carrier drift	m/s
μ	Charge-carrier mobility	$m^2/V \cdot s$
ϵ_∞	Relative permittivity of sample at very high frequency	dimensionless
D	Electric flux density	C/m^2
$f(t)$	Dielectric response function	$1/s$
$j(t)$	Current density	A/m^2
σ_0	DC conductivity	S/m
$E(t)$	Electric field stress	V/m
V_0	Voltage applied	V
C_0	Capacitance of inter-electrode	pF
a	Effective area of electrode	cm^2
$\tan \delta$	Dielectric dissipation factor	dimensionless
ϵ_r	Relative permittivity	dimensionless

ω_1	Frequency component of dielectric response at 60°C (reference curve)	<i>rad/s</i>
ω_2	Frequency component of shifted dielectric response at T2 (shifted curve)	<i>rad/s</i>
T_1	Reference temperature = 60+273 = 333°K	<i>K</i>
T_2	Temperature for the shifted curve, the new temperature	<i>K</i>
σ_1	DC conductivity at reference temperature	<i>S/m</i>
σ_2	DC conductivity at new temperature	<i>S/m</i>
ϵ'	Real part of complex dielectric permittivity	dimensionless
ϵ''	Imaginary part of complex dielectric permittivity	dimensionless
C'	Real part of complex capacitance	<i>F</i>
C''	Imaginary part of complex capacitance	<i>F</i>
χ'	Real part of complex dielectric susceptibility	dimensionless
χ''	Imaginary part of complex dielectric susceptibility	dimensionless
A	Pre-exponential value of Arrhenius equation for DC conductivity	dimensionless
S_1, S_2	Dielectric material in heterogeneous dielectric mixtures	dimensionless
ϵ_{eff}	Effective relative permittivity of dielectric mixtures	dimensionless
ϵ_e	Permittivity of homogenous dielectric material (pressboard and transformer papers)	dimensionless
ϵ_i	Permittivity of material located randomly in homogenous dielectric (insulating fluids)	dimensionless
f	Volume fraction that is occupied by ϵ_i in ϵ_e	dimensionless

1. Introduction

1.1. Background

In most transformers, the insulation systems consist of oil-impregnated paper on the copper windings and several oil-impregnated pressboard barriers between the high- and low-voltage windings. The whole construction is then impregnated in insulating fluid which acted as both insulation and coolant. Currently, the widely used insulating fluid in transformers is mineral oil. However, along with times, key issues regarding insulating fluid in transformers have been shifting since the first time of mineral oil utilization. Nowadays, with environmental issues becoming extremely important, ester fluid is an attractive alternative due to its biodegradation rates, high flash point properties and high moisture tolerance. The later might prolong solid insulation longevity [1].

Ester fluids have been used in transformers since in the middle of 1970s both in new transformers and for the purpose of refilling old transformers. To utilize ester fluids in a high voltage transformer efficiently requires a proper understanding of the behavior of dielectric properties of both insulating fluid and solid-fluid insulating system. It requires knowledge of the manner the dielectric properties behave with temperature and voltage as parameters as it affects the dielectric properties to different extent [2]. Consequently even though a given insulating fluid and solid-fluid insulating system may be only used at power frequency of 50 or 60Hz, a proper insight into its electrical behavior can only be obtained by observing its dielectric response as a function of frequency with the temperature as a parameter and also by observing the transient overvoltage behavior. Hence, the investigation of dielectric properties behavior of solid-fluid insulating system over a wide range of frequencies with temperature as parameter will provide much of the required insight to comprehend its complexity [3].

Work presented in this thesis has been carried out to investigate the dielectric properties characteristic of solid impregnated with ester fluids and time behavior of dielectric properties after fluid replacement as in refilling of transformer.

This project was started in 2011 on the recommendation of Em.-Prof. Dipl.-Ing. Dr. Techn. Dr.h.c. Michael Muhr at Institute of High Voltage Engineering and System Management (IHS) of Graz University of Technology and Siemens AG Österreich Transformers Weiz, Austria.

1.2. Thesis objectives

The first objective of this work was to improve the knowledge related to dielectric properties of solid impregnated with ester fluids by means of measurement of

different quantities in time and frequency domain. The methods to quantify the dielectric properties in time domain are the measurement of dc conductivity from long time duration charging current. In the frequency domain, the quantification of dielectric response was performed by measurements of complex capacitance and dielectric dissipation factor ($\tan \delta$) over frequency range of 1mHz-5kHz.

Laboratory investigation were carried out on macroscopically homogenous samples of solid impregnated with various insulating fluid such as mineral oil, Nytro 4000X, synthetic ester, MI7131 and natural ester Envirottemp FR3. There are seven types solid sample samples with different characteristics and thus, there are twenty one solid-fluid combinations. The measurements were performed in dependence of various parameters, such as temperature and physical characteristic of solid e.g. density, thickness and type of polymer material. From the results, a data base of dielectric properties of solid impregnated in various insulating fluids was created. The data base consists of $\tan \delta$, relative permittivity, dc conductivity, activation energy and pre-exponential factor of each solid-fluid combination.

The second objective of this work was to improve knowledge related to retrofilling of transformer with ester fluids by means of time behavior investigation of dielectric properties of pressboard after insulating fluid replacement. The measurements were performed in dependence of immersed temperature after fluid replacement as parameter. Investigation of interfacial (space charge) polarization on the surface of pressboard was also performed in order to gain knowledge on the influence of insulating fluid on the polarization behavior on the solid-fluid insulating system.

The last objective was to propose a simple mathematical formula for estimating effective relative permittivity of solid impregnated with ester fluids. The semi-empirical formula takes into account the influenced of interfacial polarization on the relative permittivity.

1.3. Thesis structure

A short description of each of the chapters in this report is given below.

Chapter 2: This chapter provides the overview of insulating fluid, pressboard and transformer papers in impregnated insulation systems. Retrofilling of a transformer is also reviewed.

Chapter 3: This chapter describes the theory of dielectric response measurement techniques on insulation systems. The temperature dependence behavior of dielectric properties solid-fluid insulation systems is discussed. The basic theory of composite material is also reviewed.

Chapter 4: Here, a description of samples investigated and their preparation procedures is presented. Specification concerning experiment scheme, measurement procedure and set-up are also given.

Chapter 5: The experiment results of solids impregnated with ester fluids are presented and discussed in the following order: linearity properties, DC conductivity, dielectric response in frequency 1mHz – 5kHz and master curve. In addition, the temperature dependence behavior of solid impregnated with ester fluids are given for each solid-fluid combination.

Chapter 6: A detailed description of laboratory experiment of retrofilling is presented in the following order: retrofilling scheme, effect of immersed temperature on the dielectric properties characteristic and time behavior of dielectric properties after insulating fluid replacement. The influence of interfacial polarization on the surface of pressboard is also discussed.

Chapter 7: A new mathematical formula for estimating effective relative permittivity of solids impregnated with ester fluids are given based on experiment results.

Chapter 8 and 9: Summarize of this dissertation and the possibilities of further work are discussed.

2. Transformers insulation system

Transformer insulation systems consist of oil-impregnated paper on the copper windings and several oil-impregnated pressboard barriers between the high- and low-voltage windings. With that being said, the insulation capability of transformer depends on the complex solid- fluid insulating system. This chapter addressed the topic of fluid and solid insulation in transformers and retrofilling of transformers.

2.1 Insulating fluid

2.1.1. Historical development

In the beginning of liquid-filled transformers, the insulating fluid has two important functions which are providing electrical insulation (in combination with solid insulation) and removing the heat generated from the windings. Insulating fluid eliminates air and gases within the cellulose which compromised its electrical insulation performance.

For more than one hundred years, the widely used insulating fluid in transformers is mineral oil. The utilization of petroleum based mineral oil is mainly because its wide-availability (in fact Nynas claims that it has enough reserves in Venezuela, thus assured supplies for the foreseeable future) good electrical and physical properties, good combination with cellulose and low cost [4]. However, some key issues on the usage of insulating fluid in transformers have been shifting since the first time of mineral oil utilization. Nowadays, with environmental issues becoming extremely important, the utilization of insulating fluids with high biodegradation rates is very attractive. Thus, the utilization of ester fluids which categorized as “readily biodegradable” attracts interest as a potential substitute for mineral oil. Figure 2.1 depicts historical development of insulating fluids and key issues when utilize in transformer.

Historically, ester fluids have been used as insulating fluid since the invention of electrical equipment in the late 1880s. Indeed, the first insulating fluid historically used in electrical equipment – capacitors was extracted from castor-oil plant which can be categorized as natural ester [5, 6]. However, the earliest simple natural ester fluids were shortly found to be incompatible with free breathing equipment because of their chemistry and were gradually replaced by mineral oils. Petroleum oils have been used in electrical equipment since 1887 [7, 8]. These low viscosity paraffinic petroleum oils served the purpose of providing superior insulation when impregnated into paper or other solid dielectrics and when used by themselves they provide an excellent heat transfer medium for removal of heat generated by electrical losses. However, paraffinic crudes such as are available from the Middle East Arabian Peninsula contain large quantities of paraffin wax and therefore have high pour points which make them unacceptable for use in electrical apparatus exposed to low temperatures [7]. Due to

that reason, after 1925, they were mostly replaced with naphthenic petroleum oils. For many years, the history of the development of insulating fluid for electrical apparatus is the history of the development of mineral oil from naphthenic crude. Naphthenic oils contain aromatic compounds which remain fluid at comparatively low temperatures such as at -40°C . One of the earliest concerns with mineral based insulating fluid was its flammability. Since mineral oils were used early in combination with cellulose based papers to insulate transformers, there was a concern for explosive or flammability hazards associated with them.

Driven by the desire for a safer non-flammable transformer fluid, mineral oils were replaced by Askarels between 1930 and the mid-1970s. Askarels comprise a group of synthetic fire resistant, chlorinated aromatic hydrocarbons used as electrical insulating fluid for applications where flammable mineral oils were not acceptable. The first transformer that utilize askarel was made in 1932 and it contained Aroclor (polychlorinated biphenyl, PCB's) mixed with varying quantities of trichlorobenzene and/or tetrachlorobenzene [7]. The use of PCB's as non-flammable insulating liquids continued until the mid-1970s when it was realized that PCB's were harmful to the environment. PCB's could not be degraded rapidly. It was found to be accumulated in fatty tissues of organisms as it progressed through the food chain. On top of that, it was also found that incomplete combustion of PCB's generated Dioxin which is more hazardous to health than PCB's themselves [9].

With the departure of PCB's in the 1970s, the industry turned to alternative insulating fluid which is equally fire resistant and available commercially i.e. synthetic ester at 1977, silicone fluids at 1979, high temperature hydrocarbons (HTH), members of the chlorofluorocarbon family (Freons), perchloroethylene (C_2Cl_4) or Perc at early 1980s and Beta Fluid (improved fire resistant petroleum oil) at 1995 [10, 11]. While those alternative insulating fluid could not be categorized as non-flammable (with the exception of Freons and Perc which are non-flammable), they have a higher fire point than mineral oils. Silicone fluids showed to have excellent electrical insulating properties, highly stable and have excellent oxidation resistance. However, its high viscosity and slow biodegradation rate limits the fluid's capability as coolant and hazard to environment. Thus, the application of silicone fluid is restricted to where additional coolers or pumps are applicable. Currently, Japan has developed a lower viscosity silicone fluid for power transformer [12].

In the mid-1970s, driven by the need for a less-flammability and safe for the environment synthetic ester were started to be used in distribution transformer as alternative to mineral oil and as a replacement of PCBs. Synthetic ester was extensively used because its less-flammable characteristics, environmental protection and good technical performance. Concerns regarding the utilization of synthetic ester in transformers are mainly due to its high cost (at the moment, three times the price of mineral oil) and high viscosity, which require changes in the design of heat transfer system in transformer [13, 14, 15].

The high cost of synthetic ester led to the evaluation of a natural (vegetable oil) ester having many of the same performance advantages of synthetic esters but much more economical. The major disadvantages of natural esters are their inherent susceptibility to oxidation and higher pour point. After a massive research of natural ester in the early of 1990s, significant improvement on low temperature was achieved. Oxidation inhibitors together with proper method-of-use overcome the oxidation stability issues. The inhibitors were found that did not adversely affect the non-toxicity or biodegradation rates [1]. In many cases the natural esters perform better than the less-flammable fluid they replace and offer significant advantages for applications where naphthenic mineral oil are traditionally applied, especially in case of ageing of cellulose and less-flammable characteristic. Finally, at 1999, natural esters that commercially available are in the market [16].

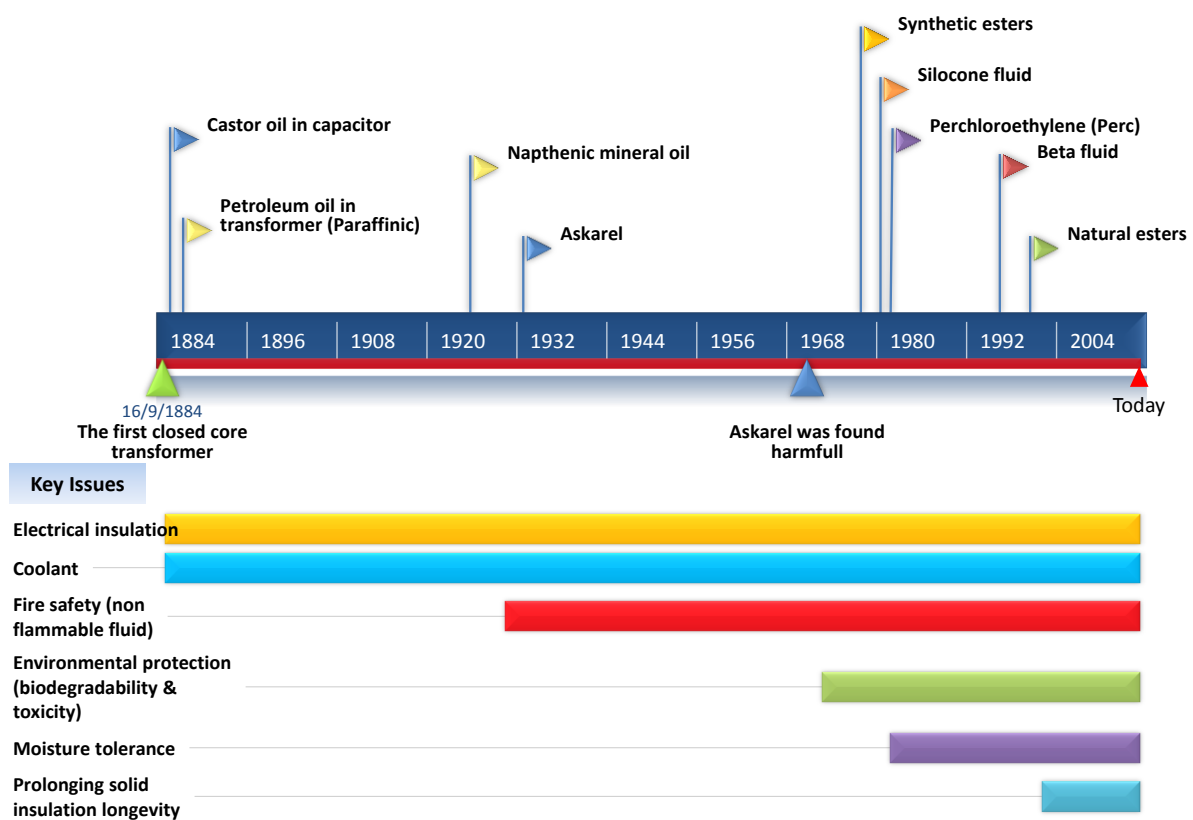


Figure 2.1: Timeline of events in the development of insulating fluid in transformers and on the key issues of insulating fluid.

2.1.2. Overview of alternative insulating fluids

In this work, alternative fluids insulation under discussion is synthetic esters and natural esters.

Mineral oil - Nytro 4000X

Mineral oil is made by refining a fraction of the hydrocarbon collected during the distillation of a petroleum crude stock. Because of the wide availability and low cost, as well as being an excellent dielectric and cooling medium, petroleum-based transformer oils are probably the most widely used electrical insulating fluid in the world for the last today and maybe for the last century. Chemically, the mineral oil consists of a complex of basic hydrocarbon liquids, as depicted in Table 2.1.

Virtually all of the hydrocarbon compounds in transformer oils are members of three classes [17, 18]:

1. Paraffinic oil

Paraffinic oil is derived from crude oil containing significant amount of n-paraffin. It has relatively high pour point and may require additives to reduce pour point. Given modern refining technology, acceptable transformer oils can be made from paraffinic crude oils that are richer in *n-alkanes* and *i-alkanes*.

2. Naphthenic oil

Naphthenic oil is derived from crude oil containing a very low level of n-paraffins. It is free of wax and has low pour point. It requires no additives to reduce pour point. It also possesses better viscosity characteristic and longer life expectancy. Naphthenic oil has more polar characteristic compared to paraffinic oil.

3. Aromatic oil

Aromatic oil is a class of organic hydrocarbon compound which have one or more unsaturated rings of carbon atom. It is characterized by double and single bond between carbon atoms. Moderate concentrations of aromatic hydrocarbon are necessary in an oil to meet the specified limits on several electrical and chemical characteristics of transformer oils.

Transformer oils may contain inhibitor which delays the oxidation of oil. It might be natural or synthetic and added to oil.

New mineral oils are produced in accordance with IEC 60296 [19]. Meanwhile, for evaluation of oil insulation quality in operational transformers is normally done in accordance with IEC 60422 [20]. Mineral oil used in this thesis was Nytro 4000X.

Nytro 4000X is an inhibited super grade manufactured by Nynas AB, Sweden. Nytro 4000X provides outstanding oxidation stability for a longer transformer life with less maintenance. It possesses extremely good heat transfer due to its low viscosity. Nytro 4000X is naphthenic based petroleum oil, thus it has very good low temperature properties. The Nytro 4000X also possesses high dielectric strength, above 70kV for moisture content less than 10ppm [21].

Synthetic ester – Midel 7131(MI7131)

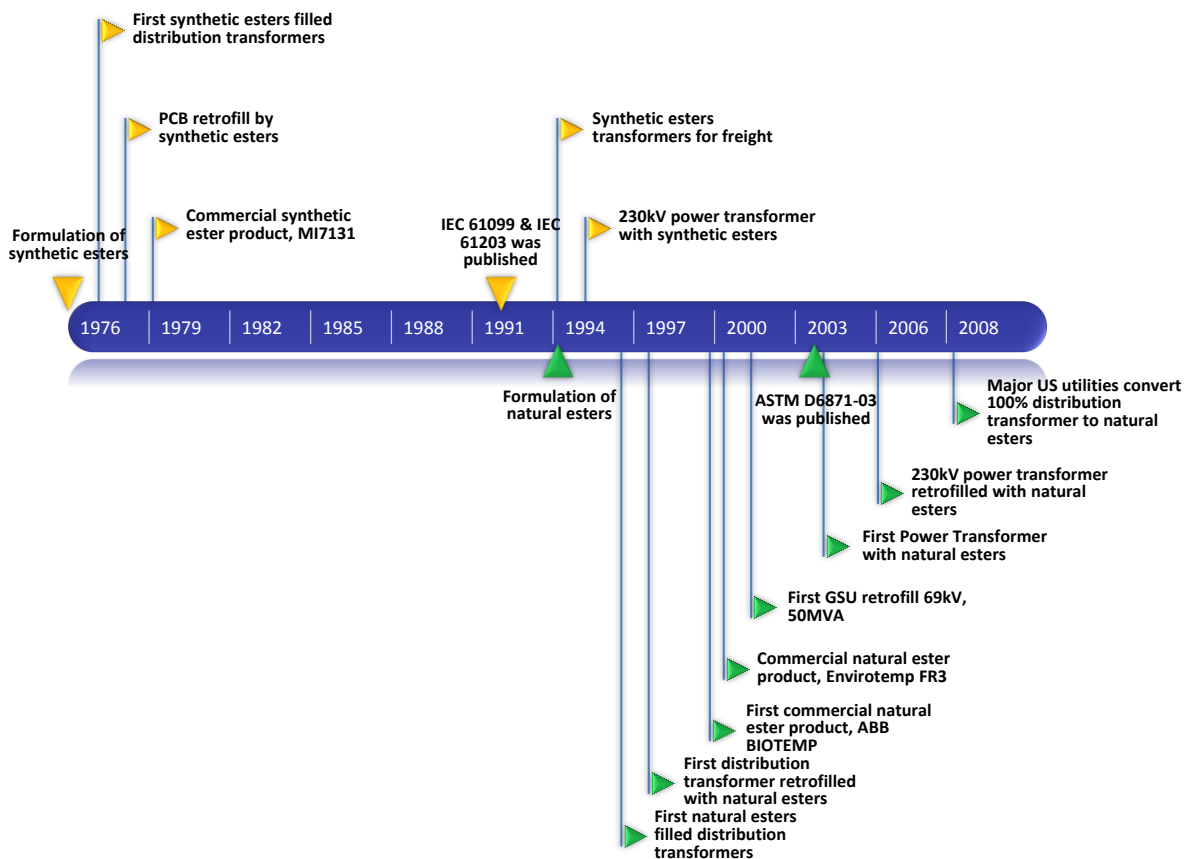


Figure 2.2: Timeline of events in the development and application of ester fluids. Yellow mark is for synthetic esters and green mark is for natural esters [12, 16]

Esters are chemical compounds consisting of a carbonyl adjacent to an ether linkage. They are derived by reaction of an oxoacid with a hydroxyl compound such as an alcohol or phenol. With that being said, esters are formed by condensing an acid with an alcohol. Esters linkage occurs in both natural and synthetic esters. The reactions involved in the manufacture of ester are relatively simple and can be expressed as [17]:

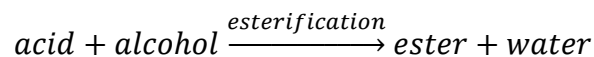


Figure 2.2 presents timeline of events in the development and application of ester fluids. In the mid-1970s, synthetic esters were begun to be utilized in distribution transformer as alternative to mineral oil and as a replacement of PCBs. Synthetic ester was extensively used because its less-flammable characteristics and environmental protection [22]. Ester fluid is somewhat in intermediate position between PCBs and mineral oil in term of flash ignition and self-ignition temperature [23]. Ester fluids are also non-toxic, well digested by micro-organism and possess low vapor pressure at the operating temperature of power transformers. During a fire, they produce neither dioxins nor toxic products and categorized as “readily biodegraded” [12]. The only

products by their biodegradation process are carbon dioxide and water. Ester fluids have been developed to resist oxidation and are able to absorb more moisture than mineral oil before their electrical performance deteriorates [24]. Ester fluids also possess good electrical insulation performance and comparable to mineral oil [25]. They have the capacity to absorb moisture produced in degradation process of cellulose which will further delay the ageing process of cellulose. However, at the first time of the utilization of synthetic ester in transformer, the superior moisture absorption in cellulose was not a key issue yet. Concerns regarding the utilization of synthetic ester in transformers are mainly due to its high cost (three times the price of mineral oil) and high viscosity, which require changes in the design of heat transfer system in transformer.

Currently they are increasingly being utilized in power transformer and in transformer where the safety of people and property could be jeopardized by fire. New synthetic esters are produced in accordance with IEC 61099 and in service maintenance is in accordance with IEC 61203 [12, 26]. Synthetic ester used in this thesis was Midel 71317 (MI7131).

MI7131 is a synthetic ester manufactured by M&I Materials in Manchester, UK. MI7131 was first commercially available in 1979, when less-flammable and environmentally friendly insulating fluid was sought.

It is derived from penta erythritol, with four fatty acid chains. Due to ester linkage in the molecular structure, MI7131 is highly biodegradable and has high moisture saturation limit, around 2600ppm at 20°C. The moisture tolerance property of MI7131 is important for assuring the longevity of cellulose material as it will absorb moisture from cellulose at equilibrium. The dielectric strength of MI7131 is comparable to Nytro 4000X, above 70kV. Due to its excellent physical, chemical and electrical properties, MI7131 is widely used in both distribution and power transformers around Europe [27].

Natural ester - Envirotemp FR3

Natural esters are produced from vegetable oils which extracted from renewable plant crops. The structure of natural esters is based on glycerol backbone, to which 3 naturally occurring fatty acid groups are bonded. Plant crops produce these esters as part of their natural growth cycle.

Natural esters offer the same advantages as synthetic esters i.e. less-flammable characteristic, provide good environmental protection and high moisture saturation point but with less cost. The major disadvantages of natural esters are their inherent susceptibility to oxidation and high viscosity. The reason for this is because many fatty acid of native oil contain two or more carbon-carbon double bonds, which undergo reactions with atmospheric oxygen. Therefore, natural esters are more susceptible to

oxidation the more of these unsaturated fatty acids are available. However, oxidation inhibitors together with proper method-of-use overcome the oxidation stability issues [1].

Natural esters can be produced from a wide variety of crop oils, but for electrical applications, they are commonly produced from soya, rapeseed and sunflower oil. This is due to their availability, low cost and good performance. Other crop such as coconut oil has been used, but the utilization limited to countries where these crops grow e.g. Srilanka. In the recent years, there is also camellia oil which is a new trend in China [28].

In recent years, natural esters are widely used in distribution transformers and its popularity has increased. Two guides are available, IEEE Guide C57.147 – “IEEE Guide for Acceptance and Maintenance of Natural Ester Fluids in Transformer” [29] and ASTM D6871 – 03 (2008) [30]. IEC is currently developing its own natural esters standard. Natural ester used in this thesis was Envirotemp FR3.

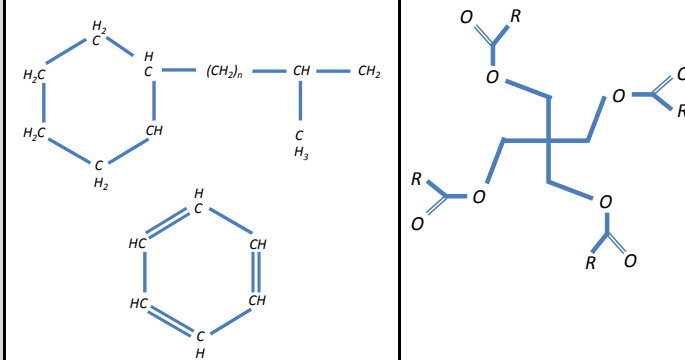
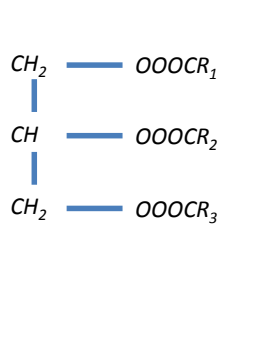
Envirotemp FR3 is a natural ester manufactured by Cargill, in the USA. FR3 was first commercially available in 2000 and has been used in distribution and power transformer around the world. FR3 is mainly used in distribution and power transformer in America.

FR3 is made from edible-seed oil. It is a natural ester (triglyceride fatty acid ester) contains a mixture of saturated and unsaturated fatty acids with 14 to 22 carbon length chains containing one to three double bonds. FR3 is highly biodegradable and has high moisture saturation limit, 1100ppm at 20°C [31]. The dielectric strength of FR3 is comparable to MI7131 and Nytro 4000X. The only disadvantage of FR3 is its oxidation stability which is not as good as MI7131.

Comparison of properties of alternative insulating fluid

An overview of properties of alternative insulating fluid is presented in Table 2.1. Meanwhile, the comparison of physical, chemical, and electrical properties of commercially available alternative insulating fluid is presented in Table 2.2.

Table 2.1: Overview of properties of alternative insulating fluid (adapted from [12, 17]).

Name	Mineral Oil	Synthetic Ester	Natural Ester
Type	Refined distilled based crude oil	Synthetic	Refined vegetable oil
Principal components	Complex mixture of hydrocarbons	Pentaerythritol tetra ester	Plant based natural ester
Chemical structure	$CH_3 - (CH_2)_n - CH_3$ 		
Source	Purified from petroleum crude	Made from chemicals	Extracted from crops
Biodegradability	Slow to biodegrade	Readily biodegradable	Readily biodegradable
Oxidation stability	Good stability	Excellent stability	Generally oxidation susceptible
Water saturation at ambient (ppm)	55	2600	1100
Flash point, °C	160 - 170	> 250	> 300
Fire point, °C	170 - 180	> 300	> 350
Fire classification	O	K*	K*

*K-Class high fire point (>300°C) according to IEC 61100

Table 2.2: Physical, chemical and electrical properties of insulating fluid [12, 21, 26, 31].

	Parameter	Units	Nytro 4000X	FR3	MI7131
PHYSICAL	Autoignition temperature	°C	>270	n.a	438
	Biodegradability (28-days)				
	- OECD 301D	%	n.a	95 - 100	readily biodegradable
	- OECD 301F	%	n.a	> 99	> 89
	Density at 20°C	kg.m-3	0.895	0.92	0.97
	Expansion coefficient	/°C	n.a	0.00074	0.00075
	Fire hazard classification to IEC 61100		O	K2	K3
	Fire point	°C	170	360	322
	Flash point	°C	140	330	275
	Gassing tendency	µL/min	n.a	-79,2	29.2
	Kinematic viscosity at 0°C	mm ² .s-1	37.5	207	240
	Kinematic viscosity at 20°C	mm ² .s-1	22	78	70
	Kinematic viscosity at 40°C	mm ² .s-1	9.1	36	28
	Kinematic viscosity at 100°C	mm ² .s-1	3	8	5.25
	Pour point	°C	-40	-21	-60
	Specific heat at 20°C	J/kg K	n.a	1883	1880
Thermal conductivity at 20°C	W.m-1.K-1	n.a	0.167	0.144	
CHEMICAL	Appearance		Light yellow	Clear light green	Petrol yellow
	Biodegradability (21-day test)	%	< 10	97	89
	Moisture before treatment	ppm	10	20	50
	Neutralization Number	mg.KOH.g-1	0.01	0.022	< 0.03
	Oxidation stability after 164 hours				
	- Acid number	mg.KOH.g-1	<0.01	n.a	0.01
	- Sludge	% per mass	<0.01	n.a	< 0.01
ELECTRICAL	Breakdown strength IEC 60156 2,5mm (after treatment)	kV	<60	56*	> 75
	Dielectric constant (50Hz) at 25°C		2.2	3.18	3.2
	Dielectric dissipation factor at 90°C	%	<0.001	0.005	< 0,008
	Interfacial tension	mN.m	49	n.a	n.a
	Volume resistivity at 90°C	Ω.cm	7.2 x 10 ¹³	>30 x 10 ¹¹	30 x 10 ¹²

* with ASTM 1816

Viscosity

Viscosity is the key parameter in determining the cooling capability of insulating fluid from the perspective of transformer design. Viscosity of fluids refers to the flow resistance of the fluid. For transformer, in which insulating fluid also acts as coolant, high viscosity slows the flow of fluid in winding ducts and thus, hampers the cooling

process. This event might increase the operating temperature of a transformer. When the transformers' operating temperature is quite high, cellulose degradation becomes an issue. Therefore, to accommodate the ester fluids in transformers, a specific design might be employed to improve the cooling process.

Figure 2.3 shows the comparison graph of alternative fluid's viscosity with temperature as parameter. Ester fluids are naturally more viscous than mineral oil over a wide range of temperature; however, at higher temperature, the difference of viscosity is diminished. Viscosity of insulating fluid also affects the impregnation process of solid insulation in the transformer manufacturing process. Normally, it takes longer time to fully impregnate solid insulation in case where ester fluids were utilized [32].

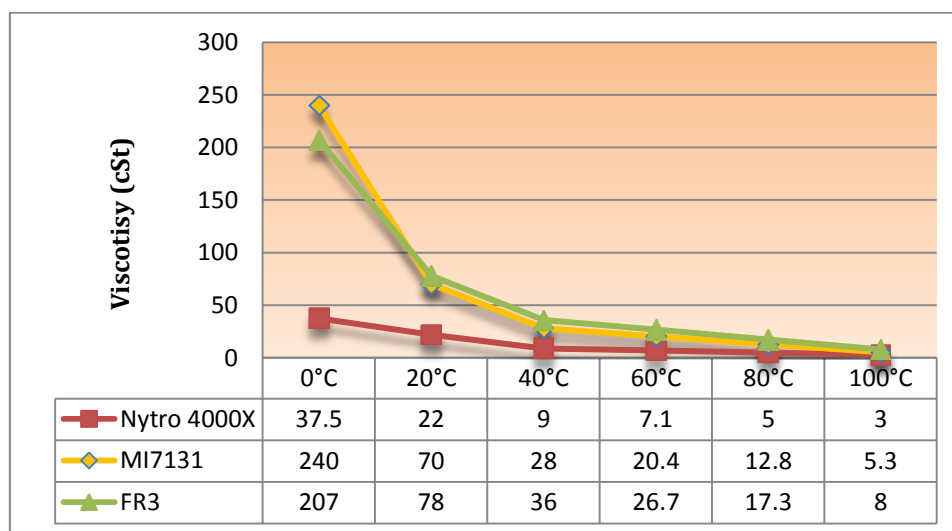


Figure 2.3: Comparison of viscosity of insulating fluid (adapted from [12]).

Moisture tolerance

Moisture tolerance is important in increasing the reliability of transformers and highly related to prolonging solid insulation longevity. Commonly, the term “moisture tolerance” is interchangeably used with the term “water solubility”. It explains the same thing which is the total amount of dissolved water (water or moisture content) in insulating fluid without free water being deposited.

Water is a polar molecule which is strongly attracted to other polar molecules. Literally, polar molecule means that the molecule has permanent dipoles, but in the context of discussion, the term “polar” refers to region of a substance which has different attractions, like pole in a magnet [12].

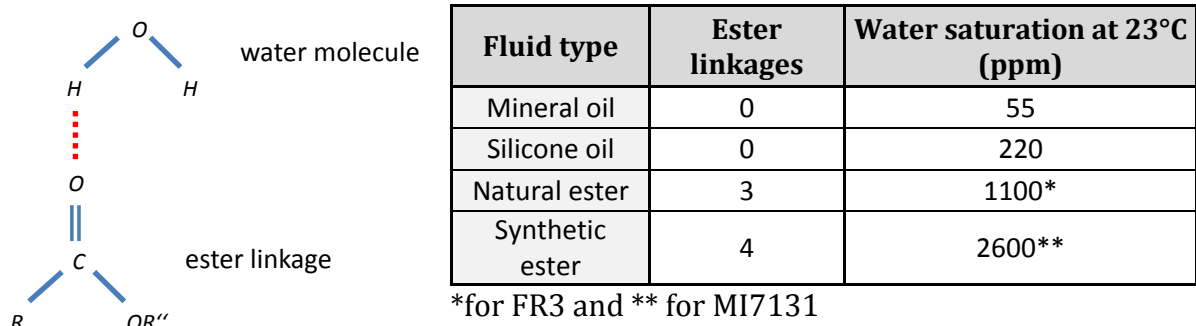


Figure 2.4: How ester linkage attracts water molecule and relation of ester linkages' number to moisture saturation (adapted from [12]).

Mineral oil is categorized as non-polar fluid. Meanwhile, ester linkages present in ester fluids make them categorized as “polar”. Different from mineral oil, the ester linkages in ester fluids attract water molecules and thus, the hygroscopic nature of ester fluids come from. Natural esters have three ester linkages per molecule, whilst synthetic esters have 2-4 linkages per molecule. The number of ester linkages is related to solubility of water in fluids as depicted in Figure 2.4. The more ester linkages in the molecule, the more water can be dissolved across temperature range as the solubility of water in fluids increases with temperature.

It should be noted that moisture in liquids is measured in parts per million (ppm) using the weight of moisture divided by weight of fluid ($\mu g/g$). It is also normally called as absolute moisture of fluid. Rather than absolute moisture, the relative moisture is more common when discussing about moisture (water) saturation of fluid. Relative moisture of fluids is the ratio of dissolved moisture (water) content in the fluid to the moisture saturation of fluid at the same temperature. Because the saturation level is a function of pressure and temperature, the relative moisture is a combined index of the environment and reflects more than only the moisture content [33]. The relative moisture W_{rel} for a given temperature is defined as ratio of absolute moisture W_{abs} (ppm) of fluid to the moisture (water) saturation limit $W_L(T)$ (ppm) as in equation (1.1).

$$W_{rel} = \frac{W_{abs}}{W_L(T)} \quad (2.1)$$

The saturation limit of moisture at a temperature T can be expressed as equation (1.2) [20, 33].

$$W_L(T) = K \cdot e^{\frac{-H}{T}} \quad (2.2)$$

Where the constant H and K depend on the fluid itself. The value of the H and K constant for mineral oil, MI7131 and FR3 is shown in Table 2.3. Figure 2.5 shows the moisture saturation limit of alternative insulating fluid.

Table 2.3: Value of H and K constant

Constant	Nytro4000X*	MI7131**	FR3***
H	1567	684	582
K	7.0895	5.3318	5.417

* according with [20]

** according to [34]

*** according to [35]

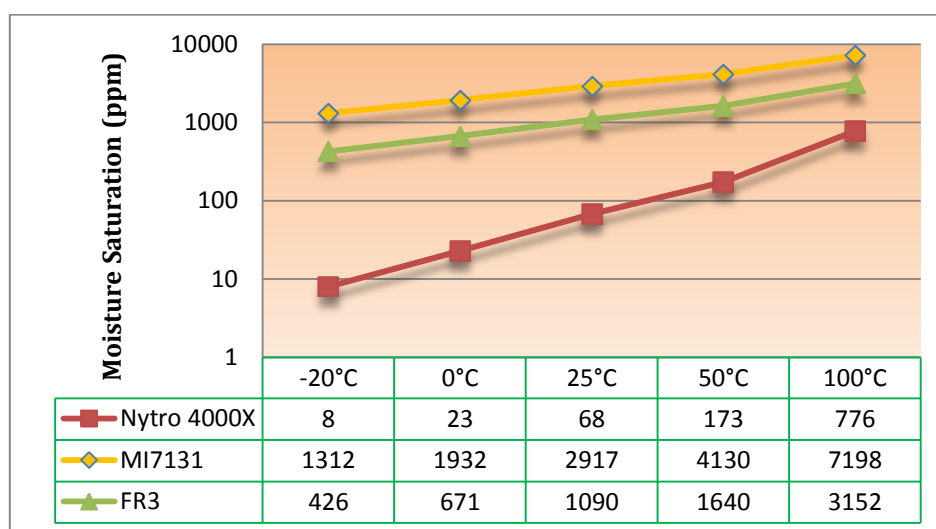


Figure 2.5: Moisture saturation limit of alternative insulating fluid. The moisture saturation was calculated in accordance with equation 1 and 2.

The reason why moisture tolerance is important can be summarized as follows [36, 37]:

1. Dielectric strength - reduces as moisture content increase

A small amount of moisture in mineral oil and silicone liquid causes a rapid deterioration in breakdown voltage. In contrast, ester fluids maintain a high breakdown voltage of >75kV even when moisture levels exceed 600ppm.

2. Rate of paper ageing - increases with higher moisture content

Studies have shown that the lifetime of the paper reduces by as much as a factor of ten for each extra 1% of moisture content in the cellulose. As the cellulose ages it releases water, thus accelerating the ageing process. Insulating fluid with high moisture tolerance at equilibrium will leach out water out of cellulose and hence reduce the ageing rate.

3. Bubble formation during overloads - bubbles formed at a lower temperature when there is a high moisture content in the paper

Bubbles in insulating fluids are undesirable since they are electrically weak. According to IEC 60076-14 [38], bubble evolution temperature is directly related to the moisture content of cellulose. For example, a paper with absolute moisture content of 2.6%, the temperature at which bubbles form will be 130°C. With absolute moisture content of 1.1%, the bubble evolution temperature is 165°C.

Therefore, insulating fluid with high moisture tolerance has the ability to keep paper drier and it gives a greater margin of safety during overloads.

4. Condensation during cool down - risk of release of free water from mineral oil
 With mineral oil there is a potential for moisture to be released (become free water) when a transformer cools down from operating temperature to ambient. This is due to the fact that mineral oil has a low moisture saturation limit which reduces as the temperature drops. For example if a transformer with mineral oil and a paper with moisture content of 1.5% was running at 90°C the moisture content of the mineral oil would be 65ppm. If the transformer then shut down the moisture would tend to stay in the mineral oil. At 20°C the saturation limit of mineral oil is 55ppm, so the mineral oil would be 118% saturated, releasing free water into the solids. However, this process takes long time. The breakdown voltage of the mineral oil would be affected and it increases the risk of failure when restarting. That event would have been protected in case of ester fluids. Using the same example for ester fluids at 90°C the moisture content would be 700ppm. The saturation limit for ester fluid at 20°C is 2700ppm, so even if all the moisture stays in the MI7131 it will only be 26% saturated. This means there is no free water and still an excellent breakdown voltage.

Fire safety

Fire safety has been a key issue of insulating fluid since the beginning of 20th century. In recent times, it becomes more important considering the utilization of transformers in highly populated areas, subway tunnels, ships, etc. When fire originating from insulating fluid in transformer, there are many consequences e.g. risk to human life, down-time cost or transformer replacement. Hence, the less-flammable and non-flammable insulating fluid is a necessity. The fire classification of transformer fluids is according to IEC 61100. Figure 2.6 compares the flash and fire point of alternative insulating fluid.

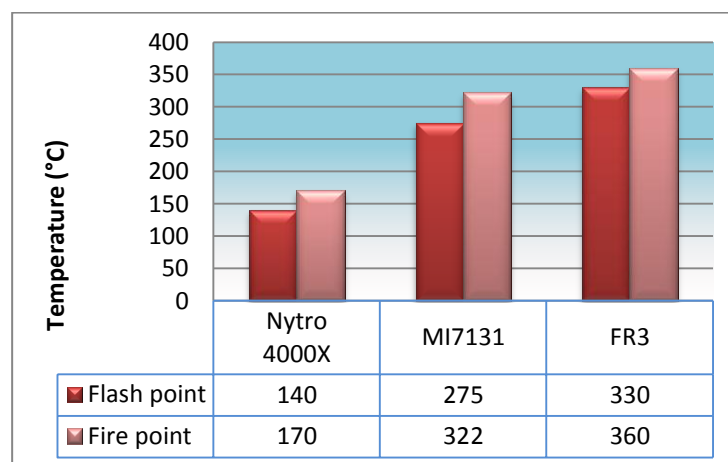


Figure 2.6: Comparison of flash and fire point of alternative fluid (compiled from [21, 26, 31])

Environmental protection

Environmental protection depends on two criteria, biodegradation rates and low-toxicity. Insulating fluids which possess a rapid biodegradation rate and demonstrates low-toxicity is classified as environmentally friendly fluid. The term “biodegradability” or “biodegradation rates” refers to the extent to which fluid is metabolized by microbes in soil or water in the event of a spillage or leak. To be classified as readily biodegradable, the fluid must satisfy these criteria [12]:

1. 60% biodegradation must occur within 10 days of exceeding 10% degradation
2. At least 60% degradation must occur by day 28 of the test.

Both natural and synthetic esters are classified as “readily biodegradable”, whilst mineral oil and silicone fluids are more resistant to biodegradation. Figure 2.7 depicts the comparison of biodegradation rates.

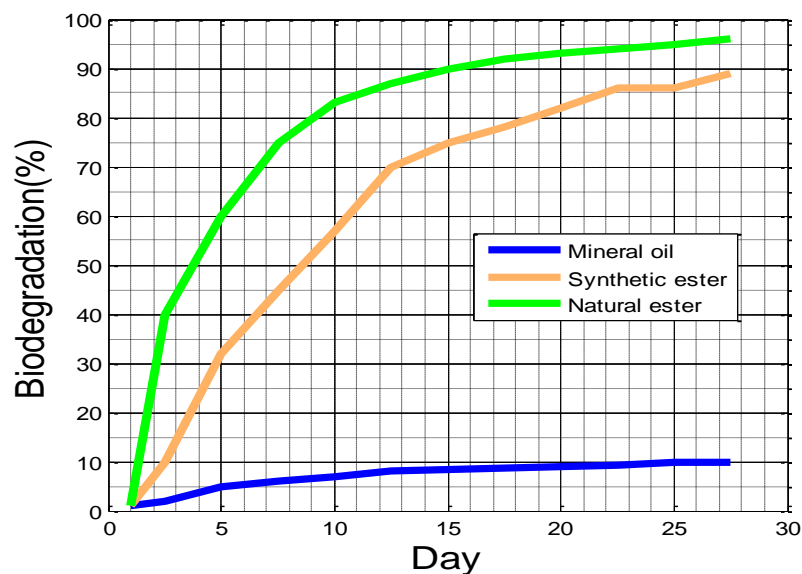


Figure 2.7: Comparison of biodegradation rates (adapted from [21])

2.2. Solid – fluid insulating system

2.2.1. Basic of solid insulation in transformer

Today’s transformers are almost entirely filled with insulating fluid, but the early transformers mainly used asbestos, cotton, hemp, silk, jute and low-grade pressboard in air. The introduction of shellac or synthetic-resin-coated paper at the late nineteenth century was a tremendous improvement. Later, it was soon discovered that air and shellac-impregnated paper could not match the thermal capabilities of the newly developed oil-filled transformers. The newly developed oil-filled transformers used kraft paper and pressboard insulation system which was supplemented from 1915 by insulating cylinders formed from phenol-formaldehyde resin impregnated kraft paper

or Bakelized paper [39]. It is usually referred as synthetic resin bonded paper. But, the introduction of oil impregnation of paper together with the invention of transformerboard in the late 1920s, led to the discontinuation of resin-impregnated paper [40].

Kraft paper is among the cheapest and best electrical insulation material known. By definition, Kraft paper is made entirely from unbleached softwood pulp. Kraft paper consists of cellulose, hemi-cellulose and some residual thio-lignin that has escaped complete removal during the Kraft pulping process. The cellulose consists of linear, polymeric chains of cyclic, β -D-glycopyranosyl units. The number of such units per chain is called the degree of polymerization (DP) [41].

Cellulose insulation has been the preferred choice for the solid insulation in power transformers not because it is the best but because it is widely available in plenty from natural renewable source—soft wood. The main disadvantage of cellulosic material for electrical use is that it is hygroscopic and thus, needs to be processed and maintained dry as depicted in Figure 2.8. The dry-out is worth the effort because dry cellulosic insulation has excellent dielectric properties.

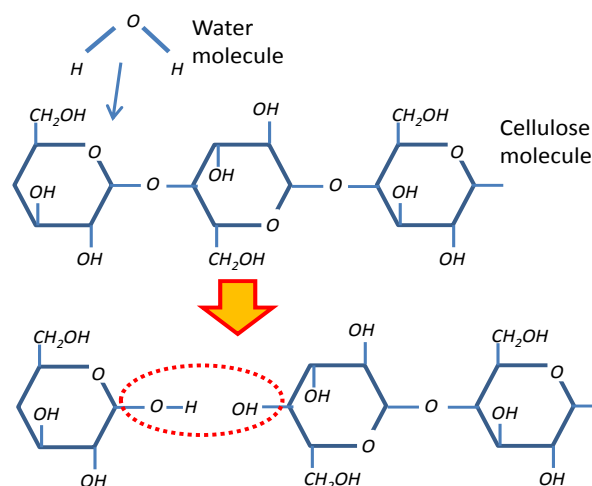


Figure 2.8: Molecular structure of cellulose and its reaction with water molecule (adapted from [41]).

There are four special types of paper whose properties have been developed to meet particular needs of transformer. These are [39]:

1. Creped paper
2. Highly extensible paper
3. Thermally upgraded paper
4. Diamond dotted press-paper

This chapter only addressed the thermally upgraded paper. Creped, highly extensible paper and diamond dotted press-paper are discussed in [39, 42]. The upgrade of Kraft paper was achieved in 1960 by adding weak, organic bases such as dicyandiamide, urea

or melamine so as to neutralize acids produced by oxidation of the oil and paper thermally upgraded paper is treated by the addition of stabilizers during manufacture to provide better temperature stability and reduced thermal degradation. Degradation of transformer is temperature dependent caused by the breakdown of the long-chain cellulose molecules. The permitted temperature rise for power transformers is based on reaching an average hot spot temperature in operation which will ensure an acceptable life for the insulation. This is usually between about 110-120°C. Within this range of temperatures insulation degradation is greatly affected by the presence of oxygen and moisture [43]. Those three factors, temperature, oxygen and moisture are present in most transformers, particularly in distribution transformers. For this situation, thermally upgraded is beneficial in degrading the ageing of paper insulation by reducing the rate of degradation at the operating temperatures normally reached. It is allowed the temperature of the winding rise to be increased by 10°C. Addition of dicyandiamide helped to make the solid insulation more resistant to heat, oxygen and oil oxidation by-product damage.

The aging of paper happens when the paper depolymerizes. The DP of Kraft pulps ranges from 1100 to 1200, but mixed pulp fibers can have much higher DP, e.g., 1400 to 1600 [42]. After processing the transformer in the factory the DP of the paper has deteriorated to about 1000. Transformer insulation with a DP of 200 is regarded as having reached the end of their reliable live, and in imminent danger of failure. Kraft is regarded a class A material, which only allows a maximum operating temperature of 105 °C. The latest development in the paper degradation analysis is furan analysis. When cellulose depolymerizes a chemical compound, a furan, is formed. By measuring the quantity and types of furans present in the transformer oil sample, the insulation's DP can be established.

Pressboard represents thick insulation paper made by piling up a number of layers of paper at the wet stage of manufacture. High density pressboard which was used for this work is standardized in IEC 60641. Pressboard is divided into two basic categories [39]:

- That built up purely from paper layers in the wet state without any bonding agent.
- That built up, usually to a greater thickness, by bonding individual boards using a suitable adhesive.

Paper and pressboard are excellent insulation materials when used in fluid filled transformer. But when it is required to eliminate fire hazard that might occur in oil-filled transformer, transformers manufactures will utilize air as main dielectric. In this case, it is not possible to utilize paper and pressboard. Without oil as coolant, the transformer must run hotter in order to be economic and paper and pressboard cannot withstand the high temperature. For this purpose, an organic polymer, aromatic polyamide produced by DuPont of Switzerland and known by their trade name of Nomex is widely used [39].

Chemically, Nomex is an aromatic polyamide and generally known as aramid. The molecular structure of Nomex is stable and does not oxidize easily. Thus, has high resistance to pyrolysis and the subsequently high temperature required for decomposition. Nomex for transformers is available as both synthetic paper and pressboard. Nomex exhibits outstanding thermal, mechanical and electrical properties but it comes at a cost and could be up to 30x the price of kraft paper [41].

Several applications have been identified where the high cost justifies the benefits achieved by using Nomex in transformers. Two ways of the designing transformers generally exist when operating with high temperature insulation, the total replacement of cellulose with high temperature insulation or a selective replacement to overcome temperature limitation due to cellulose. The selective replacement of cellulose is referred to as the hybrid insulation concept. Because of high temperature stability of Nomex, the transformer cooling ducts may be reduced in size without affecting the overall performance of insulation. The reduction in cooling duct size will increase the hottest spot temperature in the winding. Nomex has a considerably higher thermal rating (220 vs. 105°C for cellulosic paper), without significant loss of life. Reducing the cooling duct effectively reduces the overall radial build and thus the mean turn length of the conductor, effectively reducing the amount of copper used and thus reducing the load loss of the transformer. Although Nomex also absorbs moisture, the dielectric strength of Nomex is not compromised as in the case with cellulose-based insulation. Figure 2.9 depicts the chemical structure of NOMEX paper.

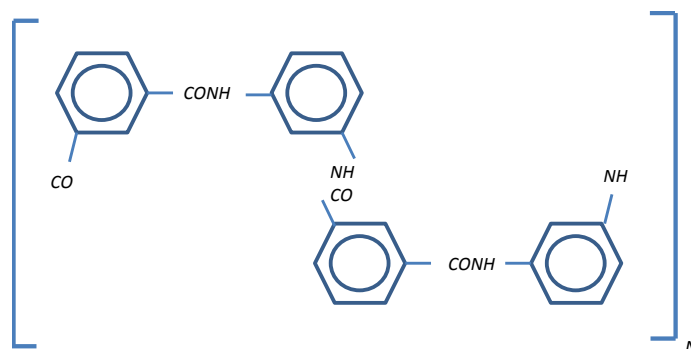


Figure 2.9: Molecular structure of Nomex (adapted from [41]).

Increasingly, synthetic ester has been successfully used in combination with aramid insulation for special applications such as in traction transformers and wind farm generators since both applications required the insulation system to operate in high temperature [12]. With the combination of ester fluids – aramid, the high power transformer can be built smaller and still maintain the environmentally friendly and fire safety characteristics.

Currently, a hybrid transformer design is being implemented in which the transformer manufactures combine the cellulose and aramid in a transformer. A hybrid transformer combines a traditional cellulose-based kraft papers at low temperature part of transformer and aramid paper in the hottest area of transformer. This strategy allows

almost equal advantages with a wholly aramid system. Naturally, ester fluids which possess high flash point are commonly used in this hybrid system [12].

2.2.2. Intrinsic viscosity

Intrinsic viscosity is one of the most important characteristic of polymer. In this work, it will be related to the polarization mechanism and the temperature dependent behavior of solid samples. Therefore, a basic knowledge regarding internal viscosity is presented in this section.

The intrinsic viscosity of a dilute solution of a polymer is related to the molar mass of the polymer given by Staudinger and Heuer [44]. The relation is described by the empirical Mark - Houwink equation:

$$\eta = KM^a \quad (2.3)$$

Where

η	Intrinsic viscosity of a sample dissolved in a specified solvent
K	Empirical parameters
M	Molar mass
a	measure of the extension of the molecule

The relationship between the intrinsic viscosity (η) and the degree of polymerization ($DP_v^{0.9}$) of cellulose samples is expressed as in equation (2.4) [45]:

$$DP_v^{0.9} = 1.65\eta \quad (2.4)$$

2.2.3. Research on dielectric properties of solid-fluid insulating system

Thus far, there have been many investigations on dielectric properties of solid-fluid insulating system both in time and frequency domain. This section highlights some of those investigations which correlate to dielectric response measurement over wide range of frequency and in time domain.

Dielectric response measurements over wide range of frequency are mainly on solid impregnated in mineral oil and silicone fluid. In the early of 1970s, Bartnikas investigated the dielectric-loss behavior of kraft-paper cable models impregnated with standard insulating oils and silicone fluids. At that time, the measurement range was only possible from 50Hz – 100kHz due to equipment limitation [46, 47]. In 1974, he continued his investigation on the electrical conduction mechanism for oil-paper insulating system on wider frequency range than before, from 0.01Hz-100kHz [48, 49].

Up to now, there are many investigations on various parameters affecting the dielectric and physical properties of solid-fluid insulating system such as aging, moisture, and acid. The influence those parameters can be found in these literatures: aging and

moisture in [50, 51, 52, 53, 54, 55, 56] and acidity in [55, 56, 57]. The investigation on low temperature behavior of dielectric response can be found in [58].

Most of the investigation on dielectric response over wide range of frequency was done on solid impregnated with mineral oil. Just until recently, there is available the investigation on dielectric response over wide range frequency of pressboard impregnated with ester fluids: for synthetic ester in [50] and natural ester in [59]. Thus, this thesis provides a rich investigation on dielectric response of solid impregnated with ester fluids including various types of pressboard and transformer papers.

2.3. Retrofilling

2.3.1. Introduction

The term “retrofilling” refers to the process of removing the insulating fluid of an existing working transformer and replacing it with new insulating fluid. The term was first used as early as mid-1970s when the environmental effect of PCB’s became known. Hence, there was a great pressure brought on the power utility industry and transformer owners to decide whether to “replace” their Askarel transformer with non-PCB units or to “reclassify” them to non-PCB status using retrofilling process. Reclassification of a transformer to non-PCB status involves the permanent reduction of the PCB concentration from > 50 ppm to < 50 ppm for the rest of its working life. When cost was considered, retrofilling of transformers were an attractive option. Thus, transformer owners began to retrofill their PCBs filled transformer with alternative insulating fluid e.g. mineral oil, synthetic esters, silicone fluids or Perc. Replacement of the PCBs with alternative insulating fluid would leach out the PCBs from the porous of solid insulation, a process that would take several years to complete.

The key issue of why transformers owner retrofilled their transformers have been shifting from just environmental protection in the PCBs era to various issues e.g. fire safety, prolonging solid insulation longevity, etc. Currently, the transformer being retrofilled are mineral oil distribution transformer with ester fluids. Some of important moments of retrofilling practice with ester fluids are depicted in Figure 2.2.

2.3.2. Reasons for retrofilling

There are many reasons why transformer owners consider retrofilling. Key issues on the purpose of retrofilling transformers have been shifting since 1970s. In 1970s, the key issue was environmental protection when it was realized that PCB’s were harmful to the environment. The same issue was applied for retrofilling Perc filled transformer (after previously retrofilled from PCBs to Perc) [33].

Currently, the fluid being replaced is mineral oil for more complex reasons. Although mineral oil is a commonly used transformer fluid, there are many reasons why transformer owners consider retrofilling it with another insulating fluid [12, 60, 61]:

- **Fire safety**
Replacing mineral oil will enhance fire safety especially in populated or sensitive areas.
- **Environmental protection**
Ester fluids are classified as readily biodegradable and considered to be environmentally friendly. Replacing mineral oil will greatly reduce environmental impact in case of spillage.
- **Moisture tolerance**
Ester fluids are much tolerant of moisture ingress than mineral oil without decreasing its electrical properties. Hence in areas prone to wet conditions, replacing mineral oil will lead to increased reliability.
- **Corrosive sulphur**
Alternative ester fluids do not suffer from corrosive sulphur as in mineral oil. Replacing mineral oil in transformer where corrosive sulphur compounds have been detected in mineral oil but has not shown signs of copper corrosion would likely to prevent further damage. But it cannot reverse the effect of corrosion that already occurred.
- **Prolonging solid insulation longevity**
There are many literatures that explain cellulose insulation last longer in ester fluids than in mineral oil. It is related to the ester's ability to retain moisture. Replacing mineral oil by ester fluids will shift the moisture equilibrium between paper and fluids. Esters will leach out the moisture from paper. Therefore this process will delay the ageing process of paper caused by hydrolysis.
- **The overload ability of ester liquid filled transformers**
Ester fluids are superior due to the higher operation temperature range of the liquid and the reduced aging of the solid insulation. Hydrolysis loses importance when using an ester liquid as the thermal capability of the transformer is primarily assigned by the solid insulation.

2.3.3. What happened to transformer insulation after retrofilling

A successful retrofilling process depends on removing as much of the original filled fluid as possible. However, the removal process could not leach out all of the original fluid, a small amount of it will remain in the unit because it has saturated in the porous of paper and pressboard. It is known by experience that during the replacement of insulating fluid, up to about 10% of the original fluid remains in the pores of the pressboard, the windings, the core and the walls of transformer [33, 61]. After certain time, the original fluid may diffuse slowly during operation and mix together with the new insulating fluid. It would certainly affect dielectric and electric properties of both insulating fluid and fluids impregnated solid will be affected.

Investigations are needed before retrofilling to assess the effect of such process in connection to existing standard or regulation and compatibility with material in transformers to achieve longevity. However, investigations that have been done mainly focused on the mixed fluids (the remaining of original fluid mix with the new fluid) and rarely on solids impregnated material. In this work, the investigation was performed on the dielectric properties of solids impregnated with ester fluids after retrofilling process.

2.3.4. Research on retrofiling

Mixed fluids as a result of retrofiling

Most of the investigations on retrofilling concerned with the mixed insulating fluids after fluid replacement. Fofana et al. investigated new mixed fluids properties for replacement of Perc with mineral oil and synthetic ester [33]. Patrick McShane et al. investigated fire and flash points and viscosity of mix fluid between mineral oil and natural ester, as depicted in Figure 2.10 [62]. However, there are only a few literatures concerns with the influence of retrofilling on the solid itself. Steve Moore et al. investigated solid insulation dry out as a result of retrofilling [63]. They concluded that insulation dry out is due to moisture migration and hydrolysis after retrofilling transformer with natural ester fluid. The same phenomenon would occur for transformer retrofilled with synthetic ester.

In this thesis, the investigation on the dielectric response of pressboard after retrofilling procedure was performed..

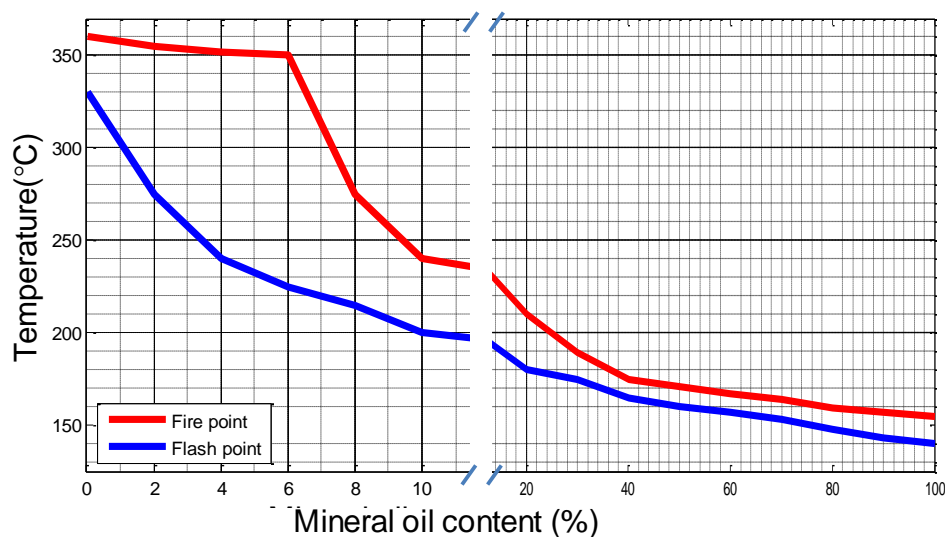


Figure 2.10: Envirotemp FR3 fluid flash and fire point variation with mineral oil content (adapted from [62]).

Miscibility

When considering retrofilling, it is important to check the miscibility between the old and the new insulating fluid. Miscibility is the property of fluids to mix in all proportions, forming a homogenous solution. Retrofilling is recommended when both fluids are miscible to make the flushing procedure to remove the old insulating fluid more effective and prevents unusual electrical stress at the fluid interfaces [12].

According to [64], there are two type of analysis to study miscibility of mixtures which are (a) a qualitative analysis to check the homogeneity of mixtures (i.e. the non-existence of emulsion in mixture) and (b) analysis of the compatibility to check the evolution of the characteristics of the mixtures. Table 2.4 list the miscibility between insulating fluids

Table 2.4: Miscibility of ester fluids with mineral oil at ambient temperature (adapted from [12]).

	Mineral oil	Synthetic ester	Natural ester
Mineral oil	X	Miscible in all proportions	Miscible in all proportions
Synthetic ester	Miscible in all proportions	X	
Natural ester	Miscible in all proportions	Miscible in all proportions	X

3. Theory of dielectric materials

In this chapter the basic theory of dielectric, dielectric response in time and frequency domain, and also theory of composite dielectric are given. This chapter also explains the practical consideration for dielectric response measurement of solid-fluid insulating system.

3.1. Introduction

Polarization in dielectric materials can be generated by many mechanisms. Before going into those mechanisms, it is important to understand the difference between electric polarization and electric conductivity [65]. Polarization originates from a finite displacement of charges in a steady electric field. Meanwhile, conduction originates from finite average velocity of motion of charges in a steady electric field.

3.1.1. Polarization Mechanism in Dielectrics

For an insulation material, there is no free charge without the application of external electric field. On atomic level, positive and negative charges are all coupled together on microscopic and macroscopic scales. The charges are balancing each other. The molecules in a dielectric material are usually distributed in such way so that the insulation material in overall is neutral.

When electric field is applied on insulating material, the positive and negative charges become oriented. They form different kinds of dipoles even on atomic level which known as polarization. A local charge imbalance is induced within neutral species (atoms or molecules). The positive and negative charges $\mp q$, become separated by a small distance d , creating a dipole with a dipole moment p :

$$p = q \cdot d \quad (3.1)$$

This formula is known as the microscopic relation of dipole moment.

Since dipole moment is related to the microscopic electric field stress E , acted on the neutral species, the dipole moment can also be written as:

$$p = \alpha \cdot E \quad (3.2)$$

Where α is polarizability of the tested samples. This formula is known as the macroscopic relation of dipole moment.

The distance d , the number of dipoles per unit and the polarizability are different for each species. Due to chemical interactions between atoms forming molecules, many of them have a constant distance d , between the charges centers thus forming permanent

dipoles. The permanent dipoles are oriented and distributed randomly when there is no electric field applied. The molecules which possess permanent dipoles are called polar molecule. The macroscopic effect of the polarizability of individual species is given in a general relation between the macroscopic polarization P , and the number of polarized species per unit volume of the material.

Each type of polarization mechanism requires time to perform. Thus, the degree of the overall polarization depends on the time variation of the electric field. There are several types of polarization mechanism: electron, atomic-ionic displacement, dipolar orientation, trapping and hopping charge carrier and ionic-interfacial polarization [66, 67, 68]:

- *Electronic polarization*

When an atom or molecule is placed in electric field, the positive nucleus and the negative electron cloud will be shifted relative to each other. This type of polarization does not contribute to conduction or dielectric loss in electrical insulating materials at power frequency. The atom requires a dipole moment which is proportional to the electric field. Electron polarization persists over entire frequency range from DC up to optical frequency.

- *Atomic-ionic polarization*

Refers to material which containing molecules forming ions. Under the influence of electric field, ions are polarized. Atomic-ionic displacement polarization persists over frequency range from DC up to infrared frequency.

- *Dipolar (dipole orientation) polarization*

Refers to material which containing molecules with permanent dipole moments with orientation distributed due to thermal energy. Under the influence of electric field, the dipoles are oriented only partially. Dipolar (dipole orientation) polarization persists over frequency range from DC up to microwave frequencies depending on the presence of dipolar molecule and resistance to molecular rotation presented by material's internal structure

- *Ionic-interfacial polarization*

Ionic-interfacial polarization is predominantly presence in insulating materials composed of different dielectric materials, such as paper/pressboard impregnated with insulating fluids. When under electric field, the mismatch product of permittivity multiply by resistivity for different insulating materials causes the movable positive and negative charge carriers to become deposited in the bulk of the material or at the interfaces between different materials. It is also formed some kind of dipoles. Ionic-interfacial polarization is involving a long range ion movement, usually observed at lower frequencies and as well as temperature dependent.

- *Trapping and hopping of charge carriers*

Trapping and hopping of charge carriers might also create polarization. In insulating materials, localized charges (ions and vacancies, or electrons and holes) can hop from one site to the neighboring site, creating so-called hopping polarization. This is a slow, but strongly temperature dependent mechanism. It is mostly found in solids.

It should be noted that if a dielectric composite involves hopping polarization, then the space charge polarization is the combination of both hopping and interfacial polarization. These two types of polarization involve the movement of charged particles; hence, it is not easy to separate these two different mechanisms [66]. When compared to dipolar polarization, typically, space charge polarization which relates to ion movement is greater than a molecular rotation and hence, it generates higher relative permittivity.

Frequency and temperature effect on the interfacial and dipolar polarization

Both interfacial and dipolar polarization depend on the effective internal viscosity material which act as resistance of the material toward movement of ions or rotation of dipole molecules. The long range movement of ions up to barriers usually takes longer time duration to develop polarization than the simple rotation of dipoles. Therefore, ionic-interfacial polarization is observed at lower frequency than dipolar polarization. Dipolar polarization usually presents up to higher frequency than interfacial space charge polarization in the same viscosity material, although the two polarization mechanisms may overlap. It should be noted that temperature dependent behavior of both interfacial and dipolar polarization is related to the frequency of the applied electric field. Internal viscosity of material decreases with increase of temperature and this, in turn, decreases the internal resistance toward movement of ions or rotation of dipole molecules (the mobility of various types of molecules is enhanced). Subsequently, the relaxation times of both polarization mechanisms take shorter time at high temperature. It means that the frequency in which maximum loss presence by the two mechanisms shifts to higher frequency [68]. In dielectric literature, time constant of material is referred to as the relaxation time and the frequency dependent polarization as dielectric relaxation phenomena.

In polymer where the dipolar groups are rigidly attached to a polymer chains, the dipoles are generally unable to rotate until the temperature is increased toward the softening point in which the chain can twist. The group dipole moments of the groups attached to polymer chains can usually be expected to be the same as in small individual molecules. However, they only contribute insignificantly to the relative permittivity, except when the polymer chain or side group can rotate easily. And this normally occurs at elevated temperature. Thus, polymer with dipoles often shows significant increase in relative permittivity with increasing temperature in the range where dipolar molecules become mobile. A good correlation between dielectric

frequency – temperature characteristics and mechanical flexibility has been shown for polar polymer and it is also apply to cellulose polymer which is polar.

In summary, dielectric polarization is the results of a relative shift of positive and negative charges in a material. During all these process, the electric field is not able not force the charges to escape from the material which would cause electric conduction. All polarization processes represent the movement of bound charges in insulation material.

Generally, insulation materials are isotropic and homogenous at least on macroscopic level. Thus, the vector of polarization P and electric field E are of equal direction as in [69]:

$$P = \chi \cdot \varepsilon_0 \cdot E \quad (3.3)$$

Susceptibility χ , accounts for all kinds of polarization mechanism within insulation. ε_0 is the permittivity of vacuum, a number with units relating the unit of electric field E , (V/m) to the electric displacement (Am/m^2). Thus, all polarization mechanism induce electric charges on the electrode when voltage is applied. Equation (3.3) also means that polarization P , will vanish if the electric field E , is set to zero. A reduction of electric field will lead to a depolarization (or relaxation process) which follow with some delay.

3.1.2. Electrical conduction mechanism of solid-fluid insulating system

Basic of conduction mechanism

Electrical conductivity can be classified into three categories (66): (a) intrinsic conductivity, (b) extrinsic conductivity and (c) injection-controlled conductivity. Intrinsic conductivity means that the conduction is caused by charge carriers which are generated in the material by its chemical structure. Extrinsic conductivity means that the conduction is caused by the presence of defects in the material. Meanwhile, injection-controlled conductivity means that conduction is caused by charge carrier injection through electrode or other process which normally occurs at high electric field stress.

As far as insulators are concerned, the origin of the charge carriers for intrinsic or extrinsic conductivity is not clear [66]. In insulating materials, the conduction is occurred when there are defects and impurities. These defects and impurities form potential wells (traps or localized states) which promote charge carriers (electrons, holes and ions) to hop. Thus, hopping charge carriers also leads to conduction besides polarization. The electrical conduction may be real dc conduction. DC conduction can be divided into two categories [70]: (a) band conduction [71] and (b) dc hopping conduction [72]. The band conduction is present in the absence of defects and

impurities. It is caused by the band structure of material. Meanwhile, dc hopping conduction occurs via defects and impurities as in insulating materials.

The localized states are disordered in insulating materials when their spatial and energy distribution are taken in account. Disturbance in energy of the localized states activate tunneling between the sites. The disturbance can be in form of temperature, pressure or applied electric field stress [66]. Under ac applied voltage, the frequency of the field affects the hopping rate as well. Furthermore, at a particular frequency, the charge carries can hop between two localized sites back and forth which is observed as if dipoles is present [70]. Hence, at low frequency or high temperatures, it is difficult to differentiate conduction and polarization mechanism in insulating materials.

Electrical conduction may be results of both electronic and ionic conduction. Further readings on this topic may be found in [66]. The basic equation for total conductivity can be written as.

$$\sigma_T = q(\mu_n n + \mu_p p) + q(\mu_- n_- + \mu_+ n_+) = \sigma + \sigma_{ion} \quad (3.4)$$

Where

n, p	Concentrations of electron and holes
μ_n, μ_p	Average mobility of of electron and holes
n_-, n_+	Concentrations of negative and positive ions
μ_-, μ_+	Average mobility of of negative and positive ions
σ	Electronic conductivity
σ_{ion}	Ionic conductivity

For solid-fluid insulating system, the more dominant process is ionic conduction and thus, the source of dc conduction is hopping of ions via defects and impurities. The increase of ionic conductivity of insulating materials with increase of temperature is a result of two superimposed effects: (a) decrease of internal viscosity (inverse of fluidity) and (b) increase in dissociation to ions with increasing of temperature. The ionic conduction through the mobility factor is governed by an activation mechanism and thus, the variation with temperature is given as

$$\mu \sim e^{\left(\frac{-\Delta F}{kT}\right)} \quad (3.5)$$

Where ΔF is the activation energy for ion motion or hopping. This possibly means that the activation energy for DC conductivity relates to energy for ion motion or hopping. Whenever there are internal boundaries or potential barriers, such as at the insulator and electrode interface which generate charge build-ups, ionic conduction is interrupted [68]. Such boundaries or barriers also led to polarization which affects the relative permittivity. This means that charge build-ups in insulating materials affect both DC conductivity and polarization.

For cellulose, not shown in the molecular structure of cellulose is the carboxyl group whose presence causes the cellulose to behave as a weak acid with an ionization constant of 2×10^{-14} . Hence, if the ionic conduction as a rate process, the carboxyl group may account for the existence of ionic losses within the cellulose [46].

Conduction mechanism in insulating materials

This specific section mostly refers to [48, 49]. In the solid-fluid insulating systems, there are several simultaneous presences of ionic loss mechanisms: long range ionic migration, interfacial space charge polarization, short range ionic jump trapping-detrapping processes within the solid paper structure and dipole orientation mechanism. The interfacial space charge polarization might occur in the fluid phase itself, in the cellulose fiber structure of the pressboard or paper and interfacial space-charge at the solid-fluid interfaces having varied geometry (one of the most dominant is on the surface of pressboard).

Dc conduction results from long range ionic migration whereby each ion must surmount a large number of different potential barriers along its path in the direction of the external field towards the electrodes. As the charge carriers drift from one defect to another in the insulation structure, a net charge drift or current is created in the direction of the external field. If the charge movement is controlled by a thermally activated process, only single charge carrier having an electronic charge e are involved and low electric field E is applied such that

$$\frac{eE\lambda}{2} \ll kT \quad (3.6)$$

Where

- λ Charge-carrier jump distance between two equilibrium positions
- k Boltzmann constant
- T Temperature

The dc resistivity ρ of the dielectric becomes [48]:

$$\rho = \frac{E}{J} = \left[\frac{2kT}{e^2 \lambda^2 n v} \right] e^{E_{DC}/k.T} \quad (3.7)$$

Where

- J Current density
- n Charge-carrier concentration
- v Vibration frequency of charge carriers in their respective energy well
- E_{DC} Activation energy of DC conduction

Activation energy of DC conduction E_{DC} is equal in value to the dc potential energy barrier separating the two equilibrium positions and generally expressed in electronvolts. The value of E_{DC} is also an indicator as to whether the charge is

transported by electrons, ions or charge macroscopic particles. In practice, normally DC resistance R_{dc} is expressed as

$$R_{dc} = \left[\frac{2kT\rho h}{e^2\lambda^2nvA} \right] e^{E_{DC}/kT} \quad (3.8)$$

Taking logarithms of equation gives

$$\ln R_{dc} = \ln \left[\frac{2kT\rho h}{e^2\lambda^2nvA} \right] + \frac{E_{DC}}{kT} \quad (3.9)$$

The phenomenon will be different if high electric field stress is applied. Under elevated electric field such that

$$\frac{eE\lambda}{2} \gg kT \quad (3.10)$$

Then the DC resistance R_{dc} is expressed as [48]:

$$\ln R_{dc} = \ln \left[\frac{2k\rho h}{e\lambda nvA} \right] + \frac{E_{DC}}{kT} + \frac{eE\lambda}{2kT} \quad (3.11)$$

Thus, R_{dc} yields an apparently field dependent value E_{DC} due to the last term of equation. At elevated electric field, there are many other conduction mechanisms which are not related to the intrinsic characteristic material such as electrode injection charge carriers. Topic on the conduction mechanism on elevated electric field can be found in [73]. Consequently, experimental work concerned with determination of conduction mechanism should be carried out at low electric field stress and the linearity property of samples is maintained.

At low frequency, it is expected that long range ionic migration across the entire dielectric material is a dominant conduction mechanism. In the presence of space-charge effects, there are charge build-ups which creates reaction field. The reaction field tends to modify the heights of potential barriers that the individual carries must exceed in their migration through dielectric bulk [48]. This phenomenon will affects E_{DC} and E_p .

If under the influence of externally high frequency electric field, a charge carrier jump back and forth between two closely separated equilibrium positions in the Potential Double Well model, the relaxation time τ of this process is related inversely to the jump probability P_j by [48, 67, 74] as in:

$$\tau = \frac{1}{2P_j} \quad (3.12)$$

And dielectric loss maximum occurs at the absorption frequency $f_m = 1/2\pi\tau$. Absorption frequency means that at that specific frequency, the molecules are having a hard time to orient themselves with change of electric field angles. Therefore, the

phase different between the molecule and electric field is large and thus, causing high displacement current. High displacement current relates to high polarization loss.

When considering long-range ionic migration across the entire dielectric thickness under dc or slow varying ac field conduction, it is necessary to introduce a different relaxation time concept. If charge carrier drift freely over potential barriers between electrodes encountering no space-charge fields at the electrodes, then the relaxation time τ' for this long-range migration is equal to charge carriers transit time across dielectric thickness as in [48, 75]:

$$\tau' = \frac{d}{2v} = \frac{d}{2\mu E} \quad (3.13)$$

Where

- v Mean velocity of charge carrier drift
- μ Charge-carrier mobility

However, in practice, the situation is more complex as mobile charge-carrier build-up at the electrodes causes the current through dielectric to become space-charge limited. Thus the relaxation time τ' for long-range charge carrier migration is modified to [76]:

$$\tau' = \frac{d}{2\mu} \left(\frac{\epsilon_{\infty}}{2\pi n k T} \right)^{1/2} \quad (3.14)$$

Note that τ' describes a long-range migration effect and consequently, $\tau' \gg \tau$ and the absorption frequency $f_{m'} = 1/2\pi\tau'$, at which the dielectric loss maximum occurs due to the space-charge effects, is very low (usually < 1 Hz). An increase in temperature and charge carriers mobility, cause the absorption peak (absorption frequency) shifting to higher frequencies (see section 3.1.1 for physical explanation on this phenomenon). The shift can also be observed from slope of polarization loss. Here activation energy E_p' was used to describe the space-charge-limited conduction process in accordance with [48]

$$\ln \tau' = \ln \tau_o' + \frac{E_p'}{kT} \quad (3.15)$$

Where τ_o' is the relaxation time of the interfacial space-charge polarization at different temperature. The determination of E_p' depends on the position of the space charge loss maxima in the frequency domain. Note that equation (3.13) is the basis of temperature dependent behavior of polarization in frequency domain which appears as shift in frequency domain if measured at two temperatures (see Section 3.4).

3.2. Dielectric response

3.2.1. Dielectric response in time domain

Under vacuum-insulated inter-electrode arrangement, the vector of dielectric flux density (or electric displacement) D , is proportional to electric field vector E , as in

$$D = \varepsilon_0 E \quad (3.16)$$

If the electric field is generated by time varying voltage, equation (3.16) become

$$D_{(t)} = \varepsilon_0 E_{(t)} \quad (3.17)$$

The dielectric flux density D and electric field E is generated by a voltage source connected to electrode. Dielectric flux density represents the positive and negative charges per unit area induced on the electrode's surface. Those charges are the source of all electric field lines. For time varying field $E_{(t)}$, the displacement current must be supplied by voltage source to maintain the area charge density on the electrode's surface.

If any kind isotropic insulation material instead of vacuum between the electrodes, polarization P , will occur. Polarization on the insulation material will increase the charge induced on the electrode's surface. The dielectric flux density in equation (3.17) increases by the polarization, P as in equation:

$$D_{(t)} = \varepsilon_0 E_{(t)} + P_{(t)} = \varepsilon_0 (1 + \chi) E_{(t)} \quad (3.18)$$

The time dependency of $P_{(t)}$ is no longer the same as the time dependency of $E_{(t)}$ because each polarization process have different time delay with respect to the appearance of E . The delay is caused by the time-dependent behavior of susceptibility $\chi = \chi(t)$. The insulation material then can be characterized by its time dependent susceptibility $\chi(t)$ and polarization $P_{(t)}$ as a response in the time domain which is the occurrence of different kinds of polarization process which developed within extremely short time (electronic polarization) or even longer time (dipolar and interfacial polarization).

The development of polarization process under a step-like electric field can be expressed by:

$$\frac{P_{(t)}}{E_0} = \chi_{(t)} \varepsilon_0 1_{(t)} \quad (3.19)$$

Where $\chi_{(t)}$ and $P_{(t)}$ represent "step response function" and $1_{(t)}$ is an indicator the unit step for electric field E_0 . The first part of this function represents the very fast polarization process, an "instantaneous polarization," $P(t = t_0) = P_\infty$, which includes

electronic and ionic polarization. This step cannot be recorded in time or the equivalent frequency domain. After all polarization processes settle in long time, the polarization becomes “static”, $P(t \rightarrow \infty) = P_s$. Thus, the step response of this simplified polarization is as follows:

$$P(t) = P_\infty + (P_s - P_\infty) \cdot g(t-t_0) \quad (3.20)$$

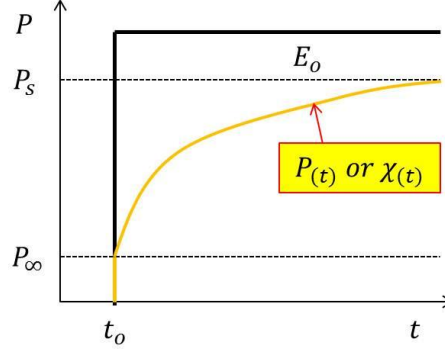


Figure 3.1: Polarization of a dielectric exposed to a step field of magnitude E_0 at $t = t_0$ (adapted from [69]).

Where $g(t)$ is monotonously increasing function and it is dimensionless. Thus, the equation (3.20) can be written as

$$P(t) = \varepsilon_0 [\chi_\infty + (\chi_s - \chi_\infty) \cdot g(t-t_0)] E_0 \quad (3.21)$$

It is now possible to estimate time dependent polarization $P(t)$ or any other time dependent electric field $E(t)$ of insulation material by utilizing Duhamel's integral which provide special solution for step excitation function [69]. Thus, equation (3.21) can be written as

$$P(t) = \varepsilon_0 \cdot \chi_\infty \cdot E(t) + \varepsilon_0 \int_{-\infty}^t f(t-\tau) E(\tau) d\tau \quad (3.22)$$

Where $f(t)$ is the dielectric response function of insulation material. It characterized the insulation material in time and frequency domain. The dielectric response function was first discovered by Curie and von Schweidler in 1907 as in $f(t) = t^{-n}$ to represent the decay of polarization in a wide range of materials [77].

$$f(t) = (\chi_s - \chi_\infty) \frac{\partial g(t)}{\partial t} = (\varepsilon_s - \varepsilon_\infty) \frac{\partial g(t)}{\partial t} \quad (3.23)$$

Polarization $P(t)$ generates polarization current in a dielectric material if electric field $E(t)$ is suddenly applied. Up to this point, the DC conductivity σ_0 has not been considered. The DC conductivity σ_0 represents the movement of the free charges in insulation material. The free charges are not involved and independent of polarization process as described in previous section.

Maxwell has postulated [78], that the total current density $j(t)$ which is generated by electric field $E(t)$ is a sum of conduction, vacuum and polarization displacement currents as in:

$$j(t) = \sigma_0 E(t) + \frac{\partial D(t)}{\partial t} = \sigma_0 E(t) + \varepsilon_0 \frac{\partial E(t)}{\partial t} + \frac{\partial P(t)}{\partial t} \quad (3.24)$$

$$j(t) = \sigma_0 E(t) + \varepsilon_0 \frac{\partial E(t)}{\partial t} + \varepsilon_0 \frac{d}{dt} \int_0^t f(t-\tau) E(\tau) d\tau \quad (3.25)$$

For $E(t)$ is constant, equation (3.25) can be written as

$$j(t) = \sigma_0 E(t) + \varepsilon_0 [\varepsilon_\infty \delta(t) + f(t)] E(t) \quad (3.26)$$

With $\varepsilon_\infty = 1 + \chi_\infty$

Therefore, the charging current (the current which flows when step DC voltage V_0 is applied) flows through the tested object can be written as

$$i_{charging}(t) = C_0 V_0 \left[\frac{\sigma_0}{\varepsilon_0} + \varepsilon_\infty \delta(t) + f(t) \right] \quad (3.27)$$

Equation (3.27) is the basis for the measurement of the dielectric response function $f(t)$ or for characterizing dielectric materials with the time-domain method. Measurement of DC conductivity of insulation material will have to utilize equation (3.27). Figure 3.2 depicts the charging current when step DC voltage V_0 is applied.

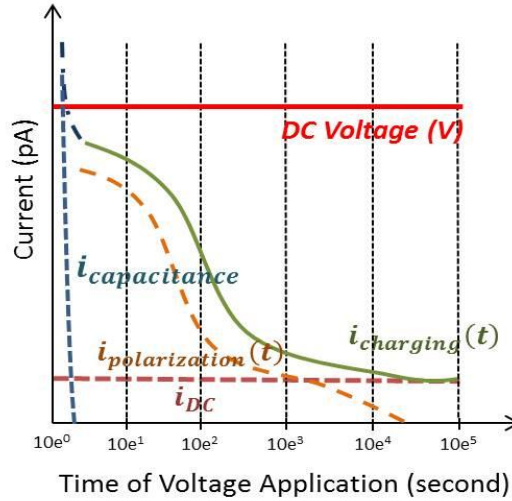


Figure 3.2: Charging current and its component under step DC voltage.

According to equation (3.27), the charging current consists of three terms [69]:

1. The first term is related to the conductivity of test object (DC conductivity).
2. The middle term is related to very fast polarization process which cannot be recorded with the current measurement instrument available.

3. The last term is related to all active polarization processes during voltage application.

3.2.2. Dielectric response in frequency domain

In materials responding linearly with respect to the amplitude of the applied signal, time domain and frequency domain are Fourier Transform of one another. The frequency dependent susceptibility $\chi_{(\omega)}$ is defined as the Fourier Transform of the dielectric response function $f_{(t)}$ as in equation (3.28):

$$\chi_{(\omega)} = \chi'_{(\omega)} + i\chi''_{(\omega)} = \int_0^{\infty} f_{(t)} \exp(-i\omega t) dt \quad (3.28)$$

Where

$$\begin{aligned} \chi'_{(\omega)} &= \int_0^{\infty} f_{(t)} \cos(\omega t) dt \\ \chi''_{(\omega)} &= \int_0^{\infty} f_{(t)} \sin(\omega t) dt \end{aligned} \quad (3.29)$$

And

$$f_{(t)} = (2/\pi) \int_0^{\infty} \chi''_{(\omega)} \sin(\omega t) d\omega = (2/\pi) \int_0^{\infty} \chi'_{(\omega)} \cos(\omega t) d\omega \quad (3.30)$$

While the time domain response corresponds to a decaying of charging current with time, frequency domain response defines two components of amplitude variation in phase and in quadrature with respect to driving harmonic signal and has to be defined as real and imaginary parts of susceptibility $\chi'_{(\omega)}$ and $-i\chi''_{(\omega)}$. These two functions are coupled to each other by Kramer-Kronig transformation which corresponds mathematically to the Hilbert integral transformation [77, 79].

Then, polarization in frequency domain can be expressed as

$$P_{(\omega)} = \varepsilon_0 \chi_{(\omega)} E_{(\omega)} \quad (3.31)$$

Transition from time to frequency domain could be done using Fourier transform on equation and become

$$j_{(\omega)} = \sigma_0 E_{(\omega)} + i\omega D_{(\omega)} \quad (3.32)$$

Using equation (3.31) and (3.32), the total current density in frequency domain can be written as

$$j_{(\omega)} = [\sigma_0 + \varepsilon_0 \omega \chi''_{(\omega)} + i\omega \varepsilon_0 (1 + \chi'_{(\omega)})] E_{(\omega)} \quad (3.33)$$

The relative permittivity of material $\varepsilon_r(\omega)$ is defined by the relation

$$D(\omega) = \varepsilon_o \varepsilon_r(\omega) E(\omega) = \varepsilon_o (1 + \chi'_{(\omega)} - i\chi''_{(\omega)}) E(\omega) \quad (3.34)$$

And can be expressed as

$$\varepsilon_r(\omega) = \varepsilon'_r(\omega) - i\varepsilon''_r(\omega) = 1 + \chi'_{(\omega)} - i\chi''_{(\omega)} \quad (3.35)$$

3.3. Practical consideration of measurement and analysis

When measuring dielectric properties, there is some practical consideration on the dielectric response of measurement that is important to be realised.

3.3.1. Time domain measurement

Actually, there is much more information can be obtained from time domain current measurement other than DC conductivity such as the transient behavior of electrical conduction. However in this work, the focus is on the DC conductivity.

In some publications [80], it was theorized that loss contribution of DC conduction is derived straight from the imaginary part of measured relative permittivity $\varepsilon''_{r(\omega)}$ as linear line which decreases with increase of frequency at low frequency range. That way of derivation is somehow over estimated and thus, the estimated DC conductivity value is too high, especially for fluid-solid impregnated samples. DC conductivity should be measured separately to get correct values.

In measuring DC conductivity, Ohm law is used to determine electrical resistance R by measuring voltage and current. However, please note that Ohm law is only valid when the relationship between voltage and current is linear. The linearity of those quantities depends on the electric field stress applied as different charge carrier might be activated when electric field stress increases.

DC conductivity measurement can be performed with several methods and measurement set-up. When measuring the DC conductivity (volume conductivity) of solid insulation (including solids impregnated samples), usually there is guidance in some international standards e.g. IEC (IEC 60093 and IEC 60247) and ASTM (ASTM D257-99 and ASTM D1169-02) [81, 82]. However, generally, there are no standardized methods to determine the DC conductivity of solid- fluid impregnated samples. In this thesis, DC conductivity was measured in accordance with IEC 60093 [81].

Measuring DC conductivity according IEC 60093 - Methods of test for volume resistivity and surface resistivity of solid electrical insulating materials

The term DC conductivity is the reversely related to DC resistivity. In this section, the term of DC resistivity was used to comply with IEC 60093. IEC 60093 covers the

determination of both volume (DC) and surface resistivity of solid insulating material. According IEC 60093, the volume (DC) resistivity is measured at predetermined times which sometimes do not comply to the correct value as the charging current has not reached steady state especially for material with high resistivity. Therefore, the recommended measurement time of 1 minute after voltage application may not reflect the real DC resistivity value. Figure 3.3 depicts the relation between time of measurement and the current measured.

IEC 60093 also gives recommendation on the electric field stress to be applied when measuring DC resistivity. However, the linearity behaviour of steady state charging current for solid-fluid impregnated system is not clear. Therefore, the preliminary measurement to justify the applied voltage level for the measurement should be performed.

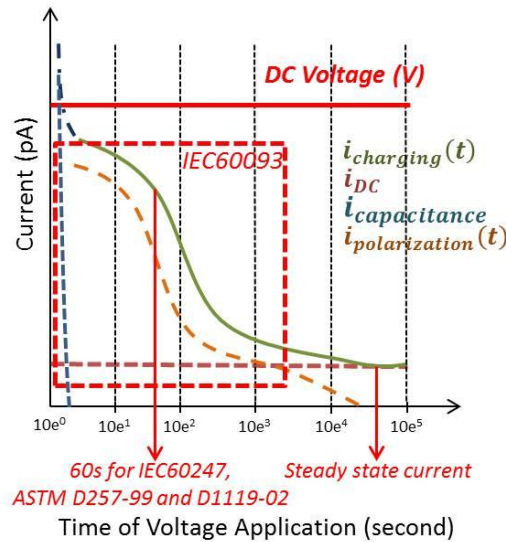


Figure 3.3: Relation between time of measurement and the current measured.

To determine the resistivity, a special measurement set-up has to be prepared. Three-electrode configuration system for DC resistivity measurement was utilized in this thesis. Those electrodes are live electrode, guarded electrode and guard electrode. Guard electrode is very important to exclude surface currents from measurement. The measurement set-up and electrode configuration in this measurement are shown in section 4.2.

Basically, the DC resistivity measurement consists of simultaneous measurement of current and voltage. Volume resistance of sample is calculated only when the current has reach steady state I_{ss} value as in equation (3.36)

$$R_x = \frac{V_o}{I_{ss}} \quad (3.36)$$

Where

- R_x Volume resistance of samples
- V Applied DC voltage
- I_{ss} Steady state current

The steady state current corresponds to the conduction current

Then DC resistivity can be calculated by

$$\rho = R_x \frac{A}{h} \quad (3.37)$$

Where

- ρ Volume resistivity of samples
- A Effective area of electrode
- h Samples thickness

Dc conductivity is then calculated

$$\sigma = \frac{1}{\rho} \quad (3.38)$$

Where σ_0 is DC conductivity. One of the elements necessary for the calculation of relative permittivity is the effective surface area of the guarded electrode A . According to IEC 60093, A is determined as:

$$A = \frac{\pi}{4} (d_a + g)^2 \quad (3.39)$$

In [83], it was explained that in IEC 60093 standard it was assumed that the guarded electrode fringing effectively extends by $g/2$. In reality the edge effect is not so large and the effective margin width is smaller than $g/2$. Therefore, it is suggested the appliance of correction of the gap width g . The calculation of the effective surface area of the guarded electrode A becomes:

$$A = \frac{\pi}{4} (d_a + B \cdot g)^2 \quad (3.40)$$

Factor B is the factor determining increase of the guarded electrode spreading margin. Determination of the effective width of the spreading margin is necessary for the calculation of the effective surface of the guarded electrode. Factor B depends on the ratio gap width (between guard and guarded electrode) to sample thickness $\frac{g}{h}$.

Factor B is determined as:

$$B = 1 - \frac{4h}{\pi g} \ln(\cosh(\frac{\pi g}{4h})) \quad (3.41)$$

The direct inter-electrode capacitance for vacuum C_o can be calculated as:

$$C_o = \epsilon_o \frac{A}{h} \quad (3.42)$$

The appliance of correction factor is important if the measured sample is thin as for transformer papers. Details on the effective area and inter-electrode capacitance for vacuum used in this work can be found in Appendix A.

Measuring DC conductivity with PDC methods

PDC stands for Polarization Depolarization Current. Actually PDC is a measurement method and is not a single measurement set-up which is patented by Allf Engineering [84, 85]. The term DC resistivity is used once again in this chapter to comply basic theory of relaxation current measurement.

The electrical conductivity of insulating material with high specific resistivity generally contains polarization behaviour. Hence, assessment of the real DC resistivity with conventional voltage-current measurement set-up as in IEC 60093 takes long time duration until the current is in steady state. The steady state current will only be reached when the polarization current has finished and sometimes it takes more than a day. It is desirable to determine dc resistivity in shorter time duration and PDC measurement method can provide this.

During the application of DC step voltage at $t = t_o$, charging current will flow as in equation

$$i_{charging}(t) = C_o V_o \left[\frac{\sigma_o}{\epsilon_o} + \epsilon_\infty \delta(t) + f(t) \right] \quad (3.43)$$

With the second term with δ function cannot be recorded in practice. Hence, equation (3.43) can be expressed as

$$i_{charging}(t) = \underbrace{C_o V_o \frac{\sigma_o}{\epsilon_o}}_{i_{DC}} + \underbrace{C_o V_o f(t)}_{i_{polarization}} \quad (3.44)$$

When the test object is short circuited at $t = t_c$ as depicted in Figure 3.4, the depolarization current can be recorded. According to the superposition principle, the sudden reduction of voltage V_o to zero is regarded as a negative voltage step at time $t = t_c$ and then for $t \geq (t_o + t_c)$, then the depolarization current is

$$i_{depolarization}(t) = -C_o V_o [f(t) - f(t + t_c)] \quad (3.45)$$

The term $f(t + t_c)$ in this equation can only be neglected if the charging period t_c is long enough to complete all polarization mechanism. The depolarization current then becomes directly proportional to dielectric response function $f(t)$. The polarization current and depolarization current will show the same response.

$$i_{polarization}(t) = i_{depolarization}(t) = C_o V_o f(t) \quad (3.46)$$

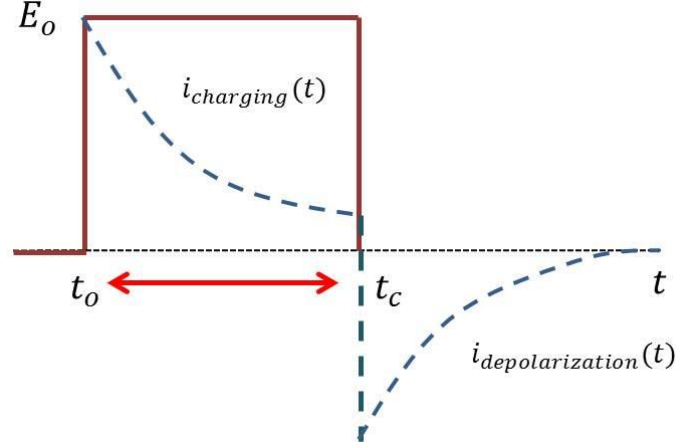


Figure 3.4: Principle of polarization and depolarization current measurement (adapted from [69]).

Hence, the dc conductivity can be calculated from difference between the charging current in equation and depolarization current in equation (3.47).

$$\sigma_0 = \frac{\varepsilon_0}{C_0 V_0} (i_{\text{charging}}(t_m) - i_{\text{depolarization}}(t_m)) \quad (3.47)$$

Where t_m represents time when the relaxation current has been measured long enough. However, insufficient charging time t_c will not force the second term $f(t + t_c)$ becomes zero and there is a “memory effect” in the dielectric due to polarization phenomena which has not been completed due to insufficient charging time [69].

A modified approach to PDC method was developed as Charge Difference Method [2]. The charging and depolarization current are integrated over time to obtain the electrical charges. By subtracting these charging and depolarization charges, the dc conductivity can be determined. The advantage of this technique is the does not have to reach steady state level as the dc conductivity can be determined from the slope of the charge time trend. Furthermore, the disturbance on the current measurement can be filtered out.

3.3.2. Frequency domain measurement

Dielectric response measurement in frequency domain is difficult to be performed, especially if the frequency range is very wide and the voltage applied is high. In frequency domain, the complex capacitance and the derived quantity, $\tan \delta$ was measured. Generally, the measurement of “Complex Capacitance – $\tan \delta$ ” is done at power frequency of 50Hz or 60Hz. However, modern measurement instrument can cover many decades of frequency and can be applied in the field e.g. Omicron Dirana [86], Allf instrument PDC-ANALYSER-1MOD [85] and General Electric IDA 200 [87].

Generally, the measurement system available cannot distinguish between the current contribution of DC conductivity σ_0 and that of polarization $\chi''_{(\omega)}$ in equation (3.33).

This means that the measured relative dielectric permittivity $\tilde{\epsilon}_{r(\omega)}$ is different than relative permittivity $\epsilon_{(\omega)}$ which is defined in equation (3.35). The imaginary part of measured relative permittivity contains both DC conductivity part and polarization part. Meanwhile, the imaginary part only contains polarization part. The measured relative dielectric permittivity $\tilde{\epsilon}_{r(\omega)}$ is defined as follows [69]:

$$j_{(\omega)} = i\omega\epsilon_0\tilde{\epsilon}_{r(\omega)}E_{(\omega)} \quad (3.48)$$

Thus:

$$\begin{aligned} \tilde{\epsilon}_{r(\omega)} &= \epsilon'_{r(\omega)} - i\epsilon''_{r(\omega)} \\ &= \epsilon'_{(\omega)} - i(\epsilon''_{(\omega)} + \sigma_0/\epsilon_0\omega) \\ &= 1 + \chi'_{(\omega)} - i(\chi''_{(\omega)} + \sigma_0/\epsilon_0\omega) \end{aligned} \quad (3.49)$$

The dissipation factor or $\tan \delta$ can then be defined from equation as

$$\tan \delta(\omega) = \frac{\epsilon''_{r(\omega)}}{\epsilon'_{r(\omega)}} = \frac{\epsilon''_{(\omega)} + \sigma_0/\epsilon_0\omega}{\epsilon'_{r(\omega)}} \quad (3.50)$$

The real part of relative permittivity of equation (3.49) calculated from the real part capacitance of samples and the imaginary part of represents both losses from DC conductivity (resistive loss) and dielectric loss (polarization loss). If “Complex capacitance – $\tan \delta$ ” measurement is made only at power frequency, the characteristic of dielectric material cannot be fully observed since those quantities are frequency dependent. Temperature, solid – fluid combination, material characteristic will change those quantities in specific frequency range. Hence, to gain insight of dielectric characteristics, it is recommended to do a wide range frequency measurement.

Tan δ is the only possible to be investigated if the geometry of the test sample is not known. If the geometry is known, the complex capacitance (hence, the complex relative permittivity) contain more information such as conductivity, frequency component of relative permittivity than only the ratio between them.

3.3.3. Equivalent circuit of pressboard impregnated system

This section gives overview on the equivalent circuit which can represent pressboard impregnated system.

The total current density in frequency domain is given in equation (3.33). Thus, the general form for the current I in dielectrics is given by

$$I = \omega\epsilon'' C_0V + i\omega\epsilon' C_0V \quad (3.51)$$

This equation implies that the dielectrics can be treated as lossless capacitor of a reactance $1/\omega\varepsilon' C_0$ in parallel with a resistor of value $1/\omega\varepsilon'' C_0$. The corresponding impedance Z_t of such admittance Y is

$$Y = \frac{1}{Z_t} = \omega\varepsilon'' C_0 + i\omega\varepsilon' C_0 \quad (3.52)$$

Using normal annotation, the current also can be represented as

$$I = I_R + iI_C = (G + i\omega C)V \quad (3.53)$$

It is often premature to conclude that a dielectric behaves like a pure capacitor in parallel with a resistor. This definition on equivalent circuit of dielectrics is widely used including in some international standards for measuring dielectrics properties. In reality, the conductance G relate to a number of different mechanism that consume energy as has been described in previous section.

This section shows equivalent circuit which exhibiting relaxation phenomena as possible equivalents to solid-fluid insulating system as shown in Table 3.1. Each circuit provided represent different type of dielectrics and it is marked by different dielectric response in frequency domain. As has been described earlier, for solid-fluid insulating system, there are three unique features over frequency range up to 10 kHz: (a). interfacial polarization, (b). dipolar orientation polarization, and (c). DC conduction. In terms of relaxation time, interfacial polarization has longer relaxation time compare to dipolar orientation polarization. Meanwhile, DC conduction is dominant at very low frequency. Thus, the equivalent circuit should be able to show the nature of mechanism which presence on solid-fluid insulating system.

The concept of dipoles giving rise to polarization was introduced by Debye in 1912 and the derivation of the dipolar response later in 1945 [77]. The equivalent circuit to represent Debye model is given in Table 3.1. The Debye response is obtained for as assembly of non-interacting ideal dipoles which have a loss of energy proportional of frequency in the Potential Double Well model – the analogy of frictional loss in a viscous medium [67, 77]. There is only single relaxation times in this model which represent the dipolar orientation polarization. The complex relative permittivity equation for Debye model is given as

$$\varepsilon'_{(\omega)} = \varepsilon_{\infty} + \frac{\varepsilon_s - \varepsilon_{\infty}}{1 + \omega^2 \tau^2} \quad (3.54)$$

$$\varepsilon''_{(\omega)} = \frac{(\varepsilon_s - \varepsilon_{\infty})\omega\tau}{1 + \omega^2 \tau^2} \quad (3.55)$$

However, it is often that there is a distribution of relaxation times or some mechanism that gives a frequency dependence which can be interpreted as a distribution of relaxation times. A distribution of relaxation times is normally presence from some heterogeneity in the inter-molecular structure, particularly in polymer.

The interfacial polarization was one of the first types of polarization to be recognized before 1900 and it is known as Maxwell-Wagner polarization [68]. To represent interfacial polarization arises from long range charge carriers migration through dielectric. The equivalent circuit to represent interfacial polarization is normally Maxwell-Wagner two layer condenser in Table. It has the physical meaning that relate to the real solid-fluid insulating system which consist of insulating fluid and pressboard. The complex relative permittivity equation for Maxwell-Wagner two layer condenser model is given as

$$\varepsilon'_{(\omega)} = \varepsilon_{\infty} + \frac{\varepsilon_s - \varepsilon_{\infty}}{1 + \omega^2 \tau^2} \quad (3.56)$$

$$\varepsilon''_{(\omega)} = \frac{(\varepsilon_s - \varepsilon_{\infty})\omega\tau}{1 + \omega^2 \tau^2} + \frac{1}{\omega C_0 (R_1 + R_2)} \quad (3.57)$$

By comparing equation (3.54) and equation (3.57), it is clear that $\varepsilon'_{(\omega)}$ is precisely the same with Debye model. Thus, by measurement of the real part of relative permittivity, it is not possible to distinguish between the effects of interfacial and dipolar orientation polarization. However, the imaginary part is different as for Maxwell-Wagner model the loss (represented by $\varepsilon''_{(\omega)}$) tend to infinity as ω tends to zero. Thus, the case of interfacial polarization may be distinguished from Debye model by observing the variation of $\varepsilon''_{(\omega)}$ at low frequency. The detail of derivation on Debye model and Maxwell-Wagner model can be read in [67].

In circumstances where the simple zero space-charge loss does not occur as in equation below:

$$\frac{\varepsilon'_1}{\sigma_1} \neq \frac{\varepsilon'_2}{\sigma_2} \quad (3.58)$$

Where

- ε'_1 Relative permittivity of insulating fluid
- ε'_2 Relative permittivity of solid
- σ_1 Conductivity of insulating fluid
- σ_2 Conductivity of solid

The following surface charge density has reached the surface discontinuity [88]:

$$q = \varepsilon'_1 E_1 - \varepsilon'_2 E_2 = \left(\varepsilon'_1 - \varepsilon'_2 \frac{\sigma_1}{\sigma_2} \right) E_1 = \left(\varepsilon'_1 \frac{\sigma_1}{\sigma_2} - \varepsilon'_2 \right) E_2 \quad (3.59)$$

Where

- E_1 Electric field stress in insulating fluid
- E_2 Electric field stress in solid

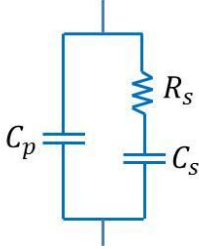
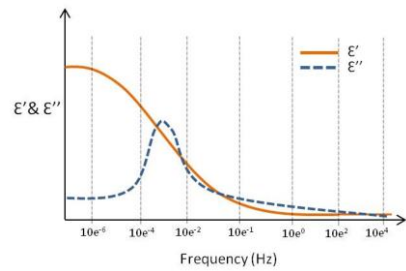
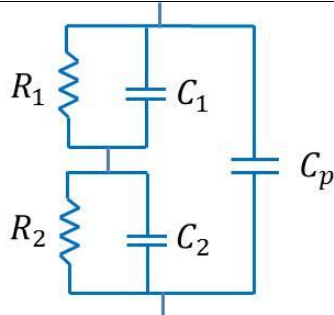
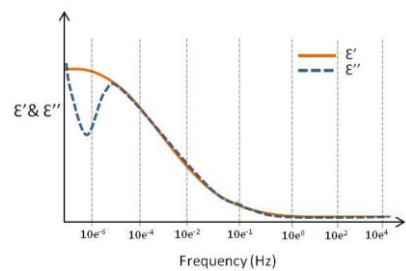
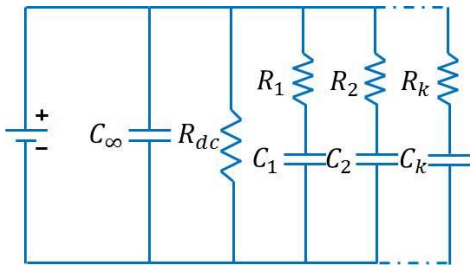
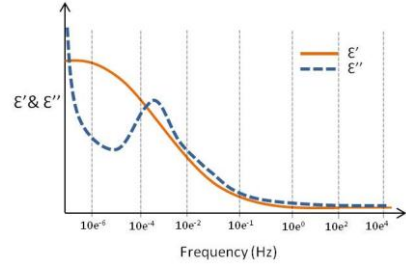
DC conduction feature on the solid-fluid insulating system is given in this paragraph. In 1963, Ochini et al. derived another equivalent circuit that represent oil impregnated paper for HVDC cables application [88]. It is called Extended Debye model, which is an expansion from the basic Debye model. In Extended Debye model, there are additional branches of series capacitor and resistor to represent the interfacial polarization and dipolar orientation characteristics. There is also R_{DC} which represent the DC conductivity on the solid-fluid insulating system. In this model, the branch that represent interfacial polarization has much longer relaxation time (greater $R_k * C_k$) compared to branch that represent dipolar orientation polarization. In 1996, Zaengl et.al developed Polarization and Depolarization Technique (PDC) technique for analysing dielectric properties of solid-fluid insulating system [84]. Along with this technique, he also showed that the depolarization current could be easily derived from Extended Debye model. Up to now the Extended Debye model is accepted as a suitable representation of solid-fluid insulating system. The derivation of Extended Debye model to be a dielectric response in time and frequency domain can be seen in Appendix B. The complex relative permittivity equation for Extended Debye model is given as

$$\varepsilon'(\omega) = \frac{C_\infty}{C_0} + \frac{1}{C_0} \sum_{k=1}^n \frac{C_k}{1+\omega^2\tau_k^2} \quad (3.60)$$

$$\varepsilon''(\omega) = \frac{1}{C_0\omega R_0} + \frac{1}{C_0} \sum_{k=1}^n \frac{\omega\tau_k C_k}{1+\omega^2\tau_k^2} \quad (3.61)$$

Table 3.1 shows the equivalent circuit and the dielectric response in frequency domain. Both Maxwell-Wagner model and Extended Debye model show similar real permittivity and $\tan \delta$ response in frequency domain. This point prove that the Extended Debye model also suitable as a representation for Maxwell-Wagner effect (interfacial polarization). However, there is some concern that the Extended Debye model could not represent dielectric characteristic of solid-fluid insulating system which is non-linear under different electric field stress and temperature [2]. It needs to employ a non-linear component to have a better representation of solid-fluid insulating system.

Table 3.1: Equivalent circuit of dielectrics.

No	Model	Circuit representation	Dielectric response in frequency domain
1	Debye model		
2	Maxwell-Wagner two layer condenser		
3	Extended Debye		

3.3.4. Dielectric relaxation in solid: review on analytical method

This section gives overview on the common analytical method of dielectric relaxation phenomena. Mainly, it explains on how researchers analyze the same phenomena and decided which one is suitable to be applied in this work.

Presentation of experimental data

The most common way of representing experimental data is on the plot of real and imaginary components in either logarithmic or linear coordinates against frequency. The frequency is usually in the logarithmic coordinates and hence, wide range dielectric data can be observed. Generally, the linear-log form is normally used to represent real part of permittivity $\epsilon'_{r(\omega)}$ or susceptibility $\chi'_{(\omega)}$ and the log-log form is used to represent either imaginary part of permittivity $\epsilon''_{r(\omega)}$ and susceptibility $\chi''_{(\omega)}$ as well as $\tan \delta(\omega)$ as depicted in Table 3.2. This kind of presentation is justified because normally the imaginary part of permittivity and susceptibility show a stronger

variation in value compared to its real part. However, according to [77], this kind of presentation is somehow mistaken due to the loss of essential link between the real and imaginary part. He suggested that both real and imaginary part of relative permittivity and susceptibility is presented in log-log form.

Another way of representing the experimental data is on polar plots of the imaginary component against the real components on a linear presentation as in Figure. The polar plot has certain limitation due to its only capability to characterize the experimental data by shape such as for Debye, Cole-cole and etc [77].

Conventional and empirical point of view of dielectric response in frequency domain

Empirical method of analysing the dielectric response in frequency domain was first suggested by Jonscher [65, 77]. His theoretical interpretation on the dielectric data rejects the conventional concept of distribution of relaxation times and suggests the plotting of both polarization loss factor (imaginary part of susceptibility) and electrical conductivity on the log-log form [68]. Another purely empirical analytical expression which is convenient for representing the loss peaks was proposed by Havriliak and Negami as in

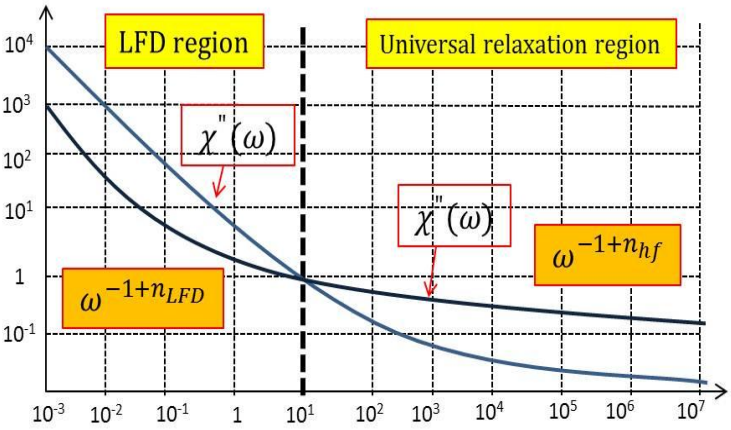
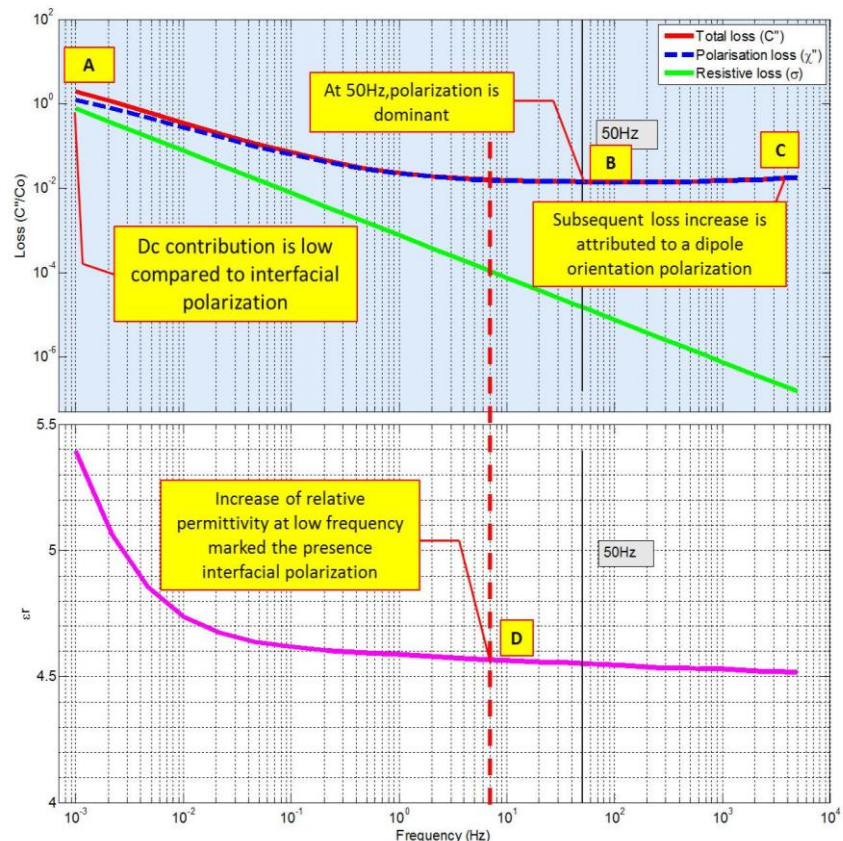
$$\chi(\omega) \approx \left[1 + \left(\frac{i\omega}{\omega_p} \right)^m \right]^{\frac{(n-1)}{m}} \quad (3.62)$$

Further reading about empirical analysis based on Havriak-Negami, Cole-Cole and Cole-Anderson can be found elsewhere. In this section, the comparison was done only between conventional method and empirical method suggested by Jonscher.

First, the summary of the different principal in the frequency domain is given in Table 3.2 and second, in time domain as shown in Table 3.3. This comparison is based on some reference: for conventional method based on [46, 47, 48, 49, 67, 68, 69] and for empirical method based on [77].

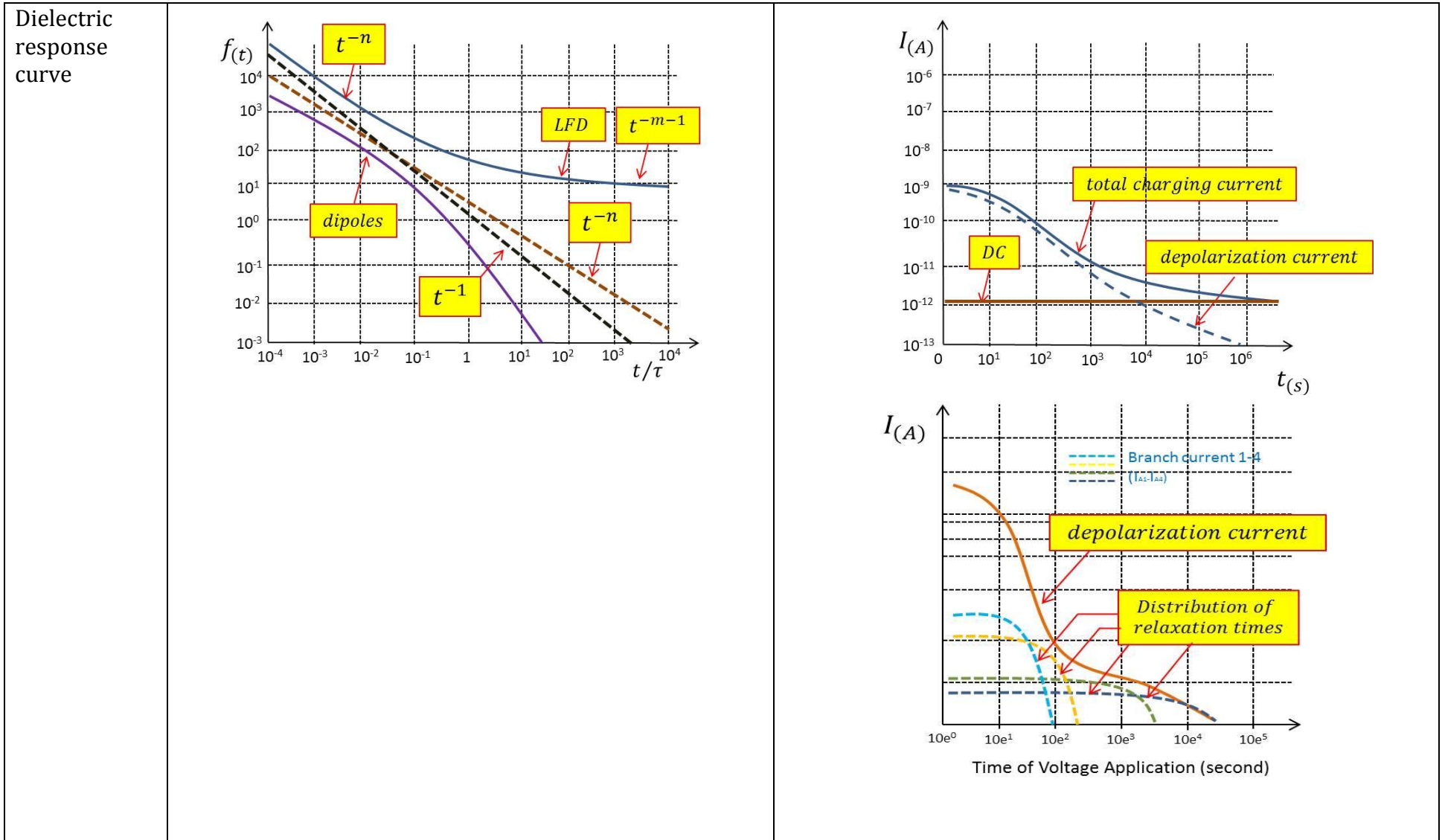
Ultimately, both approaches try to explain the same phenomenon with different purpose. The purpose of conventional method is to give detail analysis corresponding to the observed experimental results for particular case. Meanwhile, the purpose of empirical method by Jonscher is to give universal understanding regarding the phenomenon that might occur in a solid. Therefore, it explains the universality of phenomenon based on experimental results and analyse what is the physical meaning and probable causes behind it.

Table 3.2: Comparison analysis method in frequency domain.

	Empirical method by Jonscher	Conventional method
Dielectric response curve	 <p data-bbox="526 877 1108 917">- dielectric susceptibility in log-log form</p>	 <p data-bbox="1288 1220 2027 1332">- loss in log-log form - relative permittivity (real part of susceptibility) in linear-log form</p>

<p>Low frequency</p>	<p>Characterized by Low Frequency Dispersion (LFD) with typical Arrhenius temperature activation.</p> $\chi_{(\omega)} \approx (i\omega)^{n-1}$ <p>With exponents $1 - n$ closer to unity. The low frequency behavior may not correspond to DC conductivity.</p> <p>LFD analysis based on the rejection of interpretation on the rise of $C'_{(\omega)}$ in term of presence of interfacial polarization which equivalent to series of R-C combination. R-C combination corresponds to pure Debye behavior which has loss peak. However, from experimental results at low frequency, the loss peak is rarely observed.</p>	<p>Characterized by DC conductivity and interfacial polarization with typical Arrhenius temperature activation.</p> <ul style="list-style-type: none"> • When only long-range ionic migration (DC conduction) is involved, the relative permittivity value will remain constant at low frequency while the $\tan \delta$ will increase with decrease of frequency. • Meanwhile, when the interfacial space charge polarization is presence, the relative permittivity and $\tan \delta$ value will increase with decrease of frequency as $\tan \delta$ reaches maximum (loss peak). • The loss peak of interfacial polarization is rarely observed. However, for Nomex impregnated with mineral oil, the loss peak is observed over the measured frequency range.
<p>Intermediate frequency region (may stretch from below hertz to gigahertz)</p>	<p>Characterized by “Universal relaxation”.</p> <p>Material which dominates by slowly mobile hopping charge carriers do not show loss peaks in their response but instead show relatively ‘shallow’ fractional power law</p> $\chi_{(\omega)} \approx (i\omega)^{n-1}$ <p>With exponents $0.1 < 1 - n < 0.3$. This type of behavior, which is common to dipoles and to charge carriers at high frequency is referred to as “Universal dielectric response” [jonscher 1983].</p>	<p>Characterized by dipolar orientation and interfacial polarization.</p> <p>In the range of frequencies extending upwards, some residual dipole contribution to the overall total loss may occur as a result of the remnant dipole loss due to the dipole orientation of the larger molecules and it is marked by the increase of $\tan \delta$.</p>

Table 3.3: Comparison analysis method in time domain.



<p>Dielectric response function $f(t)$</p>	<p>Universal relaxation system has fractional power law response by Curie and von Schweidler.</p> $f(t) \approx t^{-n}$ <p>While the rising part of dipolar response has fractional power law response</p> $f(t) \approx t^{-m-1}$ <p>Reject the concept of distribution of relaxation times (DRT) based on the fact there is no independent ways of conforming the DRT required to give the precise fit to experimental data.</p>	<p>Debye system has exponential time dependence [67]</p> $f(t) = \left(\frac{P_0}{\tau}\right) e^{-\omega_p t}$ <p>Support the concept of distribution of relaxation time. Distribution of relaxation time can be observed from the derivation of depolarization current.</p>
<p>Characteristic</p>	<p>For charge carrier system which involved long-range ionic migration, the dielectric response function has widely extending spectra.</p> <p>The nature of long time behavior is not DC conductivity but rather LFD which has DC conductivity-like characteristic based on the idea that there is no limitation to the total polarization since the total displacement of individual charge carriers is open ended.</p>	<p>From PDC measurement technique, the depolarization current is proportional to dielectric response function</p> $i_{depolarization}(t) = C_0 V_0 f(t)$ <p>According to [69], if the dielectric was charged for long period of time, then all polarization processes will complete and it shown by the depolarization time which is died down.</p>

3.4. Temperature dependent behavior of dielectric properties

The dielectric response of insulation material is a function of frequency with temperature as one of the main parameter. For a quite large group of solid dielectric materials, it was found that the shape of the dielectric response does not alter drastically with temperature change. This is at least true for temperature ranges over which the material does not change its internal structure too much. This phenomenon allows for normalizing frequency dependent spectra for different temperatures by shifting the corresponding spectra until they coincide into a single curve, which is called a “master curve” [65, 89, 90]. For some dielectric materials including fluid impregnated solid, a shift in the spectral function due to a change in absolute temperature from T_1 to T_2 can be expressed with an Arrhenius relation. In frequency domain, a higher temperature shifts the dielectric response curve towards higher frequencies. These shifts $S(T)$ is given as [65, 74]

$$S(T) = e^{\left(\frac{-E_p}{kT}\right)} \quad (3.63)$$

Where

$S(T)$	Shift with temperature
E_p	Activation energy of polarization
k	Boltzman constant = 8.6173324×10^{-5}
T	Temperature

The activation energy of polarization has been compared to the energy (heat) of vaporization of the part of polymer participating in the polarization mechanism [68].

The temperature behavior of DC conductivity can be described Arrhenius relation as shown in equation (3.64)

$$\sigma_o = A_{DC} e^{-E_{DC}/kT} \quad (3.64)$$

Where

σ_o	DC conductivity
A	Pre-exponential value of Arrhenius equation for DC conductivity
E_{DC}	Activation energy of DC conductivity

Equation (3.64) shows that by knowing the pre-exponential factor and activation energy for every pressboard and transformer paper, it is possible to calculate DC conductivity at certain temperature.

The application of equation (3.64) for two different temperatures T_1 and T_2 , for which the measured dielectric properties σ_1 and σ_2 , respectively, gives equation (3.65):

$$\frac{\sigma_1}{\sigma_2} = \frac{e^{-E_{DC}/K.T_1}}{e^{-E_{DC}/K.T_2}} = e^{\frac{E_{DC}}{K} \left(\frac{1}{T_2} - \frac{1}{T_1} \right)}$$

$$\Rightarrow \ln \left(\frac{\sigma_1}{\sigma_2} \right) = \frac{E_{DC}}{K} \left(\frac{1}{T_2} - \frac{1}{T_1} \right) \quad (3.65)$$

For most Arrhenius activated systems, this is equal to shift of dielectric response complex susceptibility curve along the frequency axis. If the frequency is on a log scale, it is then a constant shift that is independent of frequency. It should be noted that the maximum loss peaks correspond to central relaxation time and all real polymer exhibit a distribution in relaxation times [90]. Therefore, the $\tan \delta$ spectra of solid-fluid insulating system also follow this rule.

Equation (3.63) can be generalized to be a frequency shift equation related to the shift in dielectric response $\tan \delta$:

$$\tan \delta(\omega_1) = \tan \delta(\omega_2) \quad (3.66)$$

$$\frac{\varepsilon_r''(\omega_1)}{\varepsilon_r'(\omega_1)} = \frac{\varepsilon_r''(\omega_2)}{\varepsilon_r'(\omega_2)}$$

$$\Rightarrow \frac{\frac{\sigma_1}{\varepsilon_0 \omega_1} + \chi''(\omega_1)}{1 + \chi'(\omega_1)} = \frac{\frac{\sigma_2}{\varepsilon_0 \omega_2} + \chi''(\omega_2)}{1 + \chi'(\omega_2)} \quad (3.67)$$

Where ω_1 and ω_2 are frequency set associated with $\tan \delta$ curve at different temperature, T_1 and T_2 . Based on the shifting of the complex dielectric susceptibility, set of susceptibility values at ω_1 and ω_2 are equal. Therefore, the shift in dielectric response curve of $\tan \delta$ equals the shift in complex dielectric susceptibility. However, the shift on master curve of $\tan \delta$ will only be perfect if the activation energy of DC conductivity E_{DC} and the activation energy of polarization E_p are equal as in solids impregnated with mineral oil. Hence, equation (3.67) becomes:

$$\frac{\sigma_1}{\varepsilon_0 \omega_1} = \frac{\sigma_2}{\varepsilon_0 \omega_2}$$

$$\Rightarrow \frac{\sigma_1}{\sigma_2} = \frac{\omega_1}{\omega_2} \quad (3.68)$$

Substitute equation (3.68) to equation (3.65):

$$\ln \left(\frac{\sigma_1}{\sigma_2} \right) = \ln \left(\frac{\omega_1}{\omega_2} \right) = \frac{E_{DC}}{K} \left(\frac{1}{T_2} - \frac{1}{T_1} \right)$$

$$\ln \left(\frac{\omega_1}{\omega_2} \right) = 2.30258 * \log_{10} \left(\frac{\omega_1}{\omega_2} \right) = \frac{E_{DC}}{K} \left(\frac{1}{T_2} - \frac{1}{T_1} \right) \quad (3.69)$$

The shift can be determined using equation (3.70):

$$shift = \log_{10}(\omega_1) - \log_{10}(\omega_2) = \frac{E_{DC}}{2.30258 * K} \left(\frac{1}{T_2} - \frac{1}{T_1} \right) \quad (3.70)$$

If the temperature dependence, over the whole frequency range, can be described by a single Arrhenius process with shifts proportional to $e^{-E_P/kT}$, then the fit will be perfect. The activation energy E_P can be calculated from the two shifted values from dielectric response $\tan \delta$ curve at different temperatures, T_1 and T_2 with equation (3.71):

$$E_P = \frac{\log_{10} \left(\frac{\omega_1}{\omega_2} \right) * 2.30258 * K}{\left(\frac{1}{T_2} - \frac{1}{T_1} \right)} \quad (3.71)$$

The activation energy is then the main descriptor parameter of the temperature dependent behavior solid impregnated material. In some cases there is more than one mechanism that is responsible for the dispersion and they can in general have different temperature dependence.

An advantage of the master curve technique is that the frequency range is significantly extended compared to the original measured spectra. Another useful feature of the master curve technique is that the possibility to calculate dielectric properties of pressboard at certain temperature and frequency [91]. This might be practical for transformer design purpose.

3.5. Composite dielectric

Most insulation systems found in practical applications are composites or mixtures of several different dielectric materials. The estimation of the dielectric properties of a medium formed from a composite of different dielectric material is a problem of both theoretical and practical importance [70]. The principal aim is to calculate the relative permittivity of the composite in terms of the relative permittivity of the constituents, their relative amounts and their spatial distribution. It is important to realize that each dielectric material has a dielectric response and when putting these materials together the total response will not only reflect each material but also the way they are put together. Sometimes the total dielectric response describes one physical process but the materials in the mixture have dielectric responses revealing totally different physical processes. This section will discuss several formulas for estimating of effective relative permittivity of solid – fluid insulating system. Detail on this topic can be found in [70, 92].

Two simple systems are found in Figure 3.5 representing a capacitor filled with two different dielectrics in two different ways representing a parallel and series case.

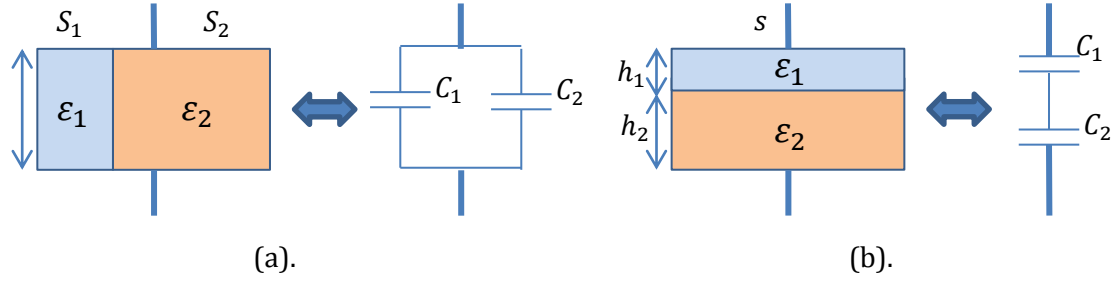


Figure 3.5: A capacitor which is filled with two dielectrics, ϵ_1 and ϵ_2 , but distributed in two different ways (a) in parallel and (b) in series.

In the first case, Figure 3.5(a), there are two dielectrics where each forms a cylinder with a cross section, of an arbitrary but uniform cross section, with its axis parallel to the applied electric field. In the second case, Figure 3.5(b), there are two dielectrics that are in parallel. However, in many practical cases, composite dielectrics are complex mixtures of several dielectrics, which are both combination in parallel and in series. Hence, the equivalent diagrams in Figure 3.5 are not sufficient to describe the effective relative permittivity of composite dielectric.

Difficulties in modelling of dielectric mixtures lead to the interest in obtaining bounds limit parameter of the effective relative permittivity. Wiener [93] and Hashin-Shtrikman [94] proposed bounds for effective relative permittivity of dielectric mixture. These bounds are called absolute bounds which mean that the effective relative permittivity ϵ_{eff} of composite dielectric cannot be present outside the limit given in equation (3.72) and (3.73) for Wiener bounds and equation (3.74) and (3.75) for Hashin-Shtrikman bounds.

Wiener assumed the dielectric mixtures consist of layered structures which had topological configuration parallel or perpendicular to applied field direction. Wiener bounds are as follows:

$$\epsilon_{eff,max} = f \cdot \epsilon_i + (1 - f) \cdot \epsilon_e \quad (3.72)$$

$$\epsilon_{eff,min} = \frac{\epsilon_i \cdot \epsilon_e}{f \cdot \epsilon_i + (1 - f) \cdot \epsilon_e} \quad (3.73)$$

Hashin-Shtrikman bounds are narrower than Wiener bounds and they were designed for homogenous and isotropic mixtures. In two dimensions, the Hashin-Shtrikman bounds are as follows:

$$\epsilon_{eff,max} = \epsilon_i + \frac{(1-f)}{\frac{1}{\epsilon_e - \epsilon_i} + \frac{f}{3 \cdot \epsilon_i}} \quad (3.74)$$

$$\epsilon_{eff,min} = \epsilon_i + \frac{f}{\frac{1}{\epsilon_e - \epsilon_i} + \frac{(1-f)}{3 \cdot \epsilon_i}} \quad (3.75)$$

There exist other bounds as proposed by Bergman and Milton [95]. However, it was found that these bounds are not valid for relative permittivity estimation at low frequency when interfacial polarization is considered.

There exist many different approaches when it comes to prediction of dielectric properties of composite dielectric with various ranges of difficulties and assumptions. Those approaches were divided into several categories which are classic theoretical approaches, spectral function approaches, percolation theory approaches, numerical approaches and experimental approaches [70].

The classic theoretical approaches consist of simple approach, mean field theory, molecular approach and regular arrangement of inclusion approach. One of the simplest approaches was expressed by Gladstone and Dale who expressed a formula for the effective relative permittivity of composite which was based on the proportionality and linearity of the concentrations and relative permittivity of constituents [96]. There is also mean field theory approach which based on the assumption that one of the phases, the inclusion phase, is inside the matrix (the main phase), in such way that both phases are embedded inside an effective medium [70]. Wagner [97] was the first to use this approach and later follow by Sillars [98], Fricke [99], and Steeman and Maurer [100, 101]. The other classic theoretical approaches approach is molecular approach, in which the dielectric behavior of the composite is assumed to be the summation of the dipole moments of each molecule in a vacuum matrix. Molecular approach was expressed by Clausius-Mosotti [92, 102, 103], Onsager-Böttcher [92, 102, 103, 104] and Kirkwood [105] who extended the Onsager theory of dielectric polarization.

There is also spectral function approach, in which a function of a composite is a compact way of expressing data over a range of frequencies. The spectral function approach expressed the effective relative permittivity of the composite as a function of dielectric permittivity of the constituents and the geometry of the composite [106].

When higher inclusion concentrations or higher ratios of electrical properties of constituents are taken into consideration, percolation theory should be included [107, 108]. It is more meaningful to apply the percolation theory in disordered system, since the question of packing density arises in that condition. In case of disordered systems, the system behavior is described by a power law with a percolation threshold and critical exponent which dependent on the geometry and on the conduction process of the system [70].

The estimation of effective relative permittivity of composite dielectric can also be expressed by numerical approaches. The finite element method is one of the most intensively used approaches in the field simulations, in which the effective medium properties of mixtures are calculated using finite element method [70, 109, 110, 111]. The effective permittivity of mixture can also be determined by calculating reflection

from a sample in which the sample is put in a TEM waveguide and fields are solved by the FDTD method [112]. However, the numerical calculation only gives little awareness to the interface problem in which dominant in case solid-ester fluids insulating system. Detail on the literature of the numerical estimation of dielectric properties can be found in [92].

Ultimately, it is desirable to found a semi-empirical formula for estimating the effective relative permittivity of composite dielectric as in solid-fluid insulating system. The formula should be simple and consider the physical phenomena which occur in solid-fluid insulating system. The mixture consists of two dielectric materials, of which one is treated as host and the other as the inclusion phase as in solid-fluid insulating system. Some of the formulas are as follows:

1. Maxwell – Garnett [113,114]

$$\varepsilon_{eff} = \varepsilon_e + 2.f.\varepsilon_e \cdot \frac{(\varepsilon_i - \varepsilon_e)}{\varepsilon_i + \varepsilon_e - f(\varepsilon_i - \varepsilon_e)} \quad (3.76)$$

2. Bruggeman or Polder-van Santen Formula [115]

$$(1 - f) \frac{(\varepsilon_e - \varepsilon_{eff})}{(\varepsilon_e + \varepsilon_{eff})} + f \frac{(\varepsilon_i - \varepsilon_{eff})}{(\varepsilon_i + \varepsilon_{eff})} = 0 \quad (3.77)$$

3. Mixing Approach [116]

$$\frac{\varepsilon_{eff} - \varepsilon_e}{\varepsilon_{eff} + \varepsilon_e + v.(\varepsilon_{eff} - \varepsilon_e)} = f \cdot \frac{\varepsilon_i - \varepsilon_e}{\varepsilon_i + \varepsilon_e + v.(\varepsilon_{eff} - \varepsilon_e)} \quad (3.78)$$

4. Coherent Potential - $v = 2$ [117, 118]

$$\frac{\varepsilon_{eff} - \varepsilon_e}{\varepsilon_{eff} + \varepsilon_e + 2.(\varepsilon_{eff} - \varepsilon_e)} = f \cdot \frac{\varepsilon_i - \varepsilon_e}{\varepsilon_i + \varepsilon_e + 2.(\varepsilon_{eff} - \varepsilon_e)} \quad (3.79)$$

5. Power Law Model - Birchak Formula $b=0.5$ [119]

$$\varepsilon_{eff}^{0.5} = f.\varepsilon_i^{0.5} + (1 - f).\varepsilon_e^{0.5} \quad (3.80)$$

6. Power Law Model - Looyenga Formula $b=0.33$ [120]

$$\varepsilon_{eff}^{0.3} = f.\varepsilon_i^{0.3} + (1 - f).\varepsilon_e^{0.3} \quad (3.81)$$

7. Lichtenecker Formula [121]

$$\ln \varepsilon_{eff} = f.\ln \varepsilon_i + (1 - f).\ln \varepsilon_e \quad (3.82)$$

For theoretical basis in this thesis, only the seven formulas above were considered and combined it with experimental approach. From the experiment, the effective relative permittivity of solid-fluid insulating system was obtained and then, utilized the theoretical approach to explain the results. Finally, based on the previous analysis, a new empirical formula was developed for estimating the effective relative permittivity of solid-ester fluids insulating system.

4. Test Object, Measurement Set-up and Measurement Performed on Test Object

The investigation in laboratory was carried out on homogenous samples of pressboard and transformer papers impregnated with alternative insulating fluids. The measurements were carried out in dependence on parameters such as temperature, polymer material of pressboard, density of pressboard and type of insulating fluid.

4.1. Laboratory samples

4.1.1. Pressboard and transformer papers samples

The dielectric response was measured for various types of pressboards and transformer papers listed in Table 4.1. The samples has round disk shape with a diameter of 120mm and absolute moisture content less than 0.5% (dry condition). The given moisture content of samples is defined as the percent ratio of moisture (water) weight absorbed from the samples to its dried un-impregnated weight. The moisture content of samples was measured using Karl Fisher titration technique [122].

Before impregnation process, solid samples were dried under vacuum ($< 1\text{mbar}$) for 3 days at 105°C to ensure the absolute moisture content less than 0.5%. Meanwhile, the insulating fluid were filtered, degassed and dried (for mineral oil, the moisture content: $< 5\text{ppm}$ and for ester fluids, the moisture content: $< 10\text{ppm}$). Then the impregnation was carried out for 2 days for samples impregnated in mineral oil and 3 days for samples impregnated in ester fluids at 105°C to ensure that the samples were fully impregnated. Impregnation with ester fluids generally takes longer time for the samples to be fully impregnated due to high viscosity values of ester fluids [32]. After impregnation, the moisture content of samples was measured as reference point. Then, the samples were stored in aluminum canisters. With this method, the absolute moisture content remains less than 0.5% for as long as eight months.

Table 4.1 shows the tested solid samples. The measurement was performed on three pressboard types and three transformer papers with different characteristics. The pressboards tested were as follows:

1. Weidmann Transformerboard B.3.1A (TIV) with 2mm and 4mm thickness (it will be referred as TIV) [123].
2. Weidmann Transformerboard B 4.1 (TIII) with 2mm thickness (it will be referred as TIII) [123].
3. DuPont Nomex pressboard T-993 with 2mm thickness (it will be referred as Nomex) [124].

In many of its applications, the density of insulating paper is varied in order to decrease the relative permittivity of the impregnated sheet [5]. In other application applications the paper density is increased in order that higher relative permittivity of the impregnated sheet may be used to obtain an improved voltage distribution of the whole insulating system. The transformer papers tested were as follows:

1. Cottrell CK 125-TU with 0.076mm thickness (it will be referred as Cottrell).
2. Tullis Russell Rotherm HIHD with 0.085mm thickness (it will be referred as Rotherm).
3. Nordic Paper Amotfors with 0.08mm thickness (it will be referred as Amotfors).

From the tested samples, the investigation was performed on the effect of material density, material thickness, and material of polymer on the dielectric properties when impregnated with alternative insulating fluid. Table 4.1 shows the characteristics of tested samples.

Table 4.1: List of tested solid samples

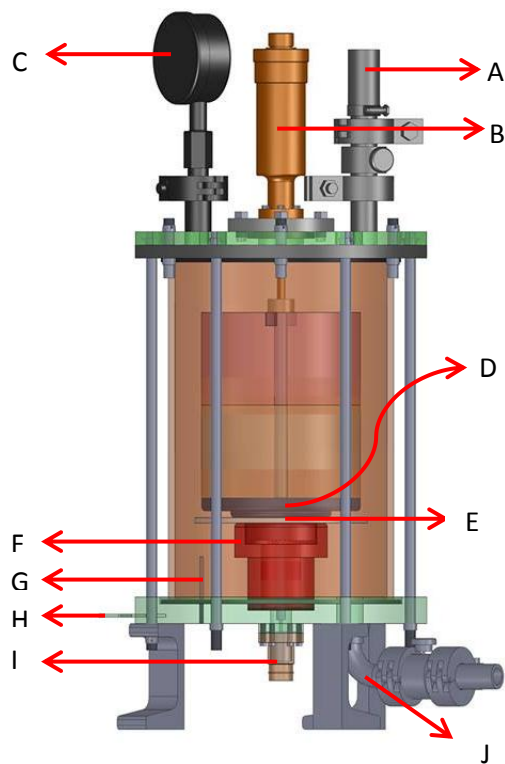
Manufacturer	Samples	Thickness (mm)	Density (g/cm ³)	BDV (kV/mm)		Comment
				in air	in oil	
Weidmann	B.3.1A (TIV)	2 and 4	1.19	n.a.	51	High density cellulose pressboard
	B.4.1 (THH)	2	0.9	n.a.	37	Low density cellulose pressboard
DuPont	Nomex T-993	2	0.76	n.a.	n.a.	Aramid pressboard with excellent thermal stability and dielectric strength
Cottrell	CK 125-TU	0.076	1.15	10.2	48	Thermally upgraded extensible kraft paper
Tullis Russel	Rotherm HIHD	0.085	0.95	12	86.6	Thermally upgraded transformer paper
Nordic Paper	Amotfors	0.08	0.8	7	n.a.	Not thermally upgraded transformer paper

4.1.2. Insulating fluid samples

The insulating fluids used in the measurement were mineral oil Nytro 4000X, synthetic ester MI7131 and natural ester Envirotemp FR3. The description of the insulating fluid can be found in section 2.1.

4.2. Test vessel

The custom vessel for the dielectric response measurements is depicted in Figure 4.1. The test vessel is equipped with temperature sensor Pt.100 and heater blanket connected to the temperature controller. The vessel can withstand maximum temperature of 180°C.



Label	Description
A	Vacuum port
B	Micrometer and power supply port
C	Pressure gauge
D	Live electrode
E	Sample
F	Measuring and guard electrode
G	Temperature sensor Pt.100
H	Ground port
I	BNC feed through
J	Exhaust port

Figure 4.1: Test vessel.

According to IEC 60093, three-electrodes-system configuration was used for measuring volume conductivity, as in Figure 4.2 [68]. The live electrode used were rounded-cornered electrode with radius 3 mm as it yields uniform electric field in the pressboard [125]. The pressure of live electrode is more than $3.3\text{N}/\text{cm}^2$ to reduce the effect of surface roughness of pressboard [91]. Detail design of test vessel and electrode system is in Appendix C.3.

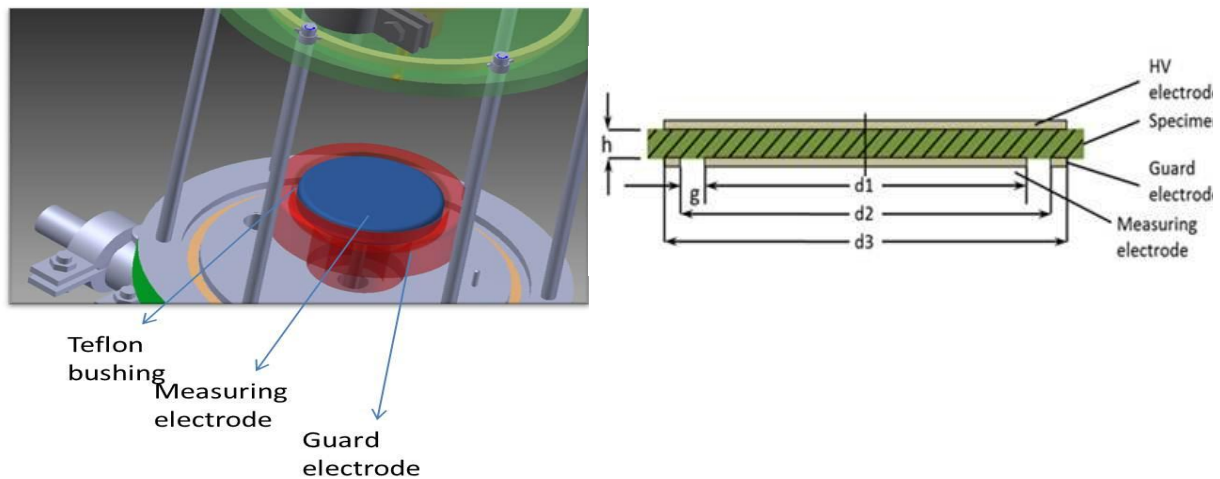


Figure 4.2: Three-electrode system configuration.

4.3. Measurement performed on test objects

4.3.1. Pressboard and transformer papers samples

Preliminary measurement

Before the primary measurement, some preliminary measurements were performed on these topics:

1. Linearity properties of pressboard samples (see section 5.1):
 - a. Capacitance – $\tan \delta$ at 50Hz with voltage applied of 200V, 500V, 1kV and 2kV.
 - b. Charging currents with voltage applied of 500V, 5kV and 10kV to obtain $250\text{V}/\text{mm}$ (low stress region), $2.5\text{kV}/\text{mm}$ (middle stress region) and $5\text{kV}/\text{mm}$ (high stress region), respectively.
2. Effect of live electrode corner shape on the distribution of electric field on the pressboard and fluid. The aim was to investigate which corner shape is suitable for dielectric response measurement. The investigation was done based on partial discharge inception voltage and partial discharge current pulse analysis on three type of live electrode corner shape which are rounded-cornered with radius 3mm and 5mm and sharp-cornered electrode (see Appendix C.1).
3. Effect of electrode pressure on the accuracy and preciseness of measurement results. The investigation on capacitance – $\tan \delta$ measurement with various

electrodes pressure of $0.6N/cm^2$, $1.9N/cm^2$, and $3.3N/cm^2$ was performed (see Appendix C.2).

Primary measurement

In the laboratory, the following quantities were measured with temperature as parameter:

1. Complex capacitance – $\tan \delta$ at 50Hz and over wide frequency range of 1mHz – 5kHz
2. Charging currents (for DC conductivity)

The dielectric response measurements were performed before the charging current measurements to avoid the relaxation process that occurred after dc source had been applied. The dielectric response in frequency domain measurement was performed by applying voltage of 200V. Meanwhile, the charging currents measurement was performed by applying voltage of 1kV. Too low of applied voltage when measuring charging current might compromise the results as the current flow might be too small and prone to noise [126] such as when measuring charging currents of Aramid pressboard which possess very low DC conductivity.

The measurement was performed in the test vessel depicted in Figure 4.1. The samples were put between parallel three-electrode configurations as in Figure 4.2 with a pressure of $3.3N/cm^2$. Temperature was the main parameter of the investigation. Three temperature levels were used 25°C (room temperature), 60°C (transformers temperature at normal condition) and 90°C (transformers temperature at overload condition). The samples were measured in insulating fluid bath within the vessel. The insulating fluid for bath is in dry condition with relative moisture content of mineral oil $< 5\text{ppm}$ and ester fluids $< 20\text{ppm}$.

4.3.2. Insulating fluid samples

In the laboratory, the following quantities were measured in accordance with IEC 60247 and using BAUR DTL with temperature as parameter [82]:

1. Relative permittivity – $\tan \delta$ at 50Hz
2. DC resistivity with 500V at 90°C

Both investigations were needed to explain the measurement result of solid samples and given in Appendix D.

4.4. Experiment scheme

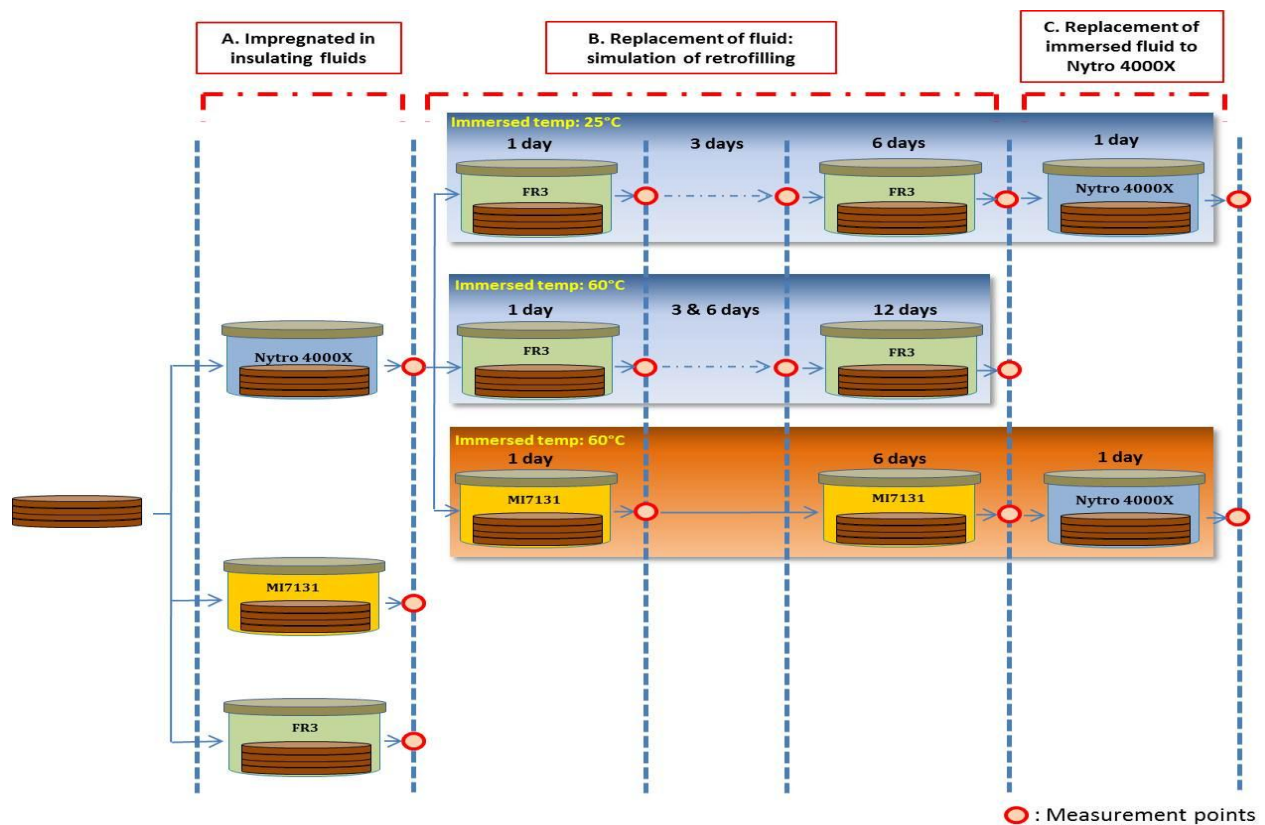


Figure 4.3: Experiment scheme.

Figure 4.3 depicts the experiment scheme in this thesis. The experiments were divided into three steps of measurement, as follows:

1. Dielectric response measurement in time and frequency domain of solids impregnated with three type insulating fluids: mineral oil Nytro 4000X (as the main reference), synthetic ester MI7131 and natural ester FR3 (as the alternative insulating fluids).
2. Simulation of retrofilling with the purpose of investigating time behaviour of dielectric properties solids impregnated with Nytro 4000X after insulating fluid replacement from Nytro 4000X to ester fluids.
3. Investigation of interfacial polarization on the surface of pressboard after the fluid replacement. It was done by replacing the ester fluids in the previous step with Nytro 4000X.

4.5. Measurement set-up

4.5.1. Complex capacitance - $\tan \delta$

Capacitance and $\tan \delta$ measurements have been performed with two different measurement set-ups. The first set-up was intended to investigate the linearity property of pressboard TIV impregnated with mineral oil as depicted in Figure 4.4.

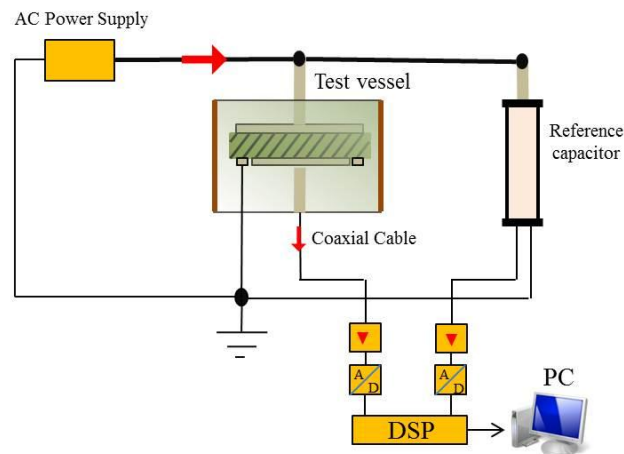


Figure 4.4: Test set-up for capacitance and $\tan \delta$ measurement at 50Hz with applied voltage up to 2kV.

The second set-up was intended to investigate dielectric response of solids impregnated with insulating fluids as depicted in Figure 4.5. Data for power frequency at 50Hz were also taken from the dielectric response measurement results. The dielectric response in frequency domain was measured using the Omicron Dirana which combined Frequency Domain Spectroscopy method (FDS) (for frequency 0.1Hz-5kHz) and Polarization and Depolarization Current method (PDC) in time domain. Data in time domain were transformed to data in frequency domain (for frequency 1mHz-0.1Hz) [86, 127]. Therefore, the dielectric response measurement can be measured over frequency range of 1mHz-5kHz in shorter time duration which is critical for the validity of measurement results.

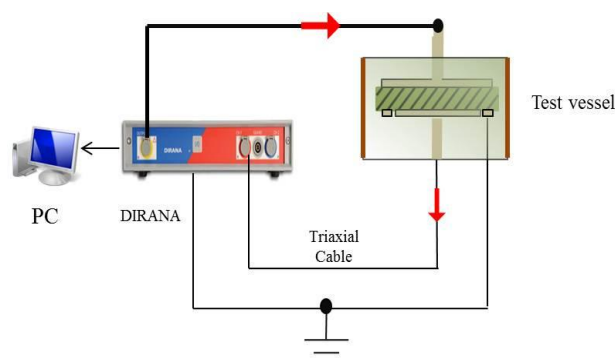


Figure 4.5: Test set-up for capacitance and $\tan \delta$ measurement over wide frequency range.

4.5.2. Electrical conductivity

Test set-up for recording charging current is depicted in Figure 4.6. The charging current was recorded with a Keithley 6514 electrometer. A stabilized DC power supply with ripple factor less than 3% was switched on immediately before recording the charging current. A custom protection circuit was applied as well.

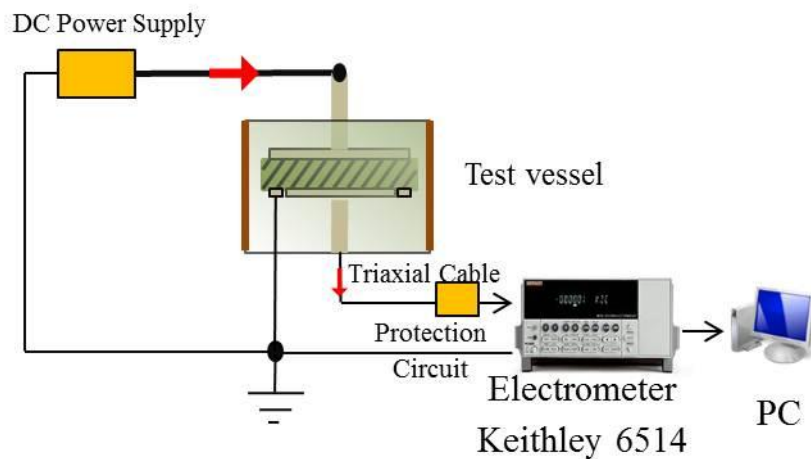


Figure 4.6: Test set-up for charging current measurement.

5. Investigation results and discussion

The results obtained with test objects are presented in this section. The influence of ester fluids on the dielectric properties, temperature dependent behaviour and characteristic of each type solid impregnated with ester fluids are discussed. All solid-fluid combinations have been analysed in total of twenty one combinations.

The samples were prepared in chemical laboratory of Institute of High Voltage Engineering and System Management, TU Graz. At least two samples were measured for each solid-fluid combination to comply with the requirement of IEC 60247. The absolute moisture content of all samples was less than 0.5% and thus, moisture content is not an influenced parameter in this thesis.

Preliminary measurements were performed to investigate the linearity of solid samples before the main measurements.

5.1. Linearity properties of samples

The application of dielectric response theory as described in section 3.2 requires preliminary measurement to check of the samples investigated. This section presents the results of preliminary measurement on linearity properties of solid impregnated samples.

5.1.1. DC conductivity

The linearity of steady state charging current is not clear for solid-fluid insulating system. The preliminary measurement was performed to investigate the influence of electric field stress on the charging current and thus, DC conductivity.

For insulating fluid, it was reported that the steady state conduction current was non-linear under different electric field stress [128]. In physical literature, the electric field stress normally divided into three regions, low (under 1kV/mm), medium (1 to 40 kV/mm), and high (more than 40kV/mm) [129, 129]. Thus, the general shape of current - electric field stress characteristics is different at those regions depend on the source of charge. However, origins of charge carriers for intrinsic or extrinsic conductivity are by no means clear as far as insulating solids are concerned [66].

In this experiment, the measurement of electrical conductivity with three electric field stress i.e. 0.1kV/mm (low), 0.5kV/mm (medium) and 5kV/mm (high) and temperature of 90°C was performed to check the linearity property. The tested object was mineral oil impregnated TIV 2mm pressboard.

Figure 5.1 shows typical electrical conductivity with long time duration of measurement at different electric field stress. In terms of DC conductivity value, higher

electric field stress (up to 5kV/mm) does not increase DC conductivity value significantly. Normally, at higher electric field stress, the conductivity does not only depend on charge carriers which generated in the test object based on its chemical structure (intrinsic conductivity) but also charge carrier which are injected into the test object mainly from metallic electrodes (injection-controlled conductivity) or other process [66, 73]. In our experiment, up to electric field stress of 5kV/mm, different conduction process did not occur and thus, the linearity properties of solid impregnated with fluid is preserved. The same result was reported in [126, 131]. Therefore Ohm's law can be applied.

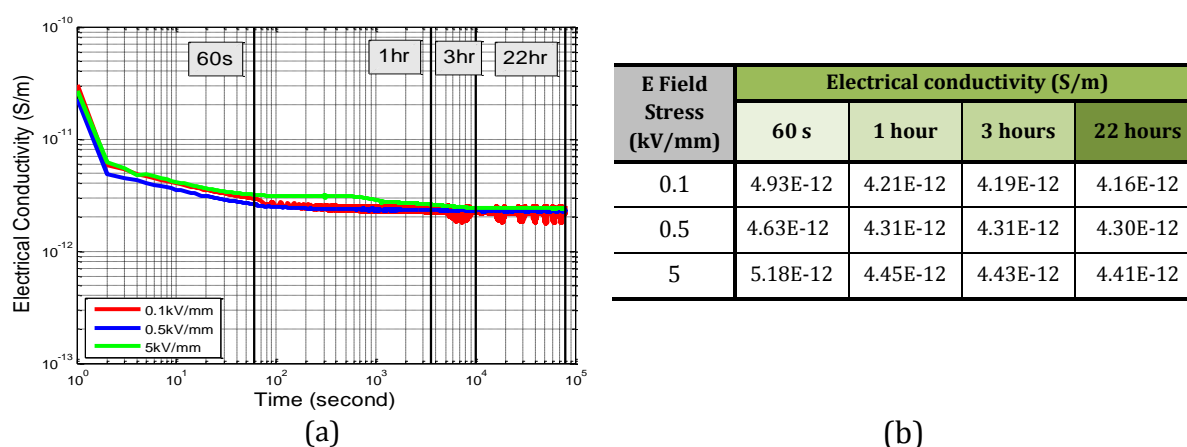


Figure 5.1: (a) Influence of electric field stress onto electrical conductivity and (b) changing of electrical conductivity with time.

5.1.2. Capacitance - $\tan \delta$

At the beginning, the investigation on the linearity properties of capacitance - $\tan \delta$ at wide range frequency using custom AC source with frequency of (0.1Hz - 1kHz) and maximum voltage of 2 kV was examined. However, it was found out that the measurement system LDIC TD Smart (Electronic Bridge) and Universal Schering Bridge were not able to measure dielectric properties at low frequency of 0.1Hz and at 1kHz. At 1kHz, measuring with LDIC TD Smart (Electronic Bridge) showed negative $\tan \delta$ value (not shown in this thesis) which is not correct. Therefore, the measured was only performed at 50Hz to investigate the linearity properties in frequency domain using LDIC TD Smart with applied voltage from 200V - 2kV. Linearity for cellulose pressboard impregnated with mineral oil at low applied voltage of 1 -140V has been investigated in [80].

The measurement on linearity properties in frequency domain was performed of pressboard TIV and Nomex impregnated with Nytro 4000X. Figure 5.2 depicts the relative permittivity and $\tan \delta$ for TIV. $\tan \delta$ and relative permittivity of dry TIV impregnated with Nytro 4000X is not influenced by electric field stress up to 1kV/mm. It was reported in [5] that $\tan \delta$ of dry un-impregnated kraft paper is not influenced by electric field stress at 30°C.

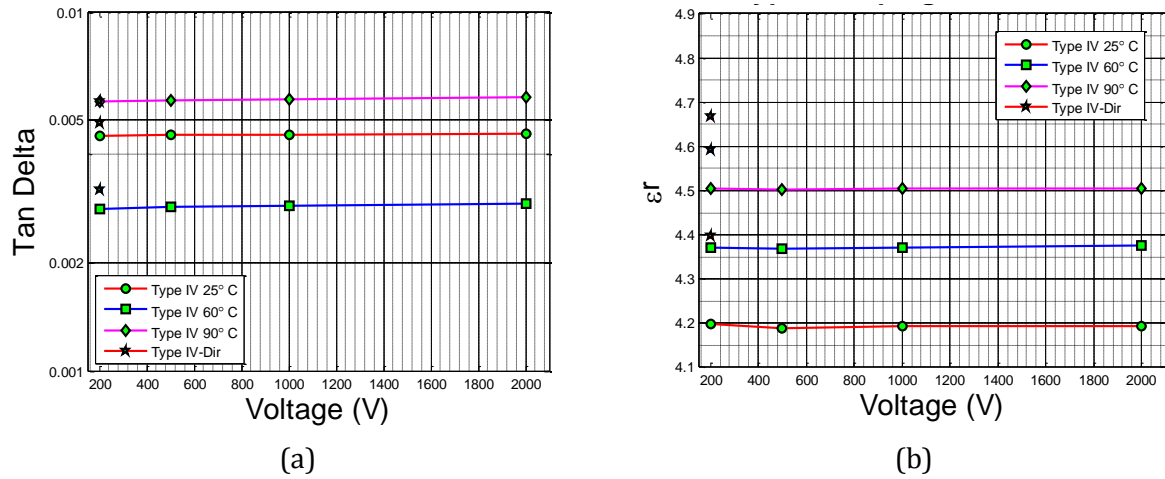


Figure 5.2: Voltage dependencies of (a) $\tan \delta$ and (b) relative permittivity of pressboard TIV 2mm.

Figure 5.3 depicts the relative permittivity and $\tan \delta$ for Nomex impregnated with Nytro 4000X. As in for cellulose pressboard TIV, $\tan \delta$ and relative permittivity of dry Nomex impregnated with Nytro 4000X is also not influenced by electric field stress up to 1kV/mm. Hence, the linearity properties of Nomex impregnated with mineral oil is preserved up to electric field stress 1kV/mm. There was no Gärton effect observed from the measurement results up to 1kV/mm. The Gärton effect refers to insulating fluid medium but it also can be applied for solids. It explains the variation of $\tan \delta$ with applied voltage in terms of an ionic cloud motion, whose amplitude becomes limited by the boundaries enclosing the fluid [46]. This behaviour would be marked by the decrease of $\tan \delta$ value with increase of electric field stress.

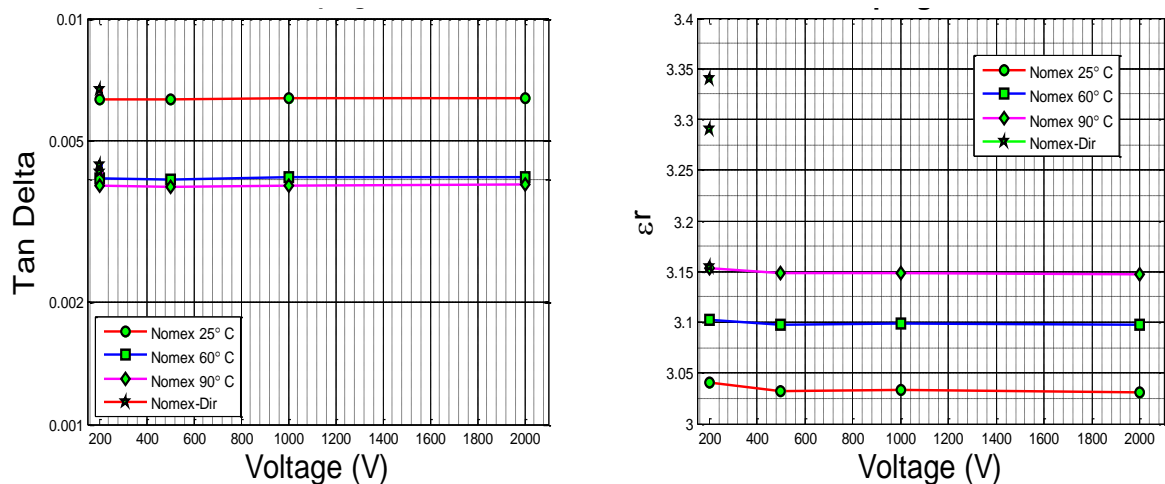


Figure 5.3: Voltage dependencies of (a) $\tan \delta$ and (b) relative permittivity of pressboard Nomex 2mm.

5.2. DC conductivity of solid impregnated with ester fluids

After the investigation on the linearity properties of pressboard impregnated with mineral oil, DC conductivity measurement of solid impregnated with ester fluids were performed on two samples.

Figure 5.4 presents typical long time duration charging current of pressboard TIV impregnated with Nytro 4000X and MI7131. A charging voltage V_c of 1kV for pressboard and 200V for transformer papers was applied until the charging current has reach steady state value. Then DC conductivity value was calculated from the steady state current.

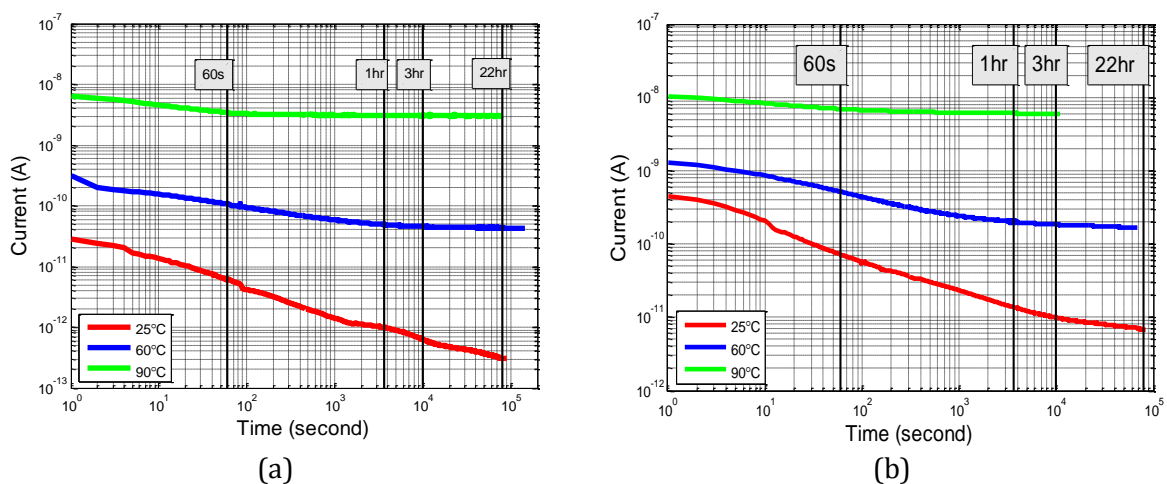


Figure 5.4: Charging current of pressboard TIV impregnated with (a) Nytro 4000X and (b) MI7131.

The DC conductivity measurement was performed on three temperature levels i.e. 25°C, 60°C and 90°C except for some samples combination impregnated with Nytro 4000X. The aim is to investigate temperature dependent behavior of DC conductivity. Temperature dependent behavior of pressboard impregnated with mineral oil can be characterized by the activation energy according to Arrhenius relation in equation (3.64) [2]. Figure 5.5 presents the Arrhenius plot of logarithmic shift for solids impregnated with (a) Nytro 4000X, (b) MI7131 and (c) FR3. DC conductivity value is very sensitive to the rise of temperature. The increase of DC conductivity of solids impregnated with ester fluids also follows Arrhenius relation.

Table 5.1 shows the DC conductivity of solids impregnated with Nytro 4000X, MI7131 and FR3. DC conductivity of solids impregnated with Nytro 4000X is generally lower than of solids impregnated with ester fluids, MI7131 and FR3. Ester fluids have higher conductivity and higher relative permittivity than mineral oil. High relative permittivity means that the insulating fluid contains more ionic impurities (high ion concentration) [68]. Ionic impurities generate high conductivity of ester fluids. Hence, solids impregnated with ester fluids have higher DC conductivity compared to solids impregnated with mineral oil. It indicates that the DC conductivity of solid

impregnated material has strong dependency on the conductivity of the insulating fluids. DC conductivity of transformer papers is generally higher compared to pressboard. It might be due to transformer papers are very thin, therefore the fluid characteristic is more dominant than in pressboard. From all solid samples, Nomex has the lowest DC conductivity and it also follows Arrhenius relation.

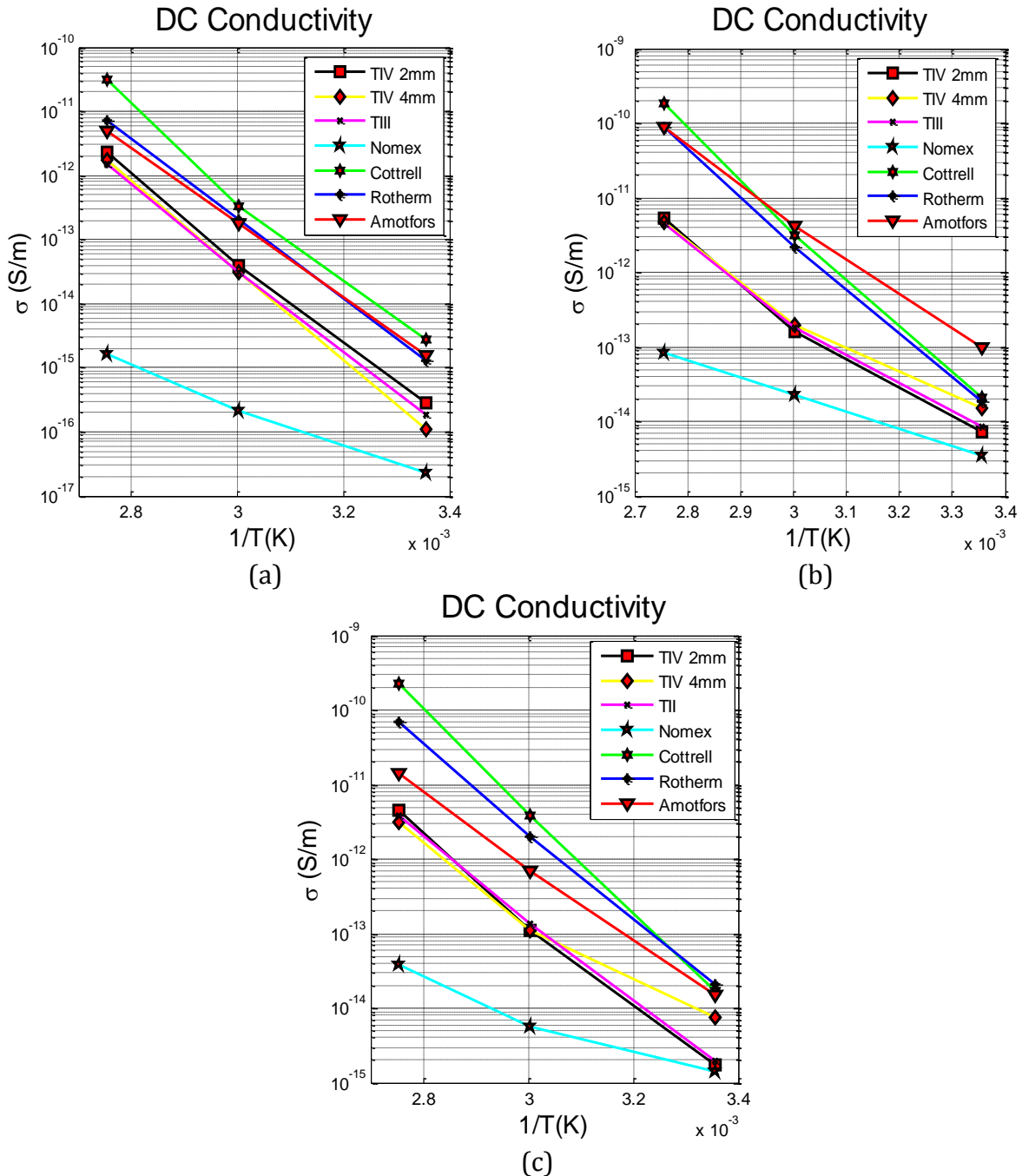


Figure 5.5: DC conductivity of solid impregnated with (a) Nytro 4000X, (b) MI7131 and (c) FR3 at temperature of 25°C, 60°C and 90°C.

Table 5.1: Dielectric properties of solid impregnated with dielectric fluid.

Type	Temp.	DC conductivity (S/m)		
		Nytro 4000X	MI7131	FR3
Weidmann B.3.1A (TIV) 2mm	25°C	2.77E-16	7.20E-15	1.75E-15
	60°C	3.89E-14	1.57E-13	1.09E-13
	90°C	2.30E-12	5.25E-12	4.60E-12
Weidmann B.3.1A (TIV) 4mm	25°C	1.11E-16	1.49E-14	7.41E-15
	60°C	3.13E-14	1.94E-13	1.11E-13
	90°C	1.70E-12	4.68E-12	3.07E-12
Weidmann B.4.1 (TIII) 2mm	25°C	1.81E-16	8.46E-15	1.93E-15
	60°C	3.06E-14	1.78E-13	1.34E-13
	90°C	1.52E-12	4.52E-12	3.78E-12
DuPont Nomex T-993 2mm	25°C	2.28E-17	3.52E-15	1.39E-15
	60°C	2.17E-16	2.26E-14	5.62E-15
	90°C	1.63E-15	8.22E-14	3.83E-14
Cottrell CK 125-TU 0.076mm	25°C	2.77E-15	2.10E-14	1.72E-14
	60°C	3.23E-13	3.11E-12	3.80E-12
	90°C	3.15E-11	1.86E-10	2.28E-10
Tullis Russel Rotherm HIHD 0.085mm	25°C	1.40E-15	1.84E-14	2.09E-14
	60°C	2.04E-13	2.19E-12	2.01E-12
	90°C	7.10E-12	8.99E-11	6.85E-11
Nordic Paper Amotfors 0.080mm	25°C	1.55E-15	9.64E-14	1.50E-14
	60°C	1.76E-13	4.08E-12	6.89E-13
	90°C	4.91E-12	8.89E-11	1.43E-11

Activation energy of DC conductivity can be calculated from (a) DC conductivity at two different temperatures with equation (3.65) and (b) gradient of DC conductivity line in Figure 5.5. Table 5.2 presents the activation energy of DC conductivity of all tested samples. Activation energy of all solids at high temperature of 60-90°C is not influenced by the insulating fluids. For cellulose solids, it is about 111-125kJ/mol and aramid pressboard, it is about 44-64kJ/mol. However, at temperature of 25-60°C, the activation energy of pressboards impregnated with ester fluids is generally lower than of pressboards impregnated with mineral oil. This might relate to the dominant effect of interfacial space charge polarization when pressboards impregnated with ester fluids. It was reported in [48] that the onset of space charge effect tends to decrease the value of activation energy of DC conductivity. The existence of space charge influences the field acting at the ionizable centres which means that the steady state applied field is modified by the presence of interfacial space charge in such a way that the resultant field appearing in each component of the compound specimen ensures that the boundary conditions for displacement and field are satisfied, and that current density is continuous. It also seems that the influence of space charge on solids impregnated samples is affected by viscosity of insulating fluids because the difference of activation energy occurs at low temperature. It is also noticeable that the activation

energy of DC conductivity of transformer papers has low dependency with the insulating fluids. It might relate to the thickness of transformer papers which is below 0.1mm.

Table 5.2: Activation energy of DC conductivity.

Type	Nytro 4000X	MI7131		FR3	
	Activation energy (kJ/mol)	Activation energy (kJ/mol)		Activation energy (kJ/mol)	
	Gradient Curve	20-60°C	60-90°C	20-60°C	60-90°C
Weidmann B.3.1A (TIV) 2mm	122.61	74.1	118.41	97.42	125.4
Weidmann B.3.1A (TIV) 4mm	133.72	60.39	106.84	63.82	111.26
Weidmann B.4.1 (TIII) 2mm	123.61	71.83	108.38	99.97	111.9
DuPont Nomex T-993 2mm	58.14	43.84	43.36	32.94	64.31
Cottrell CK 125-TU 0.076mm	128.09	119.8	132.24	127.4	137.18
Tullis Russel Rotherm HIHD 0.085mm	119.1	112.68	124.47	107.71	118.23
Nordic Paper Amotfors 0.080mm	111.52	88.31	103.25	90.24	101.61

In terms of the relaxation time, it was noticed that at higher temperature, the relaxation time is exponentially faster as shown in Figure 5.6. Faster relaxation time means that the time needed to reach steady state is exponentially faster. At 90°C, the current reaches steady state value much faster (less than 2 hours) than at lower temperature (the decreasing rate is faster) e.g. at 25°C and it takes approximately between 22-30 hours. This behavior may be explained by the change of relaxation time with temperature change. High temperature accelerates relaxation time of polarization mechanism. The temperature dependent behaviour of relaxation process (time) of solid-fluid insulating system can be expressed by Arrhenius relation, as in equation (5.1) [132]:

$$\tau = \tau_0 e^{E_{DC}/kT} \quad (5.1)$$

Yet, the measured and calculated relaxation time are slightly different.

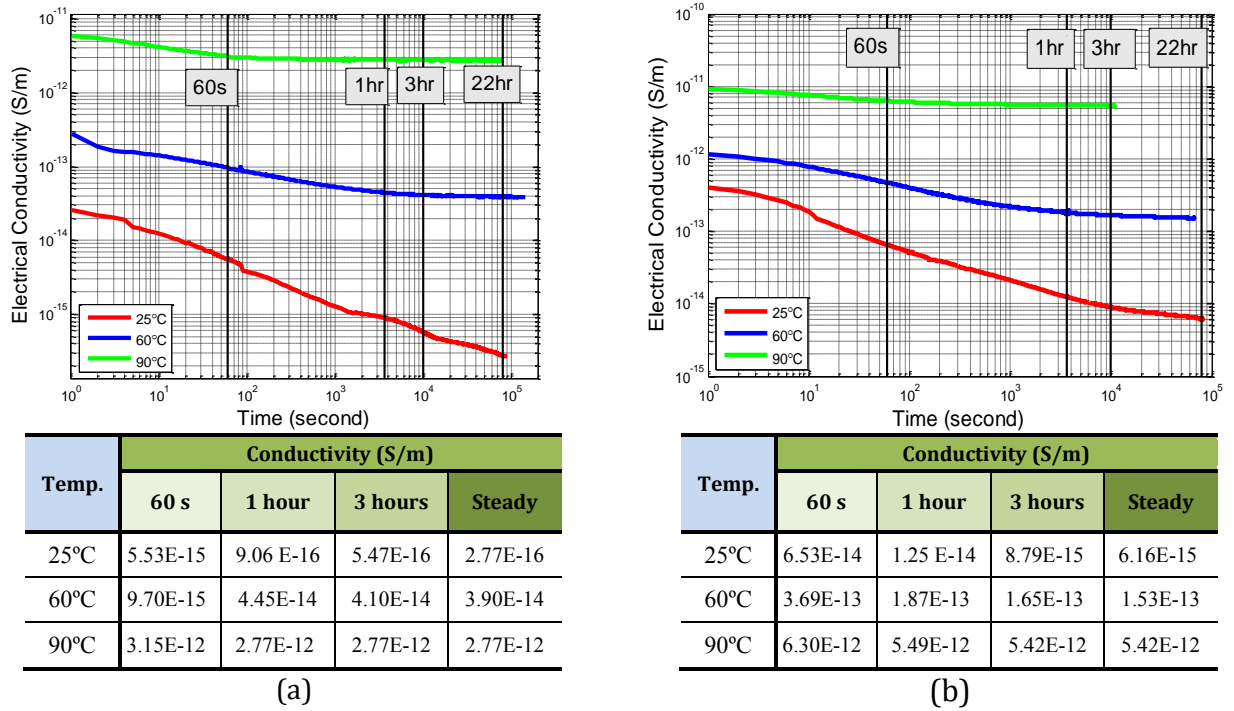


Figure 5.6: Electrical conductivity of pressboard TIV impregnated with (a) Nytro 4000X and (b) MI7131. Note: value of steady state conductivity different with DC conductivity in Table 5.1 as this figure depicts results from one sample.

Estimation of DC conductivity

Temperature dependent behavior of DC conductivity behaviour for all solid-fluid insulating combinations follows Arrhenius relation. Thus, DC conductivity can be estimated using Arrhenius relation as in equation (5.2)

$$\sigma = A_{DC} e^{-E_{DC}/K.T} \quad (5.2)$$

From the measurement results, the activation energy DC conductivity E_{DC} and pre-exponential factor A_{DC} for each combination was obtained. The pre-exponential factor was calculated from the measurement results at three temperatures and holds no physical meaning. The activation energy of DC conductivity E_{DC} was calculated from the gradient of DC conductivity with temperature in Figure 5.5 due to simplicity reason. The estimation of DC conductivity with temperature as parameter using Arrhenius relation is convenient. Table 5.3 to Table 5.5 show the comparison of measured and estimated DC conductivity and its pre-exponential factor. The estimated DC conductivity is in the same range with the measured value and below ten times of the allowable reproducibility according to IEC 60093. Therefore, the DC conductivity can be estimated for temperature other than 25°C, 60°C, and 90°C using equation (5.2).

Table 5.3: Activation energy, pre-exponential factor and estimated value of DC conductivity of solids impregnated with Nytro 4000X.

Type	Temperature (°C)	DC conductivity (S/m)		Pre-exp Factor	Activation Energy (kJ/mol)
		Measured	Calculated		Gradient Curve
Weidmann B.3.1A (TIV) 2mm	25	2.77E-16	2.47E-16	8.42E+05	122.61
	60	3.89E-14	4.48E-14		
	90	2.30E-12	1.74E-12		
Weidmann B.3.1A (TIV) 4mm	25	1.11E-16	1.09E-16	2.97E+07	133.72
	60	3.13E-14	3.16E-14		
	90	1.7E-12	1.71E-12		
Weidmann B.4.1 (TIII) 2mm	25	1.81E-16	1.69E-16	8.07E+05	123.61
	60	3.06E-14	3.18E-14		
	90	1.52E-12	1.27E-12		
DuPont Nomex T-993 2mm	25	2.28E-17	1.99E-17	3.38E-07	58.14
	60	2.17E-16	2.34E-16		
	90	1.63E-15	1.33E-15		
Cottrell CK 125-TU 0.076mm	25	2.77E-15	1.6E-15	1.03E+08	128.09
	60	3.23E-13	4.37E-13		
	90	3.15E-11	2.07E-11		
Tullis Russel Rotherm HIHD 0.085mm	25	1.3E-15	1.3E-15	1.01E+06	119.1
	60	2.04E-13	2.04E-13		
	90	7.1E-12	7.16E-12		
Nordic Paper Amotfors 0.080mm	25	1.55E-15	1.55E-15	5.45E+04	111.52
	60	1.76E-13	1.76E-13		
	90	4.91E-12	4.91E-12		

Table 5.4: Activation energy, pre-exponential factor and estimated value of DC conductivity of solids impregnated with MI7131.

Type	Temperature (°C)	DC conductivity (S/m)		Pre-exp Factor	Activation Energy (kJ/mol)
		Measured	Calculated		Curve Gradient
Weidmann B.3.1A (TIV) 2mm	25	7.20E-15	5.94E-15	4.00E+01	90.32
	60	1.57E-13	2.74E-13		
	90	5.25E-12	4.06E-12		
Weidmann B.3.1A (TIV) 4mm	25	1.49E-14	1.31E-14	5.11E-01	77.55
	60	1.93E-13	3.52E-13		
	90	4.68E-12	3.56E-12		
Weidmann B.4.1 (TIII) 2mm	25	8.46E-15	7.64E-15	6.28E+00	85.1
	60	1.78E-13	2.82E-13		
	90	4.52E-12	3.58E-12		
DuPont Nomex T-993 2mm	25	3.52E-15	3.59E-15	1.34E-07	43.21
	60	2.26E-14	2.24E-14		
	90	8.22E-14	8.14E-14		
Cottrell CK 125-TU 0.076mm	25	2.1E-14	2.03E-14	1.13E+08	123.15
	60	3.11E-12	3.92E-12		
	90	1.86E-10	1.59E-10		
Tullis Russel Rotherm HIHD 0.085mm	25	1.84E-14	1.82E-14	4.10E+06	116.13
	60	2.19E-12	2.51E-12		
	90	8.99E-11	8.04E-11		
Nordic Paper Amotfors 0.080mm	25	9.64E-14	9.35E-14	2.00E+03	93.18
	60	4.08E-12	4.87E-12		
	90	8.89E-11	7.86E-11		

Table 5.5: Activation energy, pre-exponential factor and estimated value of DC conductivity of solids impregnated with FR3.

Type	Temperature (°C)	DC Conductivity (S/m)		Pre-exp Factor	Activation Energy (kJ/mol)
		Measured	Calculated		Curve Gradient
Weidmann B.3.1A (TIV) 2mm	25	1.75E-15	1.63E-15	9.92E+03	107.18
	60	1.09E-13	1.54E-13		
	90	4.60E-12	3.77E-12		
Weidmann B.3.1A (TIV) 4mm	25	7.41E-15	6.52E-15	1.16E+00	81.32
	60	1.11E-13	2.05E-13		
	90	3.07E-12	2.32E-12		
Weidmann B.4.1 (TIII) 2mm	25	1.93E-15	1.9E-15	2.72E+03	103.59
	60	1.34E-13	1.54E-13		
	90	3.78E-12	3.39E-12		
DuPont Nomex T-993 2mm	25	1.39E-15	1.25E-15	8.22E-08	44.6
	60	5.62E-15	8.32E-15		
	90	3.83E-14	3.15E-14		
Cottrell CK 125-TU 0.076mm	25	1.71E-14	1.72E-14	1.02E+09	129.95
	60	3.8E-12	4.25E-12		
	90	2.28E-10	2.05E-10		
Tullis Russel Rotherm HIHD 0.085mm	25	2.09E-14	2.07E-14	5.27E+05	110.72
	60	2.01E-12	2.27E-12		
	90	6.85E-11	6.19E-11		
Nordic Paper Amotfors 0.080mm	25	1.5E-14	1.51E-14	3.23E+02	93.18
	60	6.89E-13	7.86E-13		
	90	1.43E-11	1.27E-11		

5.3. Dielectric response over frequency range of 1mHz – 5kHz

The objective of section 5.3 is to investigate the influence of insulating fluids and temperature on the dielectric properties behaviour. The effect of those factors could be observed over wide range frequency measurement.

5.3.1. Basic knowledge

There are several dominant ionic loss mechanisms which is active in the solid-fluid insulating systems [76]: long range ionic migration, interfacial space charge polarization and short range ionic jump trapping-detrapping processes within the solid paper structure. The interfacial space charge polarization might occur in the insulating fluid phase itself, in the cellulose fiber structure of the pressboard or paper

and at the solid-fluid interfaces having varied geometry (one of the most dominant is on the surface of pressboard).

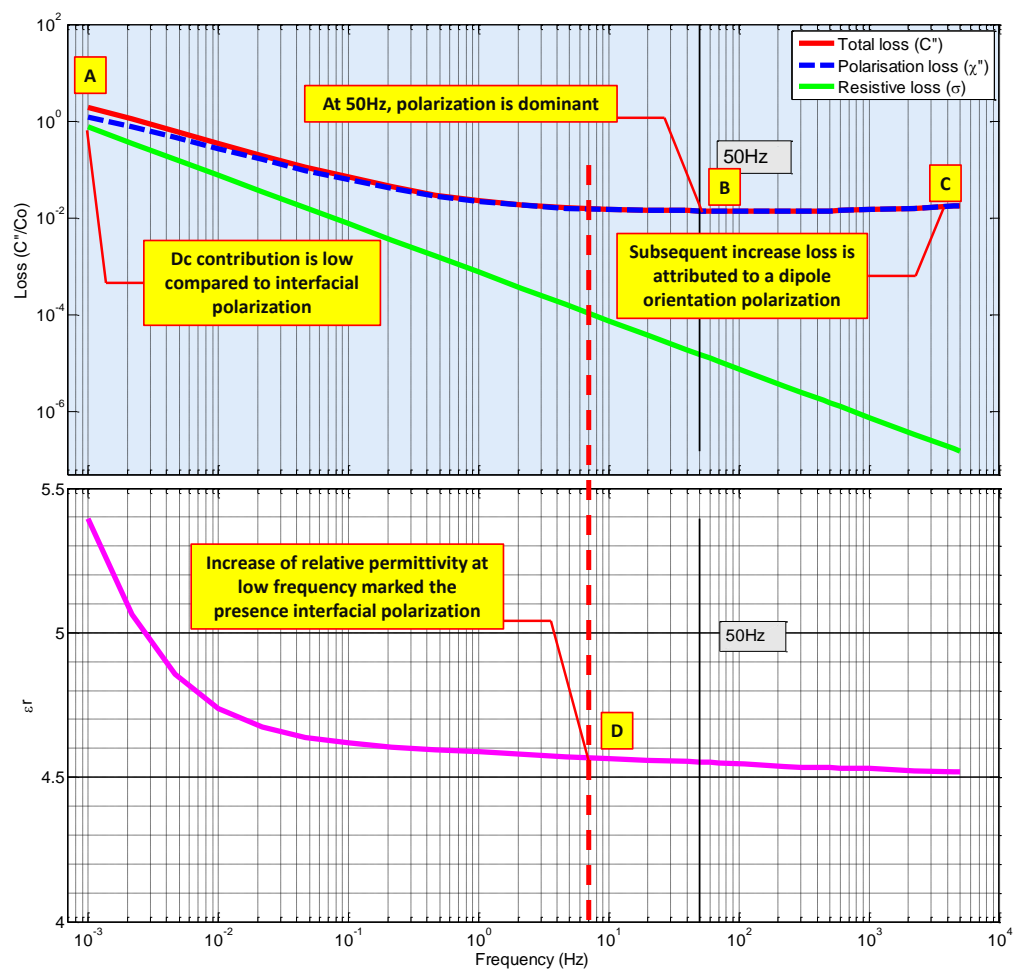


Figure 5.7: General dielectric response of loss and relative permittivity over wide range frequency.

Over wide frequency, from low (<1mHz) up to power frequency, it is either the existence of either long range ionic migration (as dc conduction), interfacial space charge polarization, or dipolar orientation polarization is most dominant. Mainly, it depends on the temperature and the characteristic of insulating materials. The existence of those mechanisms can be ascertained from wide range frequency of dielectric response $\tan \delta$ and relative permittivity. When only long-range ionic migration is involved, the relative permittivity value will remain constant at low frequency while the $\tan \delta$ will increase with decrease of frequency. Meanwhile, when the interfacial space charge polarization is presence, and then in the vicinity of the absorption frequency (see section 3.1.2), the relative permittivity and total loss ($\tan \delta$) value will increase with decrease of frequency as total loss ($\tan \delta$) reaches maximum, marked by point D in Figure 5.7.

In case of solid-fluid insulating system, generally, the dielectric response loss characteristic and relative permittivity are as depicted in Figure 5.7. At low frequency, the dominant conduction mechanism is long range ionic migration (dc conduction) and interfacial space-charge polarization (refers to polarization loss), marked by point A in Figure 5.7. It is also clear that dc conduction (marked by resistive loss (green line)) decrease rapidly with the increase of frequency and thus, at power frequency the dominant factor is interfacial polarization mechanism or dipole orientation polarization, marked by point B in Figure 5.7. The lower rate of decrease of $\tan \delta$ with increase of frequency over the power frequency indicates the presence of the dipole orientation loss, the short range charge carrier hopping and interfacial polarization mechanism. Finally, in the range of frequencies extending upwards, some residual dipole contribution to the overall total loss may occur as a result of the remnant dipole loss due to the dipole orientation of the larger molecules in the fluid and solid. It is marked by the increase of $\tan \delta$, marked by point C in Figure. However, it should be understood that the dominant polarization mechanism at certain frequency depends highly on the temperature and insulating material characteristic as it affect the relaxation time of polarization (see section 3.2). Consequently, it is possible at low temperature, the most dominant polarization mechanism is dipole orientation polarization rather than interfacial polarization.

This basic knowledge might help to explain the measurement results of dielectric response in frequency domain. In this thesis, the analysis is based on the conventional point of view as it is more appropriate for solid-fluid insulating system.

5.3.2. Influence of insulating fluids on dielectric response

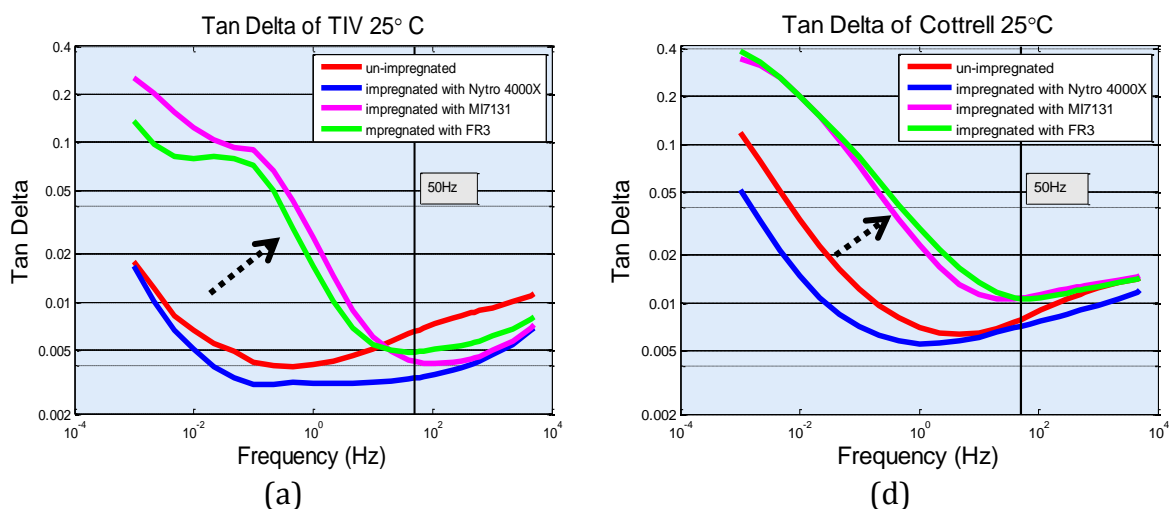
Figure 5.8 shows dielectric response $\tan \delta$ of all solid-fluid insulating system combinations at 25°C. $\tan \delta$ of solid-fluid insulating system at temperature of 25°C is mostly dominated by polarization loss in the frequency of 0.1mHz - 5kHz because the DC conductivity contributes less than 7% of total loss (see section 5.3.6). Thus, the influence of insulating fluid on polarization mechanism of the solid-fluid insulating system can be explained by dielectric response $\tan \delta$ at 25°C.

In Figure 5.8, red line represents un-impregnated solids, blue line represents Nytro 4000X impregnated solids, green line represents FR3 impregnated solids and pink line represents MI7131 impregnated solids. The dielectric response $\tan \delta$ of un-impregnated solid is used as reference. The shape of dielectric response $\tan \delta$ for solid impregnated with Nytro 4000X resembles that of un-impregnated pressboard. Meanwhile, the shape of dielectric response $\tan \delta$ for solid impregnated with ester fluids is different with that of un-impregnated solid. There is significant increase of $\tan \delta$ value and the presence of loss peak in dielectric response $\tan \delta$ at frequency between 0.01-1Hz for pressboard samples. The presence of loss peak is an indicator of relaxation time (thus, absorption frequency) of certain polarization mechanism. The loss peak at the measured frequency does not present for un-impregnated pressboard

or pressboard impregnated with Nytro 4000X. It implies that natural or synthetic ester fluids generate an additional polarization mechanism when used as impregnating fluid. The additional polarization mechanism is characterized by the presence of a new loss peak on the dielectric response $\tan \delta$. It indicates that when cellulose pressboards impregnated with ester fluids, the polarization has distribution of relaxation times at frequency $<100\text{Hz}$ marked by the presence of additional loss peak, especially for natural ester. The additional peak is also present in Nomex impregnated with ester fluids, but it is not as obvious as in cellulose pressboards TIV and TIII. Similar dielectric response $\tan \delta$ curve for pressboard impregnated with natural ester was also observed in [59], but there was no sufficient explanation on this phenomenon. Based on analysis in section 6.3, it was observed that the loss peak relates to interfacial polarization on the surface of pressboard.

The possible cause for the distribution relaxation times of interfacial space charge polarization may be from the fact that ester fluids have high kinematic viscosity, high DC conductivity (hence, the charge buildups on the surface) and coupled by its molecular characteristic because the loss peak does not occur for pressboard impregnated with mineral oil and silicone fluid (reported in [46]).

Figure 5.8 also shows that generally $\tan \delta$ of transformer papers is higher than pressboard eventhough the material density is almost equal. Actually, it relates to the extreme difference of thickness between them. The relaxation time depends on the thickness of material due to the charge carrier transit time across half of dielectric thickness. According to equation (3.14), low thickness material will have low relaxation time and thus high absorption frequency $f_{m'} = 1/2\pi \cdot \tau'$. This means that the dielectric loss maximum for transformer paper is located at higher frequency compared to pressboard due to its thickness. Hence, dielectric response $\tan \delta$ of transformer papers has high absorption frequency and therefore, high $\tan \delta$ value at 50Hz compared to pressboard.



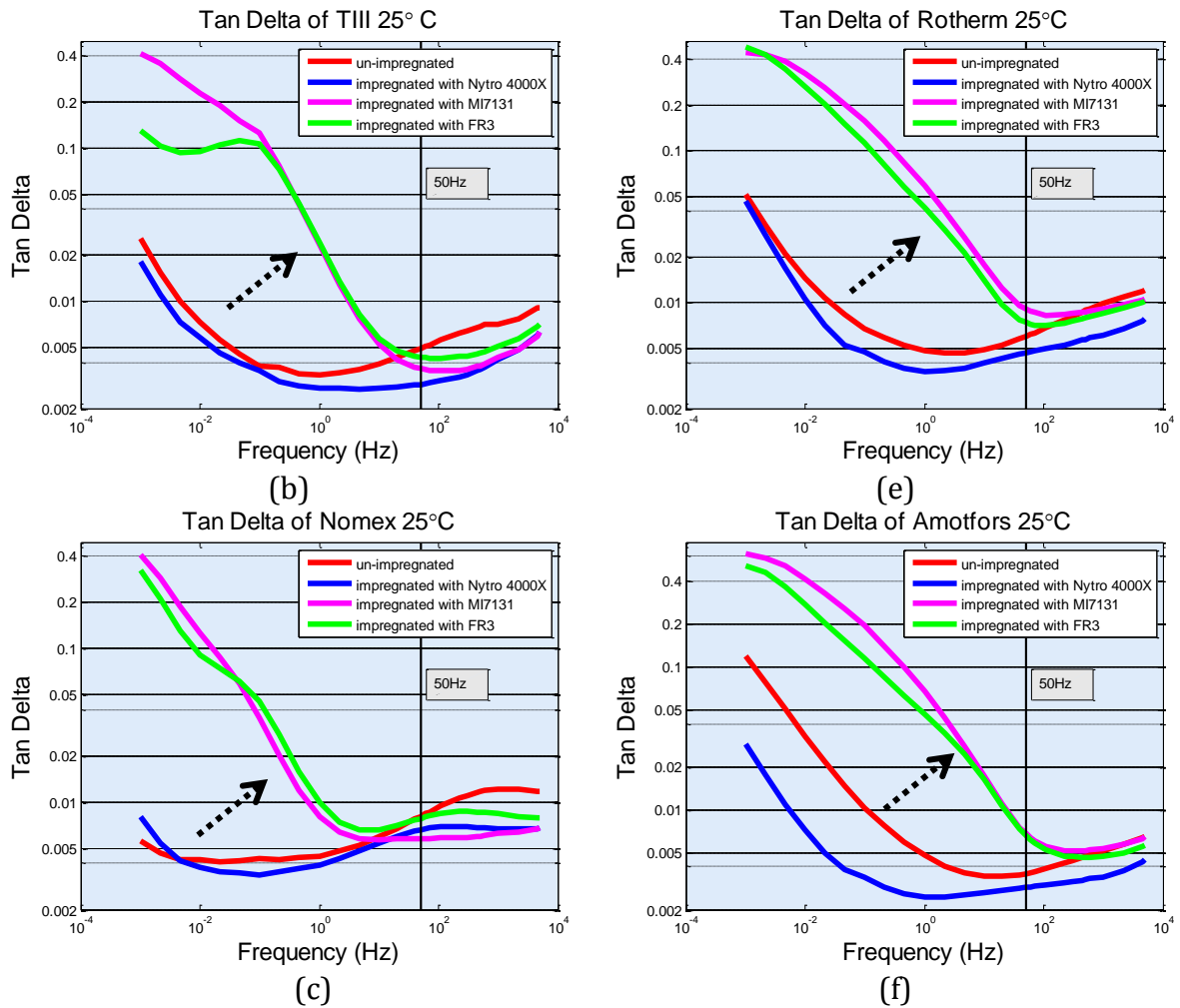


Figure 5.8: Dielectric response $\tan \delta$ of (a) TIV, (b) TIII, (c) Nomex, (d) Cottrell, (e) Rotherm and (f) Amotfors impregnated with insulating fluids at 25°C.

Figure 5.9 shows the dielectric response relative permittivity of all solid-fluid insulating system combinations at 25°C. Solids impregnated with ester fluids possess higher relative permittivity and it increases rapidly with decrease of frequency. According to the theory of effective relative permittivity of composite dielectric, higher permittivity at power frequency for solids impregnated with ester fluids is caused by the fact that ester fluids possess higher relative permittivity.

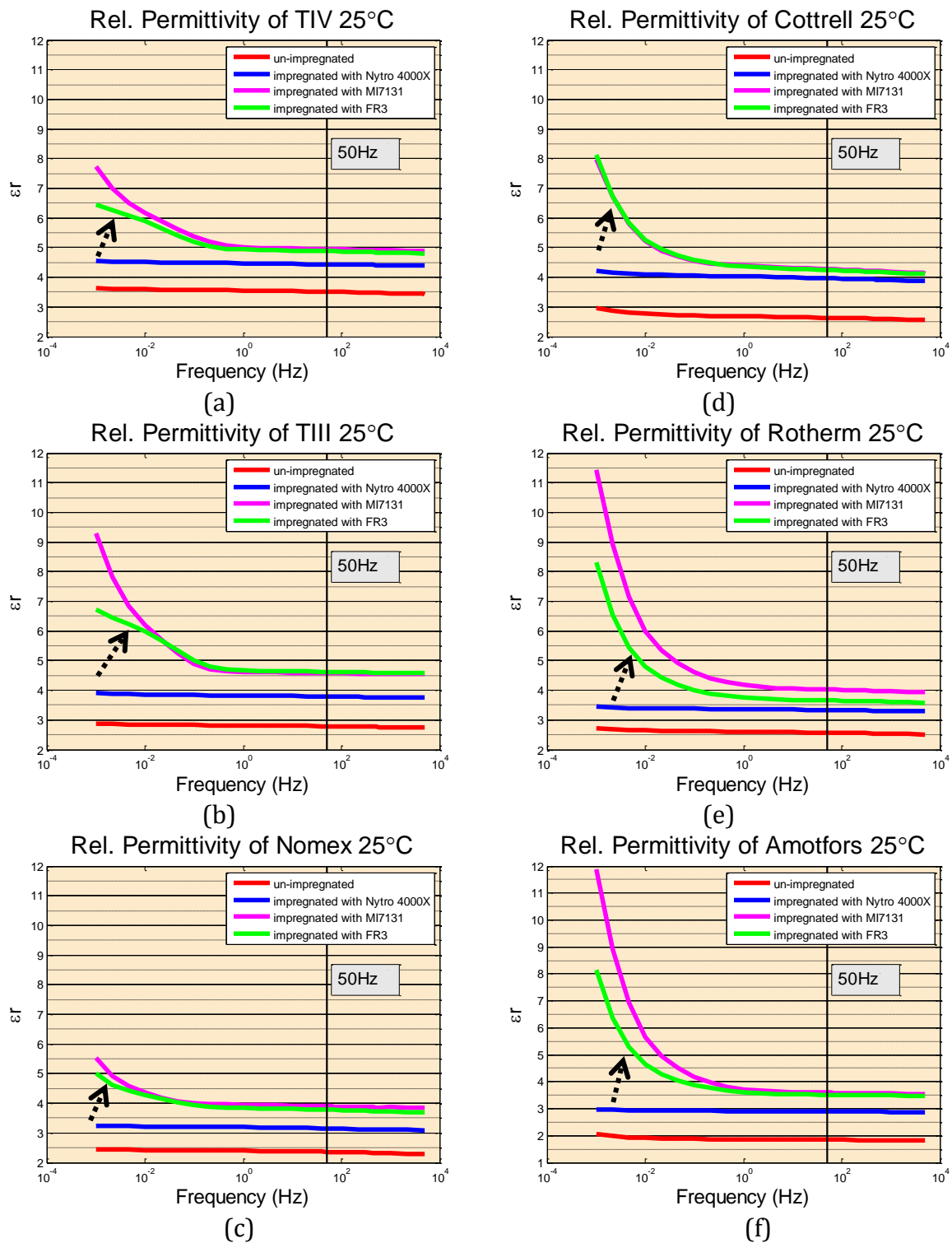


Figure 5.9: Dielectric response relative permittivity of (a) TIV, (b) TIII, (c) Nomex, (d) Cottrell, (e) Rotherm and (f) Amotfors impregnated with insulating fluids at 25°C.

Theoretically, the rapid increase of relative permittivity with decrease of frequency indicates the presence of interfacial polarization in solid-fluid insulating system. The interfacial polarization is more dominant for solid impregnated with ester fluids compared to mineral oil. The influence of synthetic ester to interfacial polarization is greater than that of natural ester. It is marked by the steeper relative permittivity

increase with decrease of frequency. Thus, it confirms that the additional loss peak is caused by distribution of relaxation time of interfacial polarization that occurs when solid impregnated with ester fluids.

It should be noticed that the polarization mechanism affects dielectric response $\tan \delta$ and relative permittivity of cellulose and aramid pressboards in different way as indicated by the presence of additional loss peak for cellulose pressboard.

Mineral oil (Nytro 4000X) influences the polarization characteristic of solid samples (indicated by different relaxation time) but does not change the characteristic of polarization mechanism, since the dielectric response curve shape of solid impregnated with Nytro 4000X is similar to the curve of un-impregnated solids. Meanwhile, ester fluids, whether it is synthetic ester MI7131 or natural ester FR3, change the polarization characteristic of solid samples. It is evident from different relaxation time of interfacial polarization and the presence of additional peak loss in dielectric response $\tan \delta$ and relative permittivity. The interfacial polarization is also more dominant for solids impregnated with ester fluids even at room temperature and it is marked by the rapid increase of relative permittivity with decrease of frequency. The explanation for this phenomenon may be related to the relaxation time of polarization due to space charge effect.

According to equation (3.14) the relaxation time depends on many factors such as temperature, relative permittivity at very high frequency and charge carrier concentration. In regard to insulating fluids characteristic, the difference of relaxation time for solids impregnated with mineral oil and ester fluids may be related to charge carrier concentration. Ester fluids possess higher relative permittivity than mineral oil. Insulating materials with high relative permittivity means that it dissolve and dissociate more ionic impurities than insulating material with low relative permittivity [68]. Hence, it is possible that ester fluids possess higher ionic concentration than mineral oil and subsequently, this decreases the relaxation time of polarization which suggests the shift of absorption peak to higher frequency.

5.3.3. Influence of polymer material on the dielectric response

Figure 5.10 compares the dielectric response $\tan \delta$ of pressboard TIV (cellulose pressboard) and Nomex (aramid pressboard) at temperature of 25°C, 60°C and 90°C. It is clear that different polymer material possess different polarization characteristic. Dielectric response $\tan \delta$ of aramid pressboard is less affected by DC conductivity over the measured frequency and temperature range (see section 5.3.6 for loss contribution characteristics of Nomex). For Nomex, the total loss mainly depends on the polarization mechanism even at high temperature.

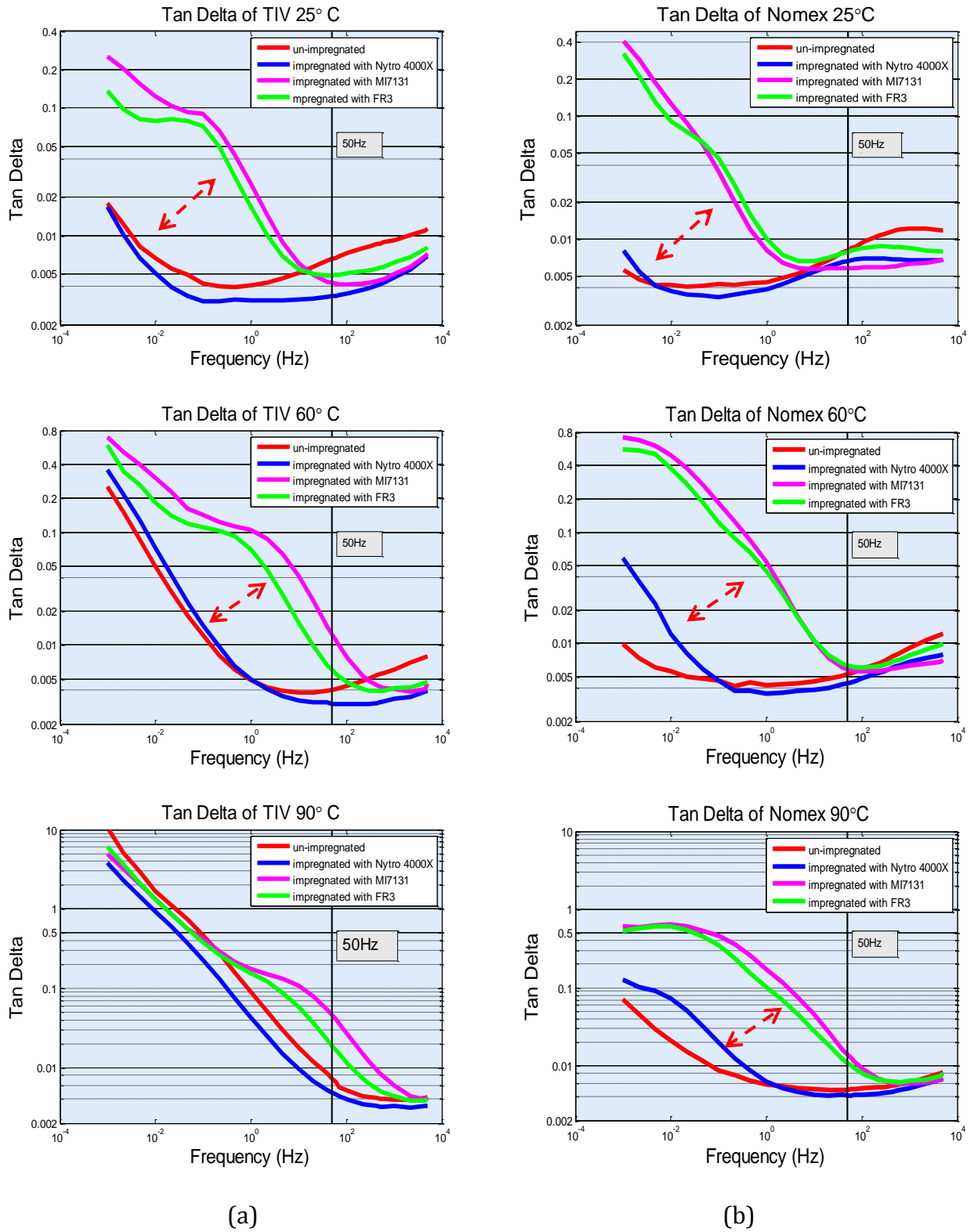


Figure. 5.10: Dielectric response $\tan \delta$ of (a) TIV (cellulose) and (b) Nomex (aramid) at temperature of 25°C, 60°C and 90°C.

Both cellulose and aramid pressboards are influenced by ester fluids which change the polarization characteristics on both polymers drastically. It is evident by the huge increase in dielectric response $\tan \delta$ caused by the interfacial polarization. The

noticeable difference is that for Nomex impregnated with ester fluids the additional loss peaks is not as obvious as in cellulose pressboard.

Figure 5.10(b) shows the loss peak of interfacial polarization for Nomex which is evident from the measurement results at temperature of 90°C. The loss peak of interfacial polarization loss for Nomex impregnated with ester fluids is about 0.5 and it seems to be significantly lower than that of TIV. The absorption frequency (indicated by the presence of loss peak) of Nomex also occurs at higher frequency than that of TIV. According to equation (3.14), the shift of absorption frequency to higher frequency might be caused by either low relative permittivity at high frequencies, high charge carrier mobility or/and concentrations of Nomex.

Another significant different is at 50Hz, the dominant polarization mechanism of Nomex impregnated with mineral oil is dipole orientation polarization which is marked by the increase of $\tan \delta$ value at higher frequency rather than interfacial polarization as in cellulose pressboard especially at high temperature.

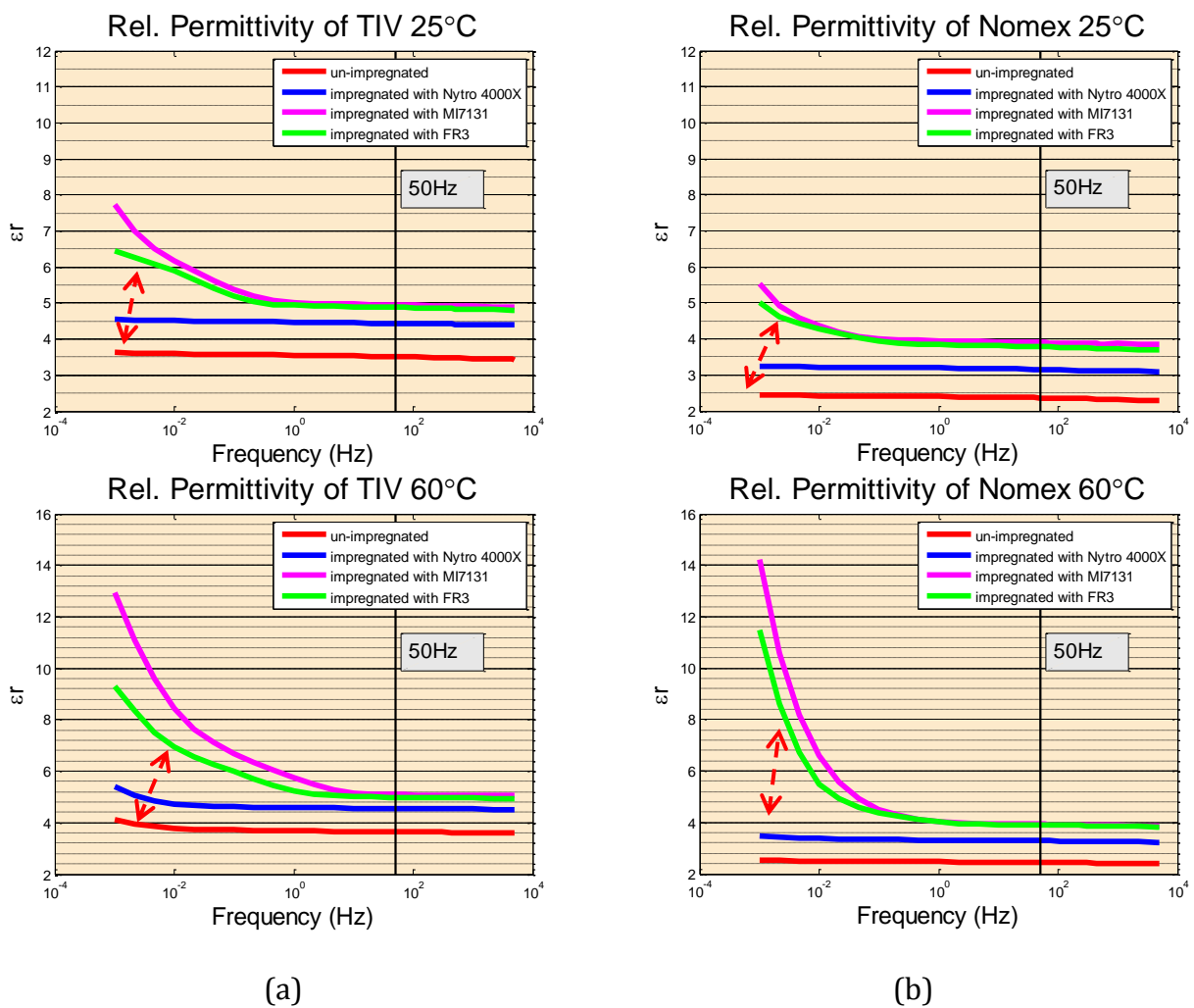


Figure. 5.11: Dielectric response relative permittivity of (a) TIV(cellulose) and (b) Nomex (aramid) at temperature of 25°C and 60°C.

Figure 5.11 compares the dielectric response relative permittivity of pressboard TIV (cellulose pressboard) and Nomex (aramid pressboard) at temperature 25°C and 60°C. It is clear that aramid pressboard possess lower relative permittivity. It is mainly due to the fact that aramid fibers possess lower permittivity value compared to pure cellulose fiber (see section 7.2 for detail). Relative permittivity of both cellulose and aramid pressboards are influenced by ester fluids in the same way. There is steep increase in relative permittivity at lower frequency that is caused by the presence of interfacial polarization when impregnated with ester fluids even at temperature of 25°C.

5.3.4. Temperature dependent behaviour of dielectric response

To study temperature dependent behavior of solid-fluid insulating system, the dielectric responses in frequency domain have been measured at temperature of 25°C, 60°C and 90°C. For solid impregnated samples, it was found that the shape of the dielectric response does not change very drastically with temperature. The dielectric response shifts in frequency domain but maintain its shape. Interestingly, the additional loss peak is also shift with temperature. It means that the relaxation time of all active polarization mechanism behave in the same manner with increase of temperature. Temperature does not change the relaxation time characteristic of each polarization mechanism as indicated by the shift of additional loss peak together with other polarization mechanism. This is true for temperature ranges over which the material does not change its internal structure too much.

As described in section 3.4, a shift in the spectral function due to a change in absolute temperature from T_1 to T_2 can be expressed with Arrhenius relation. Increase of temperature shifts the curve towards higher frequencies. Therefore, the temperature dependent behaviour of solid-fluid insulating system is characterized by the activation energy [84]. Actually, the shift of dielectric response means that the absorption frequency (frequency in which dielectric loss maximum occurs) is shifting to high frequency with increase of temperature as in equation (3.14). Physical explanation of this phenomenon is that interfacial and dipole orientation polarization depend on the effective internal viscosity material which act as resistance by the material toward movement of ions or rotation of dipole molecules. Internal viscosity of material decreases with increase of temperature and this in turn lower the internal resistance (the mobility of various types of molecules is enhanced) toward movement of ions or rotation of dipole molecules. Subsequently, the relaxation time of both polarization mechanisms takes shorter time.

Dielectric response shift for complex relative permittivity (and thus complex electric susceptibility) of oil impregnated pressboard has been presented in [133]. Section 3.4 has shown that frequency shift is also true for dielectric response $\tan \delta$. The shift in $\tan \delta$ will be perfect (it coincides into a single curve) if either the activation energy of

DC conductivity and polarization is equal or the activation energy of DC conductivity is much lower compared to activation energy of polarization.

Figure 5.12 presents the dielectric response $\tan \delta$ and relative permittivity of pressboard TIV impregnated with Nytro 4000X. The dielectric response curves shift toward high frequency with temperature increase. In all solid-mineral oil impregnated combinations, it was found that the dielectric response curve for relative permittivity and $\tan \delta$ shift perfectly with increase of temperature. For relative permittivity (dielectric susceptibility), there is also vertical shift (shift in amplitude). The shift for all dielectric properties is characterized by the same activation energy value. This is true not only for pressboard TIV but also for all cellulose solids impregnated with Nytro 4000X. The activation energy which characterized the dielectric response shift of cellulose solids impregnated with Nytro 4000X is range between 107 - 112kJ/mol for 25-60°C and between 115-131 kJ/mol for 60-90°C. Interestingly, the activation energy of polarization is equal to that of DC conductivity in case of all cellulose solids impregnated with Nytro 4000X. The activation energy of solid impregnated with mineral oil is in the same range as reported in [55].

An exception is found for Nomex impregnated with Nytro 4000X. The activation energy value which characterized the dielectric response shift is range between 78-90kJ/mol, lower than cellulose solids. The activation energy of polarization is also different to that of DC conductivity with the activation energy of polarization is a bit higher. Thus, the shift in dielectric response $\tan \delta$ is still perfect for Nomex impregnated with Nytro 4000X.

It can be summarized that for cellulose solids impregnated with Nytro 4000X, the temperature dependent behaviour of dielectric response is characterized by the same activation energy value. Meanwhile, for Nomex, the temperature dependent behavior of dielectric response depends on different activation energy value with cellulose solids. This fact leads to a conclusion that the temperature dependent behaviour of solid-fluid insulating system is highly dependent on the polymer material of solid. In this work, it was found that activation energy of cellulose solids e.g. TIV and Rotherm is higher than activation energy of aramid solid e.g. Nomex. Activation energy can be used as an indicator of material sensitivity toward temperature. Lower activation means that the material has low sensitivity toward temperature change. That is why Nomex is suitable as insulation for high temperature part in transformers.

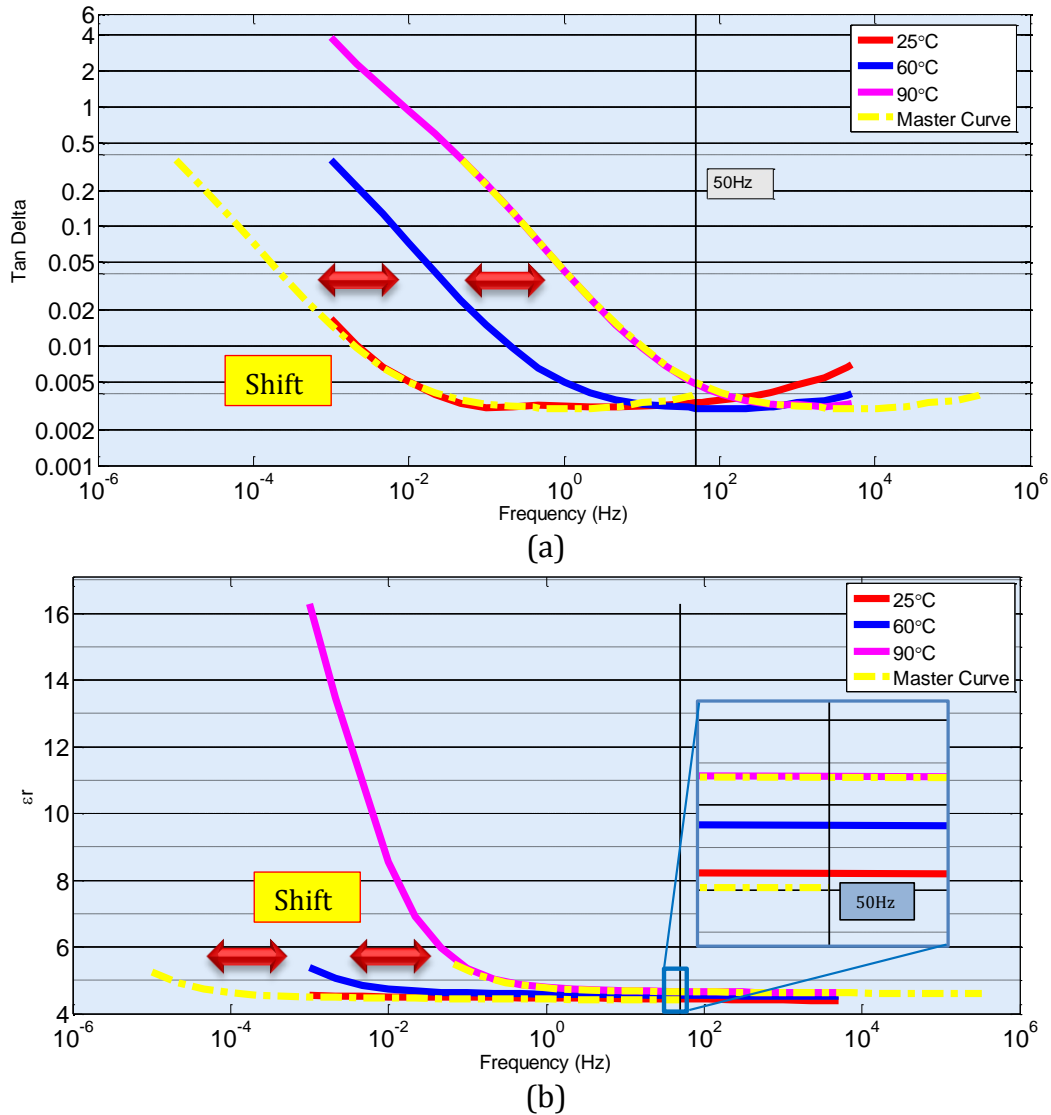


Figure 5.12: Temperature dependent behaviour of dielectric response (a) $\tan \delta$ and (b) relative permittivity for TIV impregnated with Nytro 4000X.

Figure 5.13 presents the dielectric response $\tan \delta$ and relative permittivity of TIV impregnated with MI7131. As for of solids impregnated with ester fluids, the dielectric response curves also shift toward high frequency with increase of temperature. However, it was found for dielectric response $\tan \delta$ the shift does not coincide into a single curve at temperature 90°C. There is a deviation in $\tan \delta$ curve shape from low temperature to high temperature as in Figure 5.13(a). The deviation in dielectric response was not found for relative permittivity as in Figure 5.13(b). The deviation in dielectric response $\tan \delta$ means that the activation energy of polarization at high temperature is different to that of DC conductivity for cellulose solids impregnated with ester fluids.

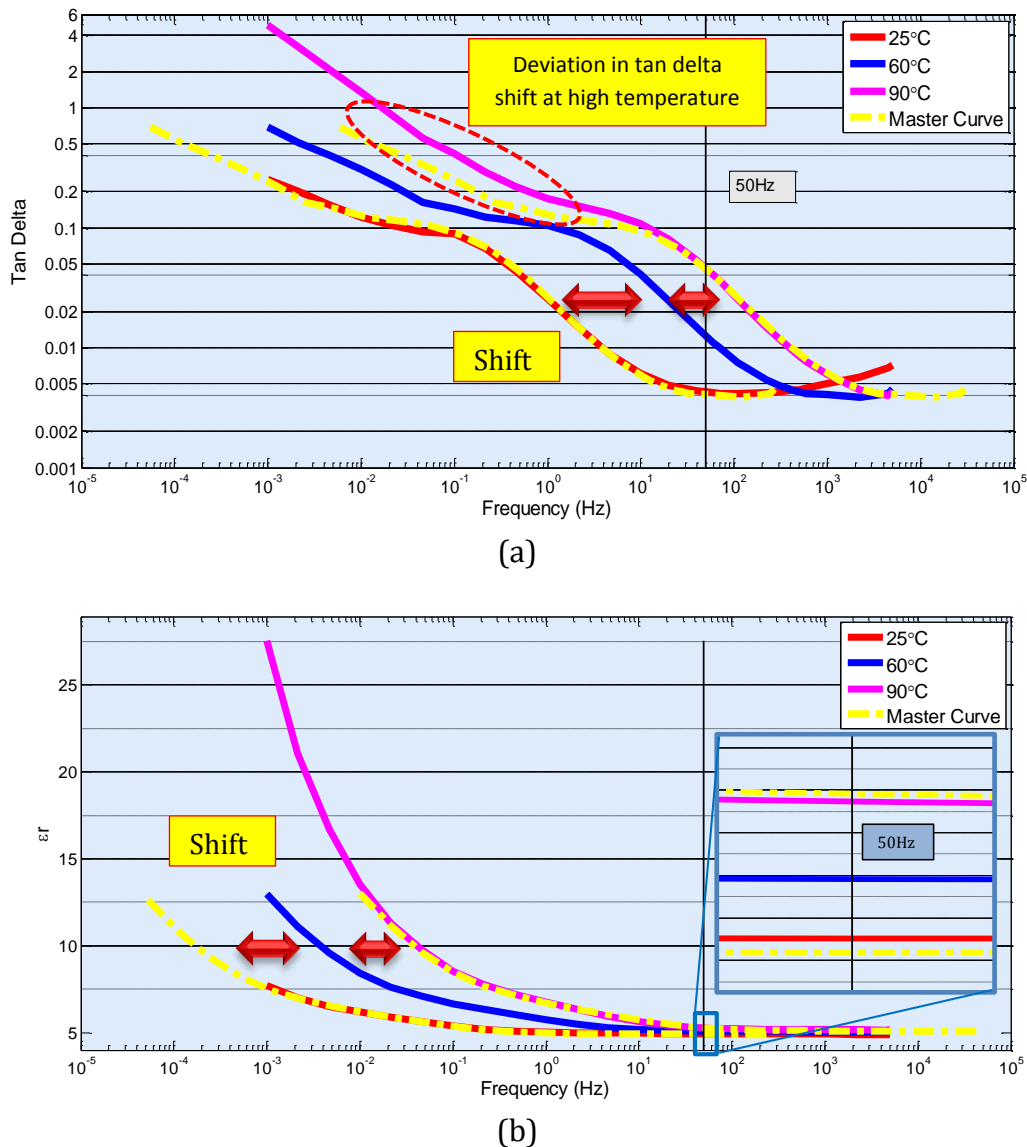


Figure 5.13: Temperature dependent behaviour of dielectric response (a) $\tan \delta$ and (b) relative permittivity for TIV impregnated with MI7131.

Different activation energy of DC conductivity and polarization at high temperature causes the deviation on dielectric response $\tan \delta$. The activation energy of complex susceptibility (polarization) is in the range between 67 - 75kJ/mol for 25-60°C and between 52-67kJ/mol for 60-90°C for cellulose solids impregnated with MI7131. The same value of activation energy of polarization for pressboard impregnated with ester fluids were also reported in [50] which is about 77kJ/mol (0.8eV). Meanwhile, the activation energy of DC conductivity for all cellulose solids impregnated with ester fluids is between 103-118kJ/mol for 60-90°C. From our measurement and literature, the activation energy value of mineral oil is in the range between 40-50 kJ/mol ([in agreement with [84]]) and the activation energy of ester fluids is reported to be about 50 kJ/mol [80]. Hence, the activation energy of ester fluids are in same range with activation energy of solids impregnated with ester fluids. It has been suggested in [48] that lower activation energy could possibly be an indication of increased space charge

effects. It supports the previous suggestion that the interfacial polarization is more dominant on solids impregnated with ester fluids than solid impregnated with mineral oil.

The possible cause for the dominant interfacial space charge polarization may be from the fact that ester fluids have high kinematic viscosity, high dc conductivity of ester fluids and coupled by its molecular characteristic as it does not occur for pressboard impregnated with mineral oil and silicone fluid (reported in [46]). Therefore, it is possible that the activation energy of polarization for solids impregnated with ester fluids depend more on temperature dependent behavior of ester fluids rather than the solid samples itself. It is also evident from the difference on activation energy of un-impregnated pressboard TIII which is about 106kJ/mol for 25-60°C compared to 62kJ/mol for TIII impregnated with MI7131. See Table 5.6 for complete list of activation energy of DC conductivity and polarization. From Table 5.6, it is also noticeable that at high temperature, the activation energy of DC conductivity of cellulose solids impregnated with Nytro 4000X and MI7131 is about equal. However, the activation energy of polarization is different.

Figure 5.14 presents the dielectric response $\tan \delta$ of pressboard Nomex impregnated with Nytro 4000X and MI7131. The same shift toward high frequency with temperature increase was observed. But there is no deviation in $\tan \delta$ curve which occurs when cellulose solids impregnated with ester fluids. It was found that the activation energy of polarization is higher compared to that of DC conductivity for Nomex impregnated with all insulating fluids. Thus, for Nomex impregnated in ester fluids, the dielectric response curve for relative permittivity, complex susceptibility and $\tan \delta$ shift perfectly with increase of temperature. The activation energy which characterized the shift is influenced by the insulating fluids used for impregnation.

It has been reported in [48] that the relatively high activation energy of DC conductivity and polarization suggested the involvement of ions in the conduction and polarization at low frequency. Thus, our results support the suggestion that for solid-fluid insulating system the main charge carrier is possibly ions.

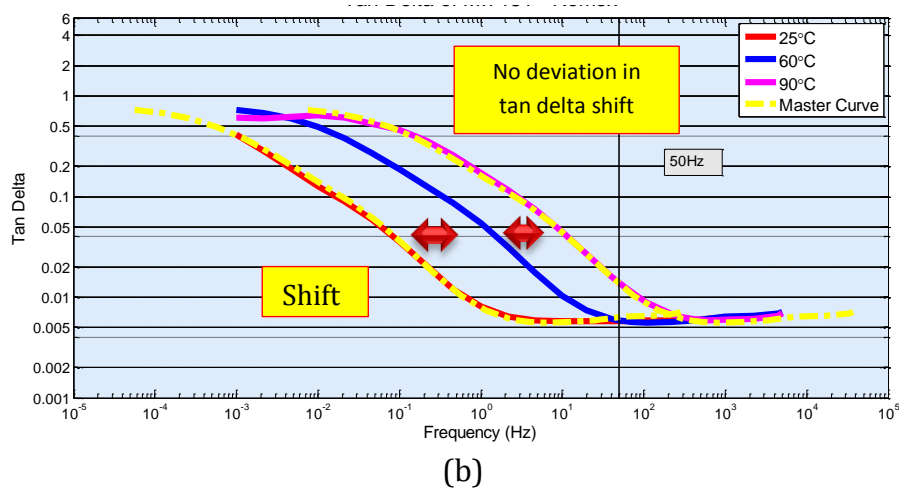
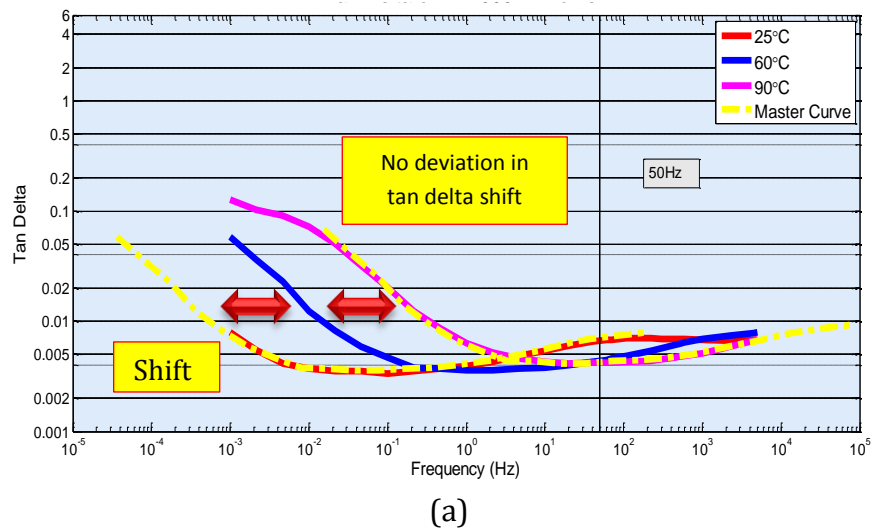


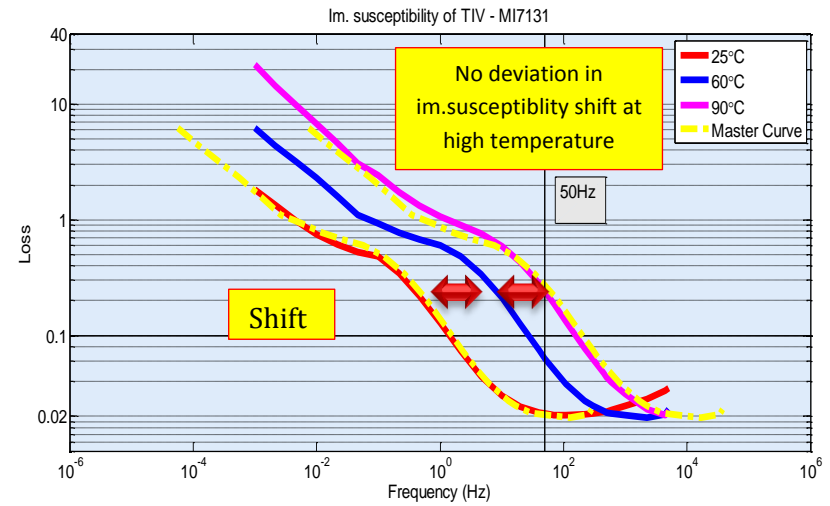
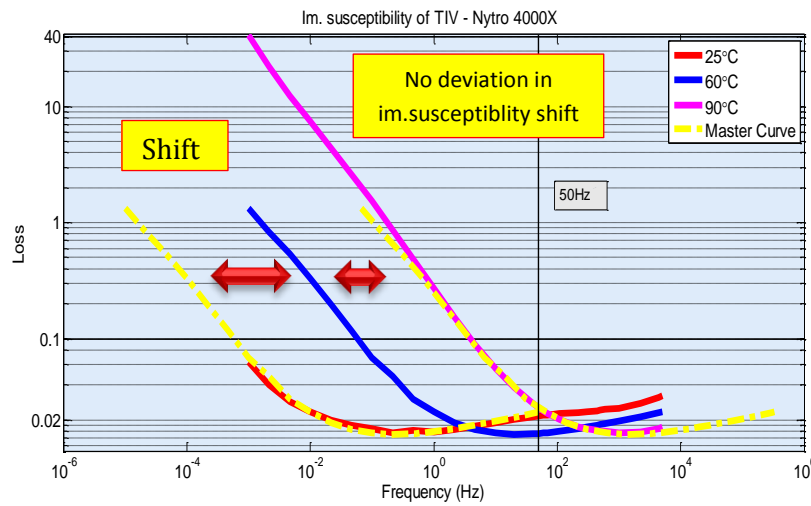
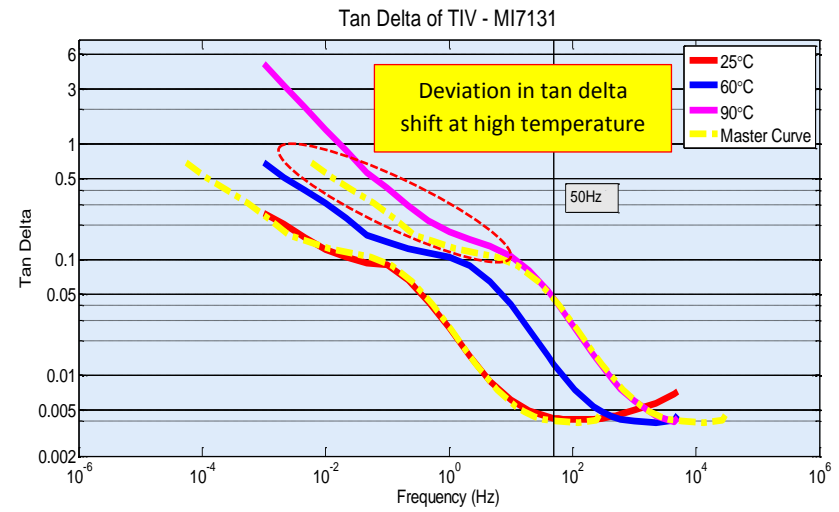
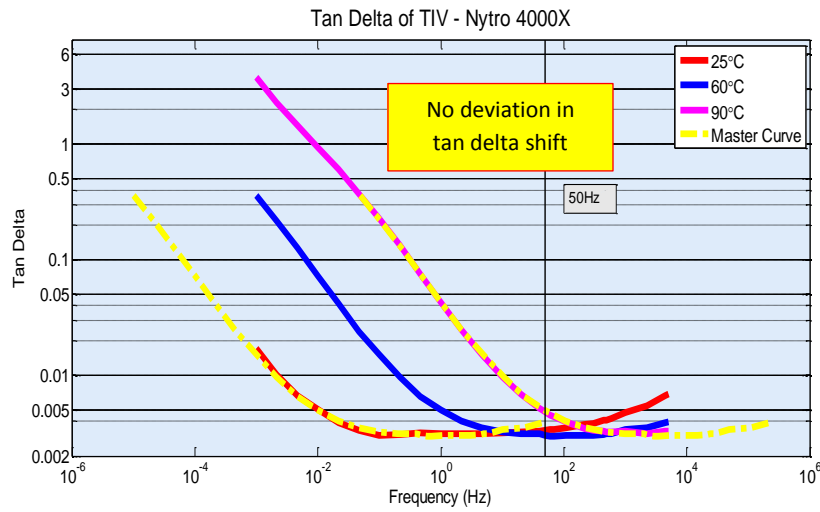
Figure 5.14: Temperature dependent behaviour of dielectric response $\tan \delta$ for Nomex impregnated with (a) Nytro 4000X and (b) MI7131.

5.3.5. Imaginary part of susceptibility

The main reason of the investigation on imaginary part of dielectric susceptibility is the presence of deviation in master curve for dielectric response $\tan \delta$ of cellulose solids when impregnated with ester fluids at temperature 60°C - 90°C as in Figure 5.13. This deviation does not occur in master curve for dielectric response $\tan \delta$ for solids impregnated with Nytro 4000X. According to equation (3.50), $\tan \delta$ of solid-fluid insulating system depends on DC conductivity and imaginary part of susceptibility. Therefore, the source of deviation is supposedly caused by the difference of temperature dependent behavior (activation energy) characteristic of DC conductivity and polarization (susceptibility). It is important to analyze imaginary part of susceptibility of solid impregnated with ester fluids to investigate the source of the deviation. Imaginary part of susceptibility was calculated from imaginary part of the complex capacitance $C''(\omega)$ which represents total loss minus DC conductivity part which represents resistive loss.

Figure 5.15 presents the dielectric response $\tan \delta$ and imaginary part of susceptibility of TIV impregnated with (a) Nytro 4000X and (b) MI7131. For TIV impregnated with Nytro 4000X, there is no deviation on both dielectric response $\tan \delta$ and imaginary part of susceptibility. The shift of dielectric response $\tan \delta$, relative permittivity and imaginary susceptibility depends on the same activation energy. However, for TIV impregnated with MI7131, though there is deviation on dielectric response $\tan \delta$ at temperature of 90°C, there is no deviation on dielectric response imaginary part of susceptibility. It suggests that the source of deviation is the difference on the activation energy of DC conductivity and polarization (imaginary part of susceptibility). It was also noticeable that the activation energy of imaginary part of susceptibility is equal to that of relative permittivity. This might be related to the fact that real part (relative permittivity) and imaginary part of susceptibility linked to each other by Kramer-Krönig relation.

Table 5.6 shows the activation energy value for solid impregnated with Nytro 4000X, MI7131 and FR3, respectively. For all solid-Nytro 4000X combinations, the activation energy of susceptibility is equal with the activation energy of DC conductivity. For solid impregnated with ester fluids, at lower temperature 25°C - 60°C, the activation energy of imaginary part of susceptibility is equal to the activation energy of DC conductivity. However, at higher temperature 60°C - 90°C, the activation energy of susceptibility is different from the activation energy of DC conductivity. The activation energy of susceptibility remains constant with increase of temperature.



(a)

(b)

Figure 5.15: Shifted dielectric response of tan δ and imaginary part of susceptibility of TIV impregnated with (a) Nytro 4000X and (b) MI7131.

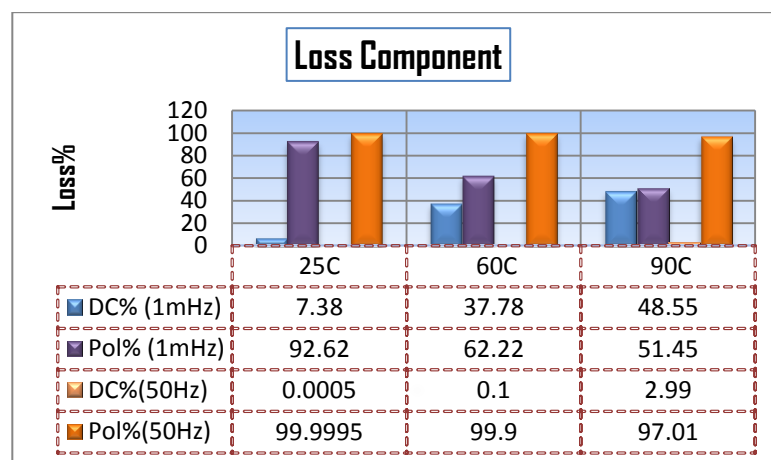
Table 5.6: Activation energy of polarization and DC conductivity.

Solid	Nytro 4000X			MI7131				FR3			
	Activation energy of polarization (kJ/mol)		Activation energy of DC conductivity (kJ/mol)	Activation energy of polarization (kJ/mol)		Activation energy of DC conductivity (kJ/mol)		Activation energy of polarization (kJ/mol)		Activation energy of DC conductivity (kJ/mol)	
	20-60°C	60-90°C	Gradient Curve	20-60°C	60-90°C	20-60°C	60-90°C	20-60°C	60-90°C	20-60°C	60-90°C
Weidmann B.3.1A (TIV) 2mm	108.56	135.41	122.61	67.55	67.55	74.1	118.41	69.48	62.73	97.42	125.4
Weidmann B.3.1A (TIV) 4mm	105.86	127.48	133.72	66.59	52.4	60.39	106.84	66.59	56.94	63.82	111.26
Weidmann B.4.1 (TIII) 2mm	103.93	133.65	123.61	62.73	56.94	71.83	108.38	56.94	50.18	99.97	111.9
DuPond Nomex T-993 2mm	78.14	86.51	58.14	67.55	67.55	43.84	43.36	51.15	60.8	32.94	64.31
Cottrell CK 125-TU 0.076mm	112.2	131.08	128.09	74.31	69.48	119.8	132.24	77.2	77.2	127.4	137.18
Tullis Russel Rotherm HIHD 0.085mm	118.7	106.15	119.1	75.27	55.01	112.68	124.47	72.38	59.83	107.71	118.23
Nordic Paper Amotfors 0.080mm	112.88	117.54	111.52	72.38	58.87	88.31	103.25	63.69	59.83	90.24	101.61

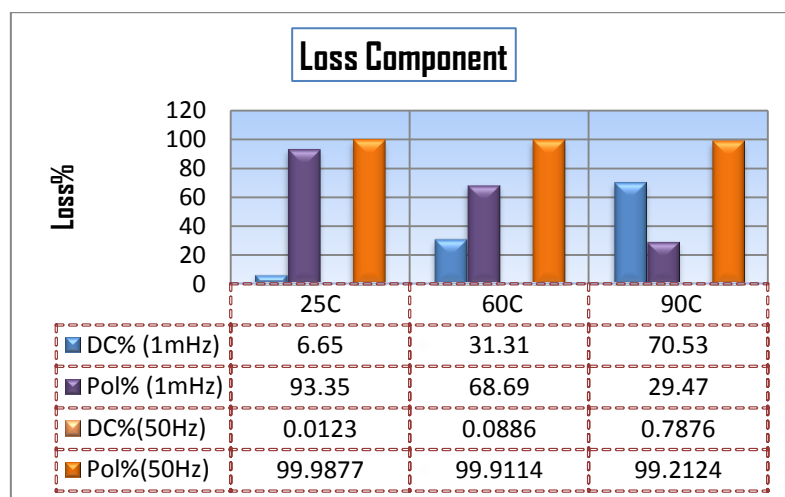
5.3.6. Loss characteristics of solid impregnated with ester fluids

Using the imaginary part of susceptibility, it is possible to analyse the loss contribution characteristic of solid-fluid insulating system. It is known for pressboard impregnated with insulating fluid that imaginary part of complex relative permittivity (loss part) contains both the resistive losses (conduction, $\sigma_0/\epsilon_0 \cdot \omega$) and the polarization losses (polarization, $\chi''(\omega)$) as in equation (3.50).

In this section, the loss contribution characteristic of solids impregnated with mineral oil and ester fluids was investigated. Results for TIV impregnated with Nytro 4000X and MI7131 is presented in Figure 5.16. The results for pressboard TIV is typical and can represent all cellulose solid samples.



(a)



(b)

Figure 5.16 Loss contribution of pressboard TIV impregnated with (a) Nytro 4000X and (b) MIDEL7131. Note: DC% refers to contribution of resistive loss and Pol% refers to contribution of polarization loss.

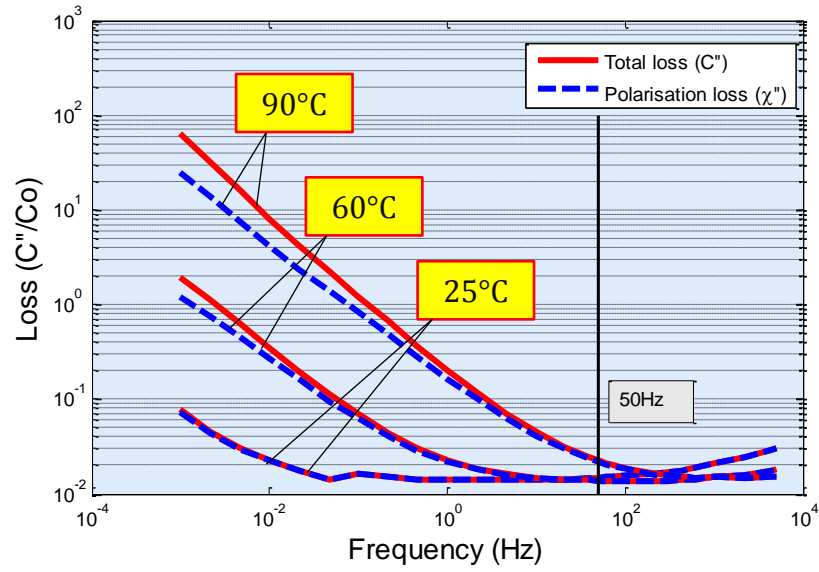
Some references have explained that resistive loss part is often dominant at low frequencies for solid-fluid insulating system. Thus, the linear increase at low frequency for $\tan \delta$ was often prematurely decided as contribution from resistive loss. However, the contrary was found in other reference which shown that the contribution of resistive loss on total loss was quite low. The same result was reported in [84]. It is of interest to investigate this matter as it will be helpful to explain the polarization characteristic of solids impregnated with ester fluids.

Figure 5.16 shows the comparison of loss contribution characteristic at two frequencies, 1mHz and 50Hz at three temperature levels. At 1mHz and 25°C, for TIV impregnated with Nytro 4000X and MI7131, resistive loss contribution is less than 8% of total loss. The contribution of resistive loss is increased along with increase of temperature. At 1mHz and 90°C, resistive loss contribution of TIV impregnated with Nytro 4000X is less 50% and when impregnated with MI7131 is about 71%. The contribution of resistive loss increases with increase of temperature as the DC conductivity increased. Different loss contribution characteristic of TIV when impregnated with Nytro 4000X and ester fluids indicates different interfacial polarization and long-range ionic migration characteristic. It is also indicated by the different activation energy of DC conductivity and polarization.

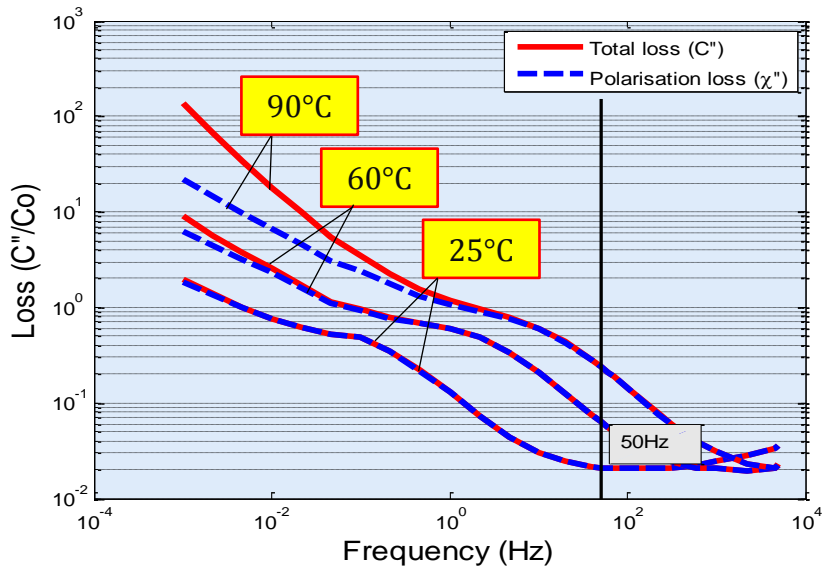
Different characteristic was found for Nomex impregnated with Nytro 4000X and MI7131. The resistive loss contribution is very small, less than 6% at 1mHz and 90°C. The increase of DC conductivity with increase of temperature for aramid pressboard is not significant as shown by the low activation energy. The activation energy of DC conductivity of aramid pressboard is about 45-58 kJ/mol.

The contribution of resistive loss is decreased linearly toward high frequency. Even at 90°C, the contribution of resistive loss at 50 Hz is less than 3% for TIV impregnated with Nytro 4000X and MI7131. Figure 5.17 shows the imaginary part of the complex capacitance $C''(\omega)$ which represent total loss and imaginary part of the susceptibility which represent polarization loss of pressboard TIV impregnated in Nytro 4000X and MI7131. Hence, it is fair to say that $\tan \delta$ at power frequency 50 Hz and 60 Hz mainly depends on the polarization loss. It can be either interfacial space charge polarization or dipole orientation polarization depends on the temperature and solid-fluid combination.

Polarization which is dominant at frequency 50 Hz and 60 Hz for solid-fluid insulating system might not exhibit the same polarization mechanism when the insulating materials, in this case pressboard and insulating fluid, are stand alone. It is important to realise that each insulating material has a dielectric response and when putting these materials together, the total response will not only reflect each material but also the way they are put together. Therefore, sometimes the total dielectric response describes one physical process but the materials in the mixture have dielectric responses revealing totally different physical processes.



(a)



(b)

Figure 5.17 Loss part (with and without DC/Resistive loss contribution of TIV impregnated with (a) Nytro 4000X and (b) MI7131 at different temperatures.

5.3.7. Master curve

As described in section 5.3.4, for solid impregnated with insulating fluids, it was found that the shape of the dielectric response does not change very drastically with temperature. The dielectric response shifts in frequency domain but maintain its shape. This phenomenon allows for normalizing frequency dependent spectra for different temperatures by shifting the corresponding spectra until they coincide into a single curve, which is called a “master curve“. Master curve is present for both dielectric responses in frequency domain and in time domain as reported in [84].

An advantage of master curve technique is that the frequency range is significantly extended compared to the original measured spectra. Another useful feature of the master curve technique is that the possibility to estimate the dielectric properties of samples at certain temperature and frequency without performed measurement at each temperature level. This might be practical for transformer design purpose. Note that, extrapolation of master curve to extreme low and high temperature might not show the correct estimation. At extreme low and high temperature, a phase transition of solid might occur and thus, the characteristic of dielectric properties will also change.

For all master curve technique presented in this section, measured curve at 60°C was used as reference curve.

Effect of insulating fluids on master curve

Figure 5.18 shows the master curve for dielectric response $\tan \delta$ and relative permittivity for TIII impregnated with (a) Nytro 4000X, (b) MI7131 and (c) FR3. The master curve of dielectric response is shifted in frequency by the change of temperature.

It is clear that each TIII impregnated with different insulating fluids has its own master curve which is characterized by different activation energy value as shown in Table 5.7. The activation energy which corresponds to frequency shift of TIII impregnated with Nytro 4000X is different from activation energy of TIII impregnated with MI7131 or FR3. The activation energy depends on many factors such as molecular characteristic of insulating fluids and solids, internal viscosity of solids, kinematic viscosity of fluids, thickness of solids and the combination of those factors. Generally, for TIII impregnated with Nytro 4000X, the frequency shift of $\tan \delta$ and relative permittivity is characterized by same activation energy value.

Table 5.7 shows that the activation energy of un-impregnated TIII is about 106-135 kJ/mol. The value corresponds to the activation energy of polarization for un-impregnated cellulose. Meanwhile, the activation energy of polarization for TIII impregnated with mineral oil is about 103-133 kJ/mol and thus, it is equal activation energy polarization of un-impregnated TIII. It indicates that mineral oil does not affect the temperature dependent behaviour of cellulose solids.

However, it was found that the activation energy of polarization for TIII impregnated with ester fluids are about 63-69 kJ/mol. It is significantly lower than activation energy of un-impregnated TIII which indicates that impregnation by ester fluid changes the temperature dependent behaviour of polarization mechanism of cellulose. It might be caused by the molecular characteristic rather than kinematic viscosity of ester fluids. It is evident from the fact that at high temperature of 100°C, the kinematic viscosity of ester fluids and mineral oil is almost equal, according to Table 2.2, it is

about $5.25 \text{ mm}^2/\text{s}$ for MI7131 to $3 \text{ mm}^2/\text{s}$ for Nytro 4000X. Thus, it is possible that different activation energy of polarization is not caused by kinematic viscosity.

It is also notable that the activation energy of DC conductivity for TIII impregnated with mineral oil is equal to activation energy of un-impregnated cellulose. At high temperature, interestingly, the activation energy of DC conductivity for TIII impregnated with ester fluids is equal to activation energy of un-impregnated cellulose which is about 108-111 kJ/mol.

However, at low temperature, the activation energy of DC conductivity for TIII impregnated with ester fluids are lower than of un-impregnated cellulose. Hence, the temperature dependent behavior of DC conductivity for solid-fluids insulating system might be influenced by the kinematic viscosity of insulating fluids. At low temperature of 20°C , the kinematic viscosity of synthetic ester and mineral oil is about $78 \text{ mm}^2/\text{s}$ for MI7131 to $22 \text{ mm}^2/\text{s}$ for Nytro 4000X.

Because of the deviation in dielectric response $\tan \delta$, it is not possible to estimate $\tan \delta$ at high temperature with master curve technique using dielectric response at 60°C as reference for cellulose solids impregnated with ester fluids.

Table 5.7: Comparison of activation energy for TIII impregnated with ester fluids.

Solid	Insulating fluids	Activation Energy			
		Polarization (kJ/mol)		DC conductivity (kJ/mol)	
		20-60°C	60-90°C	20-60°C	60-90°C
TIII	Un-impregnated	106.15	135.1	n.a.	
	Nytro 4000X	103.93	133.65	123.61	
	MI7131	62.73	56.94	71.83	108.38
	FR3	56.94	50.18	99.97	111.9

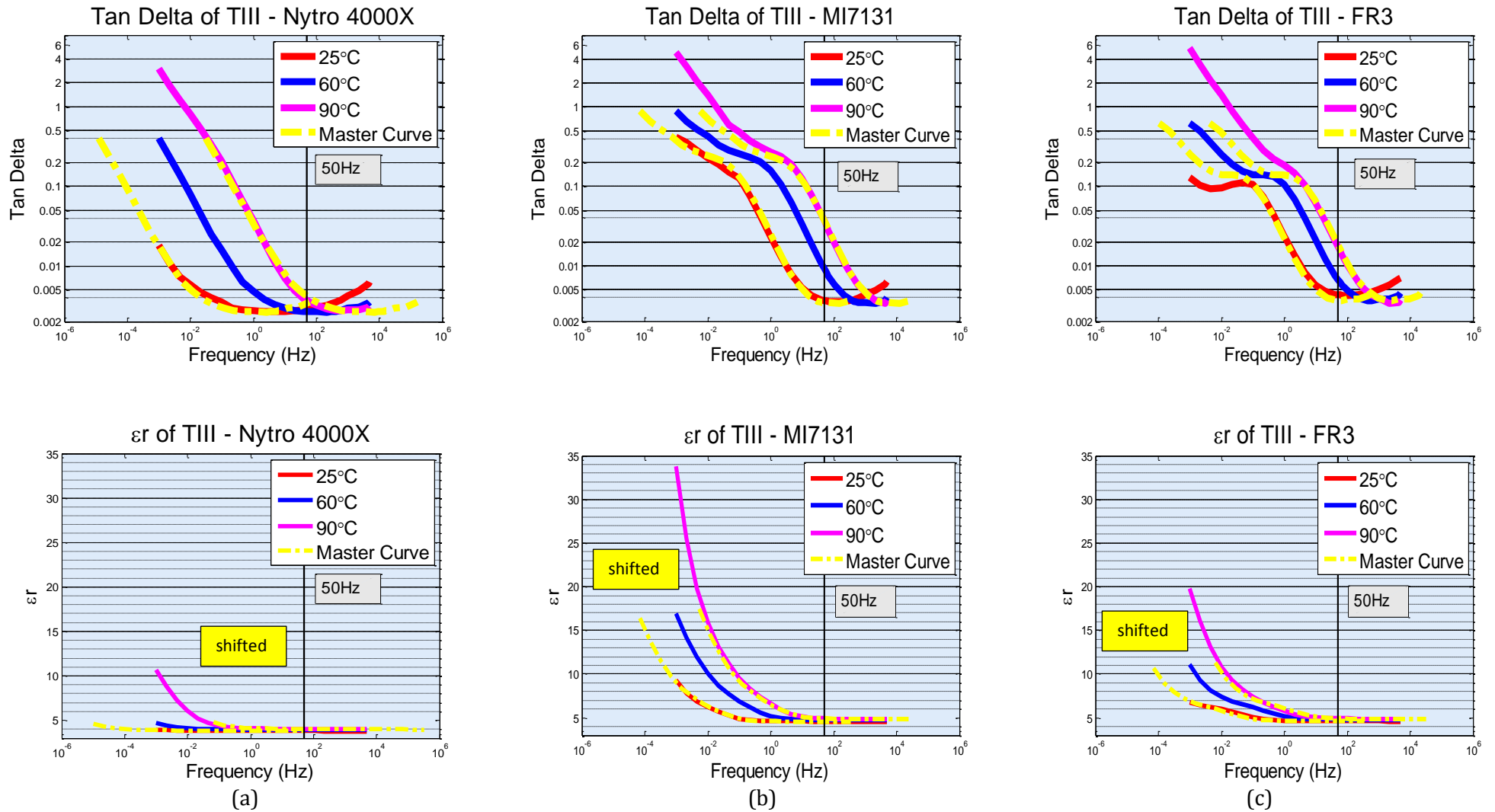


Figure 5.18: master curve for dielectric response $\tan \delta$ and relative permittivity for TIII impregnated with (a) Nytro 4000X, (b) MI7131 and (c) FR3.

Effect of polymer material on the master curve

Figure 5.19 shows the master curve for dielectric response $\tan \delta$ and relative permittivity of (a) TIII impregnated with Nytro 4000X and (b) Nomex impregnated with Nytro 4000X. The master curve of dielectric response is shifted in frequency with the change of temperature. The frequency shift of dielectric response for different polymer material (cellulose and aramid) is characterized by different activation energy even though it is impregnated with same insulating fluid. It means that for solid-fluid insulating system, polymer material is more dominant factor compared to the insulating fluids in characterizing the temperature dependent behavior.

Note that in some cases, besides the frequency shift on dielectric response, there is also vertical shift (shift of amplitude). This indicates that the temperature dependent behavior of each pressboard and transformer paper impregnated with dielectric fluids combination is unique.

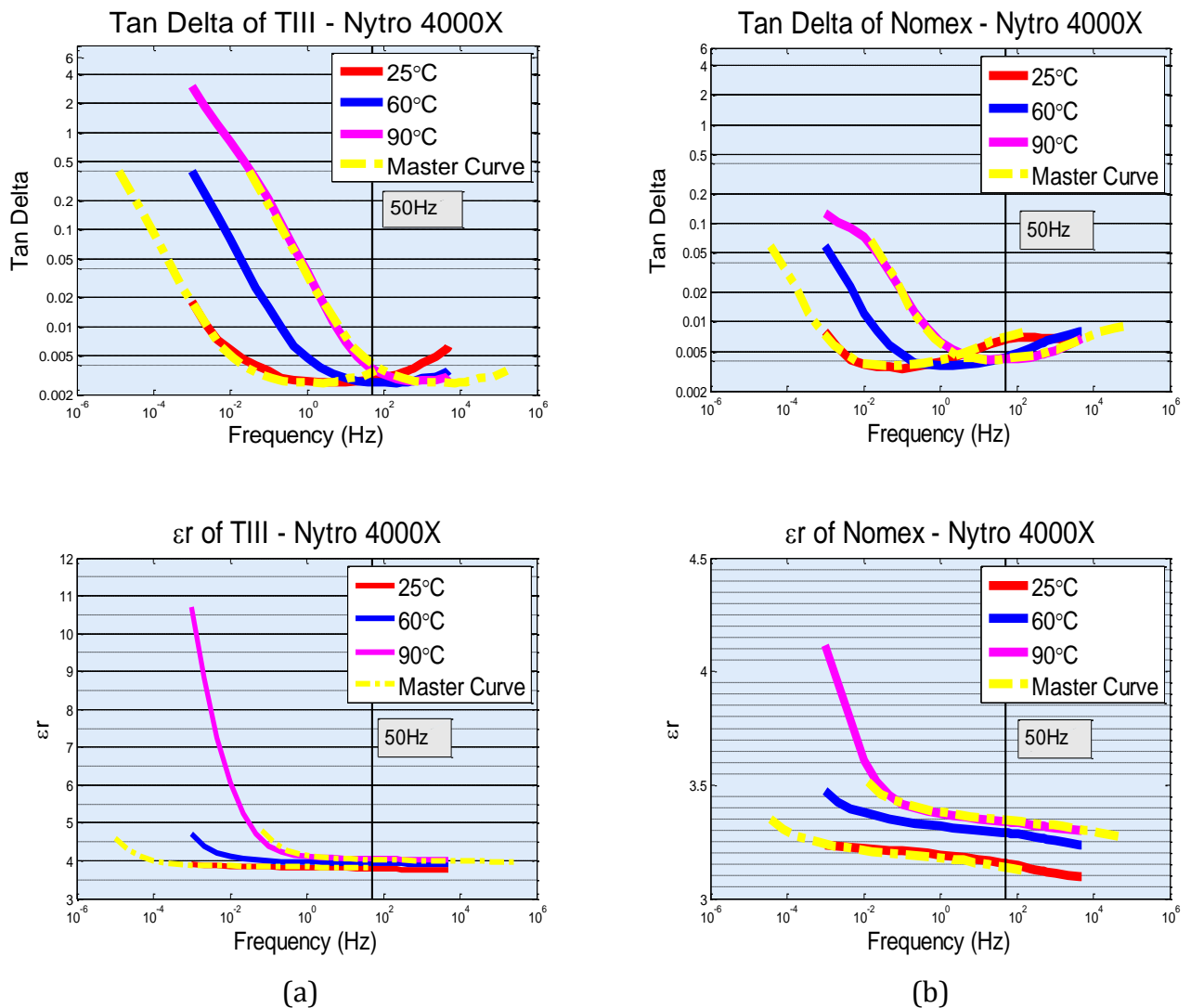


Figure 5.19: master curve for dielectric response $\tan \delta$ and relative permittivity of (a) TIII impregnated with Nytro 4000X and (b) Nomex impregnated with Nytro 4000X.

Table 5.8 shows that the activation energy of cellulose pressboard TIII is higher than aramid pressboard Nomex. The activation energy of polarization for Nomex is less influenced by the characteristic of insulating fluids compared to TIII. It indicates that temperature dependent behavior of polarization for Nomex is less influenced by the insulating fluids.

It is also notable that activation energy of DC conductivity for Nomex impregnated with all type of insulating fluids is lower than TIII. Hence, the temperature dependent behavior of DC conductivity for Nomex impregnated with insulating fluids has low dependency on the characteristic of insulating fluids.

Table 5.8: Comparison of activation energy for TIII and Nomex impregnated with alternative insulating fluids.

Insulating fluids	Solid	Activation Energy			
		Polarization (kJ/mol)		DC conductivity (kJ/mol)	
		20-60°C	60-90°C	20-60°C	60-90°C
Un-impregnated	TIII	106.15	135.1	n.a.	
	Nomex	62.7	77.2	n.a.	
Nytro 4000X	TIII	103.93	133.65	123.61	
	Nomex	78.14	86.51	58.14	
MI7131	TIII	62.73	56.94	71.83	108.38
	Nomex	67.55	67.55	43.84	43.36
FR3	TIII	56.95	50.18	99.974	111.9
	Nomex	51.15	60.8	32.94	64.31

5.4. Relative permittivity – $\tan \delta$ at 50Hz

5.4.1. Influence of density, thickness and polymer material of pressboard

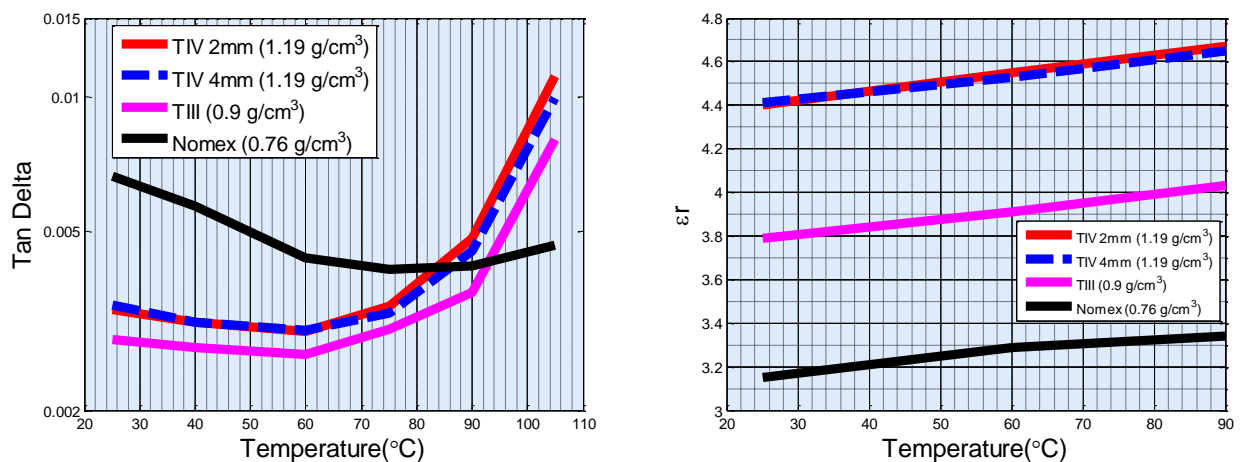
The application of different density, thickness and polymer material of pressboard has different purpose when applied in transformers as described in section 4.1. This section explains the influence of density, thickness and polymer material on dielectric properties of pressboard impregnated with alternative insulating fluids.

Figure 5.20 depicts the effect of pressboard density, thickness and polymer material on $\tan \delta$ and relative permittivity at power frequency of 50Hz. The dielectric properties value at 25°C, 60°C and 90°C was measured and at 40°C, 75°C and 105°C was estimated using master curve technique. Temperature certainly affects dielectric properties. From measurement over wide range of frequency, it is hard to quantify the effect of each factor as the detail might be disregard. Please note that measurement at different frequency might show different behavior as described in section 5.2.

Generally, for pressboards impregnated with mineral oil, high density pressboard TIV possesses higher $\tan \delta$ and relative permittivity compared than low density pressboard TIII. Similar results were found in [5]. High $\tan \delta$ may be caused by polarization of cellulose molecules. Theoretically, high density pressboard has dielectric properties characteristic similar to pure cellulose fibre. In relation with relative permittivity solid impregnated system, low density pressboard means that the pressboard possesses high volume fraction that can be filled with insulating fluids. Thus, the influence of relative permittivity insulating fluid (which filled the cellulose pores) is more dominant. It is evident from lower relative permittivity of TIII compared to TIV.

From comparison of TIV 2mm and TIV 4mm, it is clear that pressboard thickness does not change the dielectric properties characteristic of $\tan \delta$ and relative permittivity. Temperature dependent behaviour of pressboard with different thickness is also similar.

The influence of polymer material pressboard can be observed from comparing dielectric properties of cellulose pressboard TIII and TIV and aramid pressboard Nomex. Each polymer has different dielectric properties characteristic with increase of temperature. In this case, at low temperature, aramid pressboard has higher $\tan \delta$ compared to cellulose pressboard. But the behaviour changes at high temperature in which aramid pressboard has lower $\tan \delta$. It is known that the increase of temperature causes basic changes on the chemical linkage of paper which may be evident from reduce of material viscosity [5]. In this context, cellulose pressboard has lower resistance (low intrinsic viscosity) toward increase of temperature than aramid pressboard. Hence, $\tan \delta$ of aramid pressboard is lower at high temperature and its relative permittivity has lower dependency with increase of temperature compared to cellulose pressboard. Generally, aramid based pressboard has lower relative permittivity due to lower relative permittivity of pure aramid fibre ($\epsilon_r = 4$) [134] compared to pure cellulose fibre which range from 5.1-7 [5].



(a)

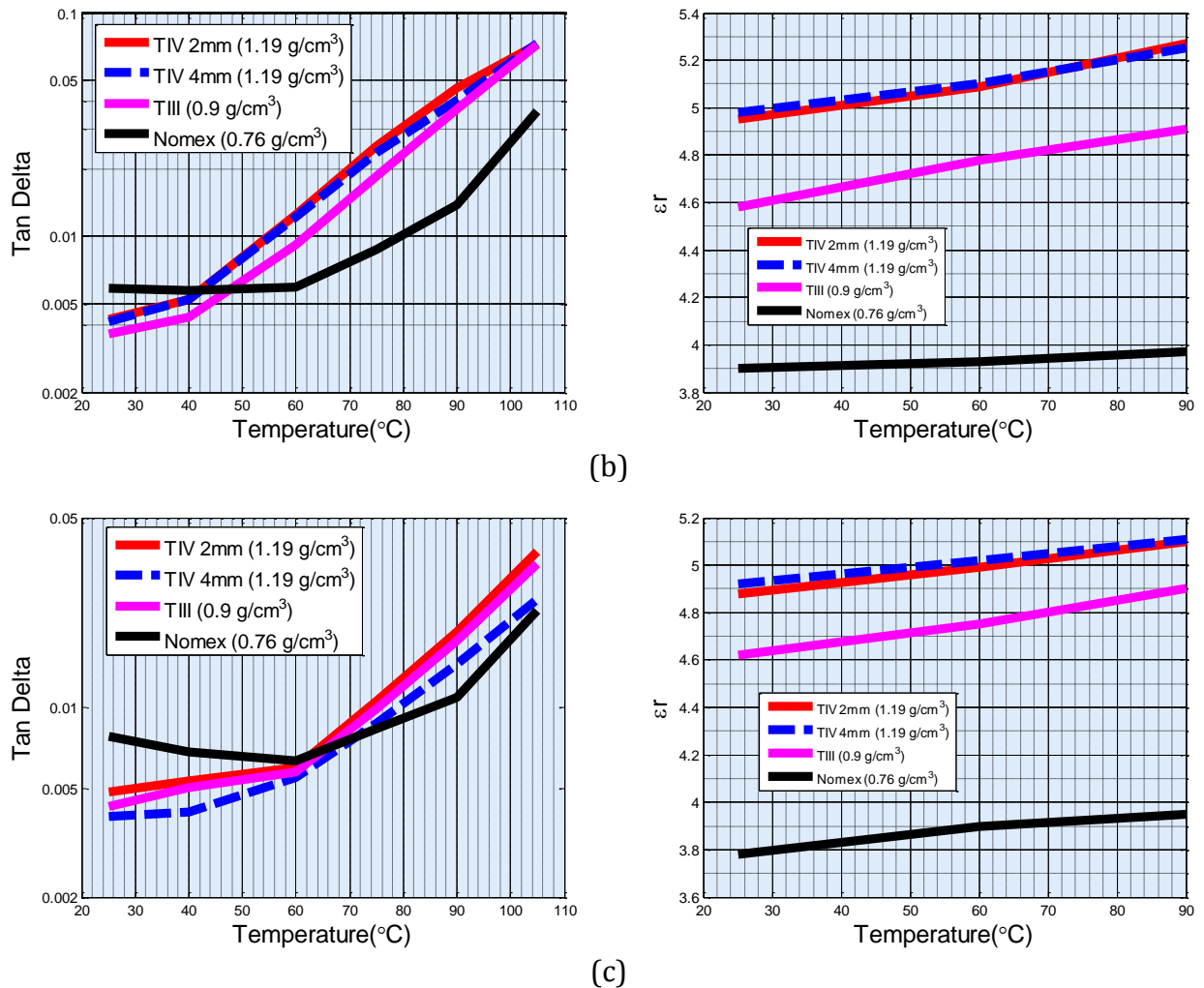


Figure 5.20: Effect of density, thickness and polymer material on $\tan \delta$ and relative permittivity at power frequency of 50Hz for pressboard impregnated with (a) Nytro 4000X, (b) MI7131 and (c) FR3.

5.4.2. Influence of density and thickness of transformer papers.

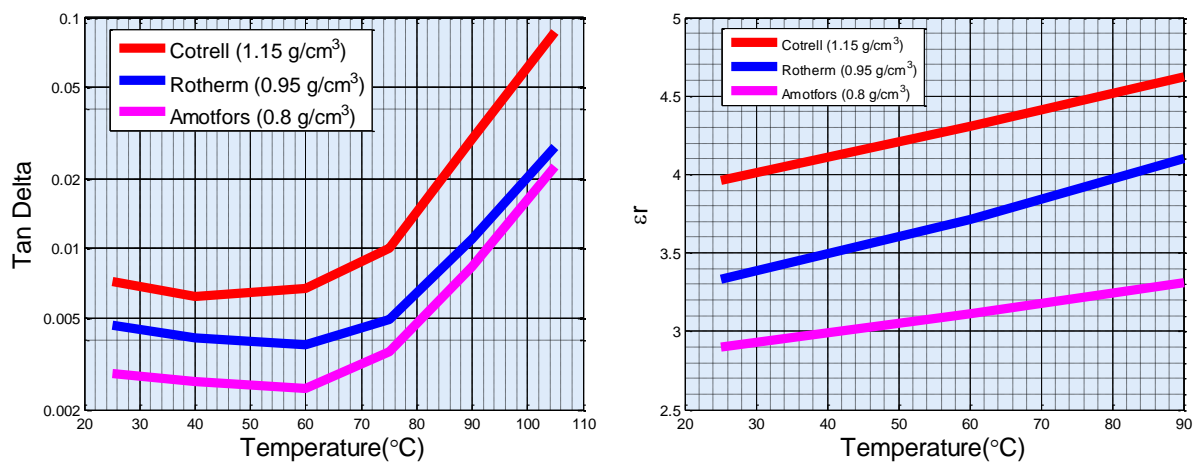
Pressboard and transformer paper were addressed separately because both has different characteristic mainly related to its thickness. Tested pressboards have thickness of 2mm and 4mm and transformer papers have thickness in range between 0.076mm to 0.085mm. In solid impregnated system, such extreme difference in thickness may have different effect due to insulating fluid layer that presence on the sample's surface and relaxation time due to long-range ionic migration, as described in section 5.3.2.

Figure 5.21(a) depicts the influence of density on dielectric properties of transformer paper impregnated with N4000X. Similar to pressboard, high density transformer papers possess higher $\tan \delta$ and relative permittivity compared to low density transformer papers. $\tan \delta$ characteristic with increase of temperature does not influenced by the density of transformer paper.

Figure 5.21(b) and (c) depict the influence of density on dielectric properties of transformer paper impregnated with MI7131 and FR3 respectively. Dielectric properties of transformer paper impregnated with ester fluids are different with pressboard. It is noticeable that the influence of paper density on $\tan \delta$ is not clear when paper is impregnated with ester fluids. It is possibly caused by the interrelation between the thickness of papers and the effect of interfacial polarization mechanism which is dominant on solids impregnated with ester fluids. The thickness of tested papers is range between 0.076-0.085mm. Hence, the influence of interfacial polarization on $\tan \delta$ is maybe more dominant than the influence of paper density itself.

Generally, relative permittivity of transformer paper possesses a positive temperature coefficient which means that it increases with increased of temperature. An exception might happen when low density paper is impregnated with insulating fluid which has higher relative permittivity than cellulose fibre [5]. Low density transformer paper has lower relative permittivity compared to high density paper. The influence of relative permittivity of insulating fluids is more dominant for low density papers. It is mainly because it has higher volume fraction. It is evident from the degree of relative permittivity increase with increase of temperature in which the increase gradient is lower for Amotfors than Cottrell. Higher density paper is less influenced by the relative permittivity of insulating fluid. Similar results also reported in [5] which described the relation between relative permittivity of paper and insulating fluid as function of paper density.

Figure 5.21 also shows temperature dependent behaviour for transformer paper impregnated with Nytro 4000X and ester fluids. The relative permittivity increase with temperature is less significant for paper impregnated with Nytro 4000X. Meanwhile, there is steep increase for paper impregnated with ester fluids. This might be related to the difference of heat transfer capability of insulating fluid.



(a)

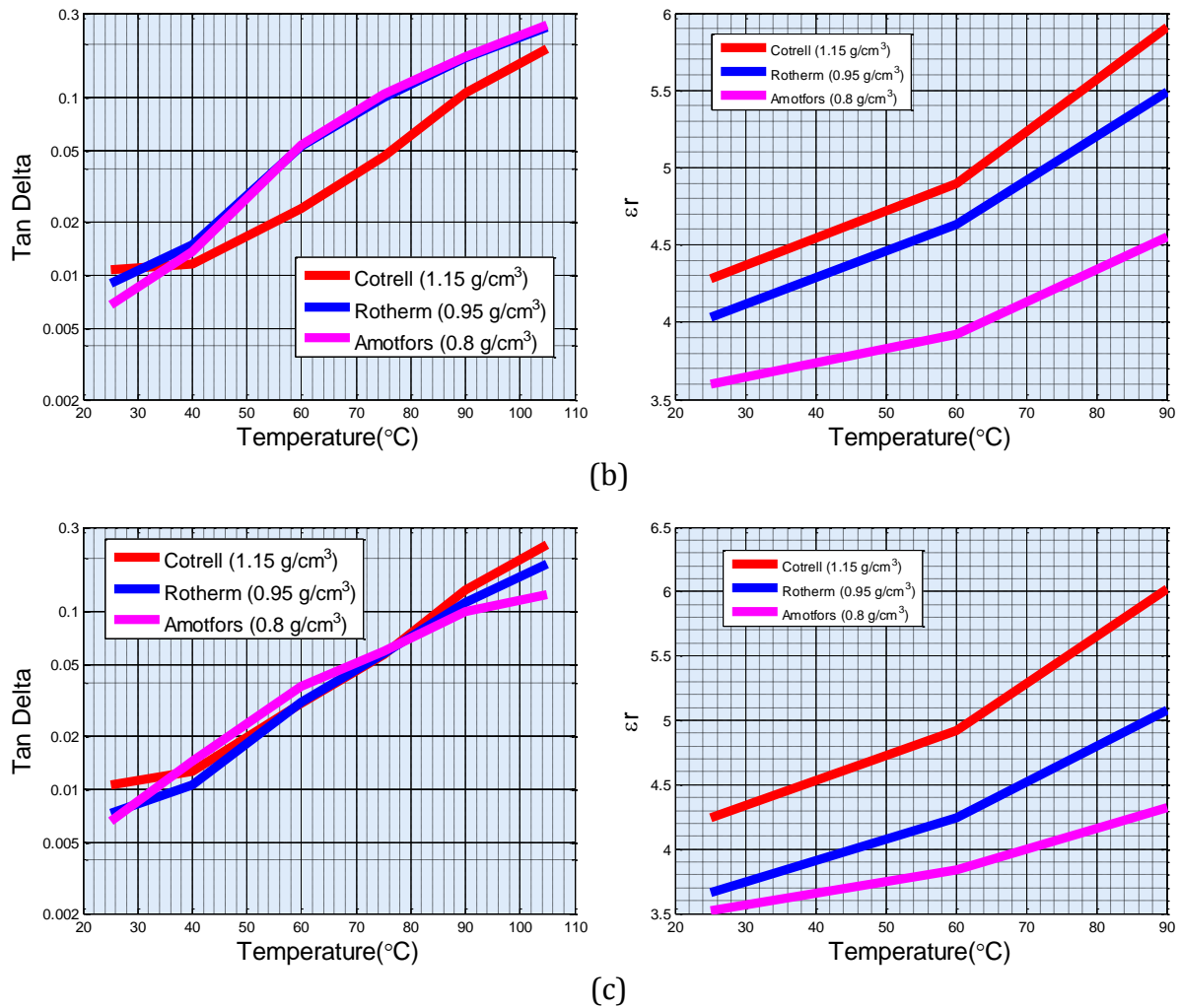


Figure 5.21: Effect of density and thickness on $\tan \delta$ and relative permittivity at power frequency of 50Hz for transformer paper impregnated with (a) Nytro 4000X, (b) MI7131 and (c) FR3.

5.4.3. Influence of insulating fluid and temperature

The influence of insulating fluids on the dielectric properties solids impregnated samples depend on many factors such as solid density, thickness, and chemical linkage of solid. Figure 5.22 depicts the influence of insulating fluids on $\tan \delta$ characteristic of pressboard and transformer paper with (a) high density, TIV and Cottrell and (b) low density, TIII and Rotherm. Generally, pressboards possess lower $\tan \delta$ compared to transformer papers when impregnated with all insulating fluids. According to equation (3.14), this phenomenon relates to the relaxation time of interfacial polarization. Thin insulating materials reduce the relaxation time of long-range charge carrier migration and subsequently, shift the peak loss (absorption frequency) to higher frequency.

$\tan \delta$ of pressboards and transformer papers impregnated with Nytro 4000X has similar characteristic with increase of temperature in which it decreases in

temperature range between 25°C to 60°C and then it increases in temperature range between 60°C to 105°C. Similar results for dry un-impregnated transformer paper can be found in [5]. It can be used as confirmation because $\tan \delta$ characteristic of un-impregnated and impregnated with mineral oil for cellulose transformer papers shows similar characteristic as in Figure 5.8.

Tan δ of pressboards and transformer papers impregnated with ester fluids are different with when it is impregnated with N4000X. It is noticeable that $\tan \delta$ increase with increase of temperature in range between 25°C to 105°C. The influence of ester fluid is more pronounced for pressboard. Pressboard impregnated with FR3 has higher $\tan \delta$ in temperature range of 40°C to 105°C. The difference is not clear for paper impregnated with ester fluids. It is possibly caused by the interrelation between the thickness of papers and the effect of interfacial polarization mechanism which presence on transformer papers impregnated with ester fluids. Hence, the influence of interfacial polarization on $\tan \delta$ is more dominant than paper characteristic itself.

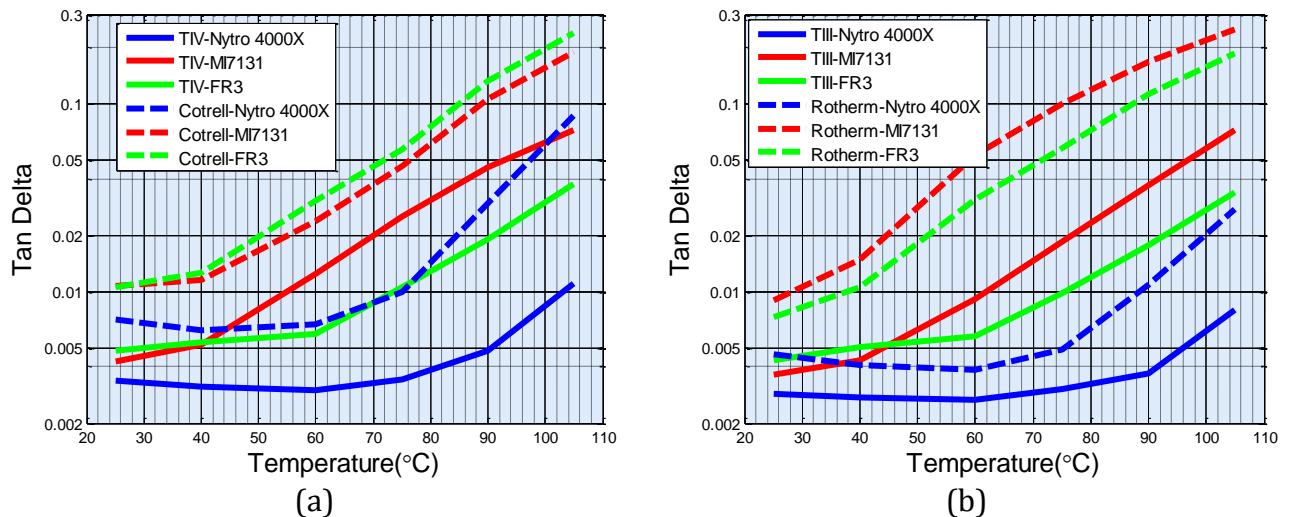


Figure 5.22: Effect of insulating fluid on $\tan \delta$ of pressboards and transformer papers with (a) high density and (b) low density.

It is well known that relative permittivity of oil at power frequency decreases with increase of temperature. For temperature above 0°C, the decrease is caused by volume expansion of oil [84, 135]. It also applies for ester fluids. Figure 5.23 depicts the influence of insulating fluids on relative permittivity characteristic of pressboard and transformer paper with (a) high density, TIV and Cottrell and (b) low density, TIII and Rotherm at 25°C. Generally, solids impregnated with mineral oil possess lower effective relative permittivity. Different characteristic of relative permittivity change with increase of temperature is observed for pressboard and transformer papers. Higher relative permittivity rise of paper compared to pressboard might be related to (a) the thermal expansion coefficient of the material and its relation to the sample dimension (e.g. Cottrell = 0.076mm and TIV = 2mm) and (b) the difference on chemical linkage of TIV and Cottrell.

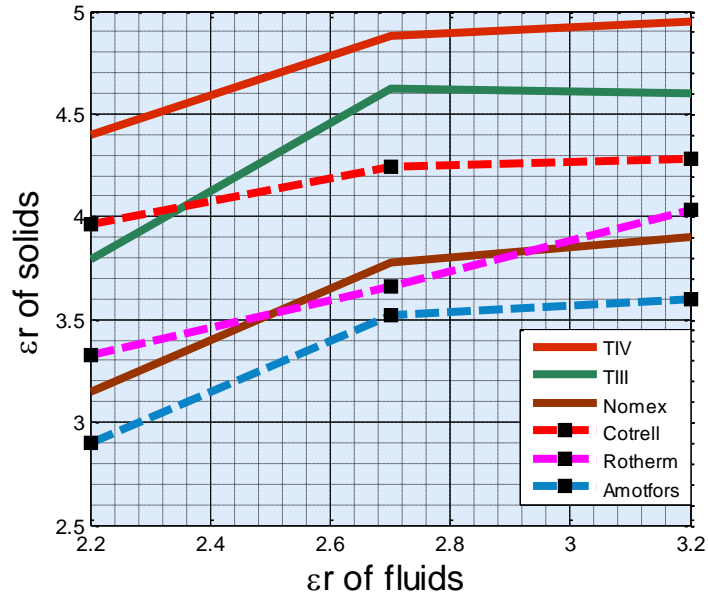


Figure 5.23: Relation of the relative permittivity insulating fluids and solid impregnated samples.

Relative permittivity is measured from capacitance of tested sample as in equation. Generally, capacitance of capacitors can be expressed as

$$C = \varepsilon_0 \varepsilon_r \frac{A}{h} \quad (5.3)$$

Based on equation (5.3), relation between temperature dependence of capacitance, relative permittivity and material dimension can be expressed as [136]

$$\frac{1}{C} \frac{dC}{dT} = \frac{1}{\varepsilon_r} \frac{d\varepsilon_r}{dT} + \frac{h}{A} \frac{d}{dT} \left(\frac{A}{h} \right) \quad (5.4)$$

Where

$\frac{1}{C} \frac{dC}{dT}$ is temperature coefficient of capacitance (TCC)

$\frac{1}{\varepsilon_r} \frac{d\varepsilon_r}{dT}$ is temperature coefficient of relative permittivity (TCE)

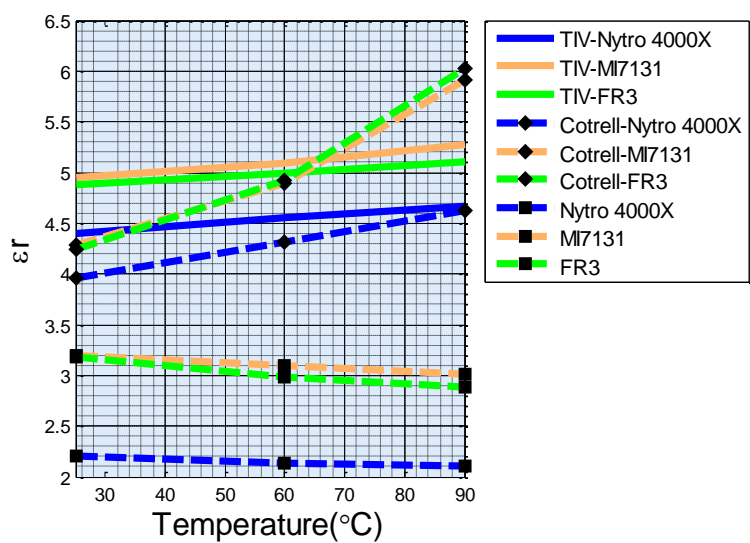
$\frac{h}{A} \frac{d}{dT} \left(\frac{A}{h} \right)$ Represents dimensional changes during thermal expansion

Therefore, temperature dependence of capacitance is determined by changes of relative permittivity and dimension of material.

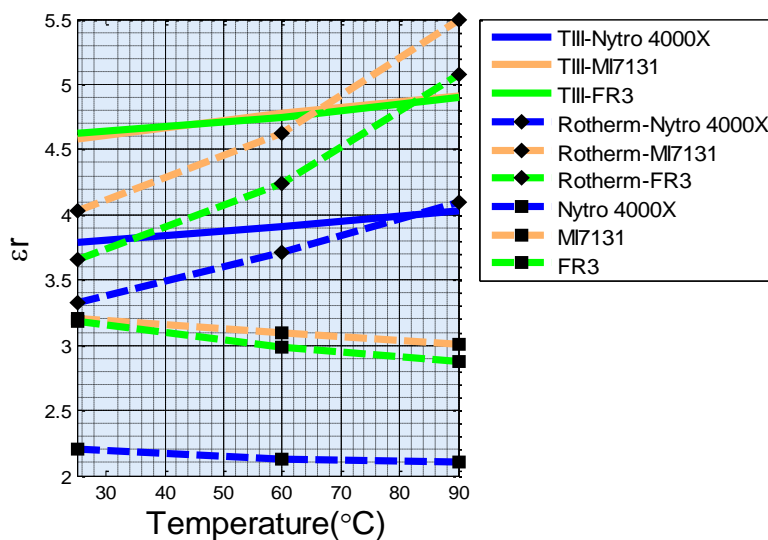
In relation to dimension changes, the same thermal expansion could have different effect on the change of capacitance due to different sample dimension. For example, dimensional change of 0.004mm is about 5% of 0.076mm (Cottrell) and only 0.2% of

2mm (TIV). Hence for thicker sample, the effect of dimensional change during thermal expansion is less pronounced. This fact might be one the reasons why the relative permittivity of paper is higher compared to pressboard at 90°C.

The other possible reason is the different chemical linkage of TIV and Cottrel. It is known that high temperature may trigger phase transition in material. A rapid increase of relative permittivity is normally observed in this instance. Different chemical linkage might change the temperature level in which phase transition occurs. Unfortunately, the information on the temperature level in which phase transition of pressboard and paper occurred was not known. This temperature level for epoxy matrix when phase transition occurred is about 90°C (136).



(a)



(b)

Figure 5.24: Effect of temperature on relative permittivity of (a) high density and (b) low density pressboard and transformer papers.

Figure 5.24 shows the effect of temperature on relative permittivity of pressboard and transformer papers with (a) high density and (b) low density and relative permittivity of insulating fluids. It shows that the relative permittivity of Cottrell impregnated with MI7131 at 90°C is higher than TIV impregnated with MI7131 (red box in Figure 5.24). However at 25°C, different relation is observed in which relative permittivity of Cottrell impregnated with MI7131 at 90°C is higher than TIV impregnated with MI7131 (blackbox in Figure 5.24). This temperature behaviour is more pronounced for solid impregnated with ester fluids and it is independent of the material density.

In solid – fluid insulating system, the volume fraction of fluid plays an important role on the effective relative permittivity ε_{eff} as in Lichtenecker formula (equation (5.5)).

$$\ln \varepsilon_{eff} = f \cdot \ln \varepsilon_i + (1 - f) \cdot \ln \varepsilon_e \quad (5.5)$$

Where

- ε_{eff} Effective relative permittivity of solid-fluid insulating system
- ε_i Permittivity of homogenous dielectric material i.e. pressboard and transformer papers)
- ε_e Permittivity of material located randomly in homogenous dielectric i.e. insulating fluids
- f Volume fraction that is occupied by ε_i in ε_e

It implies that higher volume fraction of fluid causes the effective relative permittivity ε_{eff} of solid-fluid insulating system follows the relative permittivity of fluid (e.g. MI7131 =3.2 at 25°C). It is evident from the relative permittivity of TIII, which is lower than TIV.

The odd behavior can be explained as follows. When measuring dielectric properties of solid impregnated samples, there is always thin layer of fluid on the surface. It is inevitable even with high pressure electrode and it has been reported that the dielectric response of solid impregnated material will be influenced to a considerable degree by thin fluid layer [47, 133]. This thin fluid layer can be considered as volume fraction of fluid. The effect of thin fluid layer is different on both Cottrell ($h= 0.076\text{mm}$) and TIV ($h= 2\text{mm}$). It can be visualized as in Figure 5.25.



Figure 5.25: Thin fluid layer on the surface of solid samples.

At 25°C, the thermal expansion can be neglected. Even though the thin fluid layer is equal (same thickness) for both pressboard and paper, the percentage of fluid layer on the surface of paper is higher compared to pressboard due to the sample thickness (Cottrell = 0.076 mm and TIV = 2mm). In other words, the volume fraction of fluid is higher in paper. Hence, relative permittivity of Cottrell at 25°C is lower than of TIV even though the material density is in the same range (Cottrell = 1.15 g/cm³ and TIV = 1.19 g/cm³). In conclusion, at 25°C, ϵ_{eff} of paper-fluid insulating system is lower than ϵ_{eff} of pressboard-fluid insulating system.

As described before, temperature dependent of capacitance is determined by changes of relative permittivity and dimension of material. At 90°C, the thermal expansion cannot be neglected. The effect of fluid layer is less dominant compared to thermal expansion of samples. If the effect of fluid layer still dominant then relative permittivity decreases with increase of temperature, but this is not the case. In relation to dimension changes, the same thermal expansion could have different effect on the change of capacitance due to different sample dimension.

The steep increase of relative permittivity is more pronounced for solids – MI7131 compared to solids – Nytro 4000X maybe because the differences of the heat transfer capability of insulating fluids and polarization characteristic of solid impregnated with different insulating fluids. According to equation (3.14), the relaxation time of polarization depends on many factors such as material thickness, temperature, and charge carrier concentration. Interrelation between those factors generates unique relaxation time of polarization in which the relaxation time of thin samples is more affected by increase of temperature than thick samples. The change of relaxation time with increase of temperature relates to the change of relative permittivity (it shifts to higher frequency). Hence, the change of relative permittivity with increase of temperature is more pronounced for thin samples (transformer papers) than thick samples (pressboard). All those analysis lead to conclusion, at 90°C, ϵ_{eff} of paper-fluid system is higher ϵ_{eff} of pressboard-fluid system.

6. Replacement of insulating fluids: laboratory test of retrofilling

6.1. Introduction

This chapter contains two experiments as described in the experiment scheme in section 4.4. There were two investigations performed:

1. Retrofilling simulation in laboratory scale.
The time behaviour investigation of dielectric properties for pressboard and transformer papers was performed after insulating fluid replacement the from Nytro 4000X to ester fluids.
2. Investigation of polarization mechanism after the fluid replacement.
The investigation of polarization mechanism which occurred on the surface of pressboard (interfacial polarization which presence on the surface) was performed and also the analysis of the depth of ester fluid penetration into pressboard after insulating fluid replacement. It was done by replacing again the ester fluids in the previous step with Nytro 4000X.

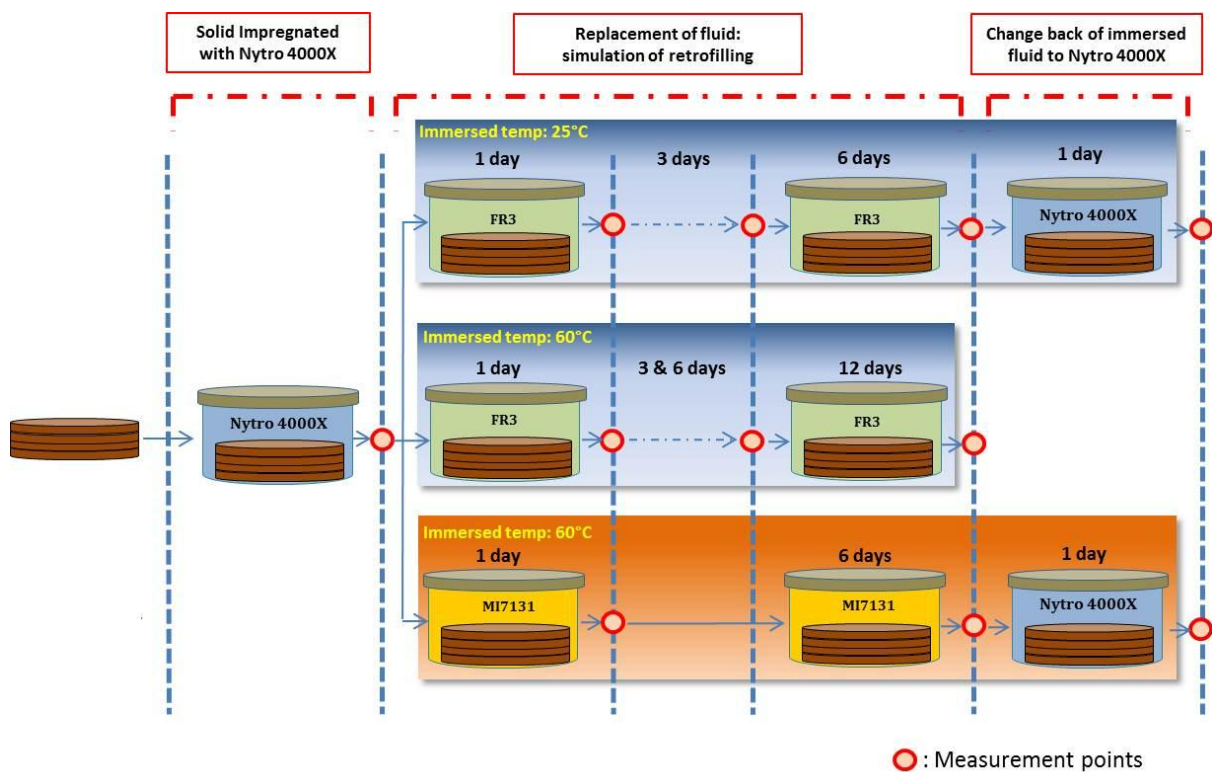


Figure 6.1: Experiment schemes for retrofilling experiment.

Figure 6.1 depicts the experiment scheme of fluid replacement from Nytro 4000X to synthetic ester, MI7131 and natural ester, FR3. For experiment in FR3, the samples were immersed at two temperature levels, 25°C and 60°C. The aim was to investigate the influence of immersed temperature on the behaviour of dielectric properties. Meanwhile for experiment in MI7131, the pressboards were immersed only at 60°C. The dielectric response measurement was performed at certain time after fluid replacement as in the schemes.

6.2. Procedure of fluid replacement

Fluid replacement procedure was designed to be similar with the recommended retrofilling procedure in field as in [137, 138] with some modifications. Pressboard impregnated with Nytro 4000X was moved into empty vessel and placed inside a vacuum oven. Shortly after that, the pressboard inside the vessel was vacuumed until the pressure below $< 1\text{mbar}$. Then, ester fluid was poured into the vessel. The low pressure was kept up to 2 hours until bubble disappeared and the vacuum was broken.

All pressboard samples in this experiment were dry with absolute moisture content is less than 0.5%. Moisture content of pressboards was measured before the experiment and after all experiments were finished.

6.3. Time behavior of dielectric response after fluid replacement

6.3.1. In frequency domain

Replacement of insulating fluid would definitely influence the dielectric properties of samples. The investigation was aimed to study the time behaviour of dielectric properties and the influence of immersed temperature on the dielectric properties.

Figure 6.2 and Figure 6.3 depict time behaviour of dielectric response after insulating fluid replacement from Nytro 4000X to FR3 at different immersed temperature, 25°C and 60°C respectively. Figure 6.2(a) shows that at frequency of 0.1-100Hz, the dielectric response $\tan \delta$ follows the shape of dielectric response $\tan \delta$ of pressboard impregnated with FR3. But at lower frequency, from 1mHz-0.1Hz, the $\tan \delta$ value return to the shape of dielectric properties of pressboard impregnated in Nytro 4000X. It is possible that at immersed temperature of 25°C, that ester fluid has not penetrated the pressboard in 6 days and only deposited on the surface of pressboard. It means that the presence of lost peak over frequency range 0.1-10Hz after fluid replacement might be caused by interfacial space charge polarization on the surface of pressboard.

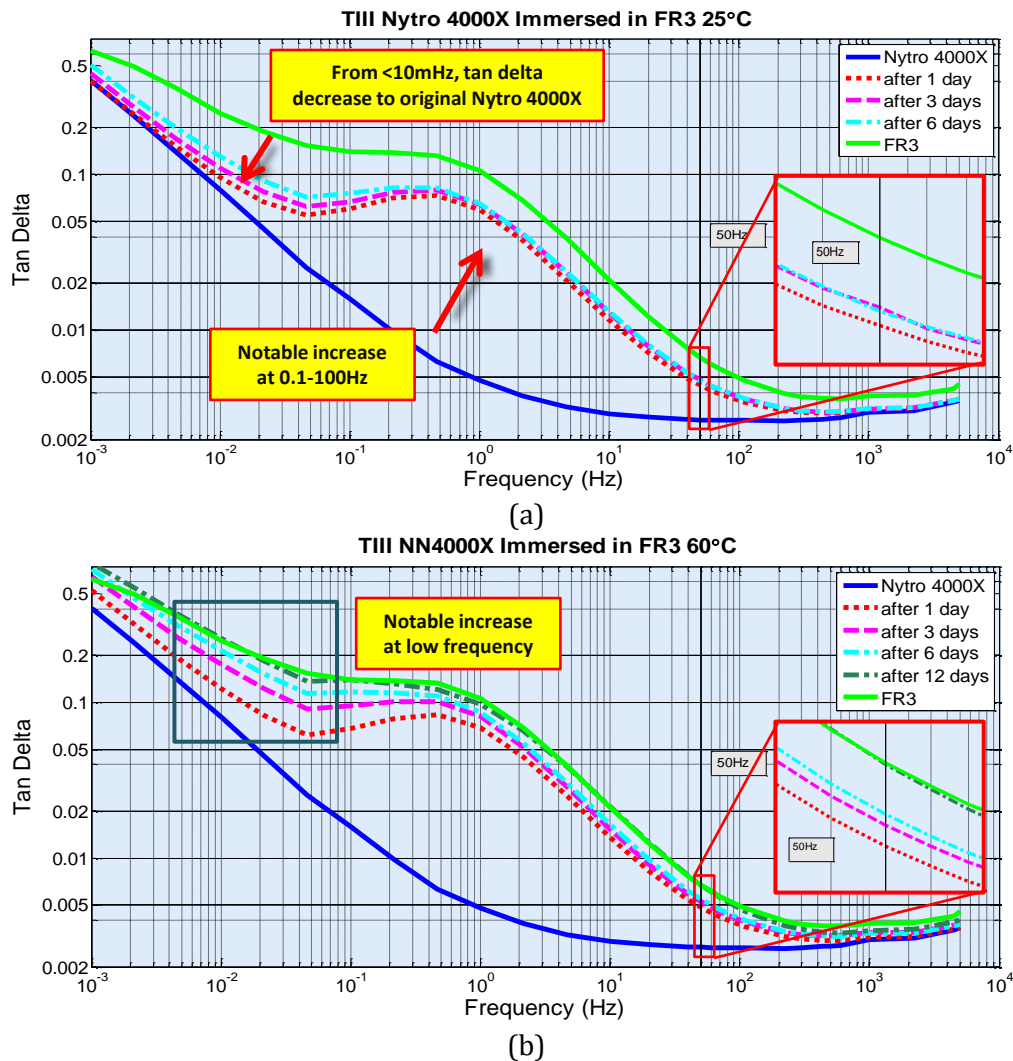


Figure 6.2: Time behaviour of $\tan \delta$ TIII after fluid replacement to FR3 measured at 60°C with immersed temperature of (a) 25°C and (b) 60°C .

Meanwhile, for immersed temperature of 60°C , the dielectric response $\tan \delta$ changes significantly with time as in Figure 6.2(b). The rate of dielectric response $\tan \delta$ change with time is faster at higher immersed temperature. At higher temperature, the kinematic viscosity of ester fluids is significantly lower and thus, it is easier to impregnate the pressboard. After immersed in FR3 for 12 days, the dielectric response is similar to dielectric response of pressboard impregnated with FR3. There is also notable increased of dielectric response $\tan \delta$ at lower frequency. The increase of $\tan \delta$ at lower frequency for immersed temperature of 60°C means it is possible that (a) ester at some level has penetrated pressboard (hence, changing of space charge polarization behaviour inside the pressboard), (b) the increased of DC conductivity value with time after replacement of insulating fluid (evident from DC conductivity measurement) and (c) additional interfacial polarization on the surface of pressboard (indicated by the presence of loss peak on dielectric response $\tan \delta$ over frequency 0.01–1Hz).

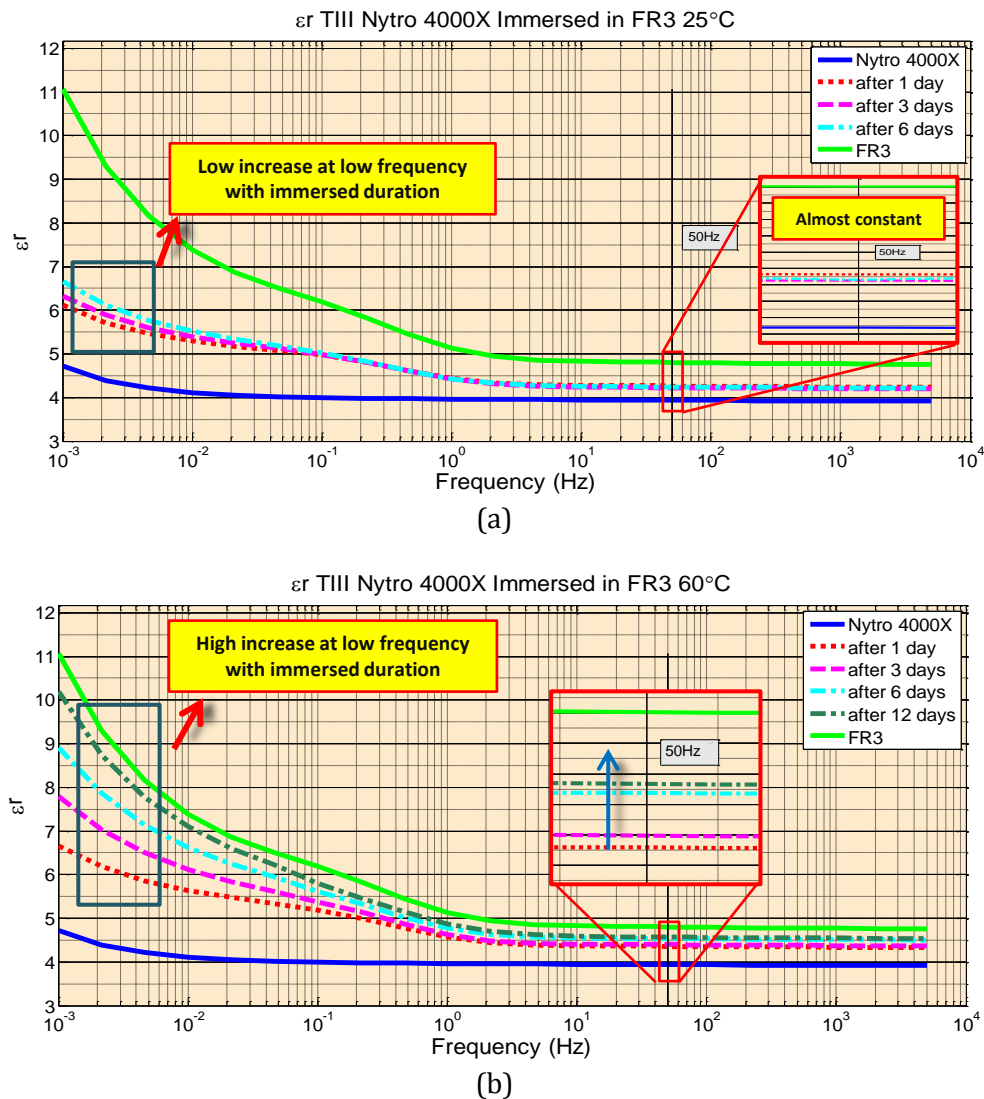


Figure 6.3: Time behaviour of relative permittivity TIII after fluid replacement to FR3 measured at 60°C with immersed temperature of (a) 25°C and (b) 60°C.

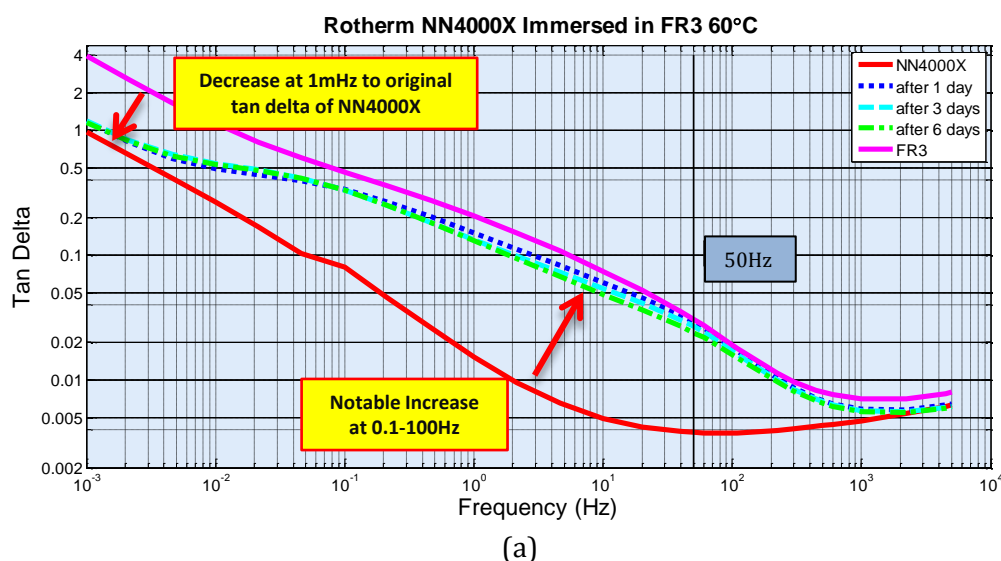
Figure 6.3(a) shows that for immersed temperature of 25°C, the relative permittivity changes after fluid replacement to FR3. But there is no significant change in relative permittivity from day one to six days after fluid replacement as in $\tan \delta$. As indicated from dielectric response $\tan \delta$, for immersed temperature of 25°C, the increase of relative permittivity relates only to the interfacial polarization on the surface pressboard. Meanwhile, for immersed temperature of 60°C, the relative permittivity changes significantly with time in wide frequency range as in Figure 6.3(b). The increase at frequency 50Hz is shown in zoom Figure 6.3(b). The increase is most significant in lower frequency which might be caused by changing behaviour of interfacial polarization mechanism, both inside the pressboard and on the surface of pressboard. Thus, for immersed temperature of 60°C, the increase of relative permittivity relates to both interfacial polarization in the cellulose fiber structure and interfacial polarization on the surface of pressboard. Hence, it is possible to conclude that interfacial polarization on the surface of pressboard is marked by the presence of

additional loss peak at frequency 1Hz (at 60°C). Meanwhile, the interfacial polarization in the cellulose fiber structure of the pressboard which filled with insulating fluid is marked by the increase of tan delta on wider range of frequency. However, the loss peak for the latter is not clear over the measured frequency range.

It was concluded that interfacial polarization on pressboard impregnated with ester fluids consist of interfacial polarization in the cellulose fiber structure and interfacial polarization on the surface of pressboard has different relaxation time. For the latter, the relaxation time is at about 1Hz at measured temperature of 60°C and marked by the presence of additional loss peak. This means that when pressboard impregnated with ester fluids, it has a distribution of relaxation time for interfacial polarization. It is not the case for pressboard impregnated with mineral oil. Those interfacial polarizations are also indicated by different characteristic of relative permittivity at low frequency.

Figure 6.4 shows time behaviour of dielectric properties transformer paper Rotherm after fluid replacement to FR3 at immersed temperature of 25°C. Figure 6.4(a) shows that at frequency of 0.1-100Hz, the dielectric response $\tan \delta$ follows the shape of dielectric response $\tan \delta$ of Rotherm impregnated with FR3. But at lower frequency, from 0.1-1mHz, the $\tan \delta$ value return to the shape of dielectric properties of Rotherm impregnated in Nytro 4000X. The change is quite similar to that of pressboard.

Figure 6.4(b) shows the relative permittivity of Rotherm after fluid replacement. The increase is most significant in lower frequency due to interfacial polarization mechanism. Hence, the increase in relative permittivity of transformer papers after fluid replacement to ester fluid indicates the changing behaviour of interfacial polarization which might be caused by interfacial polarization on surface of paper which is dominant for solid impregnated with ester fluids. The difference on the interfacial polarization characteristic for transformer paper is not obvious as in the case of pressboard due to its low thickness.



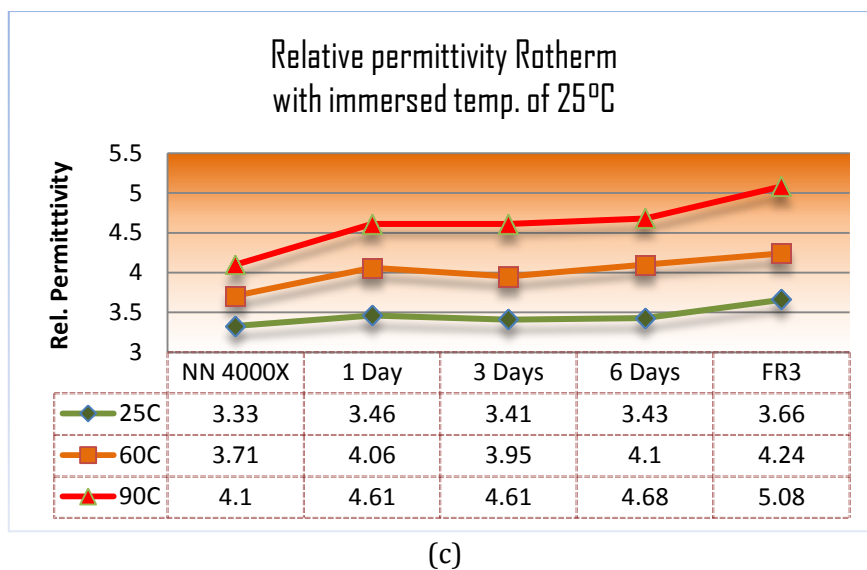
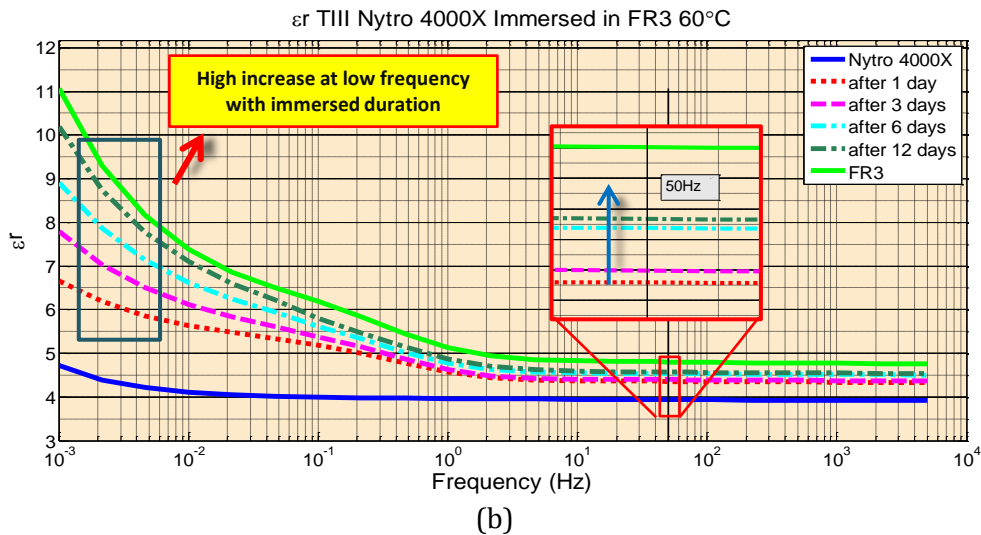
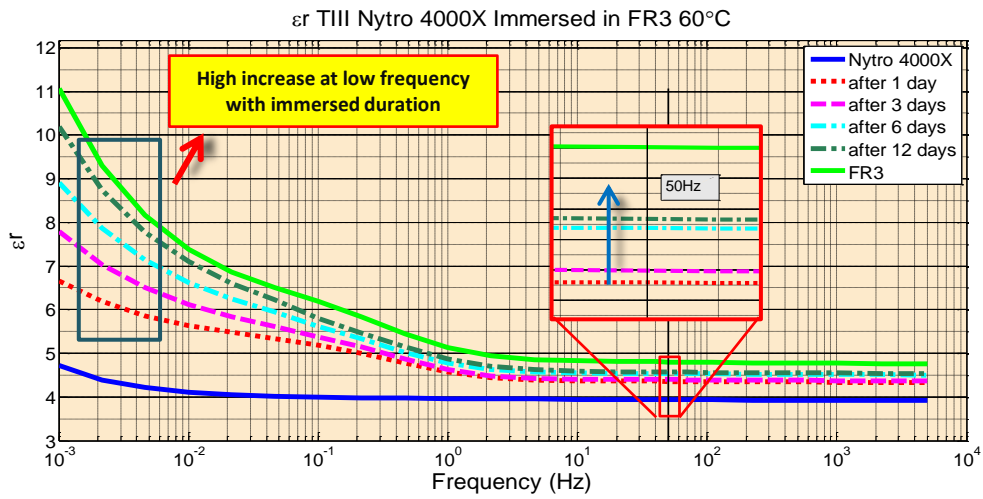


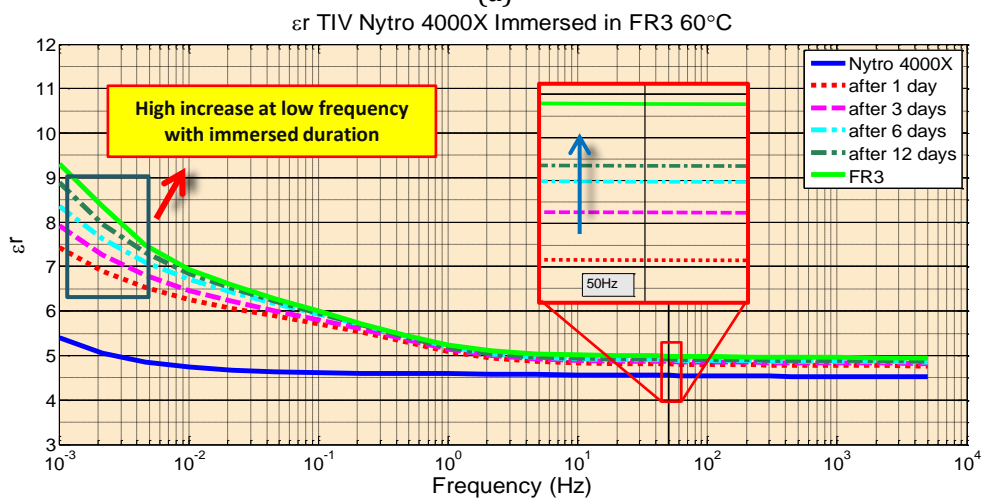
Figure 6.4: Time behaviour of dielectric properties Rotherm after fluid replacement to FR3 measured at 60°C for (a) $\tan \delta$, (b) relative permittivity and (c) table of relative permittivity changes with time.

Figure 6.5 shows the effect of material density on time behaviour of relative permittivity after fluid replacement to FR3 at immersed temperature of 60°C. Different changing behaviour of relative permittivity at low frequency was observed. It seems that the interfacial polarization more dominant for high density pressboard, notably from the increase of relative permittivity at low frequency.

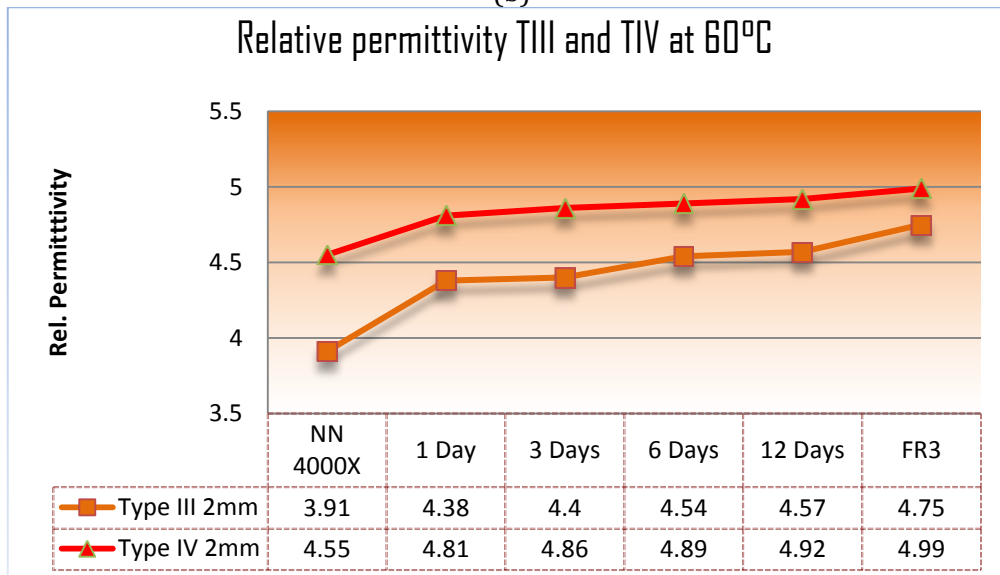
Figure 6.6 summarize the time behaviour of dielectric properties TIII and Figure 6.7 summarize the time behaviour of dielectric properties TIV after fluid replacement at 50Hz.



(a)

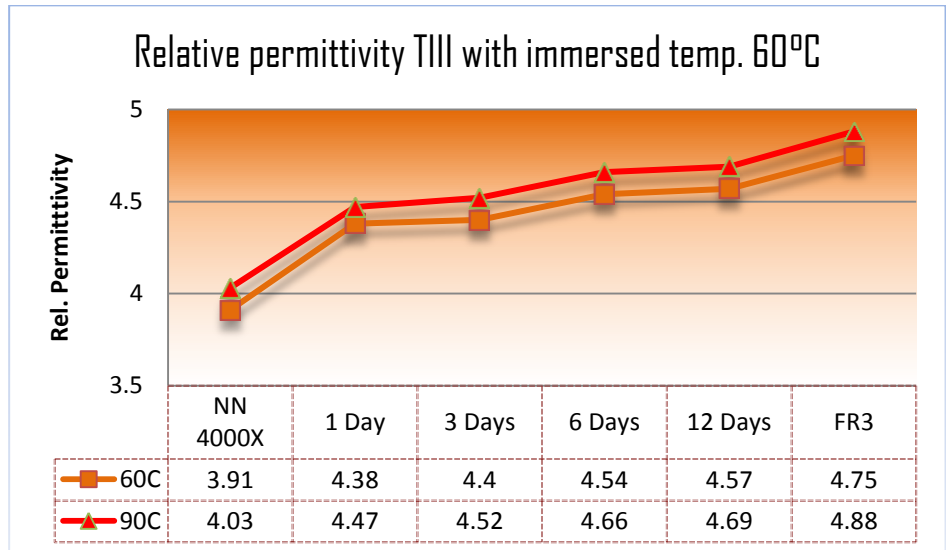
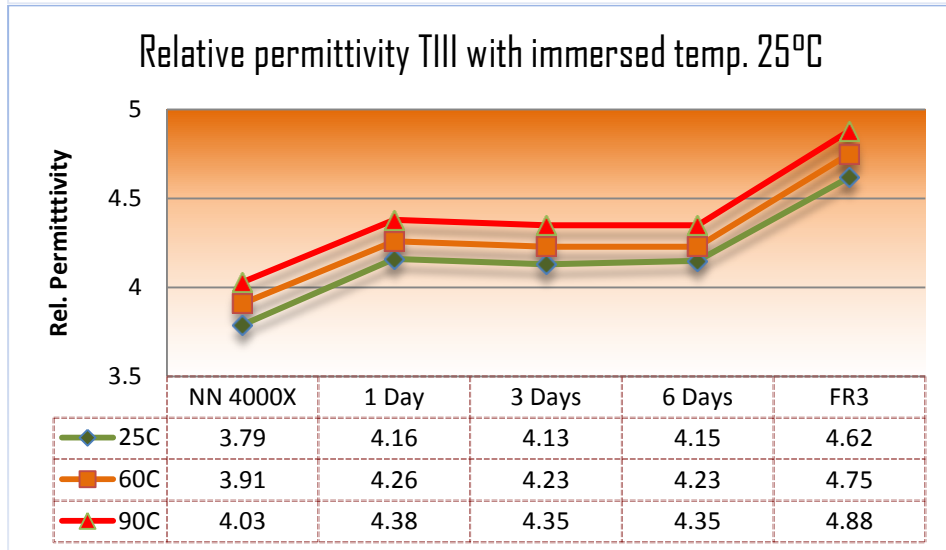
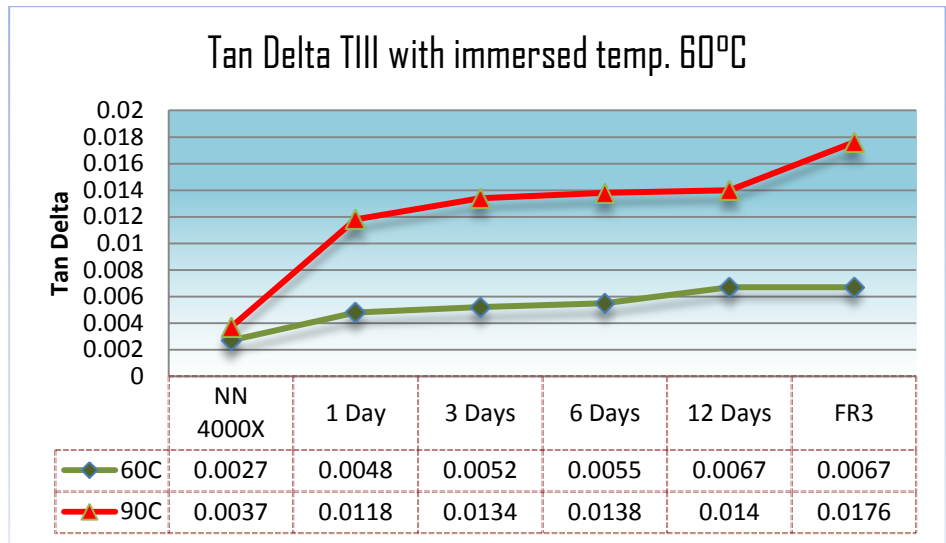
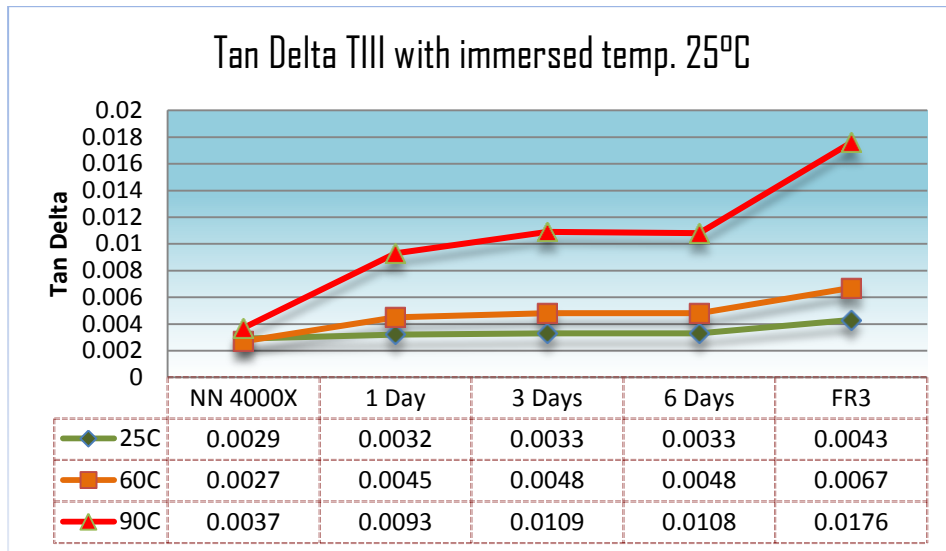


(b)



(c)

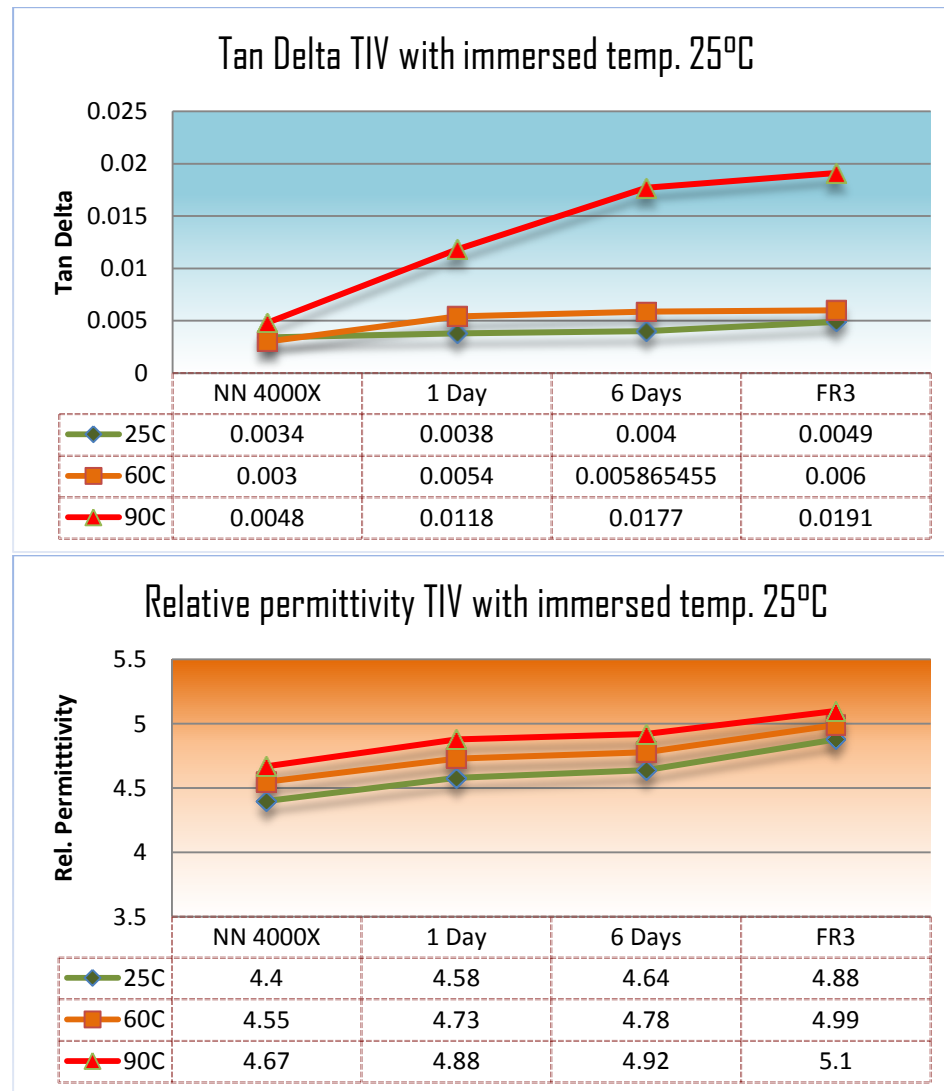
Figure 6.5: Effect of pressboard density on relative permittivity after fluid replacement to FR3 measured at 60°C for (a) TIII, (b) TIV and (c) relative permittivity comparison at 50Hz.



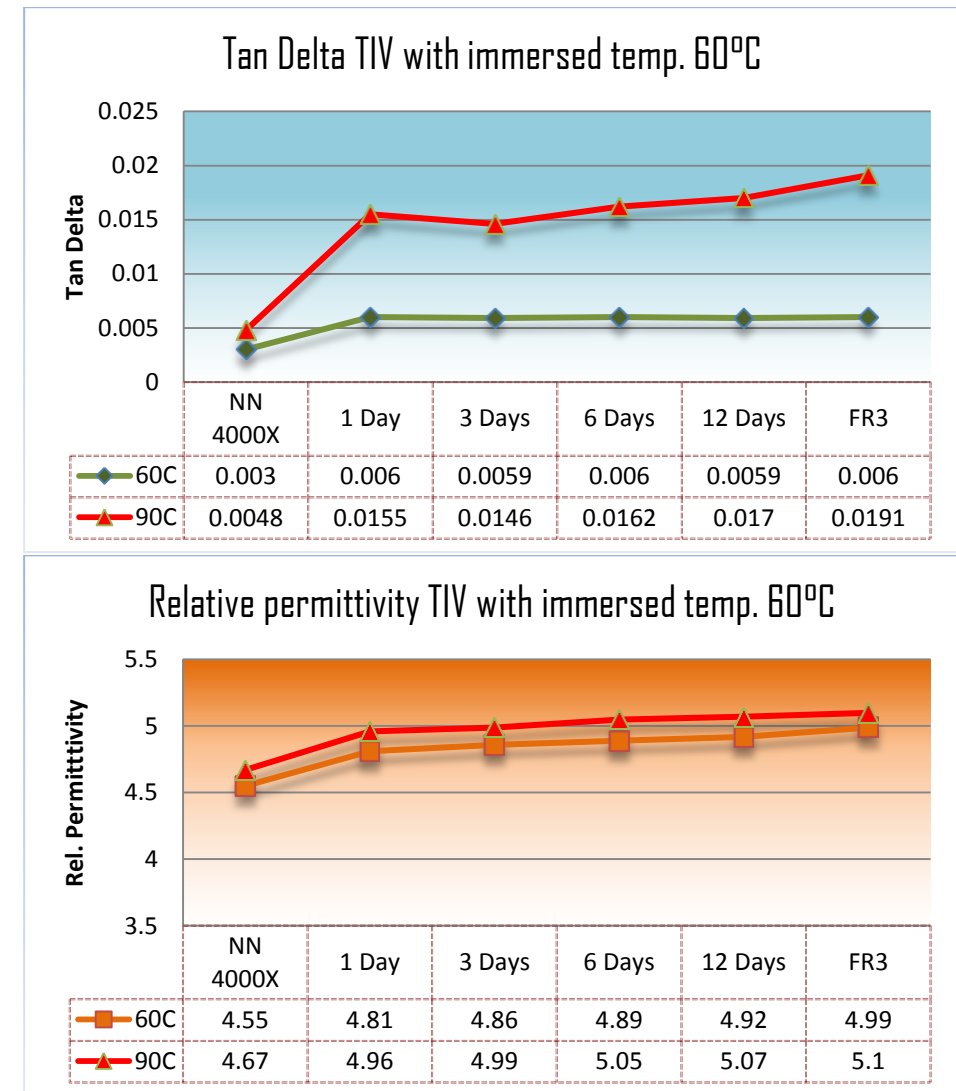
(a)

(b)

Figure 6.6: Influence of immersed temperature on dielectric properties of TIII after fluid change to FR3 at 50Hz. For immersed temperature of (a) 25°C and (b) 60°C.



(a)



(b)

Figure 6.7. Influence of immersed temperature on dielectric properties of TIV after the change to FR3 at 50Hz. For immersed temperature of (a) 25°C and (b) 60°C.

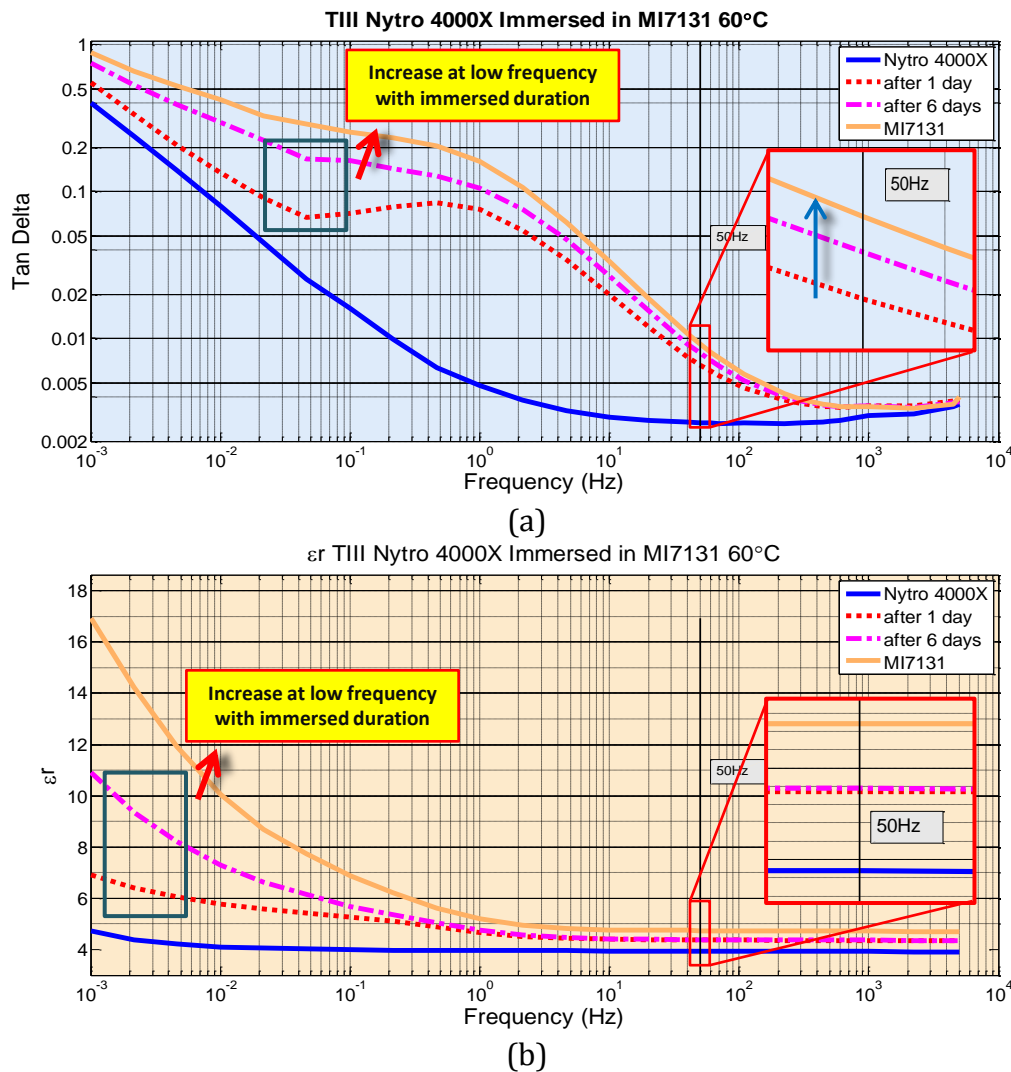


Figure 6.8: Time behaviour of dielectric properties of TIII after fluid replacement to MI7131 for (a) $\tan \delta$ and (b) relative permittivity.

Figure 6.8 depicts time behaviour of dielectric response after insulating fluid replacement from Nytro 4000X to MI7131 at immersed temperature of 60°C. The dielectric response $\tan \delta$ changes significantly with time as in Figure 6.8(a). The changing behaviour is almost the same with fluid replacement to FR3. Figure 6.8(b) shows that the relative permittivity changes significantly with time in wide frequency range. The increase at frequency 50Hz is shown in zoom Figure 6.8. The increase is most significant in lower frequency due to changing behaviour of interfacial polarization. Thus, the increase in relative permittivity at lower frequency might be caused by interfacial polarization in the cellulose fibre and on surface of pressboard. Figure 6.9 summarize the time behaviour of dielectric properties TIII and TIV after fluid replacement to MI7131 at 50Hz.

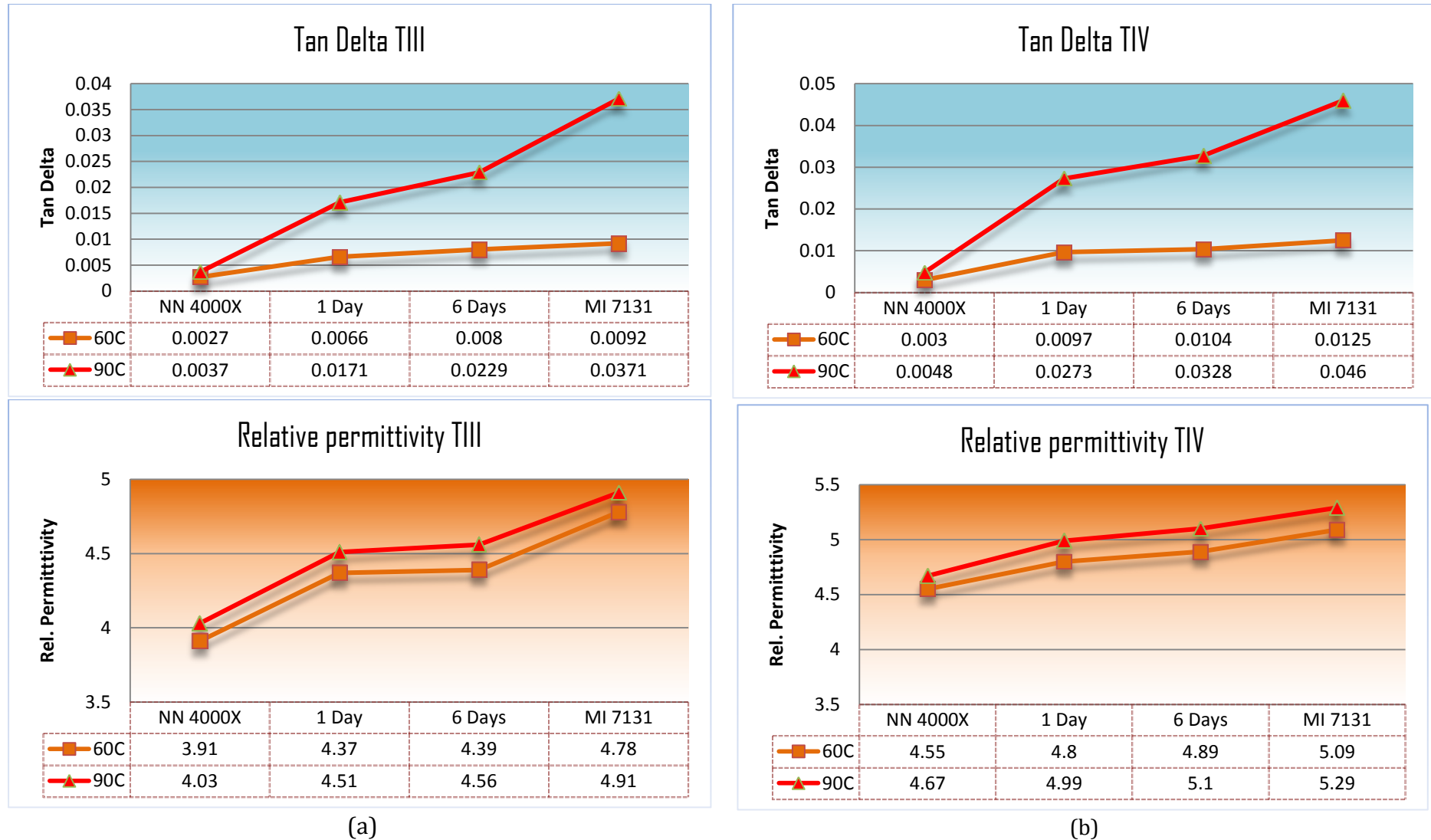


Figure 6.9: Time behaviour of dielectric properties after fluid change to MI7131 (a) TIII and (b) TIV with immersed temperature of 60°C.

There is distinction on the new dielectric response $\tan \delta$ and relative permittivity even after only one day of fluid replacement. It was changing rapidly and the new dielectric response resembles dielectric response of pressboard impregnated with ester fluids. It is interesting to investigate why it changed so fast, was it because ester fluid has impregnated the pressboard or it was caused by other mechanism. It is also important to investigate whether the change is permanent (FR3 penetrated the pressboard which has impregnated with Nytro 4000X previously) or temporary (because of interfacial polarization on the surface that can be removed). In practice, proper impregnation process of pressboard with ester fluids takes longer time (three days) and high temperature due to high viscosity of ester fluids [32]. Thus, it was suspicious if ester fluid has impregnated the pressboard in just one day.

All these questions prompted us to further investigate this phenomenon by replacing back ester fluids with Nytro 4000X. The purpose of this procedure is to remove the deposited ester fluids from the surface of pressboard.

6.3.2. In time domain

Replacement of insulating fluid would also definitely influence the DC conductivity of solid samples. A charging voltage V_c of 1kV was applied for several days to investigate the behavior of DC conductivity with time. The current measurement was performed at temperature of 90°C due to the short time to reach steady state. Thus, the investigation was performed on the steady state current and not the transient state.

Figure 6.10 presents typical long time duration charging current of after fluid replacement to FR3. In this case, the current was measured for 40 hours. It is noticeable that the time needed for current to reach steady state is longer after fluid replacement compared than that of only FR3 which is normally less than 2 hours. It is doubtful that it was caused by moisture effect (solid-fluid exchange) as the FR3 for bath had moisture content less than 20ppm and the solids had absolute moisture content less than 0.5%.

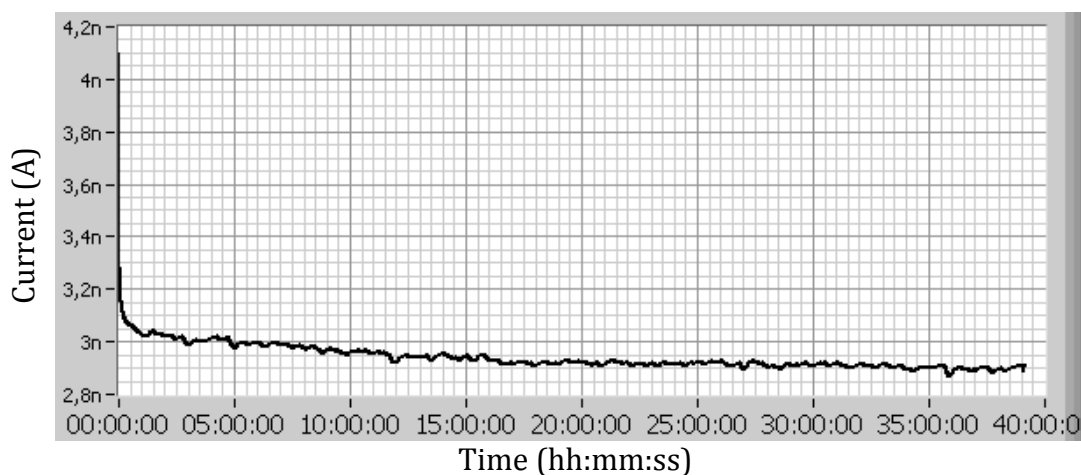
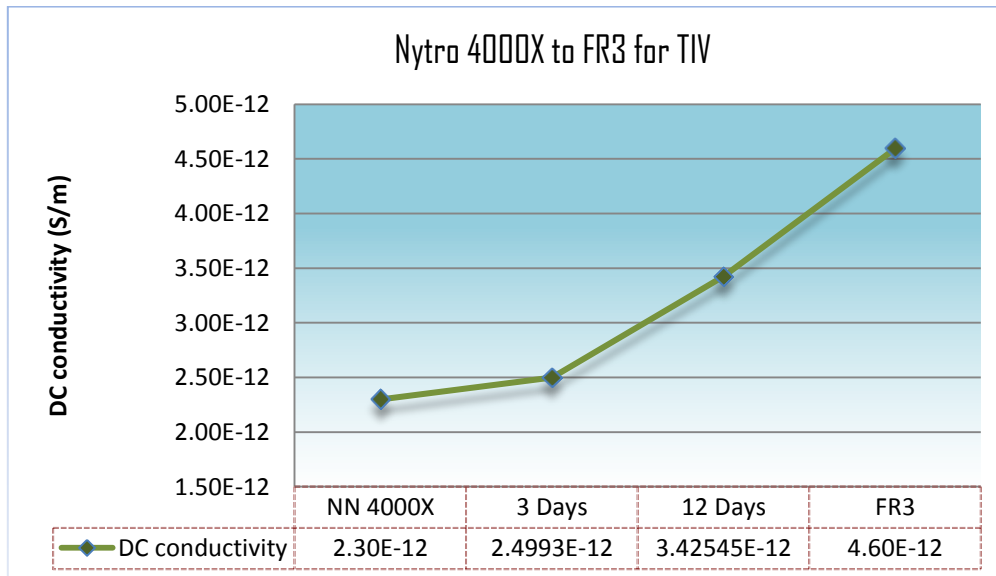
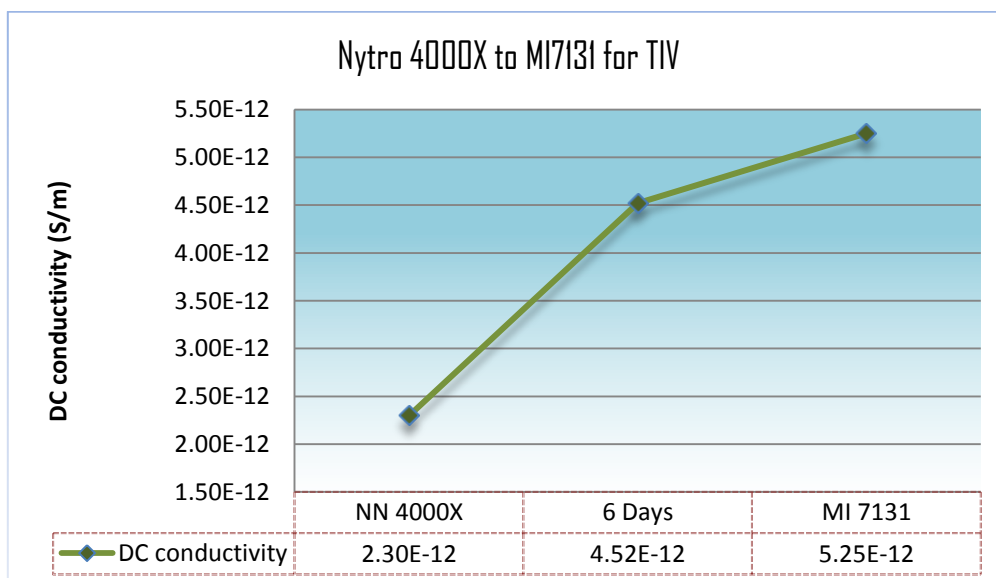


Figure 6.10: Charging current of TIV after 3 days in FR3.

Figure 6.11 shows the DC conductivity of solid impregnated with Nytro 4000X after fluid replacement to (a) FR3 and (b) MI7131. The charging current was measured for more than 16 hours for each case to ensure that the steady state value was not changed with time. It is evident that the DC conductivity of TIV increases with time after fluid replacement.



(a)



(b)

Figure 6.11: DC conductivity of TIV after fluid replacement to (a) FR3 and (b) MI7131 with immersed temperature of 60°C.

6.4. Polarization on surface of pressboard after insulating fluid replacement

This section explains the phenomenon occurred after fluid replacement. In section 6.3, it is clear that the dielectric response of pressboard impregnated with Nytro 4000X was changing after fluid replacement from Nytro 4000X to ester fluids. To have a proper explanation of this phenomenon, the ester fluids from the retrofilling experiment was changed back with Nytro 4000X to remove the deposited ester fluid from the surface of pressboard then performing the dielectric response measurement once again.

By performing this measurement, two things can be explained, (a) the penetration of ester fluids into pressboard and (b) how the polarization process on the surface of pressboard influenced the dielectric response. First, it shall answer the question of whether ester fluids really impregnated the pressboard (if it is permanent or not) or only deposited on the pressboard surface. And second, it might help us to understand the influence of interfacial polarization mechanism on the surface to the dielectric response of pressboard impregnated with ester fluids and differentiate it with the interfacial polarization within the cellulose fibre itself.

Figure 6.12 shows the fluid replacement procedure to Nytro 4000X. After the pressboard samples previously underwent change of insulating fluid from Nytro 4000X to ester fluids in the retrofilling simulation (up to 6 days in ester fluids), the ester fluid was changed back to Nytro 4000X. The pressboard samples were put back into a vessel filled with dry Nytro 4000X (relative moisture content less than 5ppm) without special treatment. The samples were kept for 22 hours at the same immersed temperature previously used before performing dielectric properties measurement. This procedure would remove the deposited ester fluids on the pressboard surface.

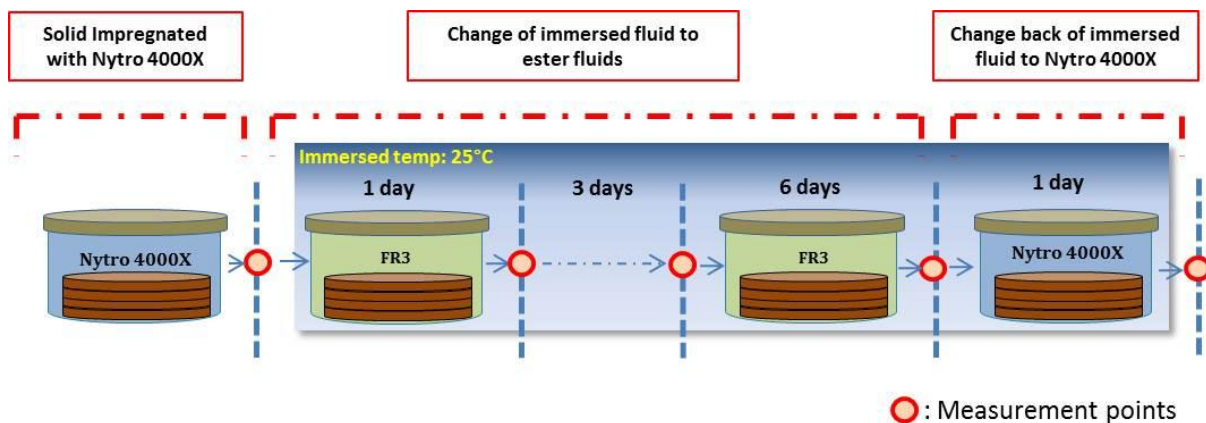


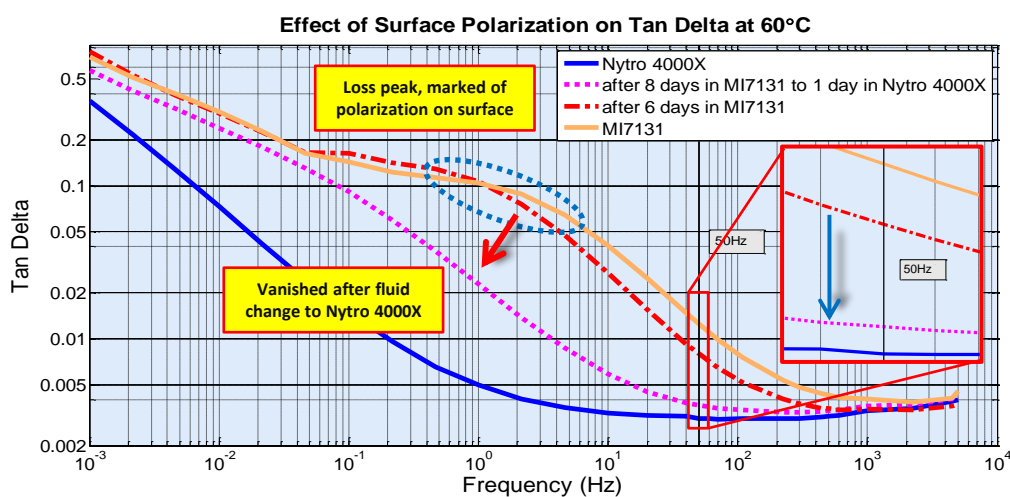
Figure 6.12: Experimental procedure of replacing the ester fluids back to Nytro 4000X.

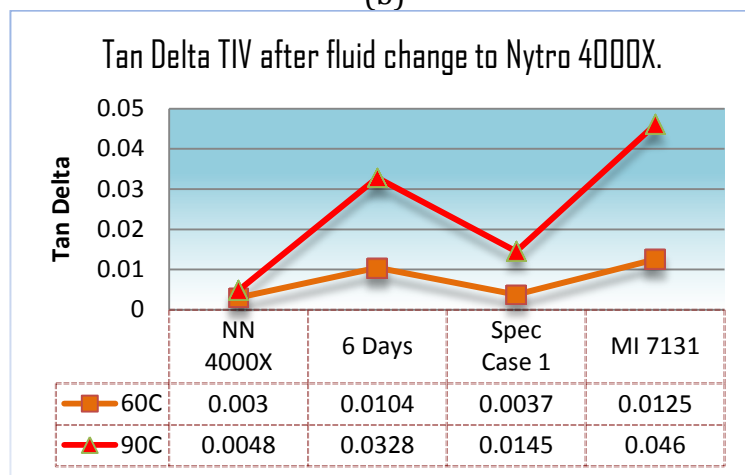
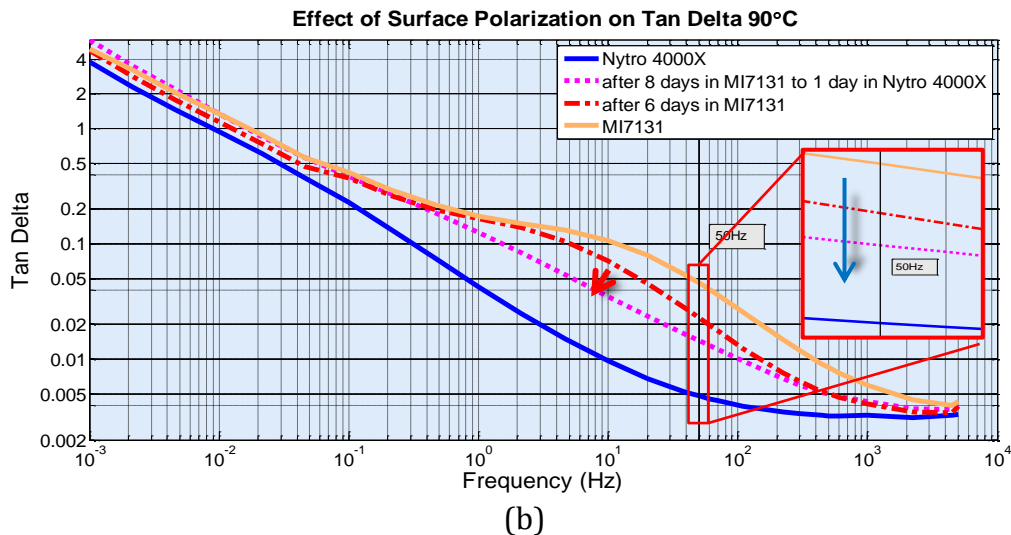
Figure 6.13 shows dielectric response $\tan \delta$ of pressboard TIV after fluid replacement from MIDEL7131 to Nytro 4000X again. The dielectric response $\tan \delta$ was changed; the loss peak in dielectric response $\tan \delta$ which previously occurred after retrofilling with ester fluid was vanished along with the removal of ester fluid from the surface of pressboard. It confirms that the presence of loss peak over frequency range of 0.1-10Hz occurred when pressboard

impregnated with ester fluid or after retrofilling is associated with interfacial polarization on the surface of pressboard impregnated with ester fluids. From previous results, the loss peak only occurs for samples impregnated in MI7131 and FR3. For samples impregnated in Nytro 4000X, there was no loss peak observed in this frequency range. Thus, it can be concluded that interfacial polarization on the surface of pressboard is dominant for pressboard impregnated with ester fluids, both synthetic and natural ester. It is marked by the presence of loss peak which is visible on dielectric response $\tan \delta$ and its contribution onto the total loss is dominant. For pressboard impregnated with mineral oil, such phenomenon is not visible.

After the removal of ester fluid from surface of pressboard, the loss peak was vanished. The new dielectric responses $\tan \delta$ were supposedly not influenced by interfacial polarization on the pressboard surface as it has been removed by replacement of MI7131 to Nytro 4000X. It is also important to note that the new dielectric response does not return to the original dielectric response characteristic of pressboard impregnated with Nytro 4000X. It means that at some level ester fluid has impregnated the pressboard samples or a small amount of Nytro 4000X has been leached out from pressboard. Nevertheless, the process changes the interfacial polarization behaviour in the cellulose fibre. Hence, the blue line in Figure 6.13 might indicate the interfacial polarization within the cellulose fibre due to ester fluids.

It is evident from the dielectric response $\tan \delta$ that after fluid replacement of MI7131 to Nytro 4000X, the loss peak that previously occurred for both pressboard impregnated with ester fluids and pressboard which underwent fluid replacement from Nytro 4000X to ester fluids were vanished. It is arguably that the loss peak is generated by interfacial polarization on the pressboard surface. The replacement of insulating fluid to Nytro 4000X had removed the ester fluids deposited on the surface. Hence, it can be concluded that the loss peak is linked to the interfacial polarization on the surface when ester fluid was applied. This loss peak does not occur for pressboard impregnated with Nytro 4000X.





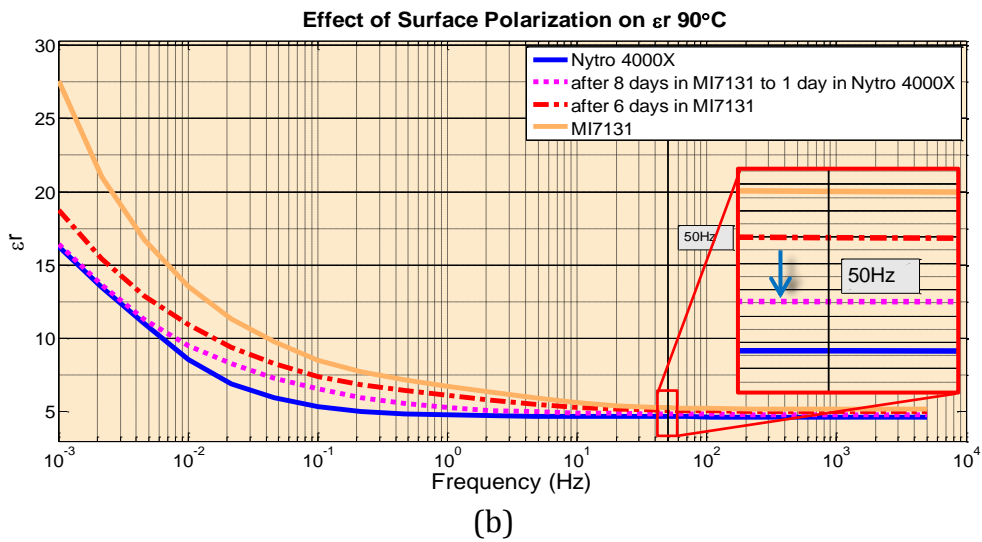
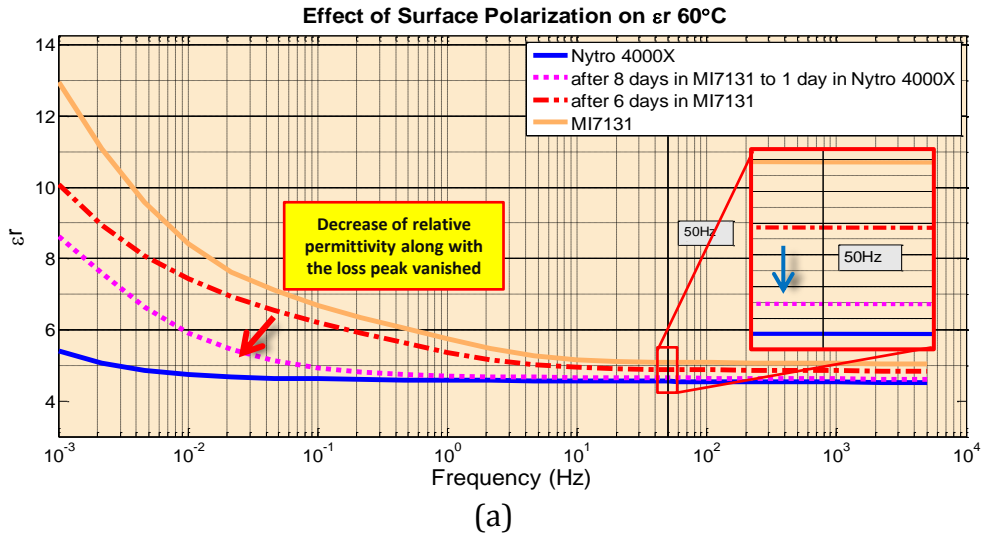
*Spec case 1 refers to pressboard after fluid change to Nytro 4000X.

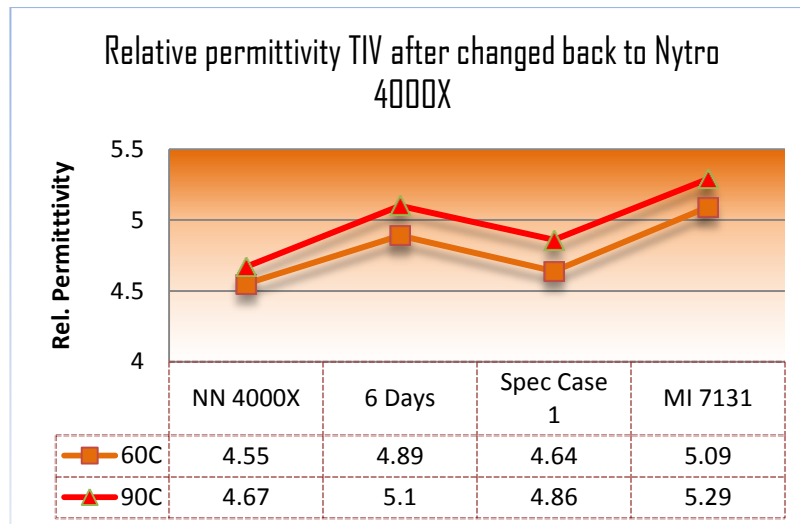
Figure 6.13: Influence of polarization on the surface of pressboard observes with dielectric response $\tan \delta$ after fluid replacement to Nytro 4000X at measured temperature of (a) 60°C and (b) 90°C. Meanwhile, (c) shows the change at 50Hz.

Figure 6.14 shows dielectric response relative permittivity of pressboard TIV after fluid replacement from MI7131 to Nytro 4000X. The relative permittivity value was decreased after replacement of insulating fluid to Nytro 4000X. It indicates that the increment of relative permittivity after retrofilling was partially caused by the interfacial polarization on the surface of pressboard. From measurement results, interfacial polarization on the surface adds up the relative permittivity value to about 0.25 for MI7131 and 0.18 for FR3 at 50Hz. In general, interfacial polarization within the cellulose fibre and on the pressboard surface increase relative permittivity value in wide range frequency but it is more dominant in lower frequency below 1Hz and both have different relaxation time.

As in the case of $\tan \delta$, the new dielectric response relative permittivity also does not return to the original dielectric response of pressboard impregnated with Nytro 4000X. There is increment of relative permittivity at low frequency after fluid replacement to Nytro 4000X. It confirms the previous conclusion from dielectric response $\tan \delta$ that at some level ester fluid has impregnated the pressboard samples or a small amount of

Nytro 4000X has been leached out from pressboard. Nevertheless, the process has changed the interfacial polarization behaviour within the cellulose fibre. Hence, the blue line in Figure 6.14 might indicate the interfacial polarization in the cellulose fibre due to ester fluids since the interfacial polarization on the surface was removed by the procedure.

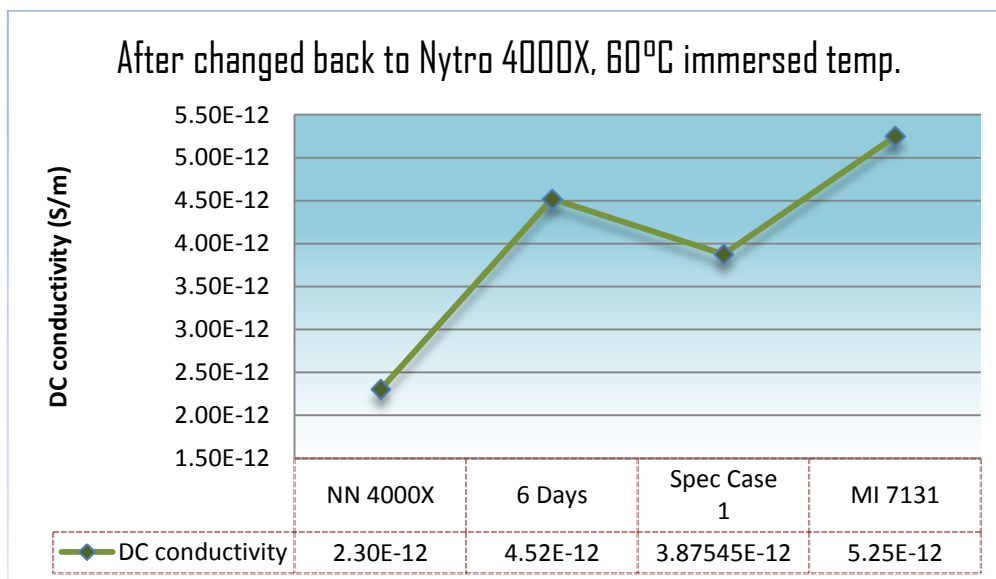




*Spec case 1 refers to pressboard after fluid change to Nytro 4000X.
(c)

Figure 6.14: Polarization on the surface of pressboard observed by dielectric response relative permittivity after fluid replacement to Nytro 4000X at measured temperature of (a) 60°C and (b) 90°C. Meanwhile, (c) shows the change at 50Hz.

Figure 6.15 presents the DC conductivity change after fluid replacement to Nytro 4000X. It is evident that the deposited ester fluid on the surface of pressboard increases the DC conductivity value. The deposited ester fluid on the surface of pressboard does not only affect the polarization mechanism but also DC conductivity. It is also noticeable that the DC conductivity value does not return to the original dielectric response of pressboard impregnated with Nytro 4000X which suggests that ester fluid influences the dc conduction process of impregnated pressboard at some level.



*Spec case 1 refers to pressboard after fluid change to Nytro 4000X

Figure 6.15: Time behaviour DC conductivity after fluid replacement to Nytro 4000X.

7. Estimating dielectric properties of solid impregnated with ester fluids

7.1. Introduction

Relative permittivity and $\tan \delta$ of solids impregnated with insulating fluids can be estimated in different way. The first approach is by semi-empirical formula. This approach has limitation especially if various parameters were taken into account. The other approach is by master curve technique. Meanwhile, the DC conductivity can be estimated using Arrhenius relation with the activation energy of DC conductivity and pre-exponential factor obtained from measurement. Both approaches are presented and discussed in this chapter

Estimation of relative permittivity and $\tan \delta$ offers flexibility when the value is not provided in the data sheets. For estimating effective relative permittivity of solids impregnated samples at 50Hz, a new semi-empirical formula was developed which takes into account the polarization process occurs on the surface of solids impregnated with ester fluids. Meanwhile, for estimating relative permittivity – $\tan \delta$ as function of frequency with temperature as parameter, the master curve of dielectric response which called the “master curve technique” was utilized. The master curve technique is more versatile than the semi-empirical formula especially for solid impregnated with ester fluids due to amount of data input needed.

7.2. Effective relative permittivity

7.2.1. Estimation of relative permittivity at power frequency of 50Hz

This section explains the semi-empirical formula for estimating relative permittivity of solid impregnated in alternative fluid. To found a suitable formula for estimating the effective relative permittivity at 50Hz, equation (2.60 to 2.66) in section 3.5 were applied to calculate the volume fraction of insulating fluid in solid. Then, the calculated volume fraction from those equations was compared with the maximum and minimum limit of volume fraction given by the Wiener Bounds and Hashin – Shtrikman Bounds as in Figure 7.1. If the calculated volume fraction for all samples is in the limit given by the bounds, then the equation was deemed to be suitable for estimating effective relative permittivity of solids impregnated with ester fluids.

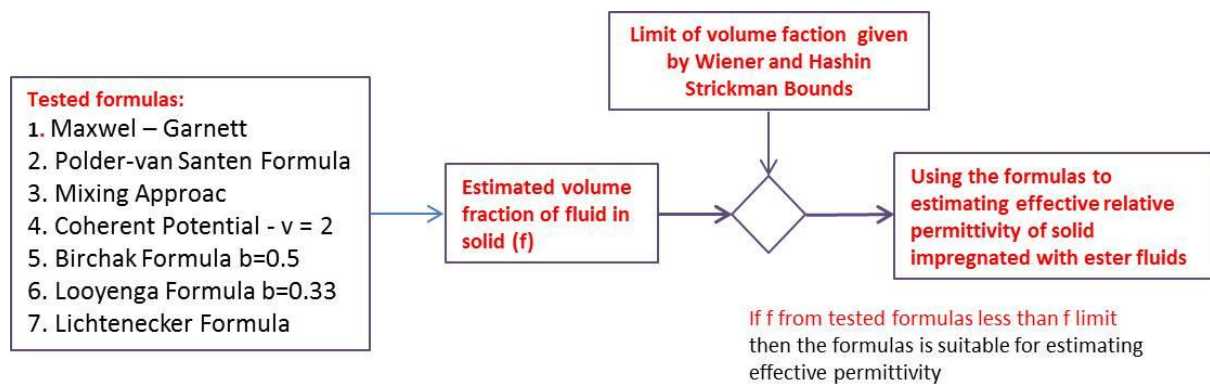


Figure 7.1: Flow chart to determine the suitable formulas to estimate effective relative permittivity.

Based on those theoretical bound, only Mixing Approach, Coherent Potential and Lichtenecker formula give reasonable estimation of volume fraction and thus, effective relative permittivity. In this work, the estimation of effective relative permittivity was based on Lichtenecker formula due to its simplicity compared to Mixing Approach and Coherent Potential.

Lichtenecker Formula

Lichtenecker logarithmic mixture formula has proven to be a useful practical formulation for estimating the effective relative permittivity of homogenous dielectric mixtures [121]. The formula itself is regarded as semi empirical in nature without theoretical justification. However, in [139], it has been shown that the Lichtenecker formula can be derived by applying Maxwell equations and the principle of charge conservation to a mixture for which the spatial distribution and orientation of the components is randomly distributed.

New semi-empirical formula for solid impregnated with ester fluids

The new semi-empirical formula is an extension of Lichtenecker formula which was found to be suitable for estimation of solids impregnated with mineral oil in but not for ester fluids. When estimating the relative permittivity of pressboard impregnated with ester fluids using Lichtenecker formula, it always generates wrong results compared to measurement results. It is possibly because the formula does not take into account the physical phenomenon such as interfacial polarization on the surface of pressboard which occur for pressboard when ester fluids is used as has been explained in section 6.4. The interfacial polarization on the surface of pressboard was found to have dominant effect on the relative permittivity of pressboard impregnated with ester fluids.

In this new formula, the interfacial polarization which occurs on the surface of pressboard was taken into consideration. The factor is called as “surface polarization factor”. The new formula is as follows:

$$\varepsilon_{eff} = e^{((f.\ln \varepsilon_i)+((1-f).\ln \varepsilon_e))} + Pe(d) \quad (7.1)$$

Where

- ε_{eff} Effective relative permittivity of dielectric mixtures
- ε_e Permittivity of homogenous dielectric material (pressboard and transformer papers). Cellulose based polymer= 5.1[5], Aramid= 4[123] at 25°C.
- ε_i Permittivity of material located randomly in homogenous dielectric (insulating fluid). Nytro 4000X= 2.2, MI7131= 3.2, FR3= 3.18 at 25°C
- f Volume fraction that is occupied by ε_i in ε_e
- $Pe(d)$ Interfacial polarization factor as a function of insulating fluids. Nytro 4000X= 0, MI7131= 0.245, FR3= 0.186.

The surface polarization factor was obtained from experiment in section 6.4. Figure 7.2 depicts the effect of surface polarization on the relative permittivity of the composite dielectric. Interfacial polarization would increase the relative permittivity value of pressboard samples. Replacing ester fluid with Nytro 4000X would remove ester fluid on the surface of pressboard samples. Thus, it removes the effect of interfacial polarization which occurs on the surface of pressboard. Based on this investigation, the surface polarization factor value was estimated. The surface polarization factor value is independent of temperature in which the samples were measured but dependent on the type of insulating fluid. The surface polarization factor value is the mean value of several measurements.

The surface polarization factor is only applied in case of pressboard. For some reason, it is not necessary to apply the factor for transformer papers. Maybe because those transformer papers are thin (less than 0.1mm). It is also obvious from dielectric response $\tan \delta$ of transformer paper impregnated with ester fluids in which the additional loss peak (signature of interfacial polarization on the surface of pressboard) is not obvious. Therefore for thin samples with thickness less than 0.1mm, the surface polarization factor of samples impregnated with ester fluids is zero.

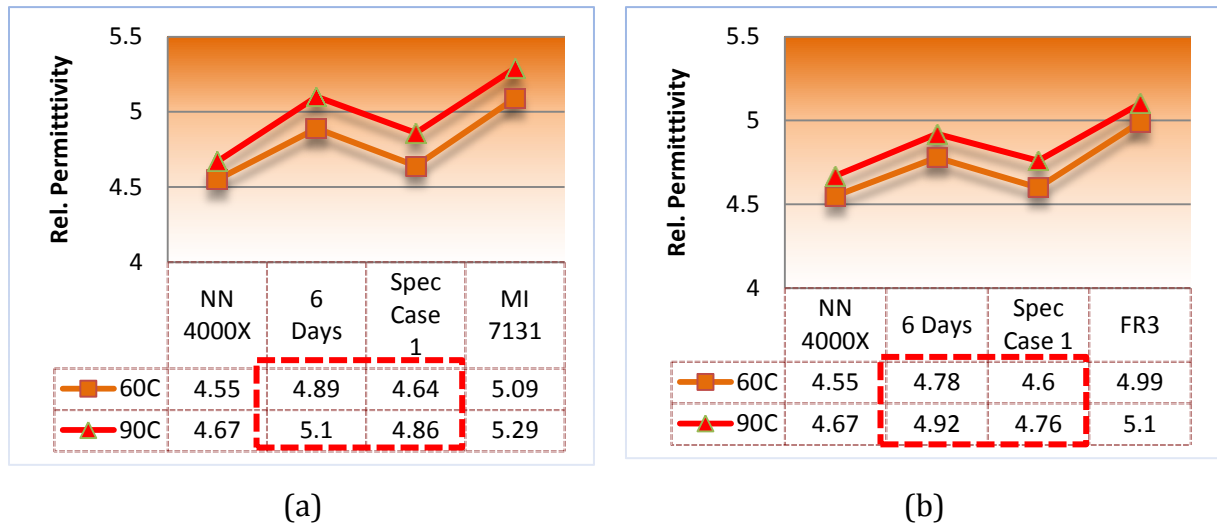


Figure 7.2: Increase of relative permittivity caused by interfacial polarization for (a) MI7131 and (b) FR3.

Other factor which plays important role in determining the effective relative permittivity is volume fraction. In solid-fluid insulating system, volume fraction is the pores of solid which is occupied by the insulating fluids. According to [32], with a correct impregnation process, the volume fraction of mineral oil and ester fluids in solid is equal. Hence, high viscosities of ester fluids do not affect the volume fraction of fluid. Volume fraction of insulating fluid can be calculated as in equation (7.2) [123]:

$$f = (1 - d/X) \quad (7.2)$$

Where

d Density (g/cm^2) of solid insulating material.

X Constant for converting density of solid to volume fraction.

The X constant was obtained from measurement. The values are different for pressboard and transformer papers. It is also different for high and low density material. It is assumed that the relative permittivity of pure cellulose fibre at 25°C is 5.1 [5] and of aramid nomex is 4 [123]. If different relative permittivity value of pure fibre is used, the volume fraction should be re-calculated.

Table 7.1: Density of samples, X constant and volume fraction

Solid samples	Density(g/cm^3)*	X	Volume Fraction
Weidmann B.3.1A (TIV) 2mm	1.19	1.41	0.156
Weidmann B.4.1 (TIII) 2mm	0.9	1.32	0.318
DuPont Nomex T-993 2mm	0.76	1.32	0.424
Cottrell CK 125-TU 0.076mm	1.15	1.85	0.378
Tullis Russel Rotherm HIHD 0.085mm	0.95	1.85	0.486
Nordic Paper Amotfors 0.080mm	0.8	2.4	0.667

*from data sheet

The semi-empirical formula has been verified by comparison with measurement results as in Table 7.2. The calculated values by equation (7.1) provide a quite good estimation of relative permittivity for solid-fluid insulating system with margin of error averagely lower than 4%. The margin of error is generally lower than the standard deviation of measurement results. For this reason, the new formula can be applied for any solid-fluid insulating system.

Table 7.2: Relative permittivity estimated by new formula.

Samples	ϵ_r in NN4000X				ϵ_r in MIDEL7131				ϵ_r in FR3			
	Measured	Calculated	Std dev (%)	Error (%)	Measured	Calculated	Std dev (%)	Error (%)	Measured	Calculated	Std dev (%)	Error (%)
Type IV	4.4	4.4	1.58	0.00	4.95	4.91	0.64	0.81	4.88	4.84	1.78	0.82
Type III	3.79	3.85	1.77	1.58	4.58	4.58	0.37	0.00	4.62	4.51	0.13	2.38
Nomex T-993	3.15	3.1	3.49	1.59	3.9	3.89	0.34	0.26	3.78	3.82	0.38	1.06
Kraft TU125	3.96	3.7	6.74	6.57	4.28	4.22	4.54	1.40	4.24	4.21	7.77	0.71
Rotherm HlHD	3.33	3.35	2.85	0.60	4.03	4.02	7.68	0.25	3.66	4.01	18.70	9.56
Amotfors	2.9	2.89	0.23	0.34	3.6	3.71	8.88	3.06	3.52	3.69	3.49	4.83

7.2.2. Estimation of relative permittivity as a function of frequency

Estimation of relative permittivity as function of frequency with temperature as parameter is not possible by a single mathematical formula. It is simply because the polarization behaviour either interfacial or dipolar orientation of solid impregnated with ester fluids is hardly predicted without performing measurement on real sample. However, it is possible to estimate relative permittivity as function of frequency by utilizing the “master curve technique”.

The dielectric response curve at median temperature, 60°C, was chosen as the origin of master curve. Other plots are shifted horizontally until they coincide into a single curve. This phenomenon allows for normalizing frequency dependent spectra for higher temperature beyond the measurement temperature especially it would be an interest to investigate the dielectric response of Nomex impregnated with ester fluids at high temperature. Figure 7.3 depicts the master curve for Nomex impregnated with MI7131.

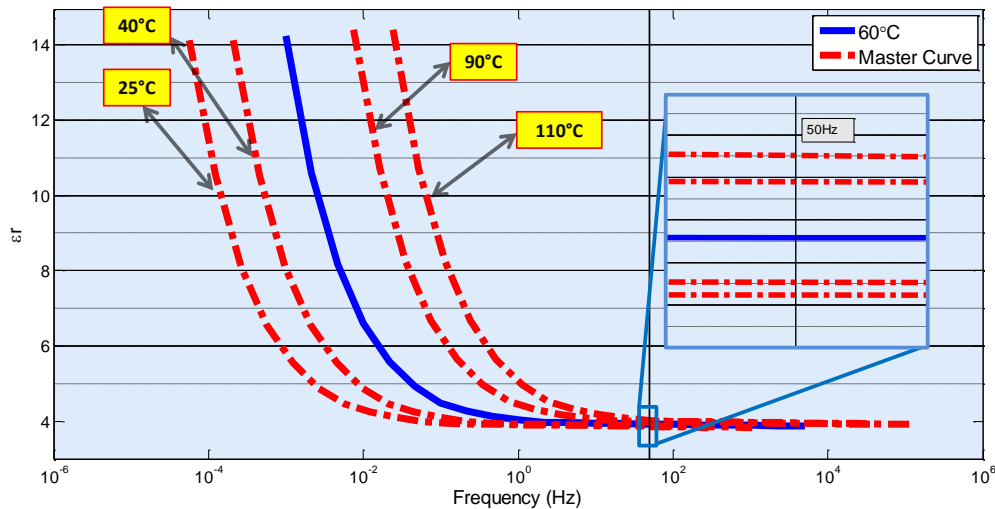


Figure 7.3: Master curve of relative permittivity for Nomex impregnated with MI7131.

7.3. Dielectric dissipation factor, $\tan \delta$

Estimating $\tan \delta$ by single mathematical equation as function of frequency with temperature, insulating fluid type, and solid type as parameters is not possible due to several reasons:

- Polarization behaviour either interfacial or dipole orientation of solids impregnated with ester fluids is hardly predicted. It is evident from the presence of additional loss peak for TIV impregnated with ester fluids as depicted in Figure 5.9.
- $\tan \delta$ depends on two factors, complex susceptibility and DC conductivity as in equation (3.50). From section 5.3.4, it is observed that for solids impregnated with ester fluids, the temperature dependent behaviour of DC conductivity and complex susceptibility is characterized by different activation energy which means the temperature dependent behaviour cannot be predicted.

For this reason, the estimation of $\tan \delta$ by one mathematical equation which is dependent on temperature, insulating fluid and solid type is not possible. $\tan \delta$ as function of frequency could be estimated using master curve technique. However, some problems arise when the master curve of $\tan \delta$ was applied for solid impregnated with ester fluids as there is deviation at higher temperature as in Figure 5.13. The behaviour of dielectric properties toward temperature change is characterized by their activation energy. In case of pressboard impregnated with ester fluids, at lower temperature 25°C - 60°C, the activation energy of susceptibility (polarization) is equal to the activation energy of DC conductivity. However, at higher temperature 60°C - 90°C, the activation energy of susceptibility is different from the activation energy of DC conductivity. The different activation energy of DC conductivity and susceptibility for solids impregnated with ester fluids causes the deviation at master curve of $\tan \delta$ as it depends on both values as in equation (7.3):

$$\tan \delta_{(\omega)} = \frac{\varepsilon_r''(\omega)}{\varepsilon_r'(\omega)} = \frac{\varepsilon_r''(\omega) + \sigma_0 / \varepsilon_0 \omega}{\varepsilon_r'(\omega)} = \frac{\chi_r''(\omega) + \sigma_0 / \varepsilon_0 \omega}{1 + \chi_r'(\omega)} \quad (7.3)$$

Thus, the application of master curve technique for estimation $\tan \delta$ is only possible for solids impregnated with mineral oil because the temperature dependent behaviour of DC conductivity and complex susceptibility is characterized by the same activation energy. That generates a good master curve as depicted in Figure 7.4.

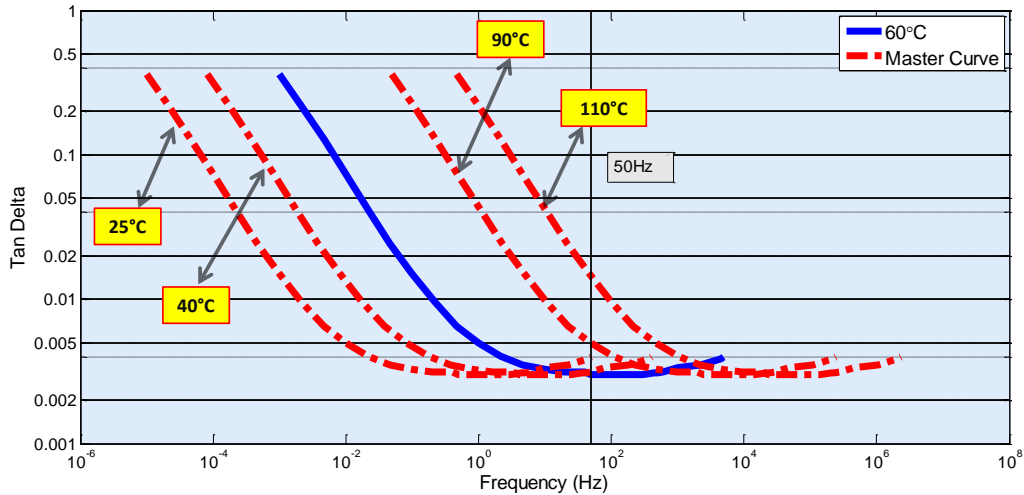


Figure 7.4: Master curve of $\tan \delta$ for TIV impregnated with Nytro 4000X.

For estimating $\tan \delta$ for solid impregnated with ester fluids could only possible by estimating each quantity, the DC conductivity and complex susceptibility separately and then estimate $\tan \delta$ as function of frequency according to equation (7.3). Figure 7.5 depicts master curve $\tan \delta$ of Nomex impregnated with MI7131.

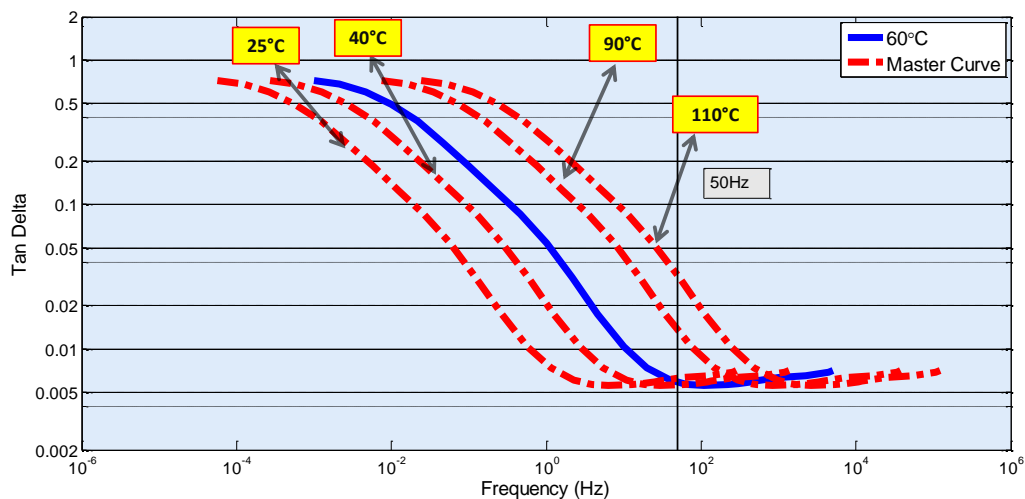


Figure 7.5: Master curve of $\tan \delta$ for of Nomex impregnated with MI7131.

7.4. DC conductivity

It has been explained in section 5.2 that DC conductivity for all solid-fluid insulating combinations follows Arrhenius relation. Thus, DC conductivity can be estimated using Arrhenius equation as in (3.64). From the measurement results, the activation energy DC conductivity (E_{DC}) and pre-exponential factor (A_{DC}) was obtained for each combination. The estimation of DC conductivity with temperature as parameter using Arrhenius relation is convenient. DC conductivity can be estimated for temperature other than 25°C, 60°C, and 90°C (see section 5.2 for details).

For example on how to estimate DC conductivity of TIV impregnated with (a) Nytro 4000X and (b) MI7131 at 75°C are shown below.

(a) Nytro 4000X

- Pre-exponential factor for TIV (B 3.1A) 2mm Nytro 4000X = 842000
- Activation energy for TIV (B 3.1A) 2mm Nytro 4000X = 122.61 kJ/mol = 1.27 eV
- Temperature = 273+75°C = 348°K
- Boltzmann constant = 8.6173324×10^{-5} (eV/K)

$$\sigma = A. e^{-E/K.T}$$

$$\sigma = 842000. e^{-1.27/8.6173324*10^{-5} * 348}$$

$$\sigma = 3.4121E - 13 \text{ S/m}$$

(b) MI7131

- Pre-exponential factor for TIV (B 3.1A) 2mm MI7131 = 40.0315
- Activation energy for TIV (B 3.1A) 2mm MI7131 = 90.32kJ/mol = 0.94 eV

$$\sigma = A. e^{-E/K.T}$$

$$\sigma = 40.0315. e^{-0.94/8.6173324*10^{-5} * 348}$$

$$\sigma = 1.1174E - 12 \text{ S/m}$$

8. Summary and Conclusions

In recent years, ester fluids become a popular alternative insulating fluids for transformers besides mineral oil due to its characteristics such as biodegradation rates, high flash point properties, high moisture tolerance and good electrical insulation capability. To utilize ester fluids in transformers efficiently requires a proper knowledge of the behavior solid-fluid insulating system with temperature as parameter because it certainly affects the dielectric properties to different extent. Consequently even though solid-fluid insulating system may be only used at power frequency of 50 or 60Hz, a proper insight into its electrical behavior can only be obtained by observing its dielectric response as a function of frequency with the temperature as a parameter. Hence, the investigation of solid-fluid insulating system over a wide range of frequencies will provide much of the required insight to comprehend the complexity of the dielectric properties behavior.

One of the objectives to start this project was to improve knowledge on the dielectric properties behavior of solids impregnated with ester fluids with the aim to study different dielectric responses as function of frequency with temperature, density and thickness of insulating solid (pressboard TIV and TIII as well as various transformer papers), and type of solid polymer (cellulose and aramid pressboard) as parameters and creating a data base of dielectric properties. The insulating fluids were mineral oil Nyro 4000X, synthetic ester MI7131 and natural ester FR3. There are seven solid types and thus, there were twenty one solid-fluid combinations in this project to gain knowledge as much as possible.

The quantification of dielectric properties of the investigated test objects in time domain was performed by means of measurement DC conductivity with conventional long time duration method. In the frequency domain, this quantification was performed by of determination complex capacitance and dielectric dissipation factor $\tan \delta$ as well as the derived values such as imaginary part of susceptibility and loss contribution over frequency of 1mHz-5kHz. According to the linear dielectric response theory (presented in chapter 3), all these quantities in time and frequency domain are related to each other by the basic function describing dielectric material which is dielectric function response $f(t)$ in the time domain and the dielectric susceptibility $\chi(\omega)$ in the frequency domain. Hence, it is important to check the linearity of tested object.

To check the linearity property of pressboard, preliminary measurement in time domain at three electric field stress i.e. 0.1kV/mm (low electric field stress), 0.5kV/mm (medium electric field stress) and 5kV/mm (high electric field stress) at temperature of 90°C and in frequency domain of 50Hz with the same electric field stress was performed. Those three electric field stress was supposed to represent three regions of electric field stress i.e. low (less than 1kV/cm), medium (1 to 40kV/cm), and high (more

than 40kV/cm). The measurement results in the frequency and time domain show that the linearity property of pressboard is maintained up to electric field stress of 5kV/mm (section 5.1). There was no Gärton effect observed from $\tan \delta$ value up to electric field stress of 5kV/mm. After the investigation of linearity property of solid samples, the main experiment of this project was performed.

In time domain, the characteristic and temperature dependent behavior of DC conductivity was observed at three temperature level i.e. 25°C, 60°C and 90°C respectively. The results of dielectric response measurement in time domain, as presented in section 5.2, have demonstrated that solids impregnated with ester fluids has higher DC conductivity compared to solid impregnated with mineral oil and generally solid impregnated with synthetic ester has higher DC conductivity compared to solids impregnated with natural ester. Aramid pressboards possess lower DC conductivity compared to cellulose pressboard, see table 5.1 (in section 5.2) for complete DC conductivity value. From measurement results, the temperature dependent behavior of solids impregnated with ester fluids was found to follow Arrhenius relation and it is characterized by activation energy of DC conductivity E_{DC} . Between temperatures of 25°C to 60°C, cellulose pressboard impregnated with mineral oil has higher activation energy compared pressboard impregnated with ester fluids. However, between temperatures of 60°C to 90°C, activation energy of pressboard impregnated with mineral oil and ester fluids are in the same range of 108-131kJ/mol (see section 5.2). Aramid pressboard impregnated with different insulating fluids has low activation energy in the range of 43-60kJ/mol. It suggests that the temperature dependent behavior of Nomex is not highly dependent on the insulating fluids as cellulose pressboard e.g. TIII and TIV. Low activation energy of Nomex means that it has low sensitivity toward increase of temperature.

In frequency domain, the dielectric response $\tan \delta$ and relative permittivity was observed over frequency range of 1mHz-5kHz and at three temperature level i.e. 25°C, 60°C and 90°C respectively. The results of dielectric response measurement in frequency domain show that for all solid-fluid fluid combinations, interfacial polarization is presence. It is marked by the increase of $\tan \delta$ and relative permittivity together at low frequency and generally at the same frequency. The increase of $\tan \delta$ without the increase of relative permittivity means that the loss increase was caused by DC conductivity rather than interfacial polarization. As presented in section 5.3, it has been demonstrated that dielectric response $\tan \delta$ and relative permittivity of solids impregnated with ester fluids has different characteristic compared to solids impregnated with mineral oil. For pressboard impregnated with ester fluids, interfacial (space charge) polarization is more dominant and has different characteristic. It is indicated by higher $\tan \delta$ and the presence of additional loss peak in dielectric response $\tan \delta$ at frequency between 0.01-1Hz for pressboards impregnated with ester fluids. The additional loss peak of solids impregnated with mineral is not visible over the measurement frequency. Parameters such as insulating fluids characteristic, density

and thickness of samples, internal viscosity of solid and kinematic viscosity of fluid, and polymer material of solid was found to be related to relaxation time of interfacial polarization and therefore, have considerable influence on the shape of dielectric response (see section 5.3.2 to 5.3.3).

Concerning temperature dependent behavior of solid impregnated samples, the temperature dependent of dielectric response in frequency domain was deduced by means of master curve technique and characterized by activation energy of polarization. The observed relaxation slope (observed in $\tan \delta$ and imaginary part of dielectric susceptibility) is shifted to higher frequency with the increase of temperature based on equation (3.15). The activation energy of polarization is not necessarily equal to activation energy of DC conductivity. Parameters such as insulating fluid characteristic, density and thickness of samples, , internal viscosity of solid and kinematic viscosity of fluid, and polymer material of solid was found to be related to activation energy of solid-fluid insulating system.

As presented in section 3.4, master curve for dielectric response $\tan \delta$ depends on the activation energy of DC conductivity and activation energy of polarization. Thus, for $\tan \delta$ the shift is perfect if either the activation energy of DC conductivity is equal to activation energy of polarization or activation energy of DC conductivity is smaller than activation energy of polarization. For solids impregnated with mineral oil, the activation energy of DC conductivity and polarization is equal. Hence, the shift in frequency domain for $\tan \delta$, imaginary part of susceptibility and relative permittivity with increase of temperature is perfect in the observed measurement temperature. It means that those dielectric properties have the same sensitivity of reaction rate to temperature. In this case, it is possible to calculate activation energy from $\tan \delta$ measurement at several temperatures.

Generally, activation energy of polarization for solids impregnated with ester fluids are lower than of solids impregnated with mineral oil (see section 5.3.2 and 5.3.7). For solids impregnated with ester fluids, the activation energy of DC conductivity and polarization is different at temperature between 60°C - 90°C. It was suspected that the discrepancy was caused by interfacial polarization behavior which is very dominant for solids when impregnated with ester fluids. Thus, it the activation energy of polarization depends more on activation energy of ester fluids rather than of the solids insulation material itself. The difference of activation energy at high temperature leads to the deviation in master curve of dielectric response $\tan \delta$.

The second objective of this project was to improve knowledge on the dielectric properties behavior of solids after insulating fluid replacement from mineral oil to ester fluids as in the case of retrofilling. The aim was to investigate the change in dielectric properties with time and the effect of interfacial polarization on the surface of pressboard after insulating fluid replacement with ester (see section 6.3 and 6.4). The shape of dielectric response was changing rapidly after fluid replacement, this is most

evident from dielectric response $\tan \delta$ (see Figure 6.2) and relative permittivity at low frequency (see Figure 6.3). After immersed in ester fluids for some days, the dielectric response is similar to dielectric response of pressboard impregnated with ester fluids (without fluid replacement). It was found out that the rapid change of dielectric response was a combination of ester fluids at some level has penetrated pressboard (hence, changing of space charge polarization behaviour inside the pressboard), increased of DC conductivity value with time after replacement of insulating fluid (evident from DC conductivity measurement) and additional interfacial polarization on the surface of pressboard (indicated by the presence of loss peak on dielectric response $\tan \delta$ over frequency 0.01 – 1Hz). The measurement results show that interfacial polarization on pressboards impregnated with ester fluids consist of interfacial polarization within the cellulose fiber structure and interfacial polarization on the surface of pressboard has different relaxation time. For the latter, the relaxation time is at about 1Hz at measured temperature of 60°C and marked by the presence of loss peak. This means that when pressboard is impregnated with ester fluids, it has a distribution of relaxation time for interfacial polarization. It is not the case for pressboards impregnated with mineral oil. Those interfacial polarizations are also indicated by different characteristic of relative permittivity at low frequency.

Second part of retrofilling experiment was to investigate if the change of dielectric response is permanent and the influence of interfacial polarization on the surface of pressboard by replacing back ester fluids with Nytro 4000X. The purpose of this procedure was to remove the deposited ester fluids from the surface of pressboard. As presented in section 6.4, the dielectric response $\tan \delta$ was changed; the loss peak in dielectric response $\tan \delta$ that previously occurred after retrofilling with ester fluids was vanished along with the removal of ester fluid from the surface of pressboard. It is also important to note that the new dielectric response does not return to the original dielectric response characteristic of pressboard impregnated with Nytro 4000X. The increase of $\tan \delta$ at low frequency indicates that there is a change of interfacial polarization inside the pressboard. It probably means that at some level ester fluid has impregnated the pressboard samples or a small amount of Nytro 4000X has been leached out from pressboard.

The last objective of this project was to propose a semi-empirical formula to estimate the effective relative permittivity of solid impregnated with ester fluids. The formula is an extension of Lichtenecker formula which was found to be suitable for estimation of solids impregnated with mineral oil but not for ester fluids. The new formula takes into account the influence of interfacial polarization on the relative permittivity. An additional factor, the “surface polarization factor” was added to the Lichtenecker formula (see section 7.1.2). The surface polarization factor value is independent of temperature in which the samples were measured but dependent on the type of insulating fluid. As presented in Table 7.1, the semi-empirical formula has been verified by comparison with measurement results. The calculated values provide a quite good estimation of

relative permittivity for solid-fluid insulating system with margin of error averagely lower than 4%. The margin of error is generally lower than the standard deviation of measurement results.

It can be concluded that the dielectric response of solids impregnated with ester fluids has different characteristic compared to solids impregnated with mineral oil. Furthermore, replacement of insulating fluid from mineral oil to ester fluids will change the dielectric response of solid drastically. This phenomenon should be considered when retrofilling a transformer. And the last one, it is possible to estimate effective relative permittivity of solid impregnated with ester fluids using the proposed semi-empirical formula.

9. Future works

Based on the conclusions presented in the previous section, there are areas for future investigation that will improve our knowledge of the behaviour of solid impregnated with ester fluids. It is as follows:

- Further dielectric properties measurement on the same solid-fluid impregnated combinations with different parameters such as moisture contents and aged samples both electrical and thermal aging. Then, the temperature dependent behaviour of new, wet and aged samples can be investigated based on its activation energy value and creates some sort of data base to characterize the insulation condition when impregnated with ester fluids.
- The specific interfacial polarization characteristic of solids impregnated with ester fluids should be deeply investigated with different sample set-up such as simplified insulation structure of core type power transformers shown in Figure 9.1.

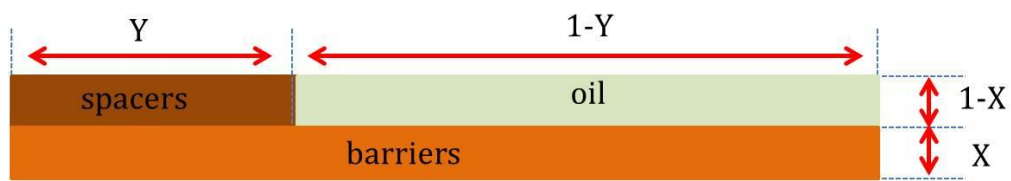


Figure 9.1: Simplified insulation structure of a core type power transformer.

- If possible, measurement over wider frequency range should be performed to have a bigger picture on the polarization behaviour of sample impregnated with ester fluids. From the results, it might be possible to investigate the distribution relaxation time of solid impregnated with ester fluids.
- It would be interesting to analyse the measurement results based on the empirical method as suggested by Jonscher [see section 3.3]. Maybe there is more information can be obtained.

References

- [1] McShane, C. P., et al. *Natural Ester Dielectric Fluid Development*. IEEE PES Transmission and Distribution Conference and Exhibition 2005/2006, 2006.
- [2] K uchler, A., et al. Parameter Determining the Dielectric Properties of Oil Impregnated Pressboard and Presspaper in AC and DC Power Transformer Application. ISH 07 International Symposium on High Voltage Engineering, 2007.
- [3] Bartnikas, R. *Engineering Dielectrics Volume III: Electrical Insulating Fluids*. ASTM, Philadelphia, 1994.
- [4] Nynas. *Base Oil Handbook*. 2001, 46 pages.
- [5] Clark, F. M. *Insulating Materials for Design and Engineering Practice*, Wiley, New York, 1962
- [6] Perrier, C. and A. Beroual. *Experimental Investigations on Insulating Liquids for Power Transformers: Mineral, Ester, and Silicone Oils*. IEEE Electrical Insulation Magazine, Vol. 25, No. 6, 2009, pp. 6-13.
- [7] Sheppard, H. R. *A Century of Progress in Electrical Insulation 1886-1986*. IEEE Electrical Insulation Magazine, Vol. 2, Issue 5, 1986, pp. 20-30.
- [8] Vishal. Transformer's History and its Insulating Oil. Proceedings of the 5th National Conference Computing For Nation Development; INDIACOM. 2011.
- [9] Fofana, I., et al. *Retrofilling Conditions of High Voltage Transformers*. Electrical Insulation Magazine, IEEE Vol. 17, No. 2, 2001, pp. 17-30.
- [10] Sheppard, H. R. *PCB replacement in transformers*. American Power Conference, April 1977
- [11] DSI. Insulating Oil Products. Product Specification and Technical Guide. 23 pages.
- [12] CIGRE Working Group A2.35. Experiences in Service with New Insulating Liquids. UK, CIGRE, 2010. 95 pages.
- [13] Dolata, B., et al. *New Synthetic Ester Fluid for the Insulation of Liquid Immersed Transformers*. Conference Record of the 2006 IEEE International Symposium on Electrical Insulation, 2006.
- [14] Gockenbach, E. and H. Borsi. *Natural and Synthetic Ester Liquids as Alternative to Mineral Oil for Power Transformers*. Annual Report Conference on Electrical Insulation and Dielectric Phenomena, 2008.
- [15] Byung-sung, L., et al. *The Characteristics of Winding Temperature for the Natural Ester Filled Transformer up to and Including 500 kVA*. Annual Report Conference on CEIDP, Electrical Insulation and Dielectric Phenomena, 2008.

- [16] Oommen, T. V. *Vegetable Oils for Liquid-Filled Transformers*. IEEE Electrical Insulation Magazine, Vol. 18, No. 1, 2002, pp. 6-11.
- [17] Wilson, A. C. M. *Insulating Liquids; their Uses, Manufacture and Properties*. The Institution of Electrical Engineers, London and New York and Peter Peregrinus Ltd., Stevenage, UK and New York, 1980.
- [18] Rouse, T. O. *Mineral Insulating Oil in Transformers*. Electrical Insulation Magazine, IEEE, Vol. 14, Issue 2, 1998, pp. 6-16.
- [19] IEC Publication 60296, edition 4.0. *Fluids for Electrotechnical Applications - Unused Mineral Insulating Oils for Transformers and Switchgear*. 2012.
- [20] IEC Publication 60422, edition 4.0. *Mineral Insulating Oils in Electrical Equipment – Supervision and Maintenance Guidance*. 2013.
- [21] Nynas. Product Data Sheet Nytro 4000X. 2013.
URL:[https://nyport.nynas.com/Apps/1112.nsf/wnpds/Nytro_4000X_IEC/\\$File/PDS_Nytro_4000X_EN.pdf](https://nyport.nynas.com/Apps/1112.nsf/wnpds/Nytro_4000X_IEC/$File/PDS_Nytro_4000X_EN.pdf)
- [22] Perrier, C., et al. *Improvement of Power Transformers by Using Mixtures of Mineral Oil with Synthetic Esters*. IEEE International Conference on Dielectric Liquids, 2005.
- [23] Senkevitch, E. D., et al. *New Synthetic Liquids for Transformers*. CIGRE Symposium, paper 500-04, Vienna, 1987.
- [24] Fofana I., et al. *Challenge of Mixed Insulating liquids for Use in High Voltage Transformers; Part 1 Investigation of Mixed Liquids*. IEEE Electrical Insulating Magazine, Vol. 18, No. 3, 2002.
- [25] Martin, D., et al. *An Overview of the Suitability of Vegetable Oil Dielectrics for Use in Large Power Transformers*. Proc. 5th Annual Euro TechCon, Chester, United Kingdom, 2006.
- [26] MIDEL. MIDEL 7131 Transformer Fluid, Technical Data Sheet. 2010.
URL:http://mimaterials.com.s3.amazonaws.com/midel/documents/technical/MIDEL_7131_Complete_Binder_of_Data_Sheets.pdf
- [27] Gockenbach, E. and H. Borsi: *Performance and New Application of Ester Liquids*. Proceedings of 2002 IEEE 14th International Conference on Dielectric Liquids, 2002
- [28] Jinhua, H., et al. *Application of Insulating Camellia Oil in High Fire Resistance Transformer*. International Conference on High Voltage Engineering and Application (ICHVE), 2012.
- [29] IEEE Guide for Acceptance and Maintenance of Natural Ester Fluids in Transformers. IEEE Std C57.147-2008, 2008, pp. 1-31.
- [30] ASTM International. ASTM D6871-03; *Standard Specification for Natural (Vegetable Oil) Ester Fluids Used in Electrical Apparatus*. 2008.
- [31] Cooper. *Envirotemp FR3 Fluid*. Brochure. 2011, 8 pages.
- [32] Pukel, G. J., et al. *Power Transformers with Environmentally Friendly and Low Flammability Ester Liquids*. CIGRE A2-201, 2012
- [33] Fofana, I., et al. *Retroilling Conditions of High-Voltage Transformers*. IEEE

- Electrical Insulation Magazine, Vol. 7, No. 3, 2001, pp. 17-30.
- [34] Martin, D. and Wang, Z.D. *A Comparative Study of the Impact of Moisture on the Dielectric Capability of Esters for Large Power Transformers*. IEEE Conference on Electrical Insulation and Dielectric Phenomena, 2006.
- [35] Cooper. Envirotemp FR3 Fluid. Testing Guide, Section R 900-20-12, 2008.
- [36] MIDEL. MIDEL 7131 Transformer Fluid, Technical Data Sheet on Moisture Tolerance. p.11, 2010.
- [37] McShane, C. P., et al. *Aging of Kraft Paper in Natural Ester Dielectric Fluid*. Proceedings of IEEE 14th International Conference on Dielectric Liquids, 2002.
- [38] International Electrotechnical Commission. *IEC 60076-7; Power Transformers Part 7; Loading Guide for Oil-Immersed Power Transformers, 1st edition*. Geneva, 2005.
- [39] Heathcote, M. J. *The J & P Transformer Book*, 12th edition; a Practical Technology of the Power Transformer. Reed Educational and Professional Publishing Ltd, Oxford, 1998. 957 pages.
- [40] Moser, H. P. *Transformerboard*. Special Print of Scientia Electrica, Translated by W. Heidemann, EHV-Weidmann Lim., St. Johnsbury, Vermont, U.S.A, 1979, 120 pages.
- [41] WILEC. Insulation in Oil Filled Transformers. Brochure. Pp.77-78.
- [42] Prevost, T. A. and T. V. Oommen. Cellulose Insulation in Oil-Filled Power Transformers; Part I – History and Development. IEEE Electrical Insulation Magazine, Vol. 22, No. 1, 2006, pp. 28-35.
- [43] CIGRE Task Force D1.01.10. *CIGRE Brochure 323; Ageing of Cellulose in Mineral-Oil Insulated Transformers*. CIGRE, Paris, 2007, 87 pages.
- [44] Berggren, R. *Cellulose degradation in pulp fibers studied as changes in molar mass distributions*. Ph. D Thesis, Superseded Departments of Fibre and Polymer Technology, Royal Institute of Technology, Stockholm, Sweden, 2003
- [45] Evans, R. and A. F. A. Wallis. *Cellulose Molecular Weights-Determined by Viscometry*. J. Appl Polym Science, 1989, pp. 2331-2340.
- [46] Bartnikas, R. *Dielectric Losses in Solid-Liquid Insulating Systems - Part I*. IEEE Transactions on Electrical Insulation, Vol. EI-5, No. 1, 1970, pp. 113-121.
- [47] Bartnikas, R. *Dielectric Losses in Solid-Liquid Insulating Systems - Part II*. IEEE Transactions on Electrical Insulation, Vol. EI-6, No. 1, 1971, pp. 4-11.
- [48] Bartnikas, R. *Electrical Conduction in Medium Viscosity Oil-Paper Films - Part I*. IEEE Transactions on Electrical Insulation Vol. EI-9, No. 2, 1974, pp. 57-63.
- [49] Bartnikas, R. *Electrical Conduction in Medium Viscosity Oil-Paper Films - Part II*. IEEE Transactions on Electrical Insulation Vol. EI-9, No. 3, 1974, pp. 85-91.
- [50] Graczkowski, A. et al. *Study of the Dielectric Response of Ester Impregnated Cellulose for Moisture Content Evaluation*. Nordic Insulation Symposium – Nord-IS 13, June 2011, pp. 67-70.
- [51] Hassan, O. et al. *Detection of Oil-Pressboard Insulation Aging with Dielectric*

- Spectroscopy in Time and Frequency Domain Measurements*. International Conference on Solid Dielectric, France, 2004.
- [52] Wang, S. Q., et al. *Investigation on Dielectric Response Characteristics of Thermally Aged Insulating Pressboard in Vacuum and Oil-Impregnated Ambient*. IEEE Transaction on Dielectrics and Electrical Insulation, Vol. 17, No. 6, 2010.
- [53] Setayeshmehr, A., et al. *Dielectric Spectroscopic Measurements on Transformer Oil-Paper Insulation Under Controlled Laboratory Conditions*. IEEE Transaction on Dielectrics and Electrical Insulation, Vol. 15, Issue 4, 2008, pp. 1100-1111.
- [54] McShane, C. P., et al. *Aging of Cotton/Kraft Blend Insulation Paper in Natural Ester Dielectric Fluid*. TechCon 2003 Asia-Pasific, 2003.
- [55] Linhjell, D., et al. *Dielectric Response of Mineral Oil Impregnated Cellulose and the Impact of Aging*. IEEE Transaction on Dielectrics and Electrical Insulation, Vol. 14, Issue 1, 2007, pp. 156-169.
- [56] Lundgaard, L. E., et al. *Aging of Oil-Impregnated Paper in Power Transformers*. IEEE Transaction on Power Delivery, Vol. 19, No. 1, 2004, pp. 230-239.
- [57] Liao, R. et al. *A Comparative Study of Physicochemical, Dielectric and Thermal Properties of Pressboard Insulation Impregnated with Natural Ester and Mineral Oil*. IEEE Transaction on Dielectrics and Electrical Insulation, Vol. 18, Issue 5, 2011, pp. 1626-1637.
- [58] Fofana, I., et al. *On the Frequency Domain Dielectric Response of Oil-Paper Insulation at Low Temperatures*. IEEE Transaction on Dielectrics and Electrical Insulation, Vol. 17, No. 3, 2010, pp. 799-808.
- [59] Hao, J. *A Comparative Study of Moisture and Temperature Effect on the Frequency Dielectric Response Behaviour of Pressboard Immersed in Natural Ester and Mineral Oil*. ISH 11 International Symposium on High Voltage Engineering, Hannover, Germany, 2011.
- [60] Moore, S. P. *Some Considerations for New and Retrofil Applications of Natural Ester Dielectric Fluids in Medium and Large Power Transformers*. IEEE PES Transmission and Distribution Conference and Exhibition 2005/2006, 2006.
- [61] Wasserberg, V. *Retrofilling of Transformers – Facts and Arguments*. Independent Condition Assessment and Concepts for the Refurbishment of Transformers, December 2004.
- [62] McShane, C. P., et al. *Retrofilling aging transformers with natural ester based dielectric coolant for safety and life extension*. Cement Industry Technical Conference, 2003.
- [63] Moore, S. P. *Transformer Insulation Dry Out as a Result of Retrofilling with Natural Ester Fluid*. IEEE PES Transmission and Distribution Conference and Exposition (T&D), 2012.
- [64] Perrier, C., et al. *Improvement of Power Transformers by Using Mixtures of Mineral Oil with Synthetic Esters*. IEEE Transaction on Dielectrics and Electrical Insulation, Vol. 13, Issue 3, 2006, pp. 556-564.
- [65] Jonscher, A. K., *Dielectric Relaxation in Solids*, Chelsea Dielectrics Press, London, UK, 1983.

- [66] Kao, W. C. *Dielectric Phenomena in Solids; with Emphasis on Physical Concepts of Electronic Processes, 1st edition*. Elsevier Academic Press, San Diego, California, 2004, 581 pages.
- [67] Anderson, J.C. *Dielectrics*. Reinhold Publishing Corporation, New York, 1964.
- [68] Dakin, T. W. *Conduction and Polarization Mechanisms and Trends in Dielectric*. Electrical Insulation Magazine, IEEE, Vol. 22, No. 5, 2006, pp. 11-28.
- [69] Zaengl, W. S. *Dielectric Spectroscopy in Time and Frequency Domain for HV Power Equipment, Part I: Theoretical Considerations*. Electrical Insulation Magazine, IEEE Vol. 19, No. 5, 2003, pp. 5-19.
- [70] Tuncer, E. *Dielectric Relaxation in Dielectric Mixtures*. Ph. D Thesis, Department of Electric Power Engineering, Chalmers University of Technology, Gothenburg, Sweden, 2001
- [71] Ashcroft. N.W and Mermin N.D. *Solid State Physics*, international ed., Harcourt Brace College Publishers, New York, 1976.
- [72] Elliot, S.R. *Physics of Amorphous Materials*, Longman Inc, New York, 1984.
- [73] Dissado, L. A. and J. C. Fothergill. *Electrical Degradation and Breakdown in Polymers*. Peter Peregrinus Ltd., Stevenage on behalf of the Institution of Electrical Engineers, 1992, 620 pages. ISBN 0-86341-196-7.
- [74] Dekker, A.J. *Solid State Physics*. Prentice Hall, Englewood Cliffs, New Jersey, 1963.
- [75] Burkhardt, P.J. *Dielectric Relaxation in Thermally Grown SiO₂ Films*. IEEE Transaction Electronic Device, vol. ED.13, pp. 268-275, 1966.
- [76] Bartnikas, R. *Performance Characteristics of Dielectrics in the Presence of Space Charge*. IEEE Transactions on Dielectrics and Electrical Insulation, Vol. 4, Issue 5, 1997.
- [77] Jonscher, A. K. *Dielectric Relaxation in Solids*. Royal Holloway, University of London, Egham, Surrey, UK, 1999, pp. R57-R70.
- [78] Maxwell, J.C. *A Treatise on Electricity and Magnetism*, vol. 1, 3rd ed. Oxford: Clarendon Press, reprint by Dover, pp. 450-464, 1981.
- [79] Landau, L.D. and Lifshitz, E.M, *Electrodynamics of Continuous Media*. 2nd ed., Course of Theoretical Physics, vol. 8, Perganom Press, New York, 1982.
- [80] Graczkowski, A. et al. *Influence of impregnating liquids on dielectric response of impregnated cellulose insulation*. IEEE International Conference on Solid Dielectrics, Postdam, 2010.
- [81] International Electrotechnical Commission. *IEC 60093; Methods of Test for Volume Resistivity and Surface Resistivity of Solid Electrical Insulating Materials, 2nd edition*. Geneva, 1980.
- [82] International Electrotechnical Commission. *IEC 60247; Insulating Liquids – Measurement of Relative Permittivity, Dielectric Dissipation Factor (tan delta) and D.C. Resistivity, 3rd edition*. Geneva, 2004.
- [83] Lisowski, M. and R. Kacprzyk. Changes Proposed for the IEC 60093 Standard Concerning Measurements of the Volume and Surface Resistivities of Electrical

- Insulating Materials. IEEE Transactions on Dielectrics and Electrical Insulation, Vol. 13, No. 1, 2006, pp. 139-145.
- [84] Houhanessian, V. D. *Measurement and Analysis of Dielectric Response in Oil-Paper Insulation Systems*. Ph.D Thesis, Swiss Federal Institute of Technology Zurich, Zurich, 1998.
- [85] Alff Engineering, Electronic Measuring Devices. PDC-Analyser-1MOD. URL: <http://www.alff-engineering.ch/analyser.htm> ALFF ENGINEERING - products - pdc-analyser
- [86] Omicron. Dirana – Dielectric Response Analysis and Moisture in Oil-Paper Dielectrics.2011. URL:https://www.omicron.at/fileadmin/user_upload/pdf/literature/DIRANA-Brochure-ENU.pdf.
- [87] GE Energy Services. IDA 200 – Insulation Diagnostics System. Programma Products. URL: <http://mldt.pl/files/ida200.PDF>
- [88] Occhini, E. and G. Maschio. *Electrical Characteristics of Oil-Impregnated Paper as Insulation for HV DC Cables*. IEEE Transaction on Power Apparatus and Systems, Vol. Pas-86, No. 3, 1967, pp. 312-326.
- [89] Ekanayake, C. *Application of Dielectric Spectroscopy for Estimating Moisture Content in Power Transformers*. Ph. D Thesis, Department of Electric Power Engineering, Chalmers University of Technology, Gothenburg, Sweden, 2003.
- [90] Gedde, U. *Polymer Physics*. Chapman & Hall, London, 1995.
- [91] Pratomosiwi, F., et al. *Dielectric Response Of Pressboard Impregnated in Mineral Oil And Synthetic Ester*. International Symposium on High Voltage Engineering, 2013.
- [92] Sihvola, A. *Electromagnetic Mixing Formulas and Applications*. IEEE Electromagnetic Waves Series, Vol. 47, The Institute of Electrical Engineers, London, 1999.
- [93] Wiener, O. *Die Theorie des Mischkorpers für das Feld der Stationären Stromung i. Die Mitterwertsätze für Kraft, Polarization und Energie*. Der Abhandlungen der Mathematisch-Physischen Klasse der Königl. Saschsichen Gesellschaft der Wissenschaften, 1912, pp. 509-604.
- [94] Hashin, Z. and Shtrikman, S. *A Variational Approach to the Theory of Effective Magnetic Pereability of Multiphase Materials*. Journal Applied Physics, 1962, pp. 3125-3131.
- [95] Milton, G. W. Bounds on the Complex Permittivity of a Two_Component Composite Material. Journal of Applied Physics, 1981, pp. 5386-5293.
- [96] Gladstone, J. H. and J. T. Dale. Researches on the Refraction, Dispersion and Sensitiveness of Liquids. Philosophical Transactions of Royal Society of London, 1863, pp. 317-343.
- [97] Wagner, K. W. *Erklärung der Dielektrischen Nachwirkungsvorgänge auf Grund Maxwellscher Vorstellungen*. Archiv für Electrotechnik II, No. 9, 1914, pp.371-387.

- [98] Sillars, R. W. *The Properties of a Dielectric Containing Semiconducting Particles of Various Shapes*. Journal of Institution of Electrical Engineers, 1937, pp 378-394.
- [99] Fricke, H. *A Mathematical Treatment of the Electric Conductivity and Capacity of Disperse Systems*. Physical Review, 1924, pp. 575-587.
- [100] Steeman, P. A. M. *Interfacial Phenomena in Polymer Systems*. Ph. D Thesis, Technische Universiteit Delft, Delft, The Netherlands, 1992.
- [101] Steeman, P, A, M and Maurer, F. H. J. *An Interlayer Model for the Complex Dielectric Constant of Composites*. Colloid & Polymer Science, 1990, pp. 315-325.
- [102] Böttcher, C. J. F. *Theory of Electric Polarization*. Elsevier Publishing Company, Amsterdam, 1952.
- [103] Greffe, J. L. and Gross, C. *Static Permittivity of Emulsion, Dielectric Properties of Heterogeneous Material (A. Priou, ed.), Progress in Electromagnetics Research*. Elsevier, 1992, pp. 41-100.
- [104] Onsager, L. *Electric Moments of Molecules in Liquids*. Journal of the American Chemical Society, 1936, pp. 1486-1493.
- [105] Kirkwood, J. G. *The Dielectric Polarization of Polar Liquids*. Journal of Chemical Physics, 1939, pp. 911-919.
- [106] Clerc, J. P., et al. *The Electrical Conductivity of Binary Disordered Systems, Percolation Clusters, Fractals and Related Models*. Advances in Physics, 1990, pp. 191-308.
- [107] Shalaev, V. M. *Electromagnetic Properties of Small-Particle Composites*. Physics Report, No. 2 and No. 3, 1996, pp 61-137.
- [108] Bideau, D. and Hansen, A. (eds.). *Disorder and Granular Media, Random Materials and Processes*. North-Holland, Amsterdam, 1993.
- [109] Tuncer, E., et al. *Dielectric Relaxation in Dielectric Mixtures; Application of the Finite Element Method and its Comparison with Mixture Formulas*. Journal of Applied Physics, No. 12, 2001, pp. 8092-8100.
- [110] Tuncer, E. and Gubanski, S. M. *Thermally Stimulated Depolarization Currents of Random Composite Structures*. NORDIS'99 Nordic Insulation Symposium. Lyngby Denmark, 1999, pp. 223-230.
- [111] Tuncer, E., et al. *Dielectric Relaxation in Dielectric Mixtures; Application of the Finite Element Method and its Comparison with Mixture Formulas*. Journal of Applied Physics, No. 12, 2001, pp. 8092-8100.
- [112] Kärkkäinen, K. K., et al. *Effective Permittivity of Mixtures: Numerical Validation by the FDTD Method*. IEEE Transactions on Geoscience and Remote Sensing, Vol. 38, No. 3, 2000, pp. 1303-1308.
- [113] Garnett, J. C. M. *Colors in Metal Glasses and Metal Films*. Transaction Royal Society, Vol. 53, 1904, pp. 385-420.
- [114] Sihvola, A. and Lindlel, I. *Polarizability Modeling of Heterogeneous Media in Dielectric Properties of Heterogeneous Materials*. PIER 6 Progress in Electromagnetics Research, A. Priou, Ed. Elsevier, New York, 1992, pp. 101-151.

- [115] Bruggeman, D. A. G. *Berechnung Verschiedener Physikalischer Konstanten von Heterogenen Substanzen, i. Dielektrizitätskonstanten und Leitfähigkeiten der Mischkörper aus Isotropen Substanzen*. Ann. Phys, 1935, pp. 636-664.
- [116] Sihvola, A. *Self-consistency Aspects of Dielectric Mixing Theory*. IEEE Transaction Geoscience Remote Sensing, vol. 27, pp. 403-415, July 1989.
- [117] Elliott, R. J., et al. *The Theory and Properties of Randomly Disordered Crystals and Related Physical Systems*. Rev. Mod. Phys, Vol. 46, 1974, pp. 465-543.
- [118] Kohler, W. E. and Papnicolaou, G. C. *Some Applications of the Coherent Potential Approximation*. In Multiple Scattering and Waves, P. L. Kohler and G. C. Papanicolaou Editions. North Holland, New York, 1981, pp. 199-223.
- [119] Birchak, J. R., et al. *High Dielectric Constant Microwave Probes for Sensing Soil Moisture*. Proceeding IEEE, Vol. 62, 1974, pp. 93-98.
- [120] Looyenga, H. *Dielectric Constants of Mixtures*. Physica, Vol. 31, 1965, pp. 401-406.
- [121] Lichtenecker K. and Rother, K. *Die Herleitung des Logarithmischen Mischungsgesetzen aus Allgemeinen Prinzipien der Stationären Strömung*. Physy. Zeitschr, Vol. 32, 1931, pp. 255-260.
- [122] IEC Publication 60814, edition 2.0. Insulating Liquids - Oil-Impregnated Paper and Pressboard - Determination of Water by Automatic Coulometric Karl Fischer Titration. 1997.
- [123] Weidmann. Transformerboard Cellulosic Insulation of Unsurpassed Quality. 24 pages.
- [124] DuPont. Nomex Pressboard. Technical Data Sheet. 4 pages.
- [125] Pratomosiwi, F., et al. *The Study of Electrode Corner Shape for Measuring Dielectric Properties of Oil Immersed Material*. International Conference on High Voltage Engineering and Application, 2012.
- [126] Judendorfer, T. *Oil-Cellulose Insulation Systems for HVDC Applications - Contribution to Ageing Behaviour, Electrical Conductivity and Charging Tendency*. Ph.D Thesis, Technische Universität Graz, Graz, April 2012.
- [127] Koch, M., et al. *Moisture Diagnostics of Power Transformers by a Fast and Reliable Dielectric Response Method*. Conference Record of the 2010 IEEE International Symposium on Electrical Insulation (ISEI), 2010.
- [128] Zaky, A. A. and Hawley, R. *Conduction and Breakdown in Mineral Oil*. Peter Peregrinus Ltd, London, 1973.
- [129] Zhakin, A. I. *Ionic Conductivity and Complexation in Liquid Dielectric*. Journal of Physics-Uspekhi, Vol. 46, No. 1, 2003.
- [130] Adamczewski, I. *Ionization, Conductivity, and Breakdown in Dielectric Liquids*. Taylor & Francis, London, 1969.
- [131] Pratomosiwi, F. et al. *Electrical Conductivity Measurement Of Oil Impregnated Pressboard with Varied Electric Field Stress And Temperature*. International Symposium on High Voltage Engineering, 2013.
- [132] Rowland, C.M. *Characteristic Relaxation Times and Their Invariance to*

- Thermodynamic Conditions*. Journal of Soft Matter, issue 12, 2008.
- [133] Ekanayake, C. et al. *Frequency Response of Oil Impregnated Pressboard and Paper Samples for Estimating Moisture in Transformer Insulation*. IEEE Transactions on Power Delivery, Vol. 21, 2006.
- [134] Internal data on calculating effecting relative permittivity of Nomex.
- [135] Bartnikas, R. *Dielectric Loss in Insulating Liquids*. IEEE Transactions on Electrical Insulation Vol. EI-2, 1967, pp. 33-54.
- [136] Jin-Gul, H., et al. *Frequency and Temperature Dependence of Dielectric Constant of Epoxy/BaTiO₃ Composite Embedded Capacitor Films (ECFs) for Organic Substrate*. Electronic Components and Technology Conference, Proceedings. 55th, 2005, pp.1241-1247.
- [137] MIDEL. MIDEL 7131 Retrofilling Guidance. Data Sheet. 2 pages.
- [138] Cooper. Envirotemp FR3 Fluid; Recommended Procedures for Retrofilling Oil-Filled Transformers. Guidance; Section A900-20-2, Reference Document. 2006.
- [139] Simpkin, R. *Derivation of Lichtenecker's Logarithmic Mixture Formula From Maxwell's Equations*. IEEE Transaction on Microwave Theory and Technique. March 2010.
- [140] Saha, T. K. and P. Purkait. *Investigation of Polarization and Depolarization Current Measurements for the Assessment of Oil-Paper Insulation of Aged Transformers*. IEEE Transaction on Dielectrics and Electrical Insulation, Vol. 11, Issue 1, 2004, pp. 144-154.
- [141] Takuma, T. and Kawamoto, T. *Field Intensification Near Various Points of Contact with A Zero Contact Angle Between a Solid Dielectric and an Electrode*. IEEE Transaction on Power Apparatus and System, vol. PAS-103, No. 9, September 1984.
- [142] Schächter, L. *Analytic Expression for Triple-point Electron Emission from an Ideal Edge*. Journal of Applied Physics, vol. 72, No. 4, 26 January 1998.
- [143] Chung, M.S. et al. *Theoretical Analysis of the Field Enhancement in a Two Dimensional Triple Junction*. Applied Surface Science, vol. 251, Issues 1-4, 15 September 2005.
- [144] International Electrotechnical Commission. *IEC 60250; Recommended Methods for the Determination of the Permittivity and Dielectric Dissipation Factor of Electrical Insulating Materials at Power, Audio and Radio Frequencies Including Metre Wavelengths*. Geneva, 1969.
- [145] Sokolov, V. et al. *Effective Methods of Assessment of Insulation System Conditions in Power Transformer: A View Based on Practical Experience*. Proceedings of Electrical Insulation Conference and Electrical Manufacturing & Coil Winding Conference, 1999.
- [146] International Electrotechnical Commission. *IEC 61294; Insulating liquids - Determination of the partial discharge inception voltage (PDIV) - Test procedure*, ed. 1.0. Geneva, 1993.
- [147] Berg, G. and Lundgaard, L. *PD Signatures of Wedge Type Discharges in Transformer Insulation*. Proceeding of 14th International Conference on

Dielectric Liquids, Graz, Austria, 2002.

- [148] Cavallini, A. et al. *Condition Assessment of Instrument Transformer by Partial Discharge Analysis: a Comprehensive Approach*. IEEE International Conference on Dielectric Liquid, 2005.
- [149] Dai, J. et al. *Creepage Discharge on Insulation Barriers in Aged Power Transformers*. IEEE Trans. On Dielectrics and Electrical Insulation, Vol. 17, No. 4, August 2010.
- [150] Tsukioka, H. et al. *Development of Low Dielectric Constant Pressboard*. Proceeding of the twenty-first symposium on electrical insulating material, 1988.

Appendix A – Calculation of direct inter-electrode capacitance for three electrodes system

One of elements necessary for the calculation of relative permittivity is the effective surface area of the guarded electrode A . According to IEC 60093, A is determined as [81]:

$$A = \frac{\pi}{4}(d_a + g)^2 \quad (\text{A.1})$$

The calculation of the effective surface area of the guarded electrode A with correction factor becomes:

$$A = \frac{\pi}{4}(d_a + B \cdot g)^2 \quad (\text{A.2})$$

Factor B depends on the ratio gap width (between guard and guarded electrode) to sample thickness $\frac{g}{h}$. Factor B is determined as:

$$B = 1 - \frac{4}{\pi} \frac{h}{g} \ln(\cosh(\frac{\pi g}{4 h})) \quad (\text{A.3})$$

The direct inter-electrode capacitance for vacuum C_o can be calculated as:

$$C_o = \varepsilon_o \frac{A}{h} \quad (\text{A.4})$$

For thick samples such as pressboard, the effective surface area (A) was calculated using equation 1. Meanwhile for transformer papers, it was calculated using equation 2 which include the correction factor. The direct inter-electrode capacitance for vacuum are presented in table below

Table A.1: Inter-electrode capacitance for vacuum.

Type of Solid Insulation	Thickness (mm)	C_o (pf)
Weidmann B.3.1A (TIV) 2mm	2	9.77
Weidmann B.4.1 (TIII) 2mm	2	9.77
DuPont Nomex T-993 2mm	2	9.77
Cottrell CK 125-TU 0.076mm	0.076	248.05
Tullis Russel Rotherm HIHD 0.085mm	0.085	221.86
Nordic Paper Amotfors 0.080mm	0.080	235.68

Appendix B – Derivation of equivalent circuit

This section provides the dielectric response in time and frequency domain of Extended Debye model that represent solid-fluid insulating system as in Figure B.1.

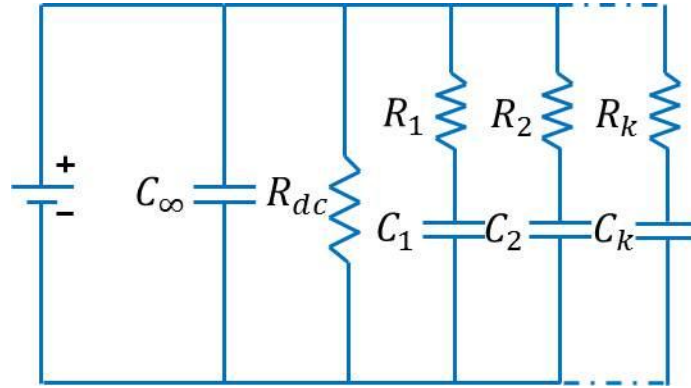


Figure B.1. Extended Debye model to represent solid-fluid insulating system.

In frequency domain

The general form for the current I in dielectrics is given by

$$I = \omega \varepsilon'' C_0 V + i \omega \varepsilon' C_0 V \quad (\text{B.1})$$

Thus, the corresponding impedance Z_t of such admittance Y is

$$Y = \frac{1}{Z_t} = \omega \varepsilon'' C_0 + i \omega \varepsilon' C_0 \quad (\text{B.2})$$

Thus, total impedance for Extended Debye model in Figure B.1.

$$\begin{aligned} \frac{1}{Z_t} &= \frac{1}{Z_\infty} + \frac{1}{R_{dc}} + \frac{1}{Z_1} + \frac{1}{Z_2} \\ \frac{1}{Z_t} &= j\omega C_\infty + \frac{1}{R_{dc}} + \frac{j\omega C_1 + \omega^2 C_1^2 R_1}{1 + \omega^2 C_1^2 R_1} + \frac{j\omega C_2 + \omega^2 C_2^2 R_2}{1 + \omega^2 C_2^2 R_2} \\ \frac{1}{Z_t} &= \frac{1}{R_{dc}} + \frac{\omega^2 \tau_1 C_1}{1 + \omega^2 \tau_1^2} + \frac{\omega^2 \tau_2 C_2}{1 + \omega^2 \tau_2^2} + j\omega \left(C_\infty + \frac{C_1}{1 + \omega^2 \tau_1^2} + \frac{C_2}{1 + \omega^2 \tau_2^2} \right) \end{aligned} \quad (\text{B.3})$$

Equating the real part of equation (B.3) with real part of equation (B.2)

$$\omega \varepsilon'' C_0 = \frac{1}{R_0} + \frac{\omega^2 \tau_1 C_1}{1 + \omega^2 \tau_1^2} + \frac{\omega^2 \tau_2 C_2}{1 + \omega^2 \tau_2^2}$$

$$\begin{aligned}\varepsilon'' C_0 &= \frac{1}{\omega} \left(\frac{1}{R_0} + \frac{\omega^2 \tau_1 C_1}{1 + \omega^2 \tau_1^2} + \frac{\omega^2 \tau_2 C_2}{1 + \omega^2 \tau_2^2} \right) \\ C'' &= \frac{1}{\omega} \left(\frac{1}{R_0} + \frac{\omega^2 \tau_1 C_1}{1 + \omega^2 \tau_1^2} + \frac{\omega^2 \tau_2 C_2}{1 + \omega^2 \tau_2^2} \right) \\ C''(\omega) &= \frac{1}{\omega R_0} + \sum_{k=1}^n \frac{\omega \tau_k C_k}{1 + \omega^2 \tau_k^2}\end{aligned}\quad (\text{B.4})$$

Equating the imaginary part of equation (B.3) with imaginary part of equation (B.2)

$$\begin{aligned}\varepsilon' C_0 &= \omega \left(C_\infty + \frac{C_1}{1 + \omega^2 \tau_1^2} + \frac{C_2}{1 + \omega^2 \tau_2^2} \right) \\ \varepsilon' C_0 &= C_\infty + \frac{C_1}{1 + \omega^2 \tau_1^2} + \frac{C_2}{1 + \omega^2 \tau_2^2} \\ C' &= C_\infty + \frac{C_1}{1 + \omega^2 \tau_1^2} + \frac{C_2}{1 + \omega^2 \tau_2^2} \\ C'(\omega) &= C_\infty + \sum_{k=1}^n \frac{C_k}{1 + \omega^2 \tau_k^2}\end{aligned}\quad (\text{B.5})$$

Equating equation (B.4) and imaginary part of equation (2.33),

$$\begin{aligned}\varepsilon''_{r(\omega)} &= \frac{C''(\omega)}{C_0} \\ \frac{\sigma_0}{\varepsilon_0 \omega} + \chi''_{(\omega)} &= \frac{1}{C_0 \omega R_0} + \frac{1}{C_0} \sum_{k=1}^n \frac{\omega \tau_k C_k}{1 + \omega^2 \tau_k^2}\end{aligned}\quad (\text{B.6})$$

Thus, the right side of equation (B.4) represents polarization loss which is interfacial polarization loss and dipolar orientation loss in solid-fluid insulating system over the measured frequency. By changing the relaxation time τ_k (series of R_k and C_k) in equation (B.4) to match the absorption frequency $f_{m'} = 1/2\pi \tau_k$ of each polarization mechanism, the loss peak of dielectric response in frequency domain can be simulated.

In time domain

The value of relaxation time τ_k (series of R_k and C_k) can also be derived from charging current measurement. Charging current flow under step DC applied voltage is given in equation (B.7)

$$i_{\text{charging}}(t) = C_0 V_0 \frac{\sigma_0}{\varepsilon_0} + C_0 V_0 f(t) \quad (\text{B.7})$$

To derive relaxation time τ_k from charging current measurement, the polarization current or depolarization current which have the same dielectric response function $f(t)$ should be analysed. With this approach, the depolarization current can be derived to

get the branches parameter in Extended Debye model that represent the relaxation time as in Figure B.2. According to [84, 140], the depolarization current can be derived as follows

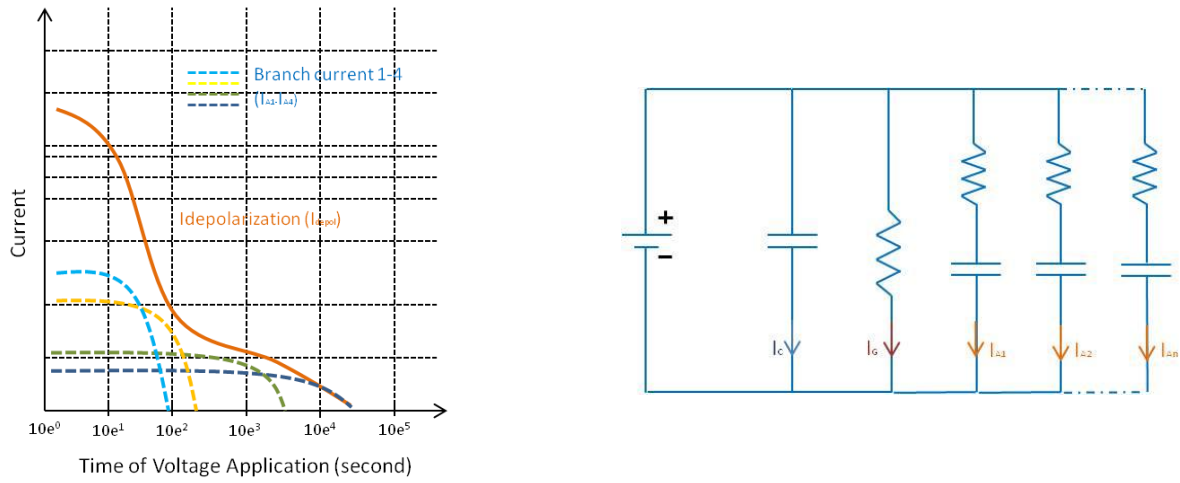


Figure B.2: Depolarization current derived from Extended Debye model.

$$i_{depolarization} = C_o V_{of}(t) = \sum_{k=1}^n A_k * e\left(-\frac{t}{\tau_k}\right) \quad (B.8)$$

Where

n number of branches in to represent loss peak

A_k amplitude of current at each branch at $t=0$

$$A_k = V \frac{(1 - e\left(-\frac{t_p}{\tau_k}\right))}{R_k}$$

t_p is the duration of time during which the sample is charged

τ_k Relaxation time on each branch $\sim R_k * C_k$

Number of branches used should correspond to the nature of polarization mechanism present. For longer polarization mechanism such as interfacial polarization, higher relaxation time should be applied.

Finally, this section shows that the Extended Debye can represent the solid-fluid impregnated system very well both in time and frequency domain. Using the Extended Debye model, data in the time domain from electrical conductivity measurement can be transformed into data in the frequency domain.

Appendix C – Design of electrode and test vessel

C.1. Electrode corner shape for measuring dielectric properties

The electrode configuration for measuring dielectric properties of solid-fluid insulating system yield an interface so called “triple junction” which is the meeting point of three materials i.e. solid, fluid and electrode. Triple junction will promote electric field stress enhancement which normally occurs with the addition of solid insulation to the insulating fluid system [141, 142, 143]. The electric field stress near or at contact point between solid dielectric surface and an electrode (triple junction) often much higher when compared with the electric field stress without solid dielectric.

Unfortunately when measuring dielectric properties according to IEC 60093 and IEC 60250, the detail of cylindrical live electrode curvature corner shape is not fully explained [81, 144]. The effect from the electrode curvature corner shape on the electric field distribution should be reduced as small as possible when measuring the dielectric response and DC conductivity of the solid-fluid insulating system. Appendix B.1 focused on comparative study of the electric field stress distribution on pressboard for three type electrode curvature corner shape i.e. rounded-cornered with radius 3 mm and 5 mm and sharp-cornered electrode as in Figure C.1.

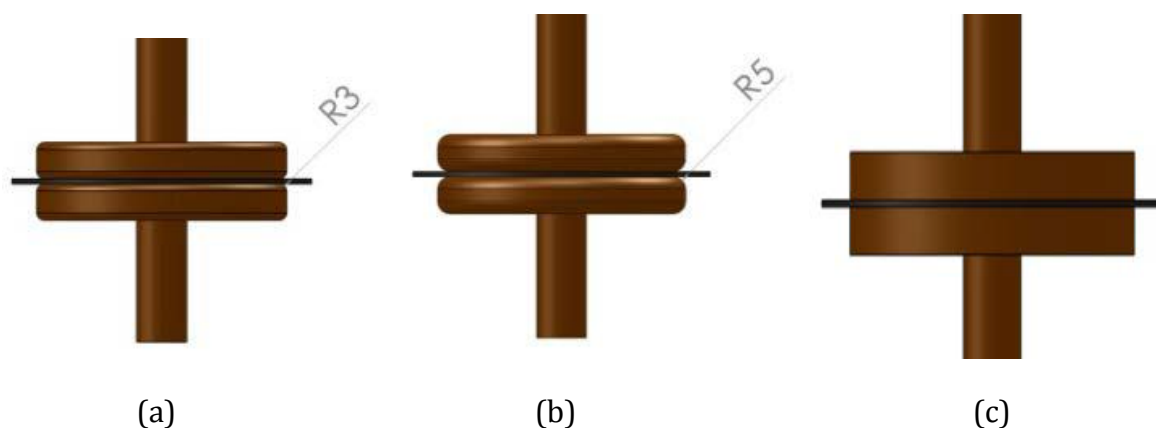


Figure C.1: Three type electrode curvature corner shape,(a) rounded-cornered with radius 3 mm,(b) radius 5 mm and (c) sharp-cornered electrode.

Investigation of the suitability of electrode corner shape for dielectric properties measurement by conducting electric field simulation and laboratory experiment for triple junction configuration was performed. The electric field simulation was done with finite element method using Infolytica Elecnet 7. The simulation results were deepened with partial discharge inception voltage (PDIV) and partial discharge (PD) measurement with the same electrode configuration to prove the effect of electric field

enhancement at the triple junction. These results could be used as a consideration on which electrode is suitable for measuring dielectric properties of solid-fluid insulating system in compliment with IEC standards.

Experimental set-up and procedure

Test circuit arrangement for PD investigation was set up according to IEC 60270, as depicted in Figure C.2. The discharge was measured at the same time with narrow bandwidth (Power Diagnostix ICM) and wide bandwidth (Oscilloscope Yokogawa DLM series) PD measurement systems. The PDIV and PD patterns were recorded using ICMsystem. Meanwhile, the PD pulse current signals were recorded with oscilloscope, and then analyzed the frequency domain in PC.

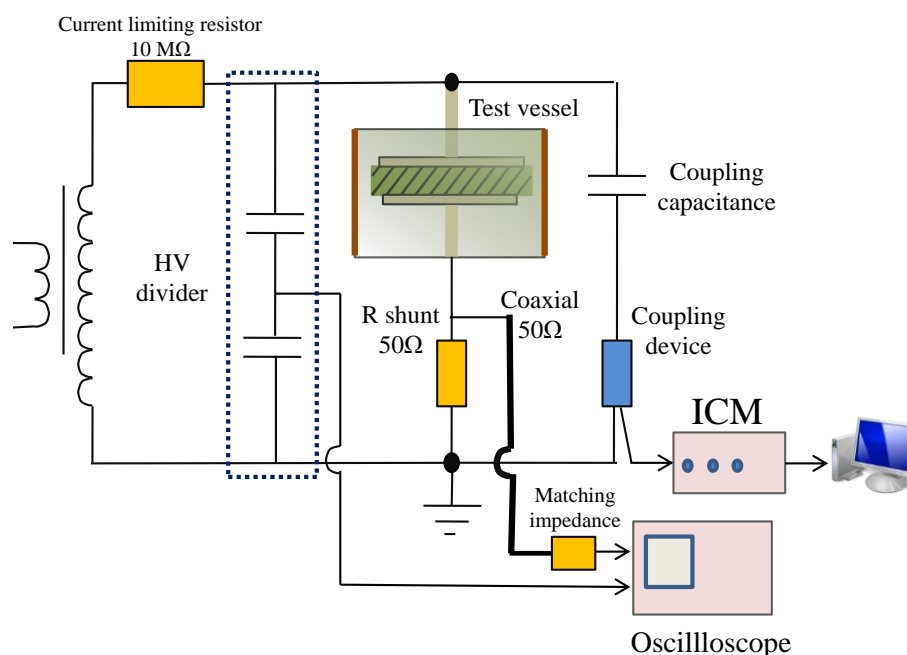


Figure C.2: PD measurement set-up.

Until recently, there is no clear definition of PDIV for PD at fluid and solid interface. In this experiment, PDIV was defined as the voltage when the apparent charge of PD was higher than 100pC. Reference [145] mentioned that the cellulose destruction (creeping discharge) begin at apparent charge 100-1000pC. Therefore at this charge magnitude, PDIV can be used as diagnostic of the onset of dangerous PD charge for insulation.

In this experiment, the voltage was applied in two consecutive ways [Figure C.3]:

(a) Ramp increased voltage at 1kV/s until PDIV ($PDIV_1$) was reached [146].

(b) And then continued measuring with step increased voltage. The voltage was raised up to 80% of PDIV mean value from the first procedure ($PDIV_1$). Then, the voltage was raised again with 1kV step until PDIV ($PDIV_2$). After that, the voltage was increase to

1.1 times PDIV_2 value and then, the PD pattern and PD pulse current signals were recorded for 5 minutes.

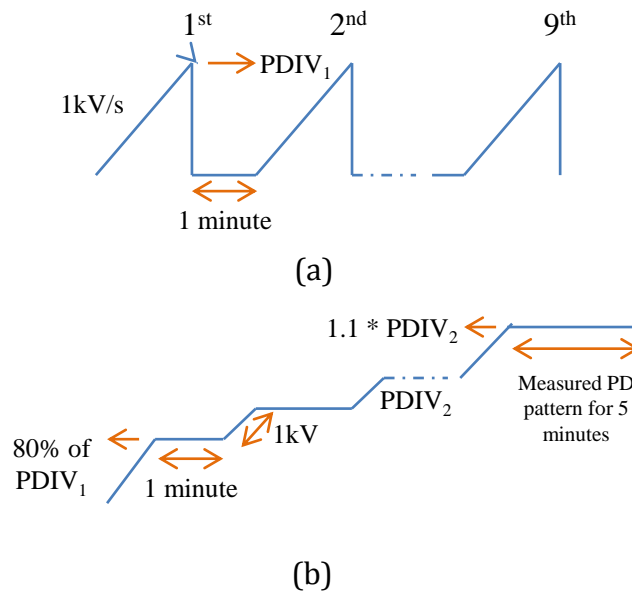


Figure C.3: Test procedures for (a) ramp method and (b) step method.

The first method of voltage appliance was intended to investigate the effect of electrode's corner shape on electric field enhancement by means of PDIV because PDIV is triggered by the highest electric field stress. Meanwhile, the second method was intended to catch PD pattern without the risk of breakdown because for this experiment, breakdown are easily occurred.

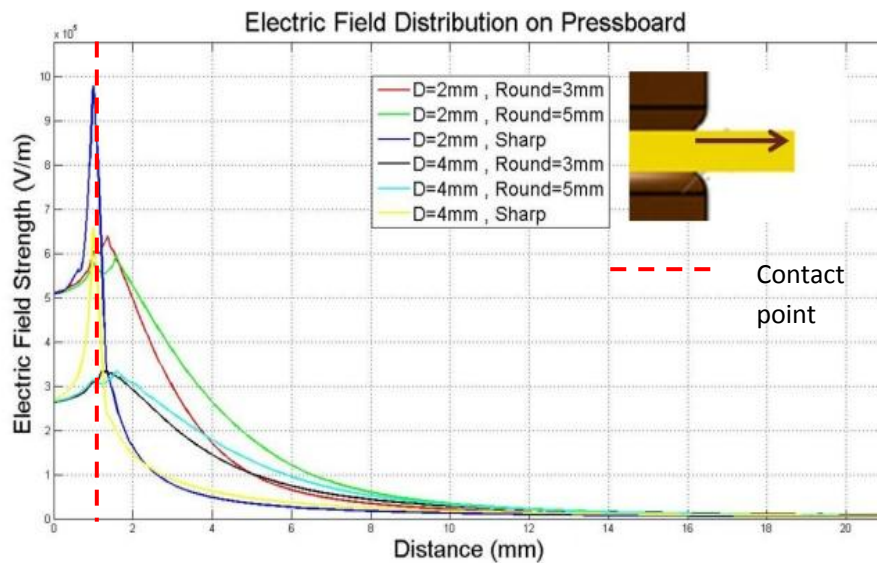
Results

- Electric Field Distribution

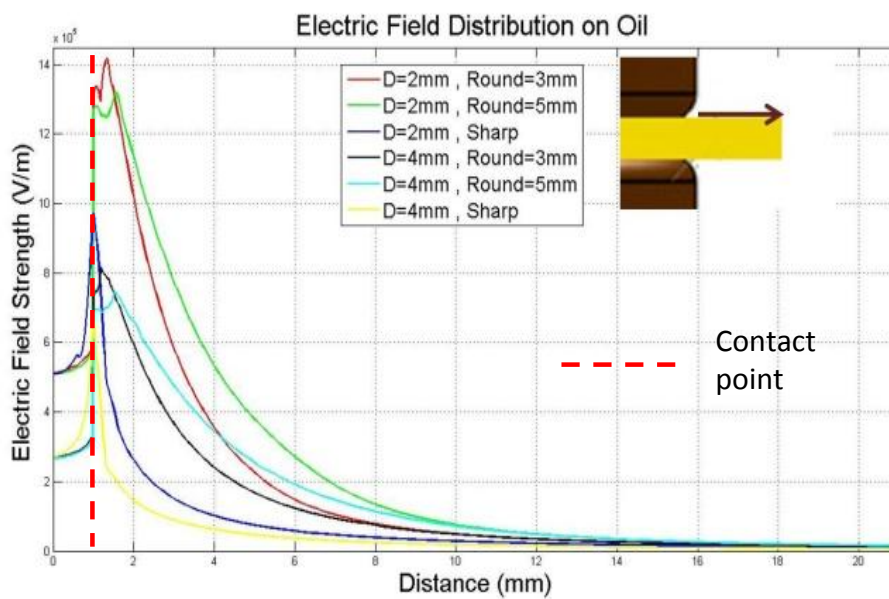
Figure C.4 (a) shows a typical electric field stress line on pressboard side from the contact point to the edge of the sample (simulated at 1kV). The electric field magnitude at the contact point of pressboard side is very high for sharp-cornered electrode compared to rounded-cornered electrode. For sharp cornered electrode, there is a steep enhancement at the contact point. Meanwhile, for rounded-cornered electrode, the electric field enhancement is much lower. In conclusion, round-cornered electrode system generates more uniform field on pressboard than sharp-cornered electrode.

Figure C.4 (b) shows typical the electric field stress line on fluid side from the contact point to the edge of the sample. The electric field magnitude for the round-cornered electrode is very high on the fluid side. The enhancement does not occur at the contact point but near the contact point of the triple junction. In reality, this steep enhancement occurs at the fluid small gap at the wedge between electrode and pressboard. The maximum electric field enhancement for rounded-cornered

electrode also occurs at this location. Furthermore, for 3mm and 5mm rounded electrode, the field enhancement is almost the equal.



(a)



(b)

Figure C.4: Electric field stress distributions from the point of contact (a) on pressboard side and (b) on oil side.

- Laboratory experiment results

PDIV experiment

Table C.1 shows PDIV₁ values of the each electrode system. It shows that the PDIV value for sharp-cornered electrode is higher than rounded-cornered electrode. This might be attributed to lower electric field enhancement at the oil side near

the contact point as shown in Figure C.4. (b) for sharp-cornered. Meanwhile, for rounded-cornered electrode, the lower PDIV value might be caused by the electric field enhancement at the oil small gap where the location of highest electric field occurs. This phenomenon could possibly explain that PD at solid-fluid insulating system interface initiates in oil as PDIV depends directly on the maximum electric field stress.

Table C.1: PDIV₁ value for three type electrode corner shape

Sample thickness	Electrode corner shape	PDIV ₁ *	
		V _{PDIV} (kV)	σ (kV)
2 mm	Rounded 3mm	31.85	1.3
	Rounded 5mm	32.01	1.6
	Sharp	34.86	1.4
4 mm	Rounded 3mm	44.73	1.9
	Rounded 5mm	46.24	1.5
	Sharp	>48	-

*PDIV₁ is PDIV value with ramp increased voltage method.

Meanwhile, for 3mm and 5mm rounded electrode, practically, there is no difference in terms of PDIV mean value especially at 2mm pressboard. These results confirm the enhancement characteristic at the oil small gap of rounded-cornered electrode as shown in electric field simulation.

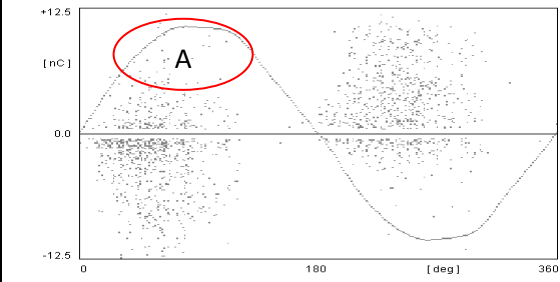
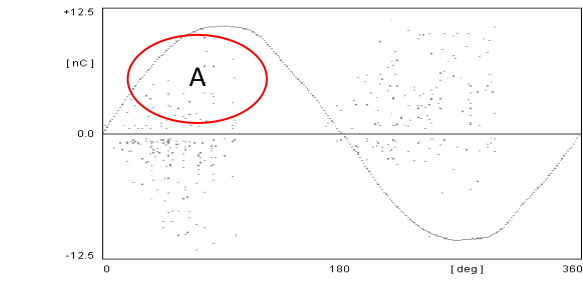
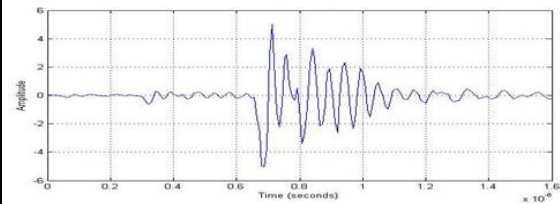
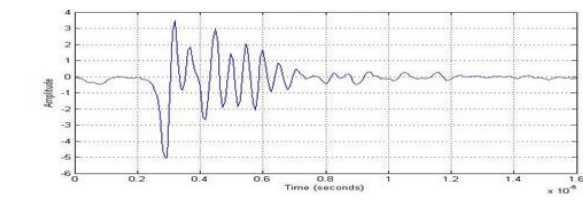
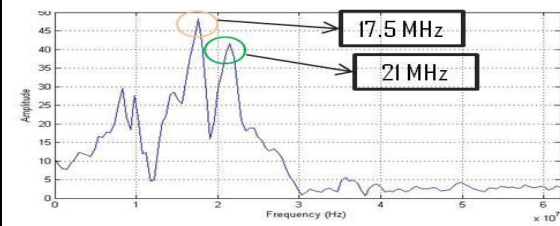
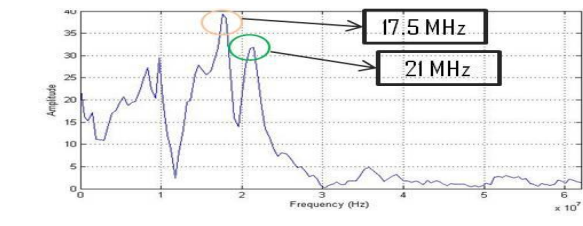
PD pattern and PD pulse current signal analysis

Table C.2 shows the comparison of typical PD pattern and PD pulse current signal for rounded-cornered electrode and sharp-cornered electrode. PD patterns for both electrodes are similar. Those scattered discharge patterns (ellipse in Table B.2) indicate the nature of surface discharge that generated at the surface of pressboard [147, 148]. References [149] also mentioned that surface discharge with this type of electrode system is similar to the corona in oil. It produces surface discharge that predominantly occurs at the oil side.

Meanwhile, from the frequency domain analysis of PD pulse current signal with wide bandwidth system, it was found that the PD signals from both electrodes have the same dominant frequency at 17.5MHz. This possibly means that the same discharge mechanism occurs with both electrode systems.

From PD pattern and PD pulse current signal analysis there is no indication internal PD occurred at this voltage level or with this electrode system. It might be attributed to characteristic of breakdown voltage of cellulose which is usually higher than oil.

Table C.2: Comparison of PD Characteristics.

PD characteristic	Rounded-cornered electrode	Sharp-cornered electrode
PD pattern		
PD current pulse		
Frequency analysis of PD current pulse		

Conclusions

Even though round-cornered electrode yields more uniform electric field at the pressboard side, it also yields steep electric field enhancement at the fluid side. This nature of rounded-corner electrode makes it easier to generate discharge in fluid at the wedge between electrode and pressboard when compared to sharp-cornered electrode [150]. When measuring dielectric properties at high voltage (for simulating the real system), this phenomenon should be taken into account.

Meanwhile, for the sharp cornered electrode, the highest electric field enhancement occurred at the pressboard side. Therefore the electric field distribution is not uniform in pressboard. It might affect the measurement results of dielectric properties because the very low charging current in the experiment. However, the extent of these two phenomena on the measurement results should be proven.

Finally, the suitability of the detail of live electrode curvature corner shape depends on the voltage stress which is going to be applied for measurement. In this thesis, the measurement was performed with maximum voltage of 1kV for DC conductivity measurement and thus, the rounded-cornered electrode with radius 3mm deemed to be appropriate.

C.2. Electrode's pressure on the measured dielectric properties

Other factor that might have influence on dielectric properties measurements of solid-fluid insulating system which was performed in a fluid bath is the pressure of the electrode. In this kind of measurement, the surface roughness of pressboard should be taken into consideration [89, 133]. These phenomena could influence the measurement results of the solid-fluid insulating system. Therefore, the pressure of electrode plays an important role to reduce the effect of surface roughness of pressboard which can reduce the measurement accuracy.

This chapter focused on the investigation of the effect of electrode's pressure on measurement results by conducting electrode's pressure simulation and laboratory experiment with various electrodes' pressure. In conclusion, it was found that electrode with pressure higher than $1.9\text{N}/\text{cm}^2$ give enough pressure to reduce the effect of surface roughness which influenced the measurement results.

Results

Electrode's pressure simulation

Figure C.5 shows the simulated electrode system in this experiment and pressure distribution on the pressboard surface. From the simulation, it was found that the maximum pressure typically occurs at the electrode's corner for rounded-cornered electrode. The pressure on the surface of pressboard is not uniform in all configurations. The average pressure of the first configuration is $0.33\text{N}/\text{cm}^2$, the second configuration is $1.9\text{N}/\text{cm}^2$ and the third configuration is $3.3\text{N}/\text{cm}^2$.

Laboratory experiment results

In this experiment, the pressure of live electrode was varied to investigate the effect of electrode's pressure to reduce the effect of surface roughness of solid-fluid insulating system. Table C.3 shows that electrode with pressure of $0.33\text{N}/\text{cm}^2$ is not enough to prevent the effect of pressboard's surface roughness because the mean value of relative permittivity is lower if compared with other configurations. It is a sign that the pressure is not enough to prevent thin fluid layer on the surface of pressboard because of surface roughness. For electrode with pressure higher than $1.9\text{N}/\text{cm}^2$, the measurement accuracy is good as shown by the relative permittivity value. However, too much pressure (from one massive electrode), usually, do not properly adhere to stiff dielectrics and may cause measuring errors and destroy the samples.

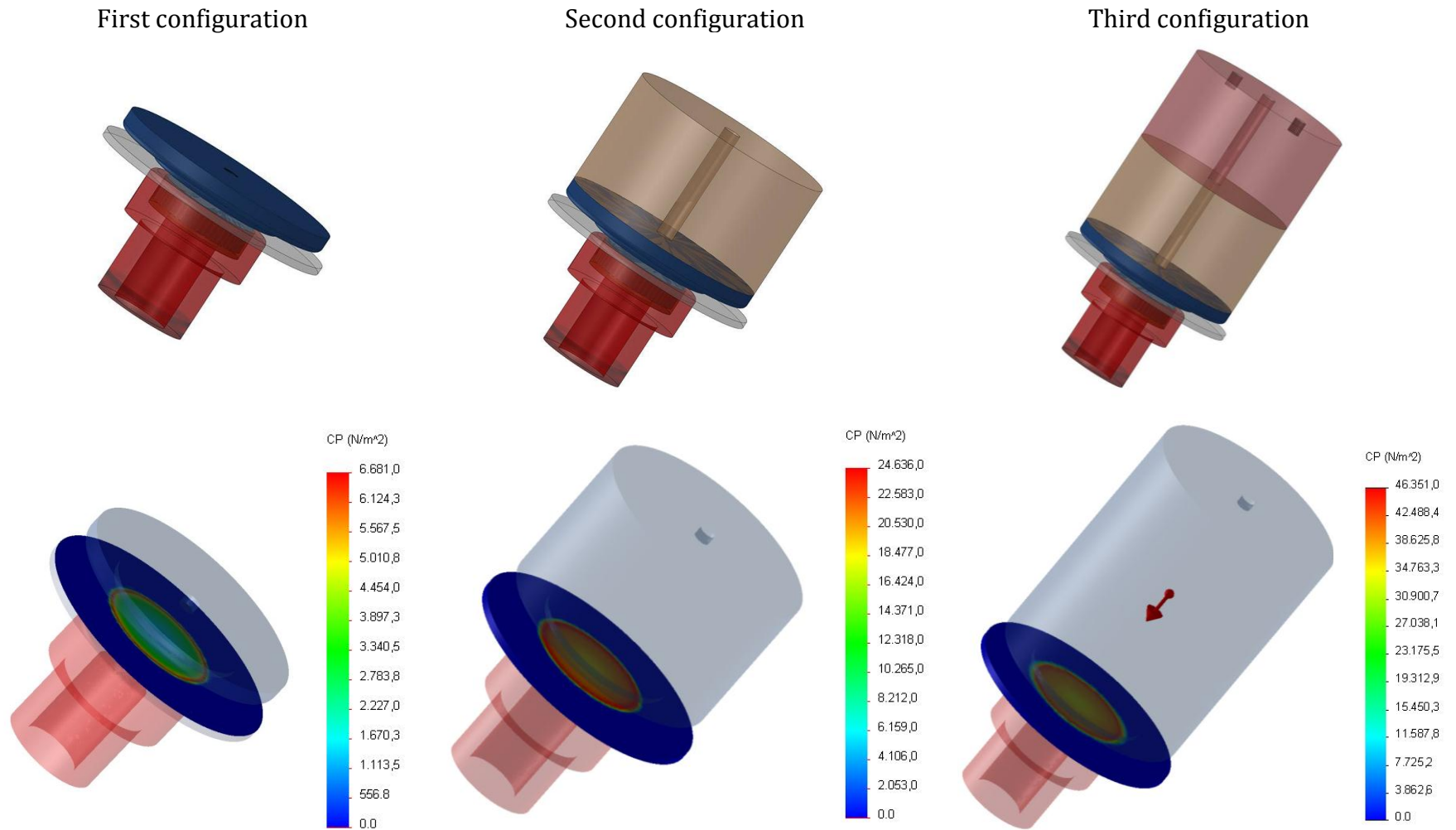
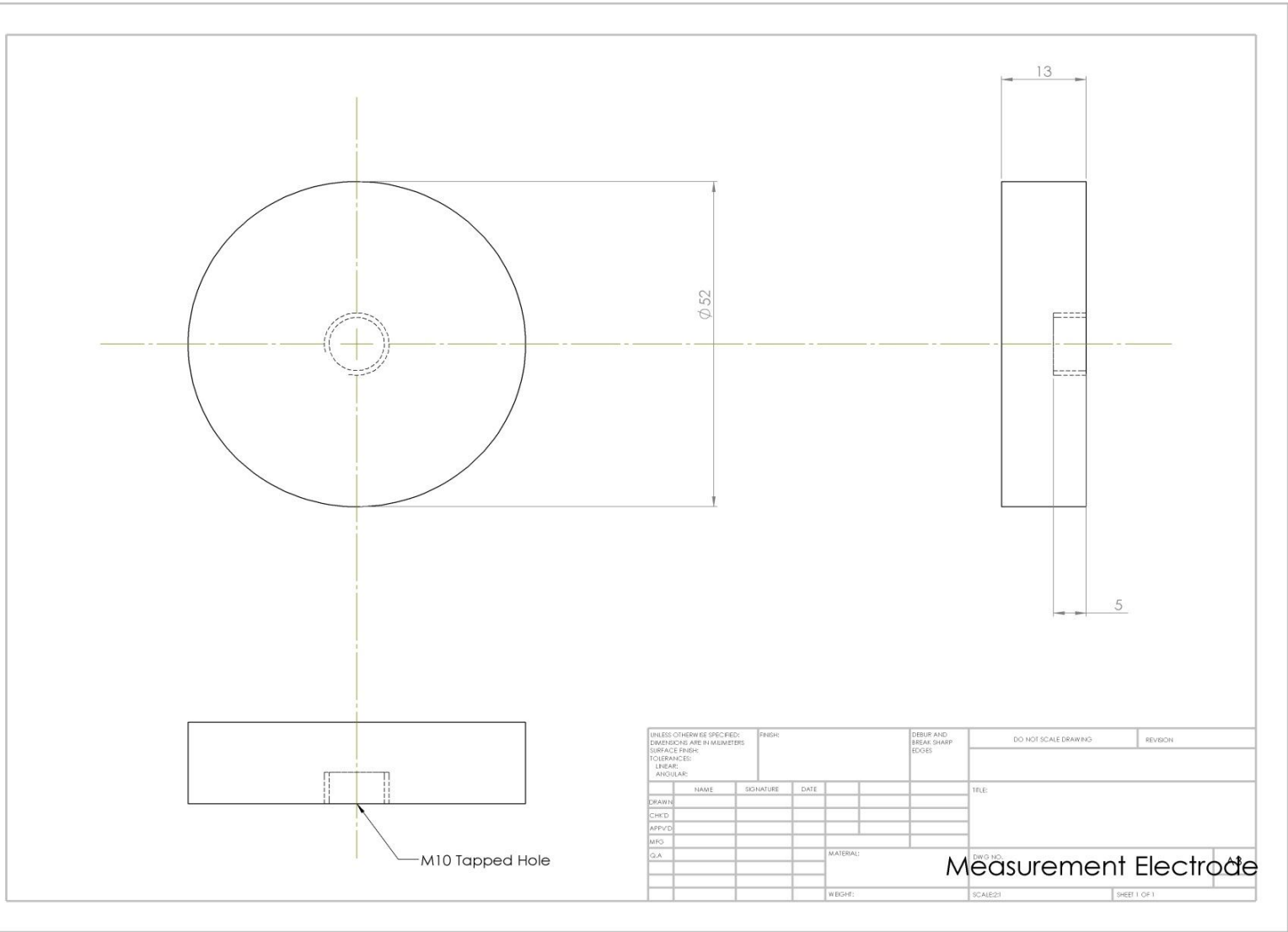
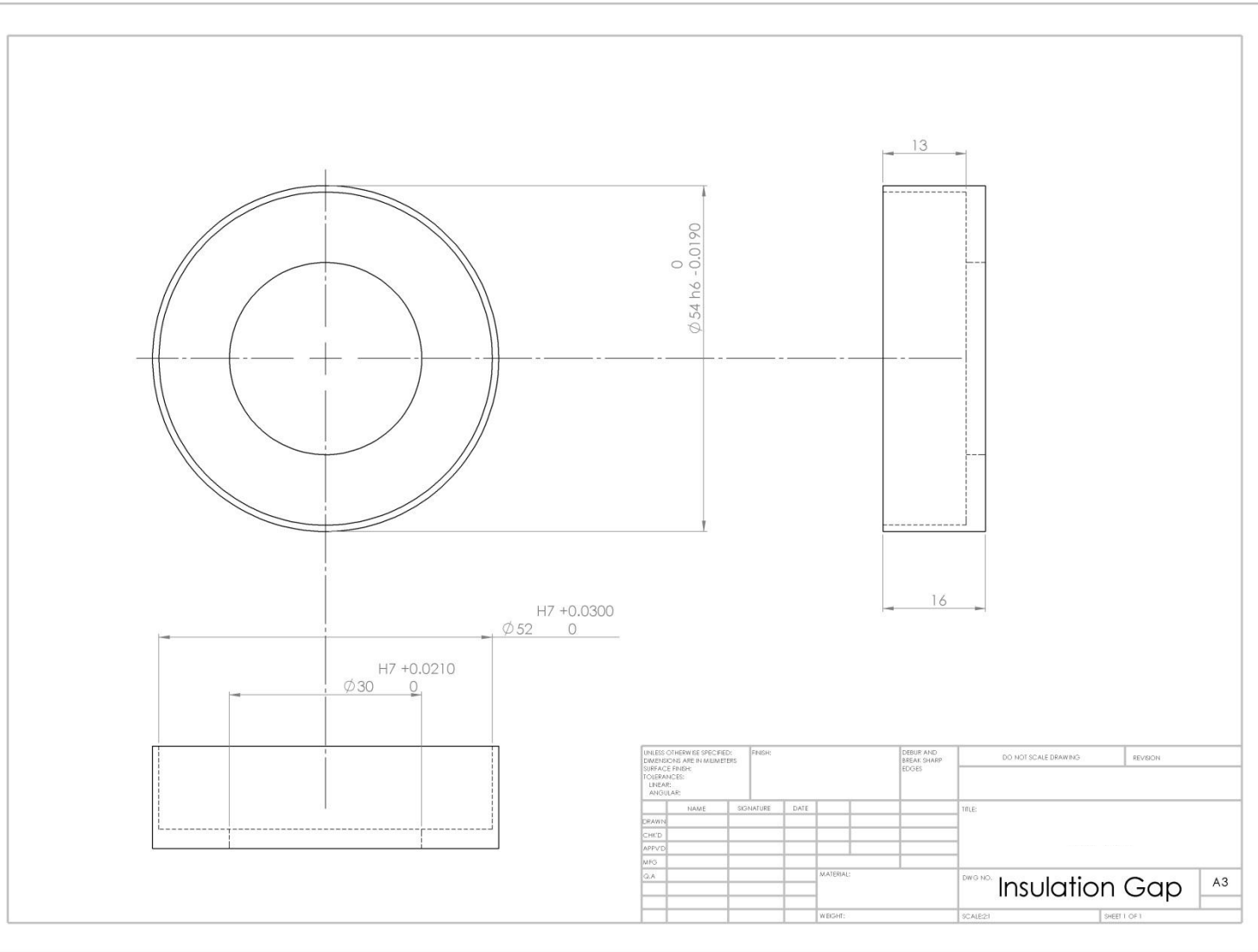


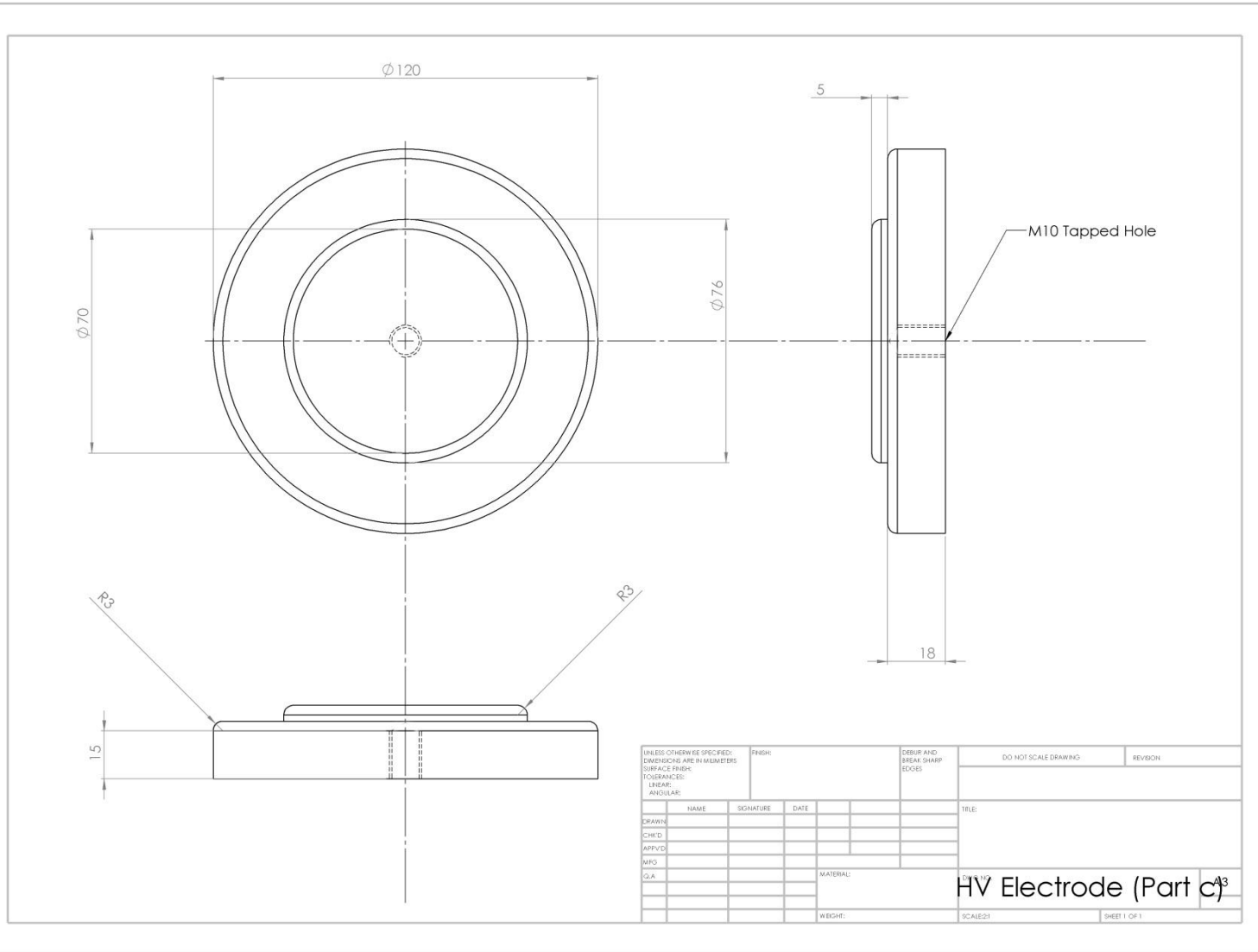
Figure C.5: Simulation of electrode system and pressure distribution on the pressboard surface.

Table C.3: Correlation between electrode's pressure & relative permittivity.

Electrode system	Electrode's Pressure		ϵ_r	
	Maximum (at the corner)	Mean (at the center)	Mean	σ
One	0.7 N/cm ²	0.3 N/cm ²	4.14	0.064
Two	2.4 N/cm ²	1.9 N/cm ²	4.25	0.067
Three	4.6 N/cm ²	3.3 N/cm ²	4.26	0.065







Appendix D – Table of Dielectric Properties

Table D.1: Dielectric properties of solids impregnated with insulating fluids.

Type	Temp.	Co (pf)	Relative permittivity at 50 Hz			Tan delta at 50 Hz			DC conductivity (S/m)		
			Nytro 4000X	MI7131	FR3	Nytro 4000X	MI7131	FR3	Nytro 4000X	MI7131	FR3
Weidmann B.3.1A (TIV) 2mm	25°C	9.77	4.4	4.95	4.88	0.0034	0.0043	0.0049	2.77E-16	7.2E-15	1.75E-15
	60°C		4.55	5.09	4.99	0.003	0.0125	0.006	3.89E-14	1.57E-13	1.1E-13
	90°C		4.67	5.27	5.1	0.0048	0.046	0.0191	2.3E-12	5.25E-12	4.6E-12
Weidmann B.3.1A (TIV) 4mm	25°C	4.88	4.41	4.98	4.92	0.0034	0.0042	0.004	1.11E-16	1.49E-14	7.41E-15
	60°C		4.53	5.1	5.02	0.003	0.0122	0.0055	3.13E-14	1.93E-13	1.1E-13
	90°C		4.65	5.25	5.11	0.0045	0.0408	0.0144	1.7E-12	4.68E-12	3.07E-12
Weidmann B.4.1 (TIII) 2mm	25°C	9.77	3.79	4.58	4.62	0.0029	0.0036	0.0043	1.81E-16	8.46E-15	1.93E-15
	60°C		3.91	4.78	4.75	0.0027	0.0092	0.0058	3.06E-14	1.78E-13	1.34E-13
	90°C		4.03	4.91	4.88	0.0037	0.0371	0.0176	1.52E-12	4.52E-12	3.78E-12
DuPont Nomex T-993 2mm	25°C	9.77	3.15	3.9	3.78	0.0067	0.0058	0.008	2.28E-17	3.52E-15	1.39E-15
	60°C		3.29	3.93	3.9	0.0044	0.0059	0.0063	2.17E-16	2.26E-14	5.62E-15
	90°C		3.34	3.97	3.95	0.0042	0.0139	0.0109	1.63E-15	8.22E-14	3.83E-14
Cottrell CK 125-TU 0.076mm	25°C	248.05	3.96	4.28	4.24	0.0072	0.0107	0.0106	2.77E-15	2.1E-14	1.71E-14
	60°C		4.31	4.9	4.92	0.0067	0.0238	0.0304	3.23E-13	3.11E-12	3.8E-12
	90°C		4.62	5.91	6.02	0.0298	0.1067	0.1329	3.15E-11	1.86E-10	2.28E-10
Tullis Russel Rotherm HIHD 0.085mm	25°C	221.86	3.33	4.03	3.66	0.0046	0.0091	0.0074	1.3E-15	1.84E-14	2.09E-14
	60°C		3.71	4.63	4.24	0.0038	0.053	0.0309	2.04E-13	2.19E-12	2.01E-12
	90°C		4.1	5.49	5.08	0.011	0.1688	0.1134	7.1E-12	8.99E-11	6.85E-11
Nordic Paper Amotfors 0.080mm	25°C	235.68	2.9	3.6	3.52	0.0029	0.0069	0.006	1.55E-15	9.64E-14	1.5E-14
	60°C		3.11	3.92	3.84	0.0025	0.0539	0.0314	1.76E-13	4.08E-12	6.9E-13
	90°C		3.31	4.55	4.32	0.0084	0.1711	0.1003	4.91E-12	8.89E-11	1.43E-11

Tabel D.2: Dielectric properties of insulating fluids.

	Relative Permittivity (50Hz)			Tan Delta (50Hz)			DC Conductivity (S.m)
	25°C	60°C	90°C	25°C	60°C	90°C	90°C (500V)
Nyro 4000X	2.19	2.13	2.1	0.00022	0.00047	0.00089	1.39E-12
MI7131	3.2	3.09	3.01	0.00211	0.00800	0.02974	1.68E-10
FR3	3.18	2.99	2.87	0.00586	0.01916	0.05140	2.87E-10